



UNIVERSITY OF  
KWAZULU-NATAL  
INYUVESI  
YAKWAZULU-NATALI

**Novel Epidermal Growth Factor Directed Cationic  
Lipoplexes Promote *In Vitro* Hepatotropic Gene Targeting**

by

**ALISHA SEWBALAS**

**Submitted in fulfilment of the academic requirements for the degree of Doctor of  
Philosophy in the School of Life Sciences, University of KwaZulu-Natal**

**Durban**

**December 2014**

**As the candidates supervisor I have approved this thesis/dissertation for submission.**

**Supervisor:** Dr M. Singh

**Signed:** .....

**Date:** .....

**Co-Supervisor:** Professor M. Ariatti

## ABSTRACT

The need for the improvement in protocols for cellular gene delivery has propelled cytofectin based liposomes as suitable non-viral gene carriers. The amenability of cationic liposomes to modification enables research based enhancement of their carrier capability. The liposomes formulated in this study show potential for cancer therapeutics, where effective delivery at the molecular level is essential. Cell specific targeting may be attained through cationic vector manipulation to favourably utilise overexpressed cancer cell specific receptors. This study serves as an evaluation of a hepatocyte-directed liposomal gene delivery system, exploiting the abundant epidermal growth factor (EGF) receptors on hepatocellular carcinoma cells (HepG2) *in vitro*. The inclusion of polyethylene glycol (PEG) served to limit steric hindrance and to increase stability of the formulations.

Four liposomes comprising cytofectins 3β[N-(N',N'-dimethylaminopropane)-carbonyl] (Chol-T) and N,N-dimethylaminopropylamidodisuccinyl-cholesterylformylhydrazide (MS09) at 50 mol%, were formulated through thin film rehydration with dioleoylphosphatidylethanolamine (DOPE) and PEG to generate liposomes that are cationic and have stealth capability. Hepatotropic lipoplexes were formed from EGF adsorption onto formulated liposomes, prior to characterisation and cell culture studies. All liposomes displayed as nano-sized particles (60 – 181 nm) with varying levels of colloidal stability and distribution as evidenced by transmission electron microscopy and nanoparticle tracking analysis. Moderate to highly cationic lipid : DNA charge ratios were observed by the mobility shift and ethidium bromide dye displacement assays. Broad range protection of plasmid DNA integrity was identified, with DSPE-PEG<sub>2000</sub>-grafted liposomes offering greatest shielding against nuclease attack. *In vitro* cytotoxicity was determined using the MTT assay, and reporter gene expression, was assayed using the luciferase and green fluorescent protein (GFP) reporter gene assays in the receptor positive HepG2 and the receptor negative Chinese Hamster ovary (CHO-K1) cell line.

These novel EGF-tagged cationic liposomes displayed negligible cytotoxicity to both cell lines and were capable of high transgene activity in the HepG2 cells compared to the CHO-K1 cells. The Chol-T-EGF liposome significantly ( $P < 0.0001$ ) potentiated transgene targeting, compared to the commercially available transfection reagent, Lipofectin. Targeting was further confirmed

from the YI-12 peptide–EGFR competitive transfection determinations in the HepG2 cell line. Results obtained for the luciferase reporter assay was corroborated by the flow cytometric quantification of GFP expression. The size distribution, physicochemical properties and *in vitro* studies strongly suggest that these targeted lipoplexes should be optimized for future applications *in vivo*.

## **PREFACE**

The experimental work described in this dissertation was carried out in the School of Life Sciences, University of KwaZulu-Natal, Durban, from July 2011 to December 2014, under the supervision of Dr. Moganavelli Singh and co-supervision of Professor Mario Ariatti.

These studies represent original work by the author and have not otherwise been submitted in any form for any degree or diploma to any tertiary institution. Where use has been made of the work of others it is duly acknowledged in the text.

## DECLARATION 1 – PLAGIARISM

I Alisha Sewbalas declare that

1. The research reported in this thesis, except where otherwise indicated, is my original research.
2. This thesis has not been submitted for any degree or examination at any other university.
3. This thesis does not contain other persons' data, pictures, graphs or other information, unless specifically acknowledged as being sourced from other persons.
4. This thesis does not contain other persons' writing unless specifically acknowledged as being sourced from other researchers. Where other written sources have been quoted, then:
  5. Their words have been re-written but the general information attributed to them has been referenced.
  6. Where their exact words have been used, then their writing has been placed in italics and inside quotation marks, and referenced.
7. This thesis does not contain text, graphics or tables copied and pasted from the internet, unless specifically acknowledged, and the source being detailed in the thesis and in the Reference section.

Signed: .....

## DECLARATION 2 – PUBLICATIONS

DETAILS OF CONTRIBUTION TO PUBLICATIONS that form part and/or include research presented in this thesis (*include publications in preparation, submitted, in press and published and give details of the contributions of each author to the experimental work and writing of each publication.*)

**Publication 1:** Peer Reviewed Published Abstract – Appendix 4

**Sewbalas, A., Ariatti, M., and Singh, M.** (2013). Epidermal growth factor targeted novel cationic lipoplexes Enhance transgene expression in HepG2 cell line *in vitro*. Human Gene Therapy, A1-A172.

Experimental work: Alisha Sewbalas

Writing of publication: Alisha Sewbalas and Dr. M. Singh

**Publication 2:** Manuscript in the preparation of submission

**Sewbalas, A., Ariatti, M., and Singh, M** (2014-2015). Targeting the HepG2 cell Epidermal growth factor receptors using cationic liposomes with EGF displays - *In preparation for submission.*

Experimental work and writing of publication: Alisha Sewbalas

# TABLE OF CONTENTS

	<b>PAGE</b>
<b>ABSTRACT</b>	II
<b>PREFACE</b>	IV
<b>DECLARATION 1</b>	V
<b>DECLARATION 2</b>	VI
<b>TABLE OF CONTENTS</b>	VII
<b>LIST OF TABLES</b>	XII
<b>LIST OF FIGURES</b>	XIII
<b>LIST OF ABBREVIATIONS</b>	XVIII
<b>ACKNOWLEDGMENTS</b>	XXII
<b>CHAPTER ONE:</b>	
<b>1. INTRODUCTION:</b>	1
<b>1.1. Cancer Gene Therapy: Turning Convention Into Innovation</b>	1
<b>1.2. Liver Cancer and Hepatocellular targeting</b>	4
<b>1.3. Delivery Systems For Hepatotropic Gene Therapy</b>	7
1.3.1. Nanoparticle systems	9
1.3.2. Polymer systems	12
1.3.3. Lipid systems	13
<b>1.4. Barriers And Modifications : How Non-Viral Systems Meet and Beat The Odds</b>	18
1.4.1. Internalisation and intracellular trafficking	18
1.4.1.1. Phagocytosis	19
1.4.1.2. Macropinocytosis	19
1.4.1.3. Clathrin mediated endocytosis (CME)	20
1.4.1.4. Caveolin mediated endocytosis (CvME)	20
1.4.1.5. Barriers to Carrier delivery	21
1.4.2. Surface modifications to liposomal systems	24
1.4.2.1. Stealth liposomes	24
1.4.2.2. Active targeting: liposomes and cellular targeting	26
	VII

<b>TABLE OF CONTENTS (continued)</b>	<b>PAGE</b>
<b>1.5. Targeting the Epidermal Growth Factor Receptor for Cancer therapy</b>	<b>28</b>
1.5.1. The epidermal growth factor receptor	28
1.5.2. EGF: the natural partner	33
1.5.3. EGFR targeted treatments	36
1.5.4. EGFR interaction, signalling and trafficking	40
1.5.5. EGF receptor mediated endocytosis	44
<b>1.6. Aims and Objectives</b>	<b>50</b>
<b>1.7. Thesis Outline</b>	<b>51</b>
<b>CHAPTER TWO:</b>	
<b>2. MATERIALS AND METHODS</b>	<b>53</b>
<b>2.1. Synthesis and Formulation</b>	<b>53</b>
2.1.1. Materials	53
2.1.2. Methods	53
2.1.2.1. Cytofectin synthesis	53
2.1.2.1.1. Chol-T Synthesis	53
2.1.2.1.2. MS09 Synthesis	54
2.1.2.2. Formulation and storage of the EGF peptide	56
2.1.2.3. Preparation of Liposomes	56
2.1.2.4. Amplification of pCMV Control Vector	58
2.1.2.5. Preparation liposome-DNA complexes or lipoplexes	59
<b>2.2. Liposome and Liposome-DNA Characterisation</b>	<b>59</b>



<b>TABLE OF CONTENTS (continued)</b>	<b>PAGE</b>
2.3.2.2.2c. Lipofectin <sup>®</sup> mediated transfection	69
2.3.2.2.2d. GFP reporter gene Analysis	70
a. Flow Cytometry	71
2.3.2.2.3. Statistical analysis	71
<b>CHAPTER THREE:</b>	
<b>3. RESULTS AND DISCUSSION</b>	72
<b>3.1. Synthesis and Characterization of Non-Viral Liposome Systems</b>	72
3.1.1. Liposome and lipoplex preparation	72
3.1.2. Transmission electron microscopy of liposome and lipoplex systems	74
3.1.3. Zeta sizing and surface potential	80
<b>3.2. Liposome – DNA Interactions</b>	85
3.2.1. Agarose gel retardation	85
3.2.2. Ethidium bromide intercalation	88
3.2.3. Liposomal display of hEGF protein for targeted formulations	91
3.2.4. Nuclease protection Assay	93
<b>3.3. Cell Line Maintenance and Transfection Activity</b>	96
3.3.1. Cell line maintenance	96
3.3.2. Cytotoxicity testing	97
3.3.2.1. Cytotoxicity in the Cho K1 and HepG2 cell lines	98

<b>TABLE OF CONTENTS (continued)</b>	<b>PAGE</b>
3.3.3. Reporter gene expression	101
3.3.3.1. Luciferase reporter gene analysis in the Cho K1 cell line	103
3.3.3.2. Luciferase reporter gene analysis in the HepG2 cell line	106
3.3.3.3. Competition Studies in the HepG2 Cell Line	110
3.3.3.4. Lipofectin <sup>®</sup> transfection in HepG2 cell line	112
3.3.3.5. GFP reporter gene analysis by Flow cytometry in the HepG2 cell line	114
 <b>CHAPTER FOUR:</b>	
<b>4. CONCLUSION</b>	124
<b>REFERENCES</b>	128
 <b>APPENDIX 1</b>	155
<b>APPENDIX 2</b>	157
<b>APPENDIX 3</b>	169
<b>APPENDIX 4</b>	171

## LIST OF TABLES

		PAGE
<b>Table 1.1</b>	Current and conventional cancer therapeutics (adapted from Dollinger <i>et al.</i> , 1997; McCrudden and McCarthy, 2013 and The International Agency for Research on Cancer, 3 February 2014).	2
<b>Table 1.2</b>	Available gene therapy vector systems and their associated advantages and disadvantages (adapted from Roth and Christiano, 1997; Lim, 1999, Mountain, 2000, , Coura and Nardi, 2008 and Katragadda <i>et al.</i> , 2010).	8
<b>Table 2.1</b>	The total lipid composition of the prepared cationic liposomes	56
<b>Table 2.2</b>	Liposome mass range tested for DNA binding. pCMV- <i>Luc</i> DNA was used at a constant amount of 0.5 µg in each lipoplex preparation.	62
<b>Table 2.3</b>	Varying liposome measurements tested for nuclease protection. DNA was constant at 1 µg and EGF used at 1 µg for all targeted formulations.	64
<b>Table 3.1</b>	The mean diameters of the various liposome suspensions examined. The data are presented as means, ±S.D. (n = 5).	75
<b>Table 3.2</b>	Sizes and Zeta potential of liposomes and lipoplexes.	83
<b>Table 3.3</b>	DNA : Liposome ratios for complete and optimal binding	87

## LIST OF FIGURES

	<b>PAGE</b>
<b>Figure 1.1</b> Nanoparticle design options and considerations for intracellular delivery.	10
<b>Figure 1.2</b> The basic structure and components of a liposomal vesicle	14
<b>Figure 1.3</b> Representation of the three basic components of a cationic lipid, using DOTMA as a structural example	16
<b>Figure 1.4</b> Schematic representation of the flip-flop mechanism favoured by cationic lipid based carriers systems for endosomal escape.	17
<b>Figure 1.5</b> Illustration of the different modes of endocytosis (within-cell).	18
<b>Figure 1.6</b> Barriers faced by cationic liposome mediated gene delivery carriers during hepatocellular delivery.	22
<b>Figure 1.7</b> Illustration of the configuration regimes for Polyethylene glycol / (PEG) polymer grafted onto the liposome surface.	26
<b>Figure 1.8</b> Crystal structure model of the inactive unbound epidermal growth factor receptor (EGFR) monomer, showing the clearly defined regions.	29
<b>Figure 1.9</b> Representation of the EGF motif with sulfhydryl bonds for the three disulphide bridges.	34
<b>Figure 1.10</b> Schematic illustration of EGFR ligand binding, activation and cellular signalling.	42

## LIST OF FIGURES (Continued)

<b>Figure. 1.11</b>	Cellular entry mechanisms favoured by the EGFR family.	47
<b>Figure 2.1</b>	Reaction scheme showing the preparation of the cationic cholesterol derivative Chol-T (T) from cholesteryl chloroformate (C) and 3-dimethylaminopropylamine.	54
<b>Figure 2.2</b>	Reaction scheme representing the preparation of the cationic cholesterol derivative, 3 $\beta$ [N(N',N',-dimethylaminopropylsuccinamidohydrazido)-carbamoyl] cholesterol (MS09)	55
<b>Figure 2.3</b>	A representative image of the DSPE-PEG molecule employed for liposomal synthesis, where n = 2000 for DSPE-PEG <sub>2000</sub> .	57
<b>Figure 2.4</b>	Illustration of the eight different liposome preparations analysed for hepatotropic efficiency.	57
<b>Figure 2.5</b>	Map of the pCMV- <i>luc</i> vector.	58
<b>Figure 2.6</b>	Lipoplex formation from the simple interaction of a liposome with DNA.	59
<b>Figure 2.7</b>	Reduction reaction of MTT by mitochondrial succinate dehydrogenase enzymes to the MTT-Formazan product.	67
<b>Figure 2.8</b>	Amino acid sequence of the Y-12 EGF competitor peptide.	69
<b>Figure 2.9</b>	Map of pCMV-GFP reporter vector.	70

## LIST OF FIGURES (Continued)

<b>Figure 3.1</b>	Transmission electron micrographs of Chol-T plain and stealth liposome, lipoplex and targeted formulations.	77
<b>Figure 3.2</b>	Transmission electron micrographs of MS09 plain and stealth liposome, lipoplex and targeted formulations.	78
<b>Figure 3.3</b>	Bar graph depiction of average mean diameter and population size deviations as determined from Cryo-TEM micrographs $\pm$ S.D. (n = 5).	79
<b>Figure 3.4</b>	Agarose retardation gels showing liposome – DNA binding of the different reaction mixtures tested.	86
<b>Figure 3.5</b>	Ethidium bromide intercalation assay for cationic liposomes in a total of 100 $\mu$ l incubation mixtures containing 1.2 $\mu$ g pCMV- <i>luc</i> DNA.	89
<b>Figure 3.6</b>	Standard curve of hEGF sample standards from 0 – 250 pg/ml.	91
<b>Figure 3.7</b>	Concentration of EGF present in each liposome formulation as determined from the linear regression equation of Figure 3.6 above.	92
<b>Figure 3.8</b>	Serum nuclease protection assay of the DNA-cationic liposome complexes containing a. Chol-T and MS09, b. Chol-T/EGF and MS09/EGF, c. Chol-T-Peg and MS09-Peg, and d. Chol-T-Peg/EGF and MS09-Peg/EGF, respectively.	94
<b>Figure 3.9</b>	Semi confluent distribution of a. CHO-K1, and b. HepG2 cells, as viewed under an Olympus inverted microscope (20x)	97

## LIST OF FIGURES (Continued)

- Figure 3.10** Growth inhibition studies of cationic liposome: pCMV-Luc DNA complexes to Cho K1 and HepG2 cells *in vitro*. DNA was kept constant at 1 µg. a. Chol-T, b. Chol-T/EGF , c. Chol-T-Peg , d. Chol-T-Peg/EGF 98
- Figure 3.11** Growth inhibition studies of cationic liposome: pCMV-Luc DNA complexes to CHO-K1 and HepG2 cells *in vitro*. DNA was kept constant at 1 µg. a. MS09, b. MS09/EGF, c. MS09-Peg, d. MS09-Peg/EGF 99
- Figure 3.12** The firefly luciferase reaction. 102
- Figure 3.13** Transfection studies of cationic liposome: pCMV-Luc DNA complexes to CHO-K1 cells *in vitro*. DNA was kept constant at 1 µg. a. Chol-T, b. Chol-T/EGF, c. Chol-T-Peg, d. Chol-T-Peg/EGF 103
- Figure 3.14** Transfection studies of cationic liposome: pCMV-Luc DNA complexes to CHO-K1 cells *in vitro*. DNA was kept constant at 1 µg. a. MS09, b. MS09/EGF, c. MS09-Peg, d. MS09-Peg/EGF 104
- Figure 3.15** Transfection studies of cationic liposome: pCMV-Luc DNA complexes to HepG2 cells *in vitro*. DNA was kept constant at 1 µg. a. Chol-T, b. Chol-T/EGF, c. Chol-T-Peg, d. Chol-T-Peg/EGF 106
- Figure 3.16** Transfection studies of cationic liposome: pCMV-Luc DNA complexes to HepG2 cells *in vitro*. DNA was kept constant at 1 µg. a. MS09, b. MS09/EGF, c. MS09-Peg, d. MS09-Peg/EGF 107

## LIST OF FIGURES (Continued)

- Figure 3.17** Transfection studies of targeted cationic liposome: pCMV-Luc DNA complexes to HepG2 cells *in vitro* in the presence of YI-12 peptide (0.5mM per well). DNA was kept constant at 1 µg. a. Chol-T-EGF, b. Chol-T-Peg, c. MS09-EGF, d. MS09-Peg/EGF 111
- Figure 3.18** Transfection studies commercial Lipofectin : pCMV-*luc* DNA complexes in HepG2 cells *in vitro*. DNA was kept constant at 1 µg. Lipofectin was introduced to DNA and HepG2 cells as per manufacturer protocol ratios of DNA to Lipofectin (<sup>w</sup>/<sub>w</sub>) 113
- Figure 3.19** Staggered overlay histograms illustrating the cytometric quantisation of GFP fluorescence produced by the varying liposomes at transfection optimal ratios 115
- Figure 3.20** Dot plot and histogram representations of GFP fluorescent intensity produced by the different liposome formulations against a positive and negative control within the HepG2 cell line. 120
- Figure 3.21** GFP fluorescence expressed as percentage produced per liposome as quantified by flow cytometry. 121

## LIST OF ABBREVIATIONS AND ALTERNATE NAMES

<b>Å</b>	Angstrom
<b>AA</b>	Arachidonic acid
<b>ABX-EGF/ Vectibx</b>	Panitumumab
<b>AIDS</b>	Acquired Immune Deficiency Syndrome
<b>AR</b>	Amphiregulin
<b>Arg</b>	Arginine
<b>AS-ODNS</b>	Antisense oligonucleotides
<b>Asp</b>	Aspartic acid
<b>ASPGR</b>	Asialoglycoprotein receptor
<b>BTC</b>	Betacellulin
<b>ChoK1</b>	Chinese hamster ovary cells
<b>Chol-T</b>	3 $\beta$ [N-(N',N'-dimethylaminopropane)-carbamoyl] cholesterol
<b>CME</b>	Clathrin mediated endocytosis
<b>Conmana</b>	Icotinib
<b>CR</b>	Cysteine rich regions
<b>Cripto 1</b>	Tetracarcinoma derived growth factor
<b>CSF-1</b>	Colony stimulating factor
<b>CvME</b>	Caveolin mediated endocytosis
<b>Cys</b>	Cysteines
<b>DCs</b>	Dendritic cells
<b>DC-Chol</b>	3 $\beta$ [N-(N', N'-dimethylaminoethane)-carbamoyl] cholesterol
<b>DCCI</b>	Dicyclohexylcarbodiimide
<b>DNA</b>	Deoxyribonucleic acid
<b>DOPE</b>	Dioleoylphosphatidylethanolamine
<b>DOTAP</b>	N-[1-(2,3-dioleoyloxy)propyl]-N,N,N-trimethylammonium chloride
<b>DOTMA</b>	N-[1-(2, 3-dioleoyloxy)propyl]-N,N,N-trimethylammonium chloride

## LIST OF ABBREVIATIONS (continued)

<b>DSPE-PEG<sub>2000</sub></b>	1,2-distearoyl- <i>sn</i> -glycero-phosphoethanolamine- <i>N</i> - [carboxy(polyethylene glycol)2000]
<b>EDTA</b>	Ethylenediaminetetraacetic acid
<b>EGF</b>	Epidermal growth factor
<b>EGFR</b>	Epidermal growth factor receptor
<b>EMD 72000</b>	Matuzumab
<b>EPN</b>	Epigen
<b>EPR</b>	Epiregulin
<b>EPR effect</b>	Enhanced permeability and retention effect
<b>erbB</b>	Erythroblastosis B
<b>ERK</b>	Extracellular signal regulated kinases
<b>FBS</b>	Foetal bovine serum
<b>Fc</b>	Fragment crystallisable
<b>FDA</b>	Food and Drug administration
<b>FPE</b>	Fluid phase endocytic mode
<b>Gln</b>	Glutamine
<b>Gly</b>	Glycine
<b>GW2016/Tykerb</b>	Lapatinib
<b>HCC</b>	Hepatocellular carcinoma
<b>HB-EGF</b>	Heparin-binding –EGF
<b>HBS</b>	HEPES buffered saline
<b>HEPES</b>	2-[4-(2-hydroxyethyl)-1-piperazinyl] ethanesulphonic acid
<b>HepG2</b>	Hepatocellular carcinoma cells
<b>hR-3/TheraCIM</b>	Nimotuzumab
<b>Ile</b>	Isoleucine
<b>IMC-C225/ Erbix<sup>TM</sup></b>	Cetuximab
<b>Iressa, ZD 1839</b>	Gefitinib
<b>KC</b>	Kupffer cells

## LIST OF ABBREVIATIONS (continued)

<b>Leu</b>	Leucine
<b>MABs</b>	Monoclonal antibodies
<b>MAPK</b>	Mitogen activated protein kinase
<b>miRNA</b>	Micro Ribonucleic acid
<b>MSO4</b>	Cholesterylformylhydrazide
<b>MSO8</b>	Cholesterylformylhydrazide hemisuccinate
<b>MSO9</b>	3 $\beta$ [N(N',N',-dimethylaminopropylsuccinamidohydrazido)- carbamoyl] cholesterol
<b>MTT</b>	3-(4,5-dimethylthiazol-2-yl)-2,5-diphenyltetrazolium bromide
<b>NGF</b>	Nerve growth factor
<b>NMR</b>	Nuclear magnetic resonance
<b>NPC</b>	Nuclear pore complex
<b>NRG</b>	Neuregulins
<b>NSCLC</b>	Non-small cell lung carcinoma
<b>NTA</b>	Nanoparticle tracking analysis
<b>ODNs</b>	Oligodeoxynucleotides
<b>PAA</b>	Polyaminoacid
<b>PA</b>	Phosphatidic acid
<b>PBS</b>	Phosphate buffered saline
<b>PDGFR</b>	Platelet derived growth factor receptor
<b>PEG</b>	Polyethylene glycol
<b>PEI</b>	Poly(ethyleneimine)
<b>PI3 K</b>	Phosphatidylinositol
<b>PLC-<math>\gamma</math>-1</b>	Phospholipase-C- $\gamma$ -1
<b>PLL</b>	Poly(L-lysine)
<b>PTB</b>	Phosphotyrosine binding
<b>RES</b>	Reticuloendothelial system
<b>RTK's</b>	Receptor tyrosine kinase
<b>SDS</b>	Sodium dodecyl sulphate

## LIST OF ABBREVIATIONS (continued)

<b>SH2</b>	Src homology
<b>shRNA</b>	Short hairpin Ribonucleic acid
<b>siRNA</b>	small interfering Ribonucleic acid
<b>STAT</b>	Signal Transducer and Activator of Transcription
<b>Tarceva/OSI-774</b>	Erlotinib
<b>TEM</b>	Transmission electron microscope
<b>TGF-<math>\alpha</math></b>	Transforming growth factor
<b>TKIs</b>	Tyrosine kinase inhibitors
<b>TLC</b>	Thin layer chromatography
<b>TMB</b>	Tetramethylbenzidine
<b>Tyr</b>	Tyrosine
<b>VEGFR</b>	Vascular endothelial factor receptor

## ACKNOWLEDGEMENTS

I wish to express my deepest gratitude to the following individuals and organisation(s):

- My supervisor, Dr. M. Singh, for her support, patience and invaluable guidance throughout this study.
- Professor M. Ariatti for his continued motivation and advice.
- Mr. Phillip Christopher of the Electron Microscope Unit (UKZN, Westville) for use of the transmission electron microscope, and consistent assistance with the cryo-preservation technique.
- The National Research Foundation (NRF) and the University of KwaZulu-Natal for the financial support that allowed completion of my studies.
- Dr. Kovashnee Naicker, the resident Post-doctoral student in the Non-viral gene therapy group, for her friendship and backing.
- Ms. Nicolisha Narainpersad for her support and assistance during this study, as well her friendship.
- Everyone in the Non-viral gene therapy group, for support and encouragement, and for always having a spare key on hand.
- To my parents (Mr. and Mrs. Sewbalas) and, thank you for the years of support, unconditional love and encouragement, throughout my studies.
- Novisha and Himlal Patel, my second parents and my darling nephews, Shiv and Yash Patel, for the love and motivation that kept me going.
- To Mr. Avish Dharamraj, who waited 13 years and then, just a bit more. Thank you for your love and understanding, and for allowing me to be myself.

THIS THESIS IS DEDICATED TO MY PARENTS,  
MR. AND MRS. SEWBALAS

## CHAPTER ONE

### 1. INTRODUCTION:

#### 1.1. Cancer Gene Therapy: Turning Convention Into Innovation

Thirteen million, that is the number of people worldwide expected to succumb to cancer over the next two decades. A staggering 70% of these cancer deaths occur in Africa, Asia, Central and South America, with one in four South Africans being personally affected by the disease. Globally the most common causes of cancer death are cancers of the lung (1.6 million, 19.4% of the total), liver (0.8 million, 9.1%), and stomach (0.7 million, 8.8%) (The International Agency for Research on Cancer, 3 February 2014). Knowledge is the key to a way forward. Through research many of the mysteries surrounding cancer and its many forms have been elucidated. We know much more today than we did two decades ago and with concerted effort in treatment development and prevention protocols, a change in statistics is possible.

Cancer therapy at present is made up of various treatment prospects as delineated by research and development over the years. Application of conventional cancer treatments such as those depicted in Table 1.1 is often insufficient against aggressive, resistant and invasive tumours possessing complex mechanisms of propagation. The limitation of traditional therapies makes alternate and hybrid treatment of cancer at the molecular level a promising venture (Morille *et al.*, 2008). Consequently new approaches are being sought with particular focus given to the investigation of genes involved in cancer development. Cancer develops from a multistep process involving numerous somatic gene alterations, many of which are not known, making correction of the abnormality or restoration of normal gene function difficult. Hence cancer was thought of as an incompatible target for classical gene therapy, but with the evolution of gene therapy together with the culmination of the Human Genome Project it has been touted as not only a viable, but an effective form of cancer therapy (Roth and Christiano, 1997; Lim, 1999; Rozema, 2008; Gascón *et al.*, 2013).

**Table 1.1.:** Current and conventional cancer therapeutics (adapted from Dollinger *et al.*, 1997; McCrudden and McCarthy, 2013 and The International Agency for Research on Cancer, 3 February 2014).

Therapy	Description	Side Effects and Pit-falls
<b>Chemotherapy</b>	Administration of cytotoxic drugs through; intravenous, muscular injection, oral or topical treatment. It may be used collaboratively as a: <b>Neo-adjuvant</b> , prior to treatment; <b>Adjuvant</b> , post treatment or as a <b>Palliative therapy</b> for symptomatic relief.	Nausea, vomiting, fatigue, appetite loss, hair loss, pain in mouth as well as infection and fever.
<b>Radiation therapy</b>	X-rays and high energy beams such as gamma rays, electron or proton beams are directed at the site of the tumour resulting in a reduction in size. This is termed external beam therapy. Brachytherapy or internal therapy involves the insertion of radioactive materials within or in the vicinity of the tumour.	Nausea, vomiting, appetite loss, changes in sense of taste as well as fatigue and tiredness
<b>Transplant therapy</b>	Blood and marrow transplantation (BMT) or hematopoietic cell transplantation (HCT) is characterized by the infusion of cells*, to restore the hematopoietic system of the patient. Used in 3 clinical scenarios: <b>Malignancy</b> treatment, Replacement or modulation of a system that is absent or functioning poorly, or <b>Genetic disorders</b> outlined by poor gene expression	Treatment intensity results in the pre-clinical state of the recipient associated with risk of transplant related mortality, as outlined by the Charlson co morbidity index.
<b>Surgery</b>	Considered an appropriate treatment, if the cancerous growth can be removed without affecting body function.	Hindered by procedural complications, duration, the patients' state of health and response to anaesthesia.
<b>Cryosurgery</b>	Use of liquid nitrogen or argon gas to remove or destroy abnormal tissue. Employed for external treatment (skin), as well as for internal tumours, through cold probe treatment accompanied by ultrasound or MRI monitoring. It is a less expensive technique with short recovery periods.	Few side effects have been noted. Some are: blisters, damage to nearby healthy tissue, scarring, ulcers, loss of sensation if nerves are affected.
<b>Laser therapy</b>	Laser light amplification by stimulated emission radiation is used to remove cancerous or pre-cancerous growths either externally or internally, lining internal organs. Reduced bleeding, normal tissue damage and risk of infection than associated with surgery.	Expensive and large equipment used. Transient effect of treatment sometimes necessitates the need for conventional surgery.
<b>Photodynamic therapy</b>	A drug called a photosensitiser is used in conjunction with light of a specific wavelength. Once exposed to light the photosensitisers produce an active form of oxygen that destroys nearby cells. Prolonged retention of the photosensitiser by cancer cells ensures tumour eradication.	Skin and eye sensitivity for up to 6 weeks post treatment. Burns, swelling and scarring to healthy tissue have been observed, but are minimal and temporary.
<b>Hyperthermia</b>	Also known as thermotherapy, involves the exposure of the body tissue to high temperatures of up to 45°C resulting in tumour reduction following damage to the protein and structures within. Used in together with Radiation and Chemotherapy.	Uncommon, however, diarrhoea, nausea and vomiting have been noted post whole body treatment.
<b>Hormone therapy</b>	Administration of drugs that block the effects of hormones on cancers deemed, hormone sensitive or dependent. The drug will act by either stopping hormone production or preventing further cancer growth.	Hormone and sex dependent but include: Tiredness, digestive problems, weight gain, memory problems and mood changes.
<b>Biological and Targeted therapy</b>	Treatment employing living organisms or synthetic variations for either exploitation of the immune systems' innate ability to detect and eradicate cancer cells or to directly target cancer cells. Examples used include: monoclonal antibodies, cytokines, adoptive T-cell transfer, therapeutic vaccines, and bacterium <i>bacillus</i> and <b>gene therapy</b> .	Treatment specific, however, reactions at the site of administration have been observed

Initially, gene therapy, considered a replacement therapy was applied to the treatment of inherited disorders such as adenosine deaminase deficiency (Candotti, *et al.*, 2012), cystic fibrosis (Burney, and Davies, 2012), Gaucher's disease (Goker-Alpan, 2010), familial hypercholesterolemia (Van Craeyveld, *et al.*, 2011), hemophilia (Skinner, 2013), and Duchenne muscular dystrophy (Chamberlain, 2002). Recently, it has been applied to the treatment of acquired diseases such as AIDS (Strayer, 2005), cancers (Cross, and Burmester, 2006), cardiovascular disease (Wolfram, and Donahue, 2013), arthritis (Robbins, *et al.*, 2003) and neuro-degenerative disorders (McMenamin, and Wood, 2010) such as Parkinson's and Alzheimer's disease. At the core, cancer gene therapy aims to effect treatment through exploitation of an included active compound or therapeutic information encoded in the DNA sequence. This has grown over the years to include, micro- (miRNA), short hairpin- (shRNA), small interfering RNAs (siRNA) and oligodeoxynucleotides (ODNs) (Lim, 1999; Nishikawa and Huang, 2001; Rozema, 2008). Moreover, the delivery of growth inhibitory or pro-apoptotic genes through a carrier system could retard the development of the cancerous growth (Mäkelä, 2008). Although this therapeutic potential of gene delivery has long been recognised, the need for safe, effective and cell specific delivery methods for exogenous genes still exists (Hasegawa *et al.*, 2002; McCrudden and McCarthy, 2013). The characteristics of these carriers or vehicles determines the efficiency and specificity of transfection and transduction, the duration of transgene expression and the host immune response to the vector. The vehicles employed for gene therapy are often classified as either biological or non-biological.

Viruses, having evolved over millions of years, are structurally and symmetrically highly complex and are considered natural vehicles for gene delivery. Viral based strategies require alterations to the intrinsic properties of the virus, with the therapeutic gene/s replacing a significant native gene/s. This produces a replication-defective particle or viral vector which is needed in efforts to regulate their safety, effectiveness and stability as vectors for human therapeutics. A general advantage associated with viral vector systems is that the transfection machinery enables the DNA to effectively access the cytosol, however, the several associated disadvantages (section 1.3, Table 1.2) have impelled research into non-viral gene therapy systems. These non-viral systems continue to be explored through physical carrier-free systems or chemical carrier-mediated systems. Cationic liposome mediated lipofection is one of the most

promising chemical carrier methods for transgene introduction into mammalian cells. This liposome based DNA delivery system involves the exploitation of ionic interactions which promote lipid-DNA complexes (Luo and Saltzman, 2000; Eming *et al.*, 2007; Mäkelä, 2008; Buñuales *et al.*, 2011).

In addition to vector development, a prominent challenge for cationic systems in particular, has been systemic tumour targeting. Several forms of cancer require systemic administration and therefore targeted cancer cell delivery. Cationic systems by nature undergo significant aggregation and degradation within the biological matrix owing to the existence of numerous negatively charged particles and defence mechanisms. Upon cellular internalization, cationic systems are faced with the additional intracellular hurdles of cytoplasmic trafficking, endosomal escape and nuclear entry which may easily reduce the efficiency of the gene therapy system (Morille *et al.*, 2008). Cancer cell targeting is achieved through exploitation of the structural features of the specific cell type. One such feature is the high expression of the specific receptors at the surface of different cancer cells (Mendelsohn, 2002). The HepG2 (human hepatocellular carcinoma) cell line is one such cell line found to overexpress the epidermal growth factor and asialoglycoprotein receptors (Buñuales *et al.*, 2011). The production of a multifunctional system composed of polyethylene glycol (PEG)-lipid, targeting ligand, nucleic peptide, fusogenic or endosomolytic peptides, could result in a sophisticated system capable of evading the many barriers to be faced. However, each of these inclusions has its own drawback, based on different results upon implementation and internalisation and interaction with other components present in the now complex system. With more research into different combinations of vector inclusions, this type of system could lead the way in cancer gene therapeutics.

## **1.2. Liver Cancer and Hepatocellular targeting**

Being a highly vascularised organ and contributing approximately 2.5% to the total human body weight, the liver is a clear target for gene therapy. This large internal organ of the body is essential for nutrient absorption, injury repair through the production of clotting factors, bile production as well as the filtration and removal of toxic waste products from the blood. The liver, having a central role in metabolism is susceptible to a vast number of inherited metabolic

diseases (Nguyen and Ferry, 2004). The progression of many of these diseases into the fibrotic stage results in a significant alteration of the liver parenchyma, vasculature and sinusoids (Jacobs *et al.*, 2012; Kamimura *et al.*, 2013).

The number of tumour types that originate in the liver is due to the divergent cell types that comprise it, viz. hepatocytes (liver parenchymal cells), Kupffer cells (KC) and sinusoidal epithelial cells. Hepatocytes which constitute the greatest proportion of the liver cells are considered important targets for gene directed therapies. The Kupffer and liver sinusoidal endothelial cells comprise the reticulo-endothelial cell system of the liver and a significant barrier to carrier mediated therapy (Nguyen and Ferry, 2004; Kamimura *et al.*, 2013). Gene therapy directed to the liver follows from early stage non-invasive *in vitro* investigations to *in vivo* involving systemic administration of the developed vectors, and to *ex vivo*, where isolated cells are genetically modified *in vitro* and transplanted into the original cellular donor (Chen and Li, 2012).

Future *in vivo* liver gene therapeutics is attractive as the hepatocytes present as easily accessible targets. Here the sinusoidal fenestrae are found clustered in sieve plates, providing a pathway to the microvilli of the protruding hepatocytes between the space of the Disse and the sinusoidal lumen. Fenestrae show a sieving action, by restricting gene delivery vectors directed to the hepatocytes on the basis of size. On average the fenestrae measure 100 – 200 nm in size, however, size divergence has been noted among various mammalian species (Jacobs *et al.*, 2010). Hence one factor considered in the design of an efficient vector system displaying potential hepatotropism, must be size so as to facilitate fenestrae mediated passage (Jacobs *et al.*, 2012; Kamimura *et al.*, 2013).

Based on point of origin, liver tumours may be classified as either primary - originating in the liver, or secondary. Secondary cancer or metastatic cancer is so termed as it originates elsewhere in the body and metastasizes to the liver. Two different types of primary liver cancer are known to exist. Hepatocellular carcinoma is the first type and bile duct cancer or cholangiocarcinoma is the second type, found commonly in women. In addition to these, primary liver diseases involving hepatocellular injury, genetic defects altering a specific hepatocellular function, form

additional candidates for liver gene therapy. Other potential targets for this type of therapy are the acquired hepatic diseases of viral hepatitis B and C (Jacobs *et al.*, 2012). Hepatocellular carcinoma (HCC) is one of the most predominant neoplasms the world over. This hepatoma arises from hepatocytes and despite being prevalent in the liver, may metastasize to other organs. It is commonly found in men and shows concomitant occurrence in liver cirrhosis patients.

For liver targeting, the point of delivery is of significance. Several earlier studies have shown that upon *in vivo* investigation, a number of liver directed liposomal systems were actually taken up by the Kupffer cells rather than the parenchymal liver cells (El Aneed, 2003). Although HepG2, Hep3B and HuH-7 cells may not directly reflect *in vitro* the tumour specific efficacy of targeting and distribution *in vivo*, they are however adequate, if not essential preliminary screening tools. They also serve as good examples of liver parenchymal cells, a primary target for most liver therapy. Cell surface characteristics also represent an important factor, as specific receptors on the cellular surface can serve as ports of entry that can be exploited for a desired therapeutic purpose. Receptor expression on hepatocellular carcinoma cells shows dependence on the differentiation status of the cells. The more highly differentiated the cells, the higher the hepatocyte specific gene levels for the receptors and vice versa. Due to recent advances, new targets for specific HCC treatment have been identified. The recent U.S. Food and Drug administration (FDA) approval of the multikinase inhibitor sorafenib that targets the vascular endothelial factor receptor (VEGFR), platelet derived growth factor receptor (PDGFR) and Raf, is one such example. Other associated targets of HCC have also been investigated for therapeutic effect. These include signaling by the epidermal growth factor receptor (EGFR) lectin EGF, telomerase and the cyclo-oxygenase (Chen and Li, 2012). The liver, therefore, serves as an important target for cancer therapy and the well differentiated hepatoma cells mentioned (e.g. HepG2) provide an effective tool for *in vitro* investigations. A positive outcome will move research toward *in vivo* clinical treatment trials and ultimately successful liver therapy (El Aneed, 2003; Fan and Wu, 2013).

### **1.3. Delivery Systems For Hepatotropic Gene Therapy**

Due to the many drawbacks associated with viral vector therapy and the numerous available cancer therapies suffering setbacks from unwanted and severe side effects, nanoparticle-based drug delivery systems are becoming a preferred research approach moving forward (Kaasgaard and Andresen, 2010). Direct gene transfer into mammalian cells without the use of viral systems is possible. The gene of interest may be incorporated into bacterial plasmid DNA together with a mammalian promoter, enhancer, and other sequences that elicit gene expression. This plasmid DNA can then be incorporated into lipid vesicles such as liposomes, complexed with proteins for tissue specific targeting, or complexed with polymers including poly(L-lysine) and polyethyleneimine. Besides these chemical methods of introducing the DNA into the mammalian cells for expression of the desired gene, many physical techniques have been applied and developed over the years as described in Table 1.2 (Rozema, 2008). Despite both these methods enabling effective and target specific delivery of genes with minimal toxicity, the chemical techniques are considered more desirable (Suda *et al.*, 2009).

**Table 1.2:** Available gene therapy vector systems and their associated advantages and disadvantages (adapted from Roth and Christiano, 1997; Lim, 1999, Mountain, 2000, , Coura and Nardi, 2008 and Katragadda *et al.*, 2010).

Vector system	Description	Advantages	Disadvantages
Viral Systems	Adenovirus	35Kb, Icosahedral, non-enveloped genome. High transfection efficiency and <i>ex vivo</i> integration Transfects many cell types High titre production	High immunogenicity Manipulation of large genome is difficult Transient gene expression
	Adeno-associated virus	5Kb, Icosahedral, non-enveloped, ssDNA genome. Wide array of cells infected <i>in vivo</i> Stable integration with prolonged expression Low immunogenicity	Capacity for transgene size limited Mutagenesis safety concerns
	Herpes simplex virus	Large 152Kb linear dsDNA genome Large capacity for foreign DNA Potential for prolonged gene expression due to latent nature	cytotoxicity
	Lentivirus	8Kb ssRNA genome Infection of quiescent and proliferative cells	Relatively low titre production Capacity for transgene size limited Insertional mutagenesis
	Retrovirus	10Kb heterodimer genome of linear positive sense ssRNA Low immunogenicity Chromosomal integration	Transfection of proliferative cells only Insertional mutagenesis Capacity for transgene size limited
Non-Viral Physical	Biobalistic	Projection of DNA coated micro-particles (gold and tungsten) by high pressure helium propellant for improved expression. High <i>in vitro</i> transfection	Poor tissue penetration Low <i>in vivo</i> expression
	Electroporation	DNA transfer occurs through the application of short electric pulses leading to transient pore formation. High levels of transgene expression	High titres of DNA required Tissue damage and inflammation
	Microinjection	Direct injection of the plasmid DNA into the target cell. Low titre of DNA required	Difficult technique with poor performance
	Naked DNA	Direct injection into target cells Broad applicability successful expression.via Hydrodynamic injection in mice	Nuclease degradation Translation to human model
	Ultrasound	Ultrasonic wave irradiation of tissue injected with DNA, allowing increased permeability for improved expression. Flexibility and safety valuable for clinical testing Successful <i>in vitro</i> and <i>in vivo</i>	Efficacy determined by frequency duration of treatment and quality of DNA introduced.
Non-Viral Chemical	Lipid	Anionic, cationic and neutral lipids are used for the production of lipoplexes with DNA, for gene delivery Ease of production and storage Low immunogenicity Broad applicability	Low <i>in vivo</i> expression of delivered gene Short period of expression
	Polymer	Natural and synthetic polymers form polyplexes with DNA, capable of cell directed gene transfer. Ease of production and storage Relatively non-pathogenic	Low <i>in vivo</i> expression Very short duration of expression
	Inorganic Nanoparticles	Nano-sized materials (gold, silica, quantum dots and carbon nanotubes) have shown direct gene delivery capability. Storage stability Low manufacturing cost Low immunogenicity	Dose related toxicity

### 1.3.1. Nanoparticle systems

Today there are a large number of non-viral vectors being employed. The potential surrounding the area of nanotechnology brings with it an anticipation of rapid and significant advancement in drug delivery, diagnostic analysis and production of enhanced biocompatible materials. The list of engineered vectors in this field has grown over the years, where the pioneers, such as cationic polymers and cationic lipids have led to more ‘highly engineered’ inorganic vectors. A basic requirement of all these particles is to compact, protect and transport the desired cargo, so as to realise many of the projected applications. A number of the earlier non-viral vectors do not completely comply with the broadly accepted definition of nanoparticles, which states that the particles should be at least one dimension below 100 nm. This fact has not, however, been found to impede the medical functionality of these materials, as their larger surface to mass ratio and carrier activity retain them as attractive nanoparticles. In fact the larger particle size may be required for sufficient loading of a drug or gene for therapeutic effect. Consequently nanomedicine may be considered as the science and technology of complex systems at the nanometer scale (10 – 1000 nm). Nanoparticle composition may vary as shown in Figure 1.1 below. Therapeutic drugs have been used as their own carrier with a number of source materials identified as biological or chemical (Cho, *et al.*, 2008, Katragadda, *et al.*, 2010, Chou, *et al.*, 2011, Guo and Huang, 2012).

Some carriers utilised thus far include, liposomes, cationic polymers, metallic nanoparticles (silver, gold and platinum), magnetic particles, quantum dots, silica nanoparticles, fullerenes, nanoshells, carbon nanotubes, lipid nanoparticles as well as supramolecular systems. The passive accumulation of nanoparticles of approximately 50 – 100 nm at tumour sites, is thought to occur due to the enhanced permeability and retention (EPR) effect, making them important tools in oncology. Moreover, they offer the option of malleability for functionalisation and active targeting to specific tumour cells. In this regard they also display the capability of acting as imaging agents. The best developed clinical imaging agents are the supraparamagnetic iron-oxide nanoparticles, which are coated with biocompatible materials, displaying magnetism only on exposure to an external magnetic field (Jong and Borm, 2008; Tang *et al.*, 2010; Guo and Huang, 2012; Rahman *et al.*, 2013).

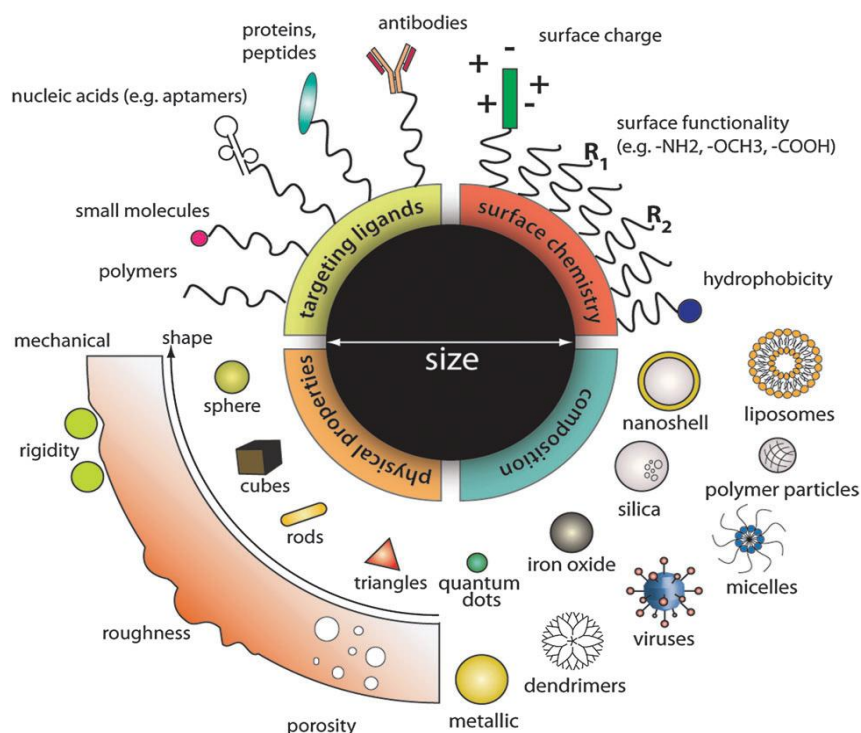


**Figure 1.1:** Nanoparticle design options and considerations for intracellular delivery. Design flexibility depicted allows for tailoring of nanoparticles for specific intracellular applications as contrast agents, drug delivery vehicles, and therapeutics (Chou *et al.*, 2010).

For delivery purposes, nanoparticle distribution is a major factor. Reports on lipid vesicles have shown that size and charge of nanoparticles were determining points of distribution. Liver uptake by these vesicles has been reported as moderate for smaller sizes and improved for sizes above 100 nm, which are terminated by clearance through the mononuclear phagocyte system. At below 100 nm, lipid vesicles displayed predominantly charge dependent distribution. As mentioned nanoparticle compositions vary, and factors such as size and shape may play more pivotal roles for other particle systems (Jong and Borm, 2008).

Silver and gold nanoparticles demonstrate broad commercial and medical application owing to their relative ease of preparation and functionalisation. Gold nanoshells, more recently, are exemplified by the flexibility and versatility of nanotechnology systems. They are described as concentric spheres comprising a dielectric core (typically silica, or gold sulphide) and a metal

(gold) shell. These nanoshells, like gold nanoparticles play a role in drug delivery with additional application in photo therapy as imaging contrast agents and in immunoassays. These nanoparticle-mediated delivery possibilities, briefly discussed here, present an optimistic potential for other combined conventional and gene therapy approaches (Katragadda *et al.*, 2010).

While the charge of the nanoparticle plays a significant role in determining biodistribution, higher surface charges appear to increase interaction with plasma proteins having isoelectric points below 5.5. Nanoparticles composed of cationic lipids have been reported to partake in significant plasma protein interaction. Knowledge of the interaction of the nanocarrier systems with biological systems is an imperative and ever continuing aspect of nanotechnology research. It is however known that upon entry of the nanoparticle into the blood system, a competition takes place not only between the proteins (opsonins) present, but also with the available lipids. Based on this, it has become accepted that nanoparticles in this environment will have their surface covered, at first by the most highly abundant proteins and later by the most high affinity proteins making up what is termed the protein corona. This corona composition depends on that of the nanoparticle and causes a change in the identity of the nanocarrier and how it is interpreted by the cells. The corona can be divided into a hard corona that directly interacts with the nanocarrier surface or a soft corona that shows weaker interaction with proteins of the hard corona and biological molecules present in the surrounding plasma (Rahman *et al.*, 2013). While this alteration of nanoparticle identity within this environment can potentially mask any predetermined or desired effect, studies on supraparamagnetic iron-oxide nanoparticles however showed little change in circulation time in the plasma. This intimates that the corona may not completely block the nanoparticle surface or functional groups. Understanding that corona composition varies and is unique to a particular nano-system, makes them important points of consideration for specific, timeous delivery of therapeutic material (Tang *et al.*, 2010; Rahman *et al.*, 2013). Due to the human health and safety risks associated, tighter regulation of nanoparticles have been proposed for nanomedicine, as these new and innovative nano-frontiers are investigated.

### 1.3.2. Polymer systems

Natural and synthetic polymeric delivery systems are popular and are commonly employed nano-scale vector systems (Li and Huang, 2000). There are two essential types of cationic polymers employed in nucleic acid delivery:

- Natural polymers, eg. chitosan and atelocollagen and
- Synthetic polymers, eg. poly(L-lysine) (PLL), poly(ethyleneimine) (PEI) and dendrimers.

In general the natural polymers are non-toxic and display mucoadhesive, biocompatibility and biodegradability in contrast to synthetic polymers which provide flexibility and the ability to be tailored to fit the size and topology of the plasmid DNA (Kawakami *et al.*, 2008). The polymers condense DNA upon binding, producing polymeric electrolyte complexes or polyplexes. The DNA is bound through electrostatic interaction and can be found entrapped within a polymeric matrix, adsorbed, or conjugated to the surface of the cationic polymer. The net positive charge produced by these complexes assists in cell attachment, internalisation and endosomal escape. A vast array of structurally divergent polymer systems have been evaluated, ranging from linear polymers (chitosan and polyethyleneimine), branched polymers (polyethyleneimine), circle-like polymers (cyclodextrin), network or cross-linked polymers (cross-linked polyaminoacid, PAA and dendrimers), cationic proteins (protamine and histones) and poly-L-lysine (PLL) (Zhu and Mahato, 2010). The effectiveness of DNA condensation and toxicity of cellular transfection produced, has been shown to be significantly divergent based on polymer architecture (Parker *et al.*, 2003; Pathak *et al.*, 2009; Gascón *et al.*, 2013).

PEI occurs either as a branched or linear polymer of varying chain lengths, with the capacity for increased transgene expression in a range of cell lines. Upon entry into the endocytic pathway, PEI-DNA complexes experience destabilisation resulting from a decrease in the environmental pH from neutral to pH 5.0. The high level of transfection efficiency produced is believed to result from an endosomal buffering capacity (Chen *et al.*, 2007). The 'proton sponge' hypothesis has been proffered as the underlying mechanism of release. However, research has shown that the addition of endosomolytic or lysosomotropic agents tend to enhance transfection activity.

Endosomal disruption may thus be attributed to a physical swelling, owing to PEI protonation and expansion of the polymer structure (Parker *et al.*, 2003; Gascón *et al.*, 2013). The cationic nature of PEI polyplexes leads to opsonisation susceptibility, higher than that seen with other polymers. PLL was the first polymer employed for gene transfer and up until the past decade was one of the most utilized. Although these cationic polymers enter the cell via the same mechanism as PEI polyplexes their transfection efficiency is not comparable, as they require co-application of lysosomotropic agents or some form of chemical alteration (Morille *et al.*, 2008). Dendrimers are highly branched, spherical polymers of which the most commonly used are the polyamines or polyamides. At their surface, they possess primary amines which are involved in DNA binding and compaction, promoting cellular uptake, while the tertiary amines act as proton sponges within, enabling endosomolysis. Due to associated toxicity with currently favoured systems, more biodegradable polymers are being designed and studied. The most successful thus far are the class of aminoesters, where the intrinsic ester bond is believed to undergo time-based destabilisation, resulting in an overall reduction in toxicity. The properties of size, modifiable surface functionality, multivalency, water solubility, and interaction capability of the available polymers makes them attractive for drug delivery (Parker *et al.*, 2003; Cho *et al.*, 2008; Gascón *et al.*, 2013).

### **1.3.3. Lipid systems**

Synthetic, spherical, self assembling structures comprising single or multiple lipid bilayers with an aqueous phase inclusion, is a broad definition for liposomes (Figure 1.2). These colloidal drug delivery systems resemble biological membranes and were thus initially investigated as model membrane systems. Initial identification as ‘Banghasomes’ following published description as swollen phospholipid bilayers by Bangham and co workers (1965), the name was later changed to ‘liposomes’. (Torchilin *et al.*, 2005). This re-terminology was accompanied by a number of applications, such as, use as drug and gene delivery systems for cancer therapy, vaccines, imaging agents, cosmetics and cosmeceuticals (MacLachlan, 2007; Cevher *et al.*, 2012; Allen and Cullis, 2013).

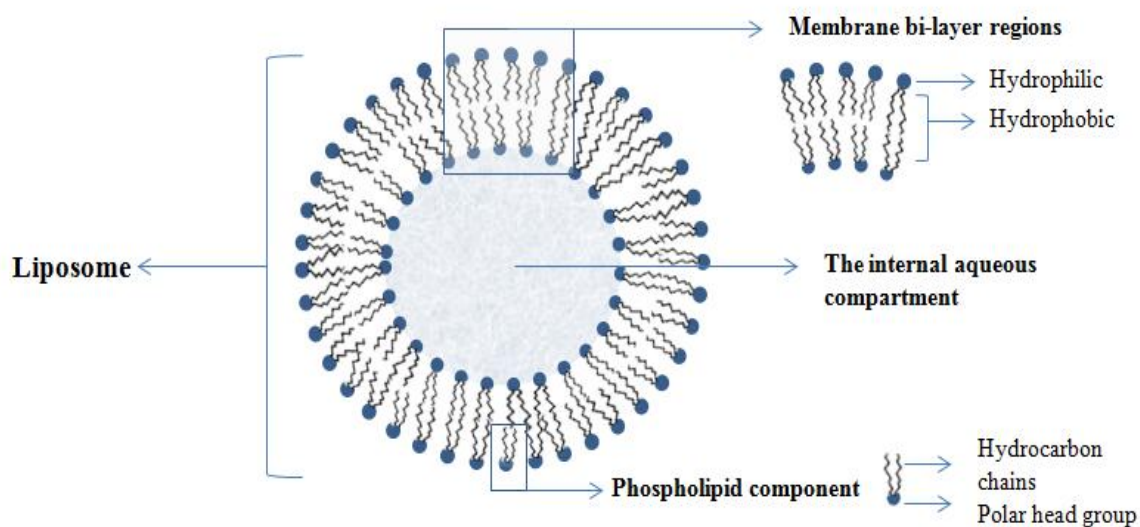


**Figure 1.2:** The basic structure and components of a liposomal vesicle. Figure not drawn to scale.

Liposomes are categorised according to their size, lamellarity (unilamellar and multilamellar vesicles) as well as preparation method. While unilamellar vesicles possess a single bilayer with a diameter in the 50 – 250 nm range, multilamellar vesicles present several concentric lipid bilayers and are generally larger in diameter (1 – 5  $\mu\text{m}$ ) (Felgner *et al.*, 1994). In addition to this classification, the functionality of the liposome is composition dependent, where its lipid make up determines its efficiency (Niidome and Huang, 2002; Katragadda *et al.*, 2010) .

Initially, the naturally occurring neutral lipids were employed for the delivery of high molecular weight DNA. This system involved encapsulation of the DNA , or low molecular weight oligo- and poly-nucleotides, while the development of cationic lipids for lipid mediated transfection favoured a ‘lipoplex’ or ‘oligoplex’ adsorption system. More recently, multiple lipid formulated systems have allowed for a more advanced lipofection system, where each lipid present offers a particular attribute for improved liposome functionality and efficient delivery. Cationic liposomes were first successfully transfected *in vitro* by Felgner and colleagues (1987) using the cationic lipid N-[1-(2, 3-dioleoyloxy)propyl]-N,N,N-trimethylammonium chloride (DOTMA). Since then a vast array of cationic lipids or cytofectins including cationic derivatives of cholesterol and diacylglycerol, quaternary ammonium detergents, and polyamine lipid

derivatives have been developed and evaluated for delivery of nucleic acids in cell culture, animal models and clinical trials. The term cytofectin is used in reference to positively charged lipid molecules that have the ability to promote the functional entry of macromolecules, polynucleotides as well as small molecules into dividing cells while being able to minimise degradation by the lysosome (Felgner *et al.*, 1994, Niidome and Huang, 2002).

Cationic lipids used in gene therapy are composed of four regions, the hydrophilic cationic head group, a spacer arm, linker bond and a hydrophobic domain or anchor. Three of these domains with variations in their chemical make up are depicted in Figure 1.3. Of the categorisation options for the polar head group, the tertiary amine and quaternary ammonium conformations have been most popular. The positive charge offered by the headgroup allows the liposome to bind with the negatively charged nucleic acid and provides the lipoplex with an overall positive charge for interaction with the anionic cell surface molecules. The spacer arm has been reported to affect transfection by the liposomal system, with longer spacers seemingly able to produce a better display of the cationic component of the liposome, thereby allowing for improved transfection or entry into the cell (Singh and Ariatti, 2006). In a similar manner, the linker component affects transfection, stability, biodegradability and associated toxicity of the cytofectin. DOTMA produces high efficiency transfection via its ether bond, however, associated stability and non-biodegradability couple this with levels of cytotoxicity. In contrast, N-[1-(2,3-dioleoyloxy)propyl]-N,N,N-trimethylammonium chloride (DOTAP) presents an ester bond that makes it more biodegradable and less cytotoxic. DC-Chol ( $3\beta$  [N-(N', N'-dimethylaminoethane)-carbamoyl] cholesterol), the first lipid used in clinical trials, comprises a carbamate linker, producing a trio of properties that make it an efficient gene delivery vector that is stable and low in cytotoxicity (Niidome and Huang, 2002, Zhao *et al.*, 2011).

Finally the hydrophobic domain of the cytofectin determines the fluidity of the bilayer, phase transition temperature, stability and toxicity of the liposome as well as the protection and release of the nucleic acid. These hydrophobic anchors comprise primarily aliphatic chains that are linear (saturated or mono-unsaturated) and a steroid domain. The single and tri-chained cationic lipids are more popular surfactants as they form micelles in solution, but are less efficient and more toxic when compared to the two-tailed DOTAP. Due to biodegradability, rigidity and

fusion activity, cholesterol is a frequently utilised alternative to aliphatic chains. The use of cholesterol containing liposomes has shown increased membrane fusion producing effective *in vivo* and *in vitro* transfection of hepatic and intra-tumoural cells (MacLachlan, 2007; Katragadda *et al.*, 2010; Zhao *et al.*, 2011; Cevher *et al.*, 2012).

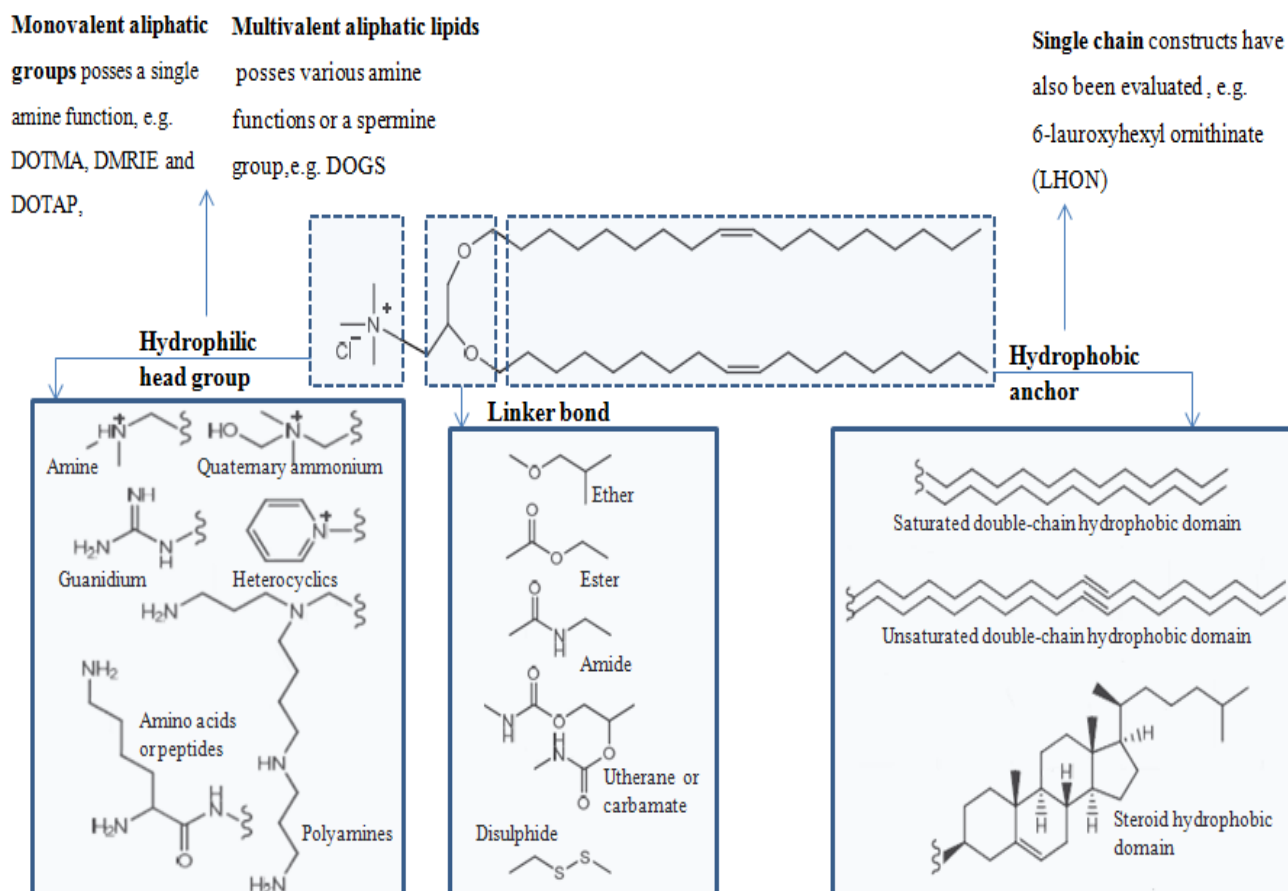


**Figure 1.3:** Representation of the three basic components of a cationic lipid, using DOTMA as a structural example (Adapted from Tang and Hughes, 1999 and Zhao *et al.*, 2011).

A problem associated with cationic systems has been its limited presence in target tissues coupled with rapid removal from the blood. Comparatively, good biodistribution with moderate internalisation has been identified for conventional liposomes displaying neutral charge. This indicates that multifunctional liposomes may prove a potential system for more effective transfection. While many cytofectins have displayed varying levels of fusogenic activity, efficient delivery is believed to require helper lipids such as dioleoylphosphatidylethanolamine

(DOPE) to improve intracellular delivery of the cargo material. The offered fusion with the target cells may take place at the plasma membrane, endosome or nuclear envelope. An important aspect for consideration is the positioning of the nucleic acid at the surface of the liposome rather than encapsulation. Here the nucleic acid is attached to the outer surface of the plasma membrane. DOPE is known to promote destabilisation of the lipid and membrane fusion, by adopting the reverse hexagonal  $H_{II}$  phase, through a flip-flop mechanism as illustrated in Figure 1.4. When the liposomes are found bound to the nucleic acid, it is in a multilamellar structure  $L^C_\alpha$  or appear as beads on a string (Felgner and Ringold, 1989; Koltover, 1998). Several studies have revealed that based on the zwitterionic lipid component, varying levels of nucleic acid interaction could be produced, thus resulting in altered lipoplex morphology. Helper lipids promote transition from the lamellar lipoplex phase to the inverted hexagonal phase for improved efficiency (MacLachlan, 2007; Katragadda *et al.*, 2010; Zhao *et al.*, 2011).

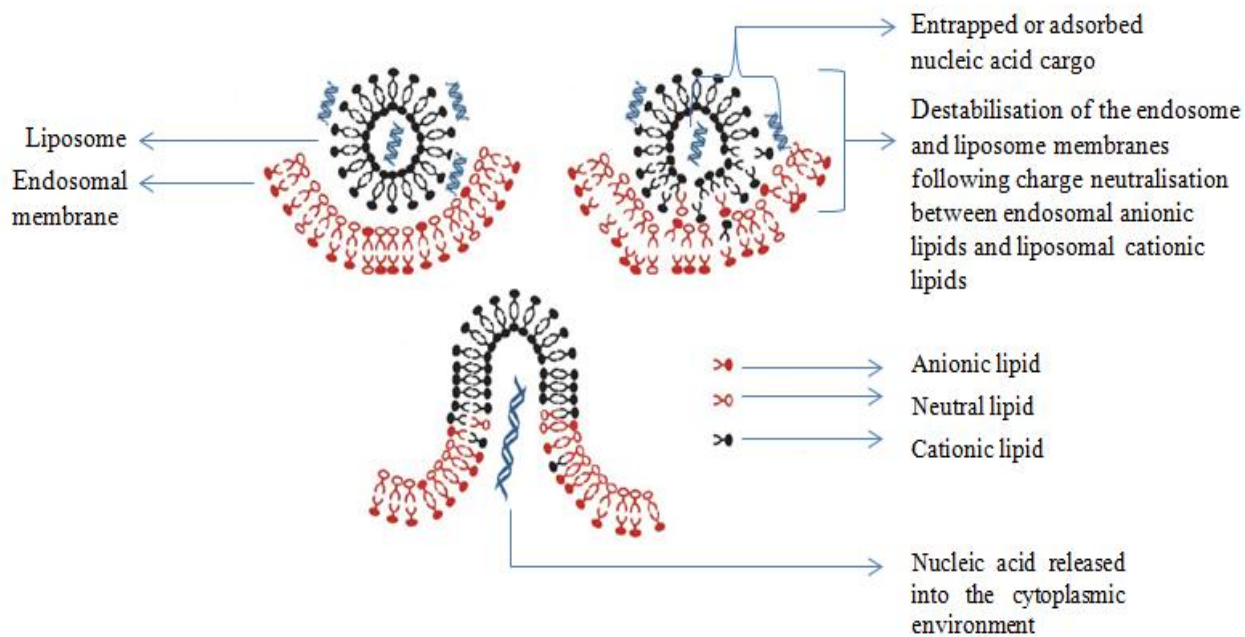


**Figure 1.4:** Schematic representation of the flip-flop mechanism favoured by cationic lipid based carriers systems for endosomal escape. The electrostatic interactions between membrane lipids, anionic and zwitterionic (endosome) and cationic (liposomes) and the formation of charge neutralised ion-pairs, allows for entry of the nucleic acid into the cytoplasm (adapted from Liang and Lam, 2012).

## 1.4. Barriers And Modifications : How Non-Viral Systems Meet and Beat The Odds

### 1.4.1. Internalisation and intracellular trafficking

Successful gene therapy shows a significant requirement for effective delivery and availability of the therapeutic agent at the intracellular target site of action. Knowledge of the favoured mechanisms of cellular uptake and the intracellular environment allows for the development of safe and effective carrier systems for delivery purposes (Gascón *et al.*, 2013; Xiang and Zhang, 2013). Moreover, efficiencies of pre-existing systems can be functionalised for active targeting to specific cell types. Peptides, proteins, carbohydrates, and others have been tested for vector functionalisation (Gascón *et al.*, 2013).

The pathways elucidated for cellular internalisation are considered as part of either an endocytic or non-endocytic mechanism. The primary method of entry has been proposed to be endocytosis. This endocytic group shows further distinction into phagocytic and non-phagocytic pathways (Figure 1.5.).

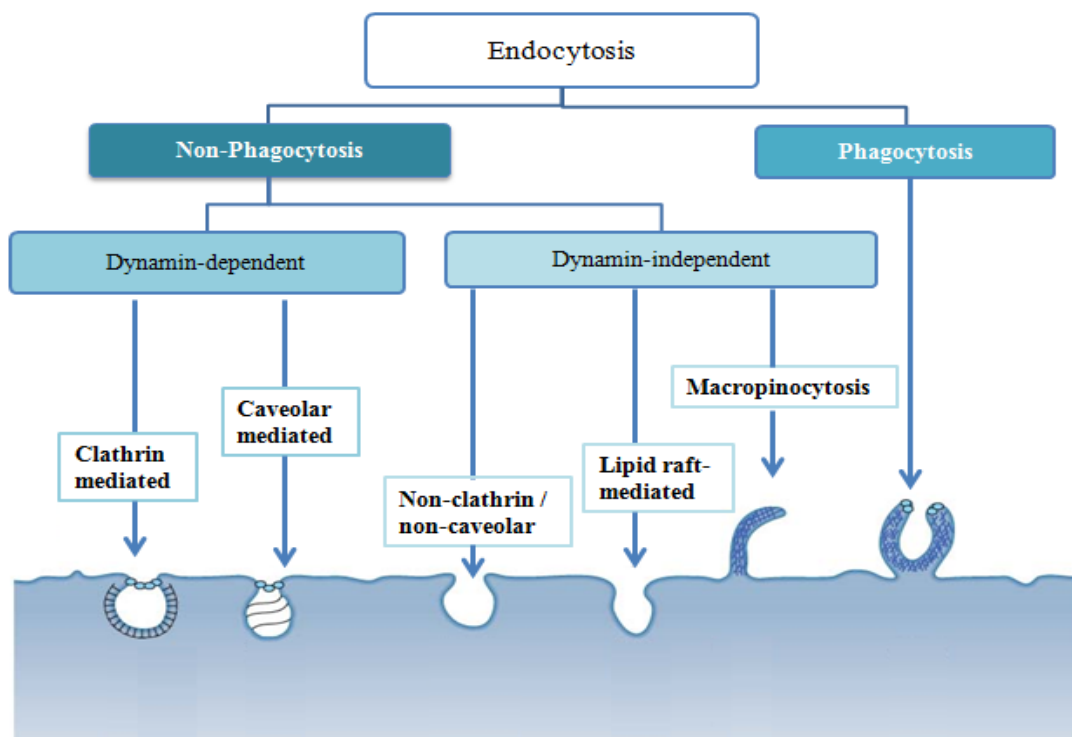


**Figure 1.5:** Illustration of the different modes of endo-cytosis (within-cell) (adapted from Mercer and Helenius, 2009).

#### **1.4.1.1. Phagocytosis**

This type of endocytic pathway has been established as the primary method of internalisation of specialised cells. The so called ‘professional phagocytes’ such as macrophages, dendritic cells (DCs), monocytes and neutrophils, adopt this mechanism in an effort to remove large pathogens and debris from the extracellular environment (Bhattarai *et al.*, 2010). This process can be stimulated by receptors such as fragment crystallisable (Fc) receptors, complement receptors, as well as mannose receptors. During opsonic phagocytosis, complexes are tagged by opsonins in the blood stream, which are recognised by the receptors, enabling binding. The mechanism of phagocytosis involves cup-like membrane conformations larger than 1  $\mu\text{m}$  which allow internalisation of the larger molecules (Belting *et al.*, 2005). Rho-family GTPases activate actin assembly and cell surface extension that closes around the complexes, engulfing them. Following phagosome trafficking, the engulfed materials reach the mature phagolysosome, where degradation occurs. Lipoplexes and polyplexes too large for traditional vector uptake through clathrin mediated endocytosis have been reported to undergo a phagocytic-like entry mechanism (Basarkar and Singh, 2007; Gascón *et al.*, 2013; Xiang and Zhang, 2013).

#### **1.4.1.2. Macropinocytosis**

Unlike the specific target cell nature of phagocytosis, this signal driven mechanism normally takes place when the membrane of cancer cells or macrophages is stimulated in response to the epidermal and platelet derived growth factors, or the colony stimulating factor (CSF-1). Vast quantities of fluid phase components are understood to be internalised non-specifically through the fluid phase endocytic mode (FPE). In a process reminiscent of phagocytic invagination, macropinocytosis is mediated by the actin derived formation of membrane protrusions. However, these protrusions do not completely encase the contents, but rather fuse with the plasma membrane following collapse onto the cell surface (Belting *et al.*, 2005). While the ultimate relationship of this mechanism with the lysosome is not clearly defined, the inherently leaky nature of macropinosomes, having no coat structures could prove to be advantageous in circumventing degradation (Khalil *et al.*, 2006; Xiang and Zhang, 2013).

#### **1.4.1.3. Clathrin mediated endocytosis (CME)**

This is well established as the major endocytic pathway of eukaryotic cells as evidenced by the considerable and intense characterisation investigations undertaken over the years. Consequently its numerous roles have been revealed, some of which include, nutrient uptake, internalisation, of the receptor-ligand complex for signal modulation and regulation. Uptake of the low-density lipoprotein and transferrin through cognate receptor recognition, are two of the most studied examples of this mechanism. During this process the receptor complexes are taken up by the clathrin coated pits, which develop into cage-like structures that ultimately bud off under GTPase dynamin action, forming the clathrin coated vesicles. These vesicles traffick the internalised components to the fate determining endosomes (Belting *et al.*, 2005; Xiang and Zhang, 2013).

#### **1.4.1.4. Caveolin mediated endocytosis (CvME)**

Caveolar endocytosis is found to occur in a large majority of cell types, but more commonly in the monolayer of endothelial cells lining the vessel walls, skeletal muscle cells and adipocytes. Caveolae are the flask shaped initiating structures of this pathway that display a diameter range of 5 - 100 nm with a neck of 10 – 50 nm. The smooth membrane invagination is rich in cholesterol and sphingolipid, and is defined by the presence of caveolin proteins. The fission produced caveosome is believed to circumvent lysosomal degradation through component or cargo delivery into the golgi and/or endoplasmic reticulum. This pathway is receptor mediated and highly dependent on cholesterol and dynamin to bring about its effect. Following almost identical pathway requirements and destination, lipid rafts, in the absence of caveolae have been united in a pathway termed caveolae/raft dependent endocytosis. This association has been postulated as a potential mode of clathrin independent endocytic regulation as driven by signaling events (Belting *et al.*, 2005; Chou *et al.*, 2011; Xiang and Zhang, 2013).

#### 1.4.1.5. Barriers to Carrier delivery

Delivery of a carrier system for the production of therapeutic effect, is one of the most important and difficult challenges for therapeutic administration. One of the first barriers to the delivery of the carrier and its cargo is the plasma membrane. Delivery vehicles must traverse this barrier for cellular internalisation, either by direct receptor interaction or indirect lipid bilayer association. Control of this mechanism of entry is of great importance, as it allows for the regulated control of the intracellular fate and consequent biological response to the vector (Parker *et al.*, 2003; Chou *et al.*, 2011; Zhang *et al.*, 2012).

The plasma membrane separates the intracellular and extracellular environments which present additional barriers, namely, proteases and nucleases, extreme pH as well as immunological and scavenger systems (Belting *et al.*, 2005). The rate of diffusion across this phospholipid barrier has shown dependency on the size, charge and hydrophobicity of the compound attempting internalisation. With many molecules unable to negotiate this barrier unassisted, successful transfection must take place via the carrier-molecule system. Conformation of this system to the following outlined criteria is thus essential:

- I. Binding and condensation of the therapeutic molecule (e.g. nucleic acid)
- II. Cargo protection from enzymatic degradation
- III. Enhanced cellular uptake of the therapeutic agent
- IV. Cytoplasmic release of contents with minimal endosomal degradation
- V. Assist with nuclear translocation to facilitate improved expression and effect

Most carrier systems possess a positive charge to aid in uptake by means of the negatively charged cell surface, a factor which also promotes non-target cell interactions and consequently reticuloendothelial system (RES) recognition. Figure 1.6 details the numerous obstacles faced by the carrier system. Recognition of this system stems from binding of these nanoparticulate systems with plasma proteins in the extracellular matrix, leading to accumulation within the RES organs (liver, spleen and bone marrow) with little therapeutic effect at the tumour site (Parker *et al.*, 2003).

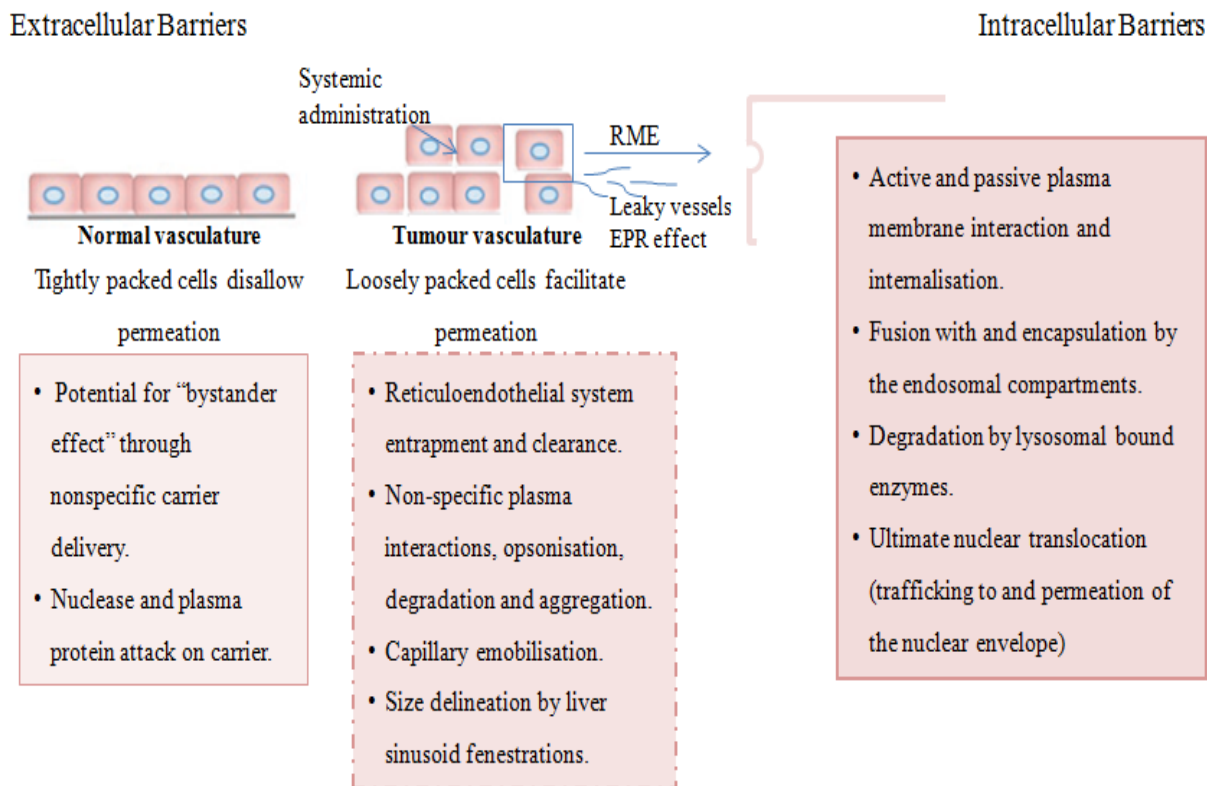


**Figure 1.6:** Barriers faced by cationic liposome mediated gene delivery carriers during hepatocellular delivery (adapted from Pathak *et al.*, 2009; Zhang *et al.*, 2012; and McCrudden and McCarthy., 2013).

The endosomal compartments pose another hurdle to successful transfection, as they limit cytosolic access and subsequent nuclear entry. Endosomal escape thus presents an alluring if not essential property for efficient transfection by the vector complex. Knowledge of the pH reduction from neutral to 6 in the early endosomes, 5 to 6 in the late endosomes and finally an approximate pH of 4.5 in lysosomes, offers an opportunity for effective design of delivery vectors for early release of contents, in an effort to avoid degradation (Khalil *et al.*, 2006; Liang and Lam, 2012). Numerous possibilities have been put forward and examined by a number of research groups as modes of escape. For carrier systems employing cationic polymers containing protonatable secondary and tertiary amine groups with pKa values correlating to the endosomal/lysosomal pH, the proton sponge hypothesis has been proffered (Xu and Skoka Jr, 1996). As previously mentioned the cationic lipid systems favour the flip-flop mechanism of escape. Use of cell penetrating peptides (TAT, GALA) as non-viral carriers have also shown

potential. The presence of zwitterionic helper lipid DOPE, adds further capacity for endosomal release. Its endosomolytic activity assists in endosomal membrane destabilisation, thought to be attributed to the cone shaped ethanolamine headgroup favouring the formation of an inverted hexagonal phase at acidic pH (Khalil *et al.*, 2006; Liang and Lam, 2012; Zhang *et al.*, 2012).

Upon cytoplasmic release the therapeutic molecules must then face the distinct chemical composition of the cytosolic 'soup' of macromolecules, cytoskeletal structures and an inherent defence mechanism. Microinjection of DNA has a reported half-life of approximately 90 min, undergoing nuclease degradation in the cytosol (Lechardeur *et al.*, 1999).

Whilst antisense oligonucleotide delivery has its ultimate delivery to the cytoplasm, presence of nucleic acid in this environment must result in nuclear translocation. Migration across the nuclear envelope presents a final impediment for the travelling nucleic acid (Khalil *et al.*, 2006). Nuclear pores display a passive transport limit of 70 KDa or an estimated 10 nm in diameter, much smaller than plasmid DNA. Two mechanisms have been elicited for transport across the nuclear membrane. The first involves mitotic membrane disruption, and the second relies on the nuclear pore complex (NPC). The NPC is a 125 MDa complex containing up to 50 nuclear pore proteins collectively known as nucleoporins. These complexes allow transportation of proteins, RNAs and ribonucleoprotein particles across the membrane and requires nuclear localisation and export signals to mediate this bidirectional membrane shuttling (Liang and Lam, 2012). Many nuclear localisation signal peptides have been developed for active nuclear import. Protamine is one such example, showing good capability for nuclear localisation despite poor effectivity as a gene delivery vector (Belting *et al.*, 2005; Zhang *et al.*, 2012; Gascón *et al.*, 2013, Xiang and Zhang, 2013).

Knowledge of the intimate details of the mechanistic barriers that cellular systems pose, allows for the improved design and strategic implementation of vector systems with the ultimate aim of producing the desired therapeutic effect.

## 1.4.2. Surface modifications to liposomal systems

### 1.4.2.1. Stealth liposomes

To meet the aims of enhanced target cell delivery and uptake with reduced ‘bystander effect’, long-surviving and cell specific vesicles must be engineered. Innovation of nanocarriers is essential to overcome the problems faced by carrier systems in an attempt to reach their desired site of action. For liver targeting, the translation of effectiveness from the *in vitro* to a biological system is often hampered by rapid clearance by the mononuclear phagocytic system. Another associated issue, discussed earlier, surrounds the inevitable protein corona that diminishes the effectiveness of the liposome complex upon entry into blood plasma (Immordino *et al.*, 2006; Milla *et al.*, 2012; Rahman *et al.*, 2013).

While many innovative colloidal systems, nanoparticles and other carriers offer some form of protection to the therapeutic cargo, the abovementioned issues still persist. The most promising approach identified thus far, requires modification of the carrier surface (Milla *et al.*, 2012). The modification of the liposomal surface with a hydrophilic polymer or glycolipid has been extensively investigated for prolonged circulation. Of these, polyethylene glycol (PEG) has proven to be the most effective for enhancing drug/gene delivery *in vivo*. The linking of one or more polyethylene glycol molecules to the carrier surface, is a technique termed PEGylation (Immordino *et al.*, 2006; Guo and Huang, 2012; Yang, 2013; Rahman *et al.*, 2013). The use of this technique was shown in the early 1990’s to improve circulation times of otherwise opsonised non-PEG liposomes upon intravenous administration (Hatakeyama *et al.*, 2013).

The average diameter of these long-circulating liposomes is known to be between 100 – 200 nm, allowing valuable accumulation at the tumour site via passive targeting. These liposomes are thus capable of taking advantage of the tumour vasculature via the EPR effect (Podesta and Kostarelos, 2009). Moreover, their ability to avoid recognition by the host immune response makes the term ‘stealth’ liposomes a very apt choice (Torchilin *et al.*, 2005; Romberg *et al.*, 2007; Franzen *et al.*, 2011; Hatakeyama *et al.*, 2013). Basically, the polyethylene glycol hydrophilic polymers possess a flexible chain that is known to occupy the peri-liposomal layer, i.e. the space that is directly adjacent to the liposome surface. The resulting sheath prevents

opsonisation by plasma proteins and consequently interactions with the macrophages of the mononuclear phagocytic system (Immordino *et al.*, 2006; Gao *et al.*, 2007; Guo and Huang, 2012).

According to deGennes (1980), the behaviour of the PEGylated liposome is dependent on the specific PEG properties at the surface. Earlier studies have proposed that the graft density and molecular mass of the polymer determine the degree of surface coverage and distance between graft sites as can be seen in Figure 1.7. The two primary chain conformations are the brush and mushroom. The low density PEG coverage favours the mushroom conformation or a thin PEG layer. This occurs as the larger molecular weight PEG, allows fewer copy numbers of the PEG graft to be loaded on the liposome surface, resulting in this mushroom structure. These PEG conformations are based on the Flory radius of the PEG graft, where the radius is directly proportional to the length of one PEG monomer ( $\approx 3.5\text{\AA}$ ) and the number of PEG monomers (molecular weight of one ethylene glycol monomer = molecular weight of the polyethylene glycol/44). The brush conformation appears as a thick PEG layer, where the distance between each monomer (PEG graft) decreases at a higher density to that of the Flory radius (Perry *et al.*, 2012). The amount of grafted PEG, molecular weight or length are major contributing factors to the circulation lifetime as well as the membrane lifetime of the PEG coated stealth liposome. A longer hydrocarbon chain length of the polymer is crucial for prolonged systemic circulation. This was reported for DSPE-PEG<sub>2000</sub>, which showed twice the amount of circulatory vehicles remaining in circulation compared to the shorter chain PEG coatings (e.g. PEG<sub>750</sub> and PEG<sub>120</sub>). The longer chain length allows this improved circulation by limiting the loss of the hydrophilic polymer to the biological molecules (Wang *et al.*, 2008; Perry *et al.*, 2012). The brush conformation on nanoparticles has produced longer lifetimes in circulation, as the highly dense coverage offers a more effective shield for the carrier during delivery (Wang *et al.*, 2008).

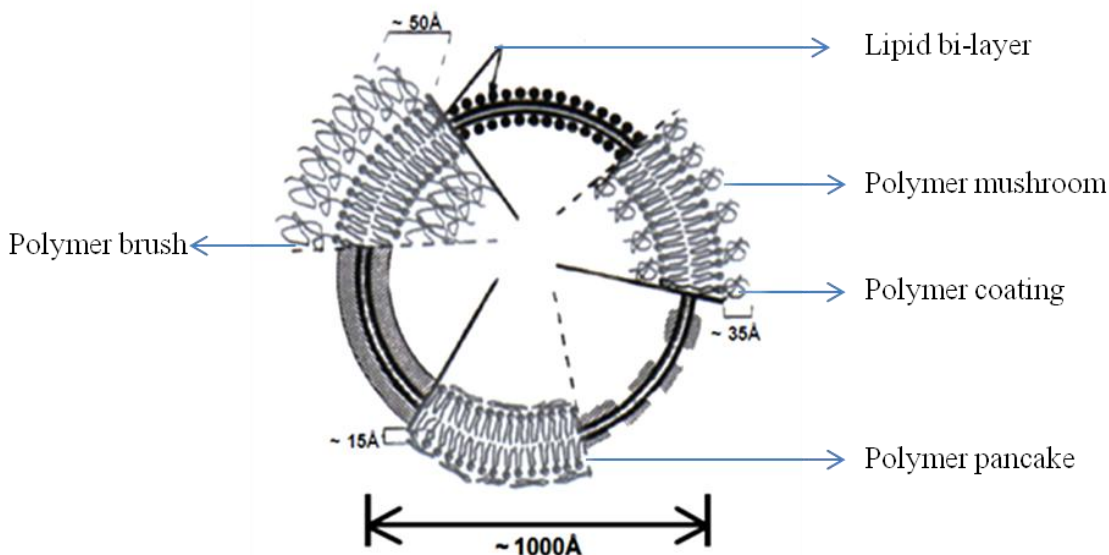


**Figure 1.7:** Illustration of the configuration regimes for Polyethylene glycol / (PEG) polymer grafted onto the liposome surface, as per studies by deGennes (1980) and adapted from Immordino *et al.*, 2006.

#### 1.4.2.2. Active targeting: liposomes and cellular targeting

Ligand targeted therapeutics is one approach under investigation for specific enhancement of delivery to a diseased or tumour site. The basic principle governing this experimental ideology, is the incorporation of targeting ligands that preferentially binds to antigens or receptors expressed either uniquely or at amplified levels on the target cancer cells compared to normal tissue types (Allen, 2002; McCrudden and McCarthy, 2013).

Improvement in specificity has been achieved with a variety of ligands which are endocytosed upon binding to cognate receptors on target cells. These ligands could present in the form of monoclonal antibodies, aptamers, antibody fragments, small molecules, vitamins and protein ligands of cell surface receptors (El Aneed, 2003). An assortment of ligands have been exploited for receptor mediated endocytosis (RME), namely: transferrin (Wagner *et al.*, 1991), asialofetuin (Wu *et al.*, 1998), asialoorosomuroid (Wu and Wu, 1988), folate (Gottschalk *et al.*, 1994) and the epidermal growth factor (EGF) (Yanagihara *et al.*, 2000). This methodology requires an understanding of receptor prevalence on the cancer cell surface compared to that of a healthy cell. A useful example is the transferrin receptor, which shows uncontrolled expression on

breast, bladder, lung and liver cancer cells. The cognate iron carrier and plasma protein, transferrin, when in a therapeutic carrier system can greatly increase targeting to these specific cell types for improved therapeutic delivery and effect (Orgis and Wagner, 2002; Singh *et al.*, 2006; McCrudden and McCarthy, 2013).

It is believed that the addition of targeting moieties to the surface of carrier systems known to undergo rapid RES clearance may not produce better delivery or efficiency than those systems utilising passive targeting to the diseased site. Despite this, targeted liposomes have been prepared by linking the ligands to the liposome either through direct interaction or adsorption, conjugated to a helper lipid, conjugated to a PEG molecule or cationic lipid (MacLachlan, 2007; Zhao *et al.*, 2011).

The asialoglycoprotein receptor (ASGPR) is found in abundance on the surface of parenchymal liver cells (hepatocytes). These receptors recognise the  $\beta$ -D-galactoside terminated glycoprotein, and bind and remove glycoproteins and lipoproteins from circulation. Ashwell and Hartford (1982) were among the first to describe the use of this information for the directed targeting of cationic vector delivery systems. More recent success in this area has been reported based on numerous investigations, where elevated levels of transfection were achieved in the hepatoma cell line (HepG2) with galactosylated cationic liposomes (Kawakami *et al.*, *et al.*, 1998, 2000). Likewise, epidermal growth factor receptor (EGFR) expression, known to be upregulated in a number of cancers serves as an attractive candidate for site specific gene delivery. EGF-targeted –polyethyleneimine delivery systems have shown successful *in vitro* and *in vivo* application with a 50 fold increase in gene transfer efficiency identified in hepatocellular carcinoma cells over normal liver tissue (Christiano and Roth, 1996; El Aneed, 2003). Hoffman and co-workers (2011) showed for the first time that the inhibition of the EGFR could sensitise HCC cells to conventional chemotherapy. Growth factor receptor targeting has been tackled with poly-L-lysine complexes, liposomes, PEI polyplexes as well as adeno-derived peptides (Kikuchi, 1996, Medina-Kauwe *et al.*, 2001; McCrudden and McCarthy, 2013).

Monoclonal antibodies have, to date, performed at a superior level to conventional therapies through their ability to selectively produce a therapeutic effect at a target location, with little or

no damage to the surrounding tissue or cells as a consequence of the ‘Bystander effect’. Furthermore, studies on aptamer targeting, have revealed these targeted systems are capable of eliciting 2.5 fold greater accumulation within a tumour site as compared to untargeted, passive alternatives. Whilst identification of an optimal hepatotropic lectin may pose a time consuming challenge, the efficacy of this yet infant methodology, distinguishes this as an attractive therapeutic treatment option (Wang *et al.*, 2008; McCrudden and McCarthy, 2013).

## **1.5. Targeting the Epidermal Growth Factor Receptor for Cancer therapy**

### **1.5.1. The epidermal growth factor receptor**

The Epidermal growth factor receptor (EGFR), erbB1 or HER 1 is a 170 KDa transmembrane glycoprotein consisting of 1186 amino acid residues (Figure 1.8). It is a prototypical member of the erythroblastosis B (erbB) family which comprises four structurally very similar members, namely; HER1/erbB1; HER2/erbB2; HER3/erbB3 and HER4/erbB4. All members of this class 1 receptor family display the following 3 major structural domains:

1. The extracellular domain,
2. The transmembrane domain, and
3. The intracellular tyrosine kinase domain

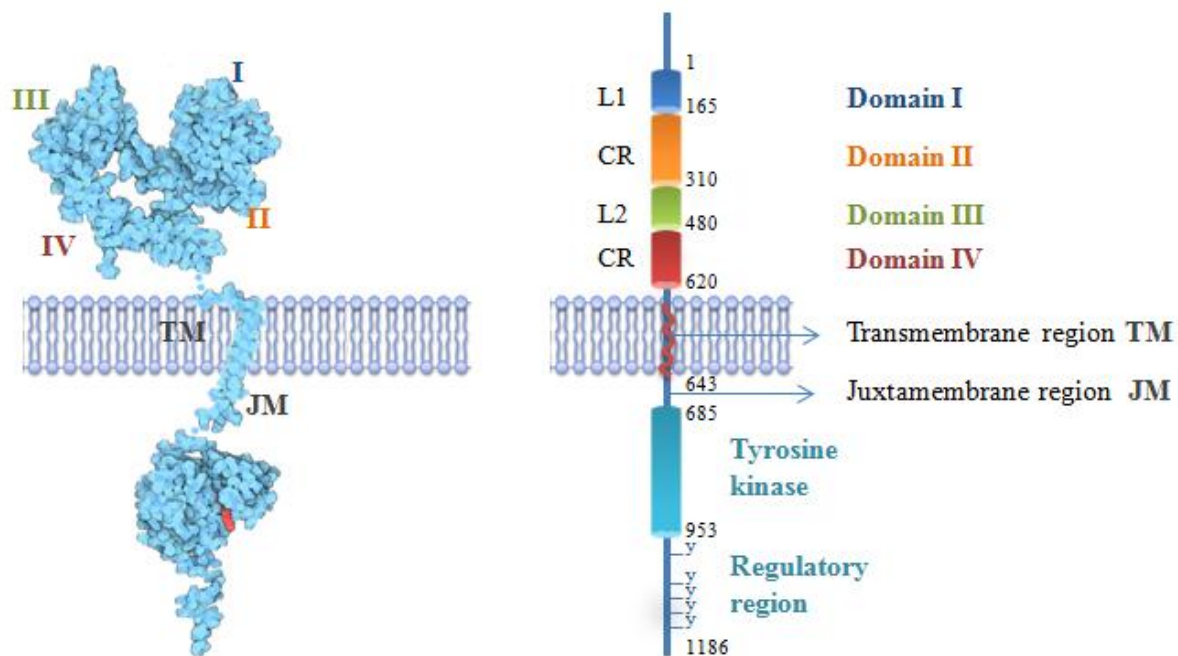


**Figure 1.8:** Crystal structure model of the inactive unbound epidermal growth factor receptor (EGFR) monomer, showing the clearly defined regions. To the right of this model is a representation of the domain architecture of the receptor. Amino acid numbers are outlined for each domain boundary based on a conventional numbering system. In this system the first amino acid at the amino (N) terminal of the mature protein is assumed to be amino acid number 1. (Adapted from Ferguson, K., 2008; Sengupta *et al.*, 2009 and Goodsell, D., 2010).

The extracellular region of the receptor is divided further into four distinct domains designated I – IV, comprising two tandem repeat sequences that make up the ligand binding domain. Of these, domains I and III also referred to as L1 and L2 are members of the leucine rich repeat family. Domains II and IV presents points for ligand attachment owing to the two homologous cysteine rich regions (CR1 and CR2) found at the amino terminal. These cysteine rich domains contain numerous small disulphide-bonded molecules that closely resemble those found in the laminin. The L1 and L2 domains contain  $\beta$ -solenoid or  $\beta$ -helix folds, and serve for the provision of a binding pocket for the growth factor polypeptide. The fourth and fifth helical turn of the  $\beta$ -helical folds present an intercalation point for the conserved tryptophan residues of the CR1 and CR2 regions. Research has shown that the receptor structure is locked in an auto-inhibitory conformation, in an apparent effort to limit or prevent exposure of the dimerisation motifs. During dimerisation the CR1 of one EGFR monomer links with the CR1 of the dimer partner

forming a large loop protrusion (Ward and Garrett, 2001; Jorissen *et al.*, 2003; Edwin *et al.*, 2006).

This major extracellular region is connected via a single  $\alpha$ -helical hydrophobic transmembrane domain to the intracellular protein tyrosine kinase region (Ward *et al.*, 1995). It is this region that is composed of a short juxtamembrane region, a tyrosine kinase region and a terminal carboxy tail consisting of receptor regulatory motifs and numerous tyrosine residues, serving as critical autophosphorylation sites. A significant problem associated with the understanding of EGFR structure, comes in the form of the transmembrane and juxtamembrane regions found running through the cell membrane, as the structural coupling mechanisms of these segments is yet unknown (Ferguson, 2008). Functionally, the transmembrane domain of the receptor not only serves as a membrane anchor, but has also been recognised to enhance receptor dimerisation upon ligand-extracellular domain interaction. The juxtamembrane region displays an intrinsically disordered and natively unfolded structure that offers flexibility. This flexible 'string' conformation proves advantageous during ligand binding and dimerisation. Additionally, it is believed, that this domain may undertake a regulatory function within the receptor (Edwin, *et al.*, 2006; Sengupta *et al.*, 2009; Arkhipov *et al.*, 2013).

Post activation, autophosphorylation of the kinase domain tyrosine residues results in the recruitment of specific substrates and adapter proteins responsible for various processes involved in the downstream signalling cascade (Mamots *et al.*, 2003; Ranson, 2004; Czyzewska, 2011). Recent research into the crystal structure of the receptor kinase core revealed that the unphosphorylated activation loop (A-loop) located in the catalytic active site, displays a constitutively active conformation in spite of its inaccessible nature. This evidence is in contrast to other protein kinases that possess low basal kinase activity until phosphorylation of the A-loop. This exhibits the catalytic independent nature of the EGFR kinase domain, making modulation of kinase activity an important factor of consideration. The EGFR possess 3 major and 2 minor autophosphorylation sites in the carboxy terminal tail, located at Y<sup>1068</sup>, Y<sup>1148</sup>, Y<sup>1173</sup>, and Y<sup>991</sup> and Y<sup>1086</sup> respectively (Edwin *et al.*, 2006). The C-terminal is considered an adequate modulator of receptor function as it retards kinase activity without autophosphorylation (Jorissen *et al.*, 2003). This tail of the receptor has been described as the most variable region, with the

majority of identified phosphorylated tyrosine residues being conserved in the erbB1, erbB3 and erbB4 (Arteaga, 2001). Despite this so called conservation, there is little homology in the short sequences either preceding or following these sequences. In addition to the critical tyrosine residues, several serine and threonine residues serving as important phosphorylation points for receptor downregulation, as well as many endocytosis imperative sequences are also present within the C-terminal tail (Fan *et al.*, 2005; Lee *et al.*, 2006; Bunuales *et al.*, 2011).

EGFR is a readily accessible cell surface receptor that when overexpressed provides an opportunity for the application of specific and selective targeting. The genes responsible for encoding the receptor are referred to as protooncogenes and are found under normal state conditions in all cells of an organism. These so called precursor genes can undergo activation through several processes causing structural genomic changes such as point mutations, translocations or amplifications (Czyzewska, 2011). The glycoprotein has been commonly observed to be amplified and overexpressed in numerous solid tumours, via gliomas, bladder, breast, brain, lung, cervical and colon cells. Of particular interest is the overexpression of the EGF receptor in liver cancer, especially, hepatocellular carcinoma and hepatoblastoma (Bunuales *et al.*, 2011). Receptor signalling plays a significant role in the invasion and metastasis in the hepatocellular carcinoma, HepG2, cell line. Evidence for this has been observed through increased migration levels of EGF treated cells. This activated direct migration of the hepatoblastoma cells is critical for tumour progression. Other responses activated in this manner following particular signaling pathways include, proliferation, differentiation as well as homeostatic functioning (Mamot *et al.*, 2003). Like its cognate ligand, EGFR is considered a pleiotropic signaller, producing various cellular responses in a broad range of cells. Reports have shown the signaling brought about by EGF during HCC development to be the most thoroughly examined, in an effort to fully understand the numerous signalling cascades. (Wells, 1999; Hu *et al.*, 2012; Zhao *et al.*, 2013).

A number of cancer types such as glioblastomas, non-small cell lung cancer as well as adenocarcinoma, are known to express the mutated form of this gene (Lynch *et al.*, 2004; Shigematsu *et al.*, 2005; Tang *et al.*, 2005). The gene encoding the receptor is found on the short arm of chromosome 7p, specifically at position 12.3 – 12.1 with any rearrangement or mutation

at this position resulting in the appearance of mutant gene variants. These mutated forms have been identified as : EGFR I, EGFR II and EGFR III. The most commonly occurring of these mutations involves EGFR III and results in a loss of ligand binding capability in addition to a permanent spontaneous activation of the protein kinase domain (Czyzewska, 2011; Nathanson *et al.*, 2014). This loss, stems from the deletion of exons 2 – 7 within the extracellular domain, which produces an 801 in frame deletion of the coding sequence that has a novel glycine residue at the binding or fusion junction. This type of mutation has been found predominantly in brain tumours, non-small lung carcinomas and gliomas (Mamot *et al.*, 2003).

A key issue regarding the receptor involves EGFR preformed dimers. On normal cells the receptor is found as monomers in an inactive state, however, when abnormal or elevated levels of expression are observed, this has been coupled with the presence of inactive preformed dimers. Despite a lack of structural understanding of these inactive dimers, evidence has suggested that they are primed to receive the cognate ligand. Based on this a potential similarity to the active dimer extracellular domain has been proposed. The erbB receptors, with the exception of erbB3 exhibit ligand inducible dimerisation, transphosphorylation and tyrosine kinase activity (Amin *et al.*, 2006). An erbB family member can undergo either homodimerisation or heterodimerisation with another member. The erbB2 receptor, having no known natural cognate ligand, is considered the preferred heterodimeric partner for other members of the erbB family. This functionality alleviates the need for tyrosine kinase induction through ligand binding to either erbB1, erbB3 or erbB4 receptors. A great many studies have proposed that EGFR mediated phosphorylation of erbB receptors such as the erbB1, is dictated by the dimerisation partners, which in turn is determined by specific ligand binding (Fan *et al.*, 2005). The epidermal growth factor receptor binds a number of natural ligands belonging to the EGF family of polypeptide growth factors. In addition to these natural ligands, synthetic ligands that produce little or no mitogenic effect have been produced. The GE11 ligand is one such example, while more recently, the YI-12 was synthesized for comparative EGF effect (Li *et al.*, 2005). A number of viruses and viral proteins have also been reported as capable of activating the EGFR. The erbB1 and related transmembrane tyrosine kinases thus play an important role in modulation of growth factor signalling. (Ranson, 2004; Muraoka-Cook *et al.*, 2006; Arkhipov *et al.*, 2013).

### 1.5.2. EGF: the natural partner

Following the discovery of the nerve growth factor (NGF) in the 1950's, Dr. Stanley Cohen made a vital addition to the Levi-Montalcini group. Cohens' observations of precocious murine development post treatment with salivary gland extract, led to the isolation of the epidermal growth factor (EGF). The growth factor has been identified to stimulate murine development and corneal cellular proliferation. Being able to enhance mitogenesis, development and implantation in varying mammalian species, has brought about characterisation of the polypeptide as an embryotropic factor. The growth factor is capable of exerting a wide variety of biological effects, chiefly inclusive of mesenchymal and epithelial cell stimulation toward proliferation and differentiation. The pleiotropic nature of EGF positively corresponds to the presence of its associated receptor on the surface of cells of vast origin (Cohen, 1990; Edwin *et al.*, 2006).

Since then, a number of EGF-like polypeptides have been listed as part of the EGF family of growth factors. Making up this family, in addition, to the EGF polypeptide are the; transforming growth factor (TGF- $\alpha$ ), amphiregulin (AR), epiregulin (EPR), heparin-binding -EGF (HB-EGF), betacellulin (BTC), neuregulins 1 – 4 (NRG 1 – 4), epigen (EPN) and the tetracarcinoma derived growth factor (Cripto 1). The erbB receptor ligands are categorised as either EGF agonists, capable of EGFR activation or neuregulins (NRG) capable of binding erbB3 and erbB4 (Wang, 2012). All erbB ligands are produced as type one transmembrane precursor proteins. These precursor proteins undergo processing until proteolytic release in the form of the mature growth factor possessing erbB1 binding capability. The EGF precursor termed prepro-EGF is 1207 AAs long in humans and 1217 AAs in mice (Olayioye *et al.*, 2000). This is known to then undergo proteolysis through cleavage stimulation by calcium ionophores and tyrosine phosphatases. The role of the metalloproteinases, although present, has yet to be fully understood in this transitory situation. The final, mature state EGF is a small, single chain polypeptide comprising 53AAs and a molecular weight of 6045 D (Savage *et al.*, 1972; Jorissen *et al.*, 2003; Edwin *et al.*, 2006).

Structurally EGF consists of asparagine at the amino (NH<sub>2</sub>-) terminus, four arginine residues at the carboxyl (COOH) end and 6 half cysteine residues found in a general consensus (Figure 1.9). These cysteine residues spatially conserved in this sequence are known as a major characteristic

feature of EGF and EGF-like peptides and is referred to as the EGF motif (Benedetta *et al.*, 2000). The presence of this motif determines the specificity of binding to receptors of the erbB family of receptor tyrosine kinases (RTK's). On evaluation of the EGF structure, no freely available sulphhydryl groups were found, indicating the later confirmed presence of disulphide bridges. The cysteine residues interact with each other in the sequence of C1 – C3, C2 – C4, C5 – C6, to form these three intramolecular disulphide bridges (Savage *et al.*, 1972; Barnham *et al.*, 1998; Raymond, *et al.*, 2004).

Features common to EGF as well as EGF-like domains are 2 anti-parallel  $\beta$ -sheets. This is composed of a triple-stranded  $\beta$ -sheet and a double-stranded  $\beta$ -sheet anchored to the major  $\beta$ -sheet by the three disulphide bonds present. The larger triple-stranded  $\beta$ -sheet results from residues at the amino terminal producing the third strand. The smaller two-stranded sheet is found closer to the C-terminal, in proximity to the C1 – C3 and C2 – C4 disulphide bonds. A  $\beta$ -hairpin forms within the EGF motif as a result of the linkage of C5 – C6 (Barnham *et al.*, 1998; Benedetta *et al.*, 2000).

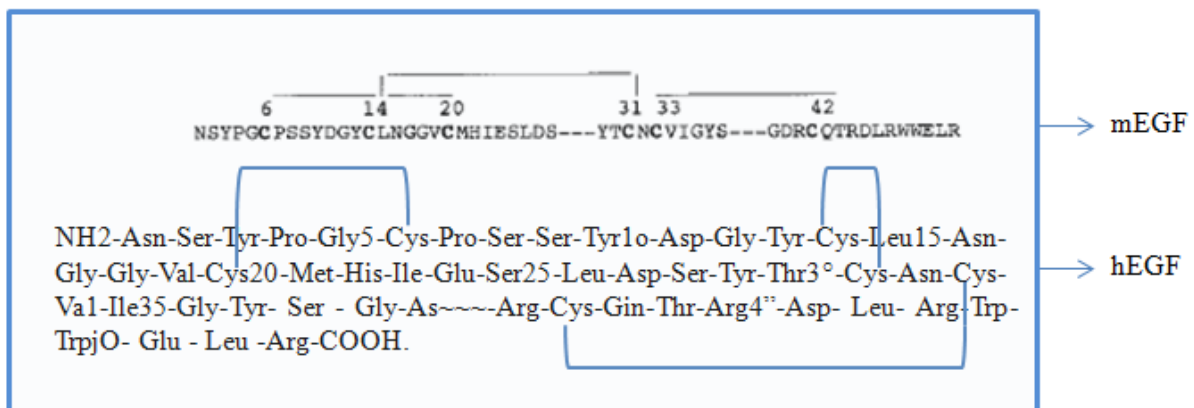


**Figure 1.9:** Representation of the EGF motif with sulphhydryl bonds for the three disulphide bridges (adapted from, Savage *et al.*, 1972 and Bennedetta *et al.*, 2000).

EGF has been found to be acidic in nature, with a relatively dynamic, non-helical conformation as determined by NMR spectroscopy studies, revealing multiple loops with a lack of secondary structure. Native structure stabilisation of proteins such as this, is thought to be attributed to a

multitude of weak interactions (hydrogen bonding, hydrophobic, electrostatic and dipole-dipole), while covalent cross-links such as the disulphide bonds present are also considered a stabilising factor. They are believed to afford levels of stability based on either a singulatory or combined enthalpic or entropic contribution (Savage *et al.*, 1972; Barnham *et al.*, 1998; Benedetta *et al.*, 2000).

While the disulphide bonds offer levels of stability to the polypeptide growth factor, the unique bonding pattern resulting from the formation of bridges may not necessarily be essential for biological activity. The folding and biological activity of the cysteine residues making up the EGF motif, however, play a vital role in determining receptor binding specificity. This results from the EGF motif being such a predominant structural feature of the polypeptide that comprises the EGF-like domains of many EGF-like polypeptides. In this regard, the multiplicity and potential for redundancy are of concern. However, ligands such as EGF and NRG-4 show narrow specificity, binding only EGFR and erbB4 respectively. Others, termed bispecific ligands, show the capability of binding to two distinct primary receptors (e.g. EPR and BTC). Research into these natural ligands and the EGF family of growth factors, illustrates that, although there are points of concern, these natural systems offer a high standard of performance, which synthetic systems could possibly better emulate (Yarden, 2001; Benedetta *et al.*, 2000).

At present, basic methods for conjugation of the peptide to a nanocarrier for therapeutic potential are limited. Buñuales and co workers (2011) recently prepared EGF-lipoplexes for transfection of the HepG2 and SW620 (human cervix carcinoma-receptor negative control) cell lines. In their investigation preformed liposomes were mixed prior to *in vitro* studies with EGF, but their attempts at adsorption conjugation achieved only moderate success. EGF polypeptide conjugation to liposomes has also been achieved through the use of a micelle transfer method. This method involved the conjugation of the epidermal growth factor to the distal end of a DSPE-PEG lipid molecule within a solution. The ligand-PEG-DSPE lipids form micelles in solution that were transferred to preformed liposomes. At a high enough temperature the ligand-PEG-DSPE lipids then transfer from the micelles into the liposome membrane. Song and co-workers (2009), modified the N terminus of the EGF peptide with SPDP followed by conjugation to DSPE-PEG 2000-Mal by standard sulfhydryl-maleimide coupling. Finally, a

streptavidin – biotin system was developed for the examination of a non-viral gene delivery formulation based on mono-PEGylated recombinant human epidermal growth factor (EGF). This system was achieved by conjugating a biotin-PEG-NHS derivative to EGF, followed by purification and immobilisation onto a polyethylenimine – plasmid DNA complex that was coated with negatively charged streptavidin. These studies showed that the EGF-PEG-biotin–streptavidin–PEI–DNA complexes exhibited high transfection efficiency. Similar work using quantum dots conjugated to the epidermal growth factor ligand for EGFR targeting has also been examined. Complexes tethered with the EGF ligand and or PEGylated through construction via biotin–avidin interaction have been established and more easily produced, compared to those prepared by direct chemical conjugation (Lee *et al.*, 2002; Sigot *et al.*, 2010).

### **1.5.3. EGFR targeted treatments**

Based on the autocrine hypothesis, cancer cells have the innate ability to circumvent retardation of their growth by producing and autostimulating their own growth factors on the cell surface. EGFR overexpression on the surface of numerous cancer cell lines with frequent ligand co-expression, allows for activation via autocrine/paracrine mechanisms. Activation and signalling have been deemed important for proliferation, angiogenesis, metastasis and sensitivity to chemotherapy and radiation therapy, in addition to inhibition of apoptosis (Arteaga, 2003). This knowledge together with the fact that EGFR plays an essential role in epithelial, mesenchymal and neuronal cancer biology, makes the receptor an attractive and viable anticancer target. Four treatment strategies that target or block the EGFR signaling pathways have been developed:

- I. Receptor blockage via antibodies
- II. Tyrosine kinase inhibition
- III. Oligonucleotide binding to EGFR or mRNA
- IV. EGFR mediated gene delivery

Of these the tyrosine kinase inhibitors and monoclonal antibodies (MAbs) constitute the two most predominant EGFR inhibitor agents in clinical development. Their sites of action can be seen in Figure 1.10 of section 1.5.4. The potential of targeting EGFR for anticancer therapy

continues to be investigated in both pre-clinical and clinical investigations (Mendelsohn, 2002; Mamot *et al.*, 2003; Ranson, 2004; Buñuales *et al.*, 2011).

The first successful cancer-targeted therapy involved the use of a monoclonal antibody (MAb). These target the extracellular domain of the EGFR, thereby competing with ligands EGF and TGF- $\alpha$ , preventing activation and subsequent signaling cascades, whilst allowing receptor dimerisation and down-regulation. MAbs show certain advantages over the tyrosine kinases, such as improved *in vivo* stability, reduced levels of gastrointestinal toxicity, and promotion of antibody-dependent cell mediated cytotoxicity. This is thought to result from an accumulation of immune effector cells to target cancer cells, by virtue of the high presence of the antibody's Fc region. The clinically advanced members of this therapeutic category are Cetuximab (IMC-C225, Erbitux<sup>TM</sup>), Matuzumab (EMD 72000) and Panitumumab (ABX-EGF, Vectibx) (Pines *et al.*, 2010). Nimotuzumab (hR-3, TheraCIM), similar to Panitumumab is a fully humanised EGFR antibody that binds the extracellular domain of the receptor (Zeineldin *et al.*, 2010). Cetuximab alternatively, displays a chimeric protein nature, originating from the murine MAb (mAb225) which was chimerised with the human IgG1 to decrease potential immunogenicity. Chimerisation and production of the C225 resulted in the inclusion of several mouse antibody variable regions to the human constant regions of IgG. Cetuximab was the first of the EGFR MAb approved by the FDA and shows greater affinity for the EGFR, binding the L2 or DIII domain of the extracellular region. Its activity has been clinically examined for patients displaying metastatic colorectal, head and neck and small-cell lung cancer (Arteaga, 2003; Mamot *et al.*, 2003; Arteaga, 2004; Reddi, 2013). Matuzumab, like Cetuximab prevents EGFR activation by interfering with ligand binding. It was originally isolated from mice as mAb 425 (EMD55900), but was humanised through grafting of the murine complementary regions onto the IgG1 framework. A fully humanised Panitumumab, approved by the FDA also acts by blocking ligand binding. Unlike the aforementioned monoclonal antibodies, it cannot induce antibody-dependent cell-mediated cytotoxicity, but its activity has been identified in the treatment of metastatic colorectal cancer. The effectivity of Nimotuzumab is currently under investigation in glioblastoma and anaplastic astrocytoma patients in early phase clinical trials (Yang *et al.*, 2001; Mamot *et al.*, 2003)

Tyrosine kinase inhibitors (TKIs) can be conveniently administered orally, they show reduced chance of inducing allergic reactions when compared to monoclonal antibodies. These small molecule drugs (MW = 300 – 500 D) act by blocking EGFR action and are categorised on the basis of their binding sites (Ladislau *et al.*, 2013). Tyrosine kinases type 1 and 2 act as ATP competitors, binding the catalytic domain of the receptor tyrosine kinase ATP binding site. Type 1 differs from type 2 in this class by targeting the active conformation rather than the inactive, preferred by type 2. The third type of tyrosine kinase inhibitor is more specific, making use of an allosteric mechanism of inhibition for binding to unique sequences from the receptor tyrosine kinase external region of the ATP binding site. Lastly the type 4 inhibitors or covalent inhibitors, irreversibly bind to the EGFR tyrosine kinase active site generally via a reaction with a nucleophilic cysteine residue, providing longer half-life at the receptor ATP binding site. All four inhibitor types mentioned, although capable of binding the same region should not be considered interchangeable, as their Mg-ATP site binding properties may vary due to structural modification. This blockage of the EGFR by TKIs results in an inhibition of autophosphorylation, downstream signalling, retardation in cell proliferation, and apoptosis (Arteaga, 2004; Ranson, 2004; Reddi, 2013).

The reversible TKIs Gefitinib (Iressa, ZD 1839) and Erlotinib (Tarceva, OSI-774) were the first to be approved by the FDA in 2003 and 2004 respectively. Since its approval, Gefitinib has undergone some revision and is used for the treatment of patients with non-small cell lung carcinoma (NSCLC), head and neck, prostate and gastric cancer. Erlotinib also has been used for treatment of patients with NSCLC as well as in a combination treatment for first line pancreatic adenocarcinoma and is currently in clinical trials for ovarian, head and neck, and hepatocellular cancer. Unlike the aforementioned inhibitors, Lapatinib (GW2016/Tykerb), a thioquinazolin that is also FDA approved (2007), is able to act as a dual reversible TKI to the kinase domain of EGFR and erbB2 (HER-2) for the treatment of metastatic breast cancer. In 2011, Icotinib (Conmana) was approved by the FDA of China. It is another reversible EGFR inhibitor, however, it is not at present approved by the American association, despite positive antitumour activity in first phase clinical trial reports. Of these the most advanced inhibitors in clinical trial development are the quinazolines, Gefitinib and Erlotinib, which are effective in a small number of the NSCLC harbouring kinase domain mutations that render tumour cells EGFR

dependent (Mamot *et al.*, 2003; Pines *et al.*, 2010; Ladislau *et al.*, 2013). The ability of TKIs to target any tyrosine kinase makes them less specific than MAbs, and despite those mentioned that directly target EGFR, the general clinical effectiveness has been noted in only a small subset of patients in spite of EGFR over expression. Mutation of the receptor gene downstream pathways have been known to affect the clinical outcome of the TKI treatment. A known side effect of these treatments is an acne rash and in some cases, diarrhoea (Ranson, 2004; Riese, 2011; Reddi, 2013).

Another therapy that focuses on EGFR involves mRNA interference for a reduction in EGFR protein production. This employs ribozymes, DNA enzymes (DNAzymes), antisense oligonucleotides (AS-ODNS) and small interfering RNAs (siRNA) as therapeutic agents (Bohl and Kullberg, 2003). This approach looks primarily at the ability of these gene-silencing nucleic acids to hybridize with the target mRNA. In this system, the structure of mRNA as well as the physiochemical properties of the chosen agent present potential problems for translation to human testing. This stems from the predominant negative charge, large size and requirement for intracellular delivery. Consequently, for positive future development an effective delivery system is required to target the mRNA in an effort to retard the production of the EGFR (Mamot *et al.*, 2003; Ladislau *et al.*, 2013).

EGFR targeting can also be actively achieved with the aid of gene delivery systems where cognate ligands enable directed EGFR targeting. These targeted treatment systems have been developed and several are currently under investigation. For this, an EGF polypeptide may be conjugated to either polymer based vehicles, nanoparticles or liposome vesicles, producing a targeting vector. These EGFR targeting vehicles are capable of actively carrying therapeutic DNA, oligonucleotides, siRNA, chemotherapeutic drugs, toxins, or any desired therapeutic construct required to produce an anti-cancer effect. The EGFR similar to integrins, is found expressed in selective regions and tissues of the body, making it an ideal model for targeted delivery and treatment. Both EGF and transforming growth factor alpha (TGF- $\alpha$ ) have also been linked to DNA for *in vitro* and *in vivo* delivery. This form of therapy is a particularly attractive cancer therapeutic due to the distinct overexpression and receptor mutations observed in

cancerous cells and tissues, which are absent in normal cells and tissues (Mamot *et al.*, 2003, Huang *et al.*, 2014).

#### **1.5.4. EGFR interaction, signalling and trafficking**

A number of aggressive cancer forms are characterised by overactive epidermal growth factor receptor signalling, growth factor overproduction, or receptor mutation. The basis for these effects involve EGFR activation. This activation develops from the presence and engagement of a cognate ligand or agonist with the receptor. EGFR-EGF interaction initiates an ultimate receptor dimerisation state (Figure 1.10) involving members of the erbB family of RTKs. Dimer formation may be considered homo- (EGFR/EGFR bound) or heterodimeric (EGFR bound to erbB2, erbB3, erbB4) (Franklin, 2004; Ferguson, 2008; Leahy, 2010).

Within the inactive receptor, the domain II  $\beta$ -hairpin loop of the extracellular domain, recognised as the dimerisation arm is found in an unavailable or inaccessible state. The hidden nature of this structure is a consequence of the intramolecular interactions between the  $\beta$ -hairpin loop and domain IV. Unliganded structural interactions such as these are distinctive features of the 'closed' receptor conformation. Once bound by the ligand, the receptor undergoes significant rearrangement of the four ectodomains, opening the structural conformation for protrusion of the dimerisation arm. These rearrangements result in the simultaneous docking of the ligand (EGF) to the domains I and III, following domain repositioning from distant to proximal (Jorissen *et al.*, 2003). The Arginine 41 (Arg41) residue of EGF plays an important role in binding to the receptor, as it forms bidentate hydrogen bonds with the aspartic acid 355 (Asp355) of the L1 and L2 domains. Moreover, it achieves correct orientation as dictated by the presence of tyrosine 13 (Tyr13) and leucine 15 (Leu15), which show additional shielding of salt bridges. Residues of the EGFR extracellular domain I (L1), glutamine 16 (Gln16) and glycine 18 (Gly18) supplement cysteines 31 and 33 (Cys31 and Cys33) of the EGF ligand with 3 hydrogen bonds. This mainchain – mainchain binding causes an extension of the triple-stranded  $\beta$ -sheet of the EGF into the receptor. Aliphatic side chain interactions between the EGF isoleucine 23 (Ile23) and the leucine (Leu14) of the EGFR have also been noted. While the smaller cysteine rich regions of

ectodomain I presents a major ligand binding point, the ectodomain III serves as an important docking site for the N-terminal of the EGF polypeptide (Lee *et al.*, 2002; Ward *et al.*, 2013).

Ligand induced dimerisation is made possible by the exposure of the dimerisation arm during the abovementioned structural alterations. During dimerisation, the close proximity of the intracellular kinase domains results in the formation of an asymmetric kinase dimer (Jorissen *et al.*, 2003). The subsequent effect of the asymmetric dimerisation between the receptors is the activation of the tyrosine kinase of one receptor monomer within the dimer. The consequence of this is the linkage of the rear loop from CR1 (C-loop) of the activator monomer (donor receptor) with the base of the CR1 domain loop (N-loop) of the partner monomer (receiver receptor). This interaction activates the C-terminal of the initial activator receptor, indicating an interchangeable activation effected by both dimer receptors. The receiver receptor shows the ability to stabilise the dimer through additional interaction between the juxtamembrane region and the C-lobe of the activator receptor (Ferguson, 2008). Trans-autophosphorylation of both engaged receptor intracellular domains is a known collateral effect. While experiments involving ligand binding to EGFR have shown the intracellular domains to be relevant to EGFR asymmetry, they are in contrast to the early X-ray crystallography studies of ligand-receptor binding. These early investigations showed the interactions to be symmetric in nature. The complete active dimer that follows from ligand binding is believed to display a symmetrical conformation that is stabilised by the  $\beta$ -hairpin dimerisation arm (Bublil *et al.*, 2010; Leahy, 2010; Riese, 2011).

The mechanism of ligand binding described, has been revealed by early Scatchard analysis plots to be 'concave up' where initial high affinity binding decreases to a diminutive affinity (Salazar and Gonzales, 2002). Negative cooperativity of the receptor-dimer systems or receptor populations have resulted in varying ligand affinities. It has been suggested that negative cooperativity may play a role in the response of the receptor to ligands of different affinities, and the presence of different ligand concentrations. Further scatchard studies have identified the presence of both low and high affinity states. It is believed that ligand binding occurs with domain I of the low affinity state receptor, and upon restructuring the dependent association with domain III, the receptor attains a high affinity state, that is favourable for induction of receptor

dimerisation. EGF has been reported to bind both the low and high affinity EGFR cell surface sites (Jorissen *et al.*, 2003; He and Hristova, 2012).

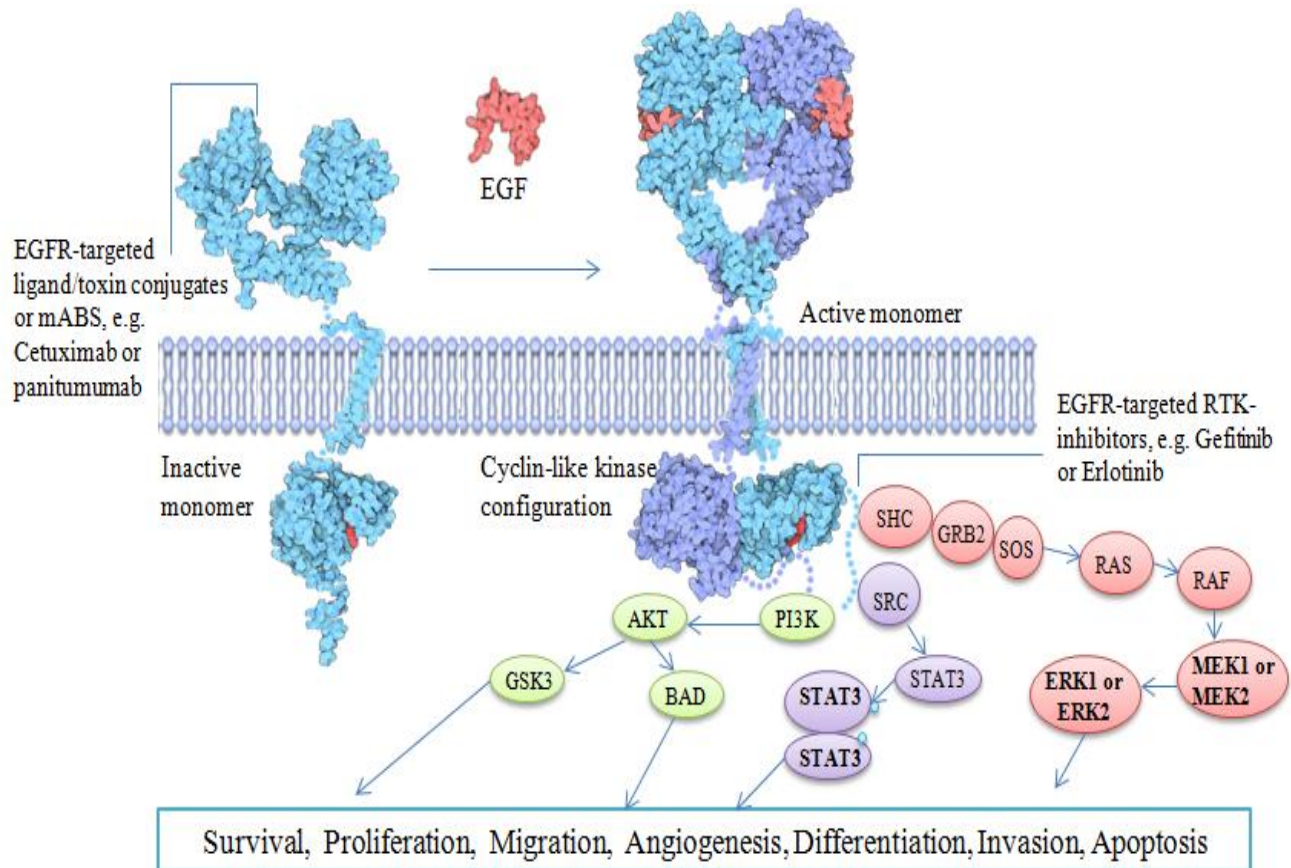


**Figure 1.10:** Schematic illustration of EGFR ligand binding, activation and cellular signalling. Binding of the EGF ligand to the EGFR initiates activation through receptor dimerisation, instigating numerous signalling pathways. EGFR can be targeted for cancer therapy by gene delivery- approaches for inhibition of EGFR are also shown (adapted from Ciardiello and Tortora, 2008, Grandal and Madhus, 2008, Sengupta *et al.*, 2009, Goodsell,D., 2010, Holohan *et al.*, 2013).

Following from ligand-receptor kinase domain activation, C-terminal tyrosine phosphorylation presents docking sites for adaptor and intracellular signal transducer proteins displaying Src-homology-2 (SH2) or phosphotyrosine binding (PTB) domains. The co-localisation of scaffold and adaptor proteins devoid of enzyme activity, is thought to aid in the recruitment of signalling proteins. A number of other signalling proteins known to participate in this system include, growth factor receptor-bound protein 2 (Grb2), Src homology 2 domain containing (transforming

protein) (Shc), phospholipase-C- $\gamma$ -1 (PLC- $\gamma$ -1), the P85- $\alpha$  subunit of phosphatidylinositol-3-kinase (PI3-K), P120 rasGap, Src (c-Src), Signal Transducer and Activator of Transcription (STAT) and Cbl. Phosphotyrosine site recognition and binding produces a ligand dependent multicomponent signalling complex necessary for initiation of multiple signalling pathways that ultimately end in cellular mitogenesis and survival (Figure 1.10). There are three major pathways implicated in receptor activation induced downstream signalling. They are the mitogen-activated protein kinase (MAPK), protein kinase B (AKT) of PI3-K and the STATs (Mamot and Rochlitz, 2006).

A strategic factor in the EGF-dependent Ras/MAPK pathway activation, is the Grb2 adaptor protein constitutively bound to the Sos (Son of sevenless homolog) Ras exchange factor. Resulting from activation dependent autophosphorylation, the SH2 domain of this cytosol localised protein binds the EGFR either directly at the tyrosine (Y<sup>1068</sup> and Y<sup>1086</sup>) residues, or indirectly via coupling with the tyrosine phosphorylated Shc that is associated with the receptor (Jorissen *et al.*, 2003). Ras activation leads to Raf 1 activation which phosphorylates and activates the extracellular signal regulated kinases (ERK1 and 2) allowing for nuclear translocation. ERK1 and 2 are responsible for the catalysis of phosphorylation of transcription factors (Elk1 and c-fos) imperative for cellular control of mitogenesis. This pathway additionally, is capable of activating a number of nuclear proteins. The cyclin-D1 is one example, that upon activation, progresses the cell cycle out of the G-phase and into the S-phase, showing a clear impact on cell proliferation (Ciardiello and Tortora, 2001; Wang, 2012).

EGF cellular stimulation has been known to affect phospholipid metabolism in phosphatidylinositol turnover, and phosphatidic acid (PA) and arachidonic acid (AA) production. EGFR shows direct activation of three pathway enzymes including, PLC- $\gamma$ -1, PI3-K and phospholipase-D. The activation of the class Ia PI3-K by EGFR occurs through either direct interaction with P85- $\alpha$  or indirectly through Ras activation. The downstream serine-threonine-AKT of this pathway mediates signals for the suppression of pro-apoptosis, promotion of growth and cellular survival (Jorissen *et al.*, 2003; Wang, 2012).

Proliferation and transformation as mediated by the EGF in fibroblasts and epithelial cells have shown significant improvement from the signal transducers, such as c-Src and other cytosolic kinases. The SH2 domain binds the phosphotyrosine residues of the kinase domain (Y<sup>891</sup>, Y<sup>920</sup>, and the later elucidated Y<sup>845</sup> and Y<sup>1101</sup>). The latter sites appear imperative for STAT5b activation and Src binding. The STAT proteins, regarded as inactive transcription factors, undergo activation and nuclear translocation upon receptor stimulation and dimerisation. The EGFR ligand activation of STATs 1, 3, and 5, unlike that observed for cytokine receptors, displays no requirement of the JAK family kinases. In contrast to the other pathway proteins discussed, the STATs show a constitutive association with the receptor, rather than with phosphotyrosine binding. Pathway cross-connections have also been made evident, where the c-Src activation has been linked to the activation of PI3-K. This cross-connection stems from the binding of the P85- $\alpha$  subunit to the receptor domain site Y920 which is associated with c-Src (Jorissen *et al.*, 2003; Wang, 2012).

C-terminal sequence divergence between the erbB family of receptors promotes specific and preferential associations with the signal proteins and dimers. Consequently, heterodimerisation is regarded as a more potent conformation for signal transduction. This shows credence based on varying levels of phosphotyrosines present, as well as very distinct phosphorylation and downstream signalling patterns. It can thus be stated that the specificity and potency of the signal output is determined by the specific ligand and the presence and concentration of potential dimerisation partners (Arteaga, 2001; Jorissen *et al.*, 2003).

#### **1.5.5. EGF receptor mediated endocytosis**

Activated EGFR downstream signalling as effected by ligand attachment, shows a regulation requirement. This comes in the form of a constant equilibrium state between kinase activity and protein tyrosine phosphatase inhibitory activity. Another important mechanism by which this signalling is regulated is endocytosis. In this regulatory mechanism, endocytosis shows promotion of receptor signalling, possibly leading to receptor eradication through lysosomal delivery (Segatto *et al.*, 2011).

Ligand mediated endocytosis can be either clathrin-dependent or clathrin-independent as depicted in Figure 1.11. Of these, clathrin dependent endocytosis appears to be the predominant choice in response to physiological ligand concentrations. All endogenous forms of the EGFR family of ligands allow receptor internalisation via the abovementioned entry mechanisms. The formation of the ligand receptor complex follows the predominant clathrin mediated endocytic (CME) pathway at physiological concentrations. Within this mechanism the early endosome acts as a sorting compartment for the ligand-receptor complex. Natural maturation of the vesicle promotes trafficking of the EGF-EGFR into the late endosome or multivesicular body. Plasma membrane recycling, delivery to the endoplasmic reticulum and nuclear trafficking present alternate routes for the ligand-receptor complex. This indicates that not all ligand directed EGFR complexes are bound for lysosomal degradation (Mills, 2007; Ceresa, 2011).

This multi-destination sorting follows from the distinctive nature of the endocytic compartments, in addition to the specific ligand affinity and response to the endocytic environment. Within this locale, the greater the distance from the plasma membrane, the greater the density and acidic nature of the compartments, presenting unique protein populations at the different locations. Furthermore, investigations by Roepstorff and colleagues (2009) into the ability of the different endogenous EGFR ligands to induce internalisation, degradation and recycling within the human hepatocellular carcinoma cell model (HepG2), showed EGF to target receptor degradation. Similarly, HB-EGF and BTC produced the same effect, while TGF- $\alpha$ , NRG-1 and epiregulin promoted receptor recycling. Ligand binding sensitivity to pH, and knowing that the endosome has a general pH of  $\approx 6.8$ , is important for understanding the activity at the various endocytic destinations. At neutral or physiological pH (7.3 – 7.4) both EGF and TGF- $\alpha$  bind EGFR with comparable affinity, however, ligand dissociation is known to be effected at approximately 5.9 and 6.8 respectively. This explains the preference of one for recycling and the other for ubiquitinylation and lysosome delivery (Olayioye *et al.*, 2000; Ceresa, 2011).

Of the vast amount of proteins and protein complexes that partake in ligand induced clathrin mediated endocytosis, the specific binding of Eps-15 with the clathrin-adaptin (AP2) protein complex is considered an important component of the early endocytic pathway. Eps-15 and epsin are proteins with ubiquitin binding capacity that are localised to clathrin coated pits. This is as a

result of the adaptin assisting in the arrangement of the polyhedral/polygonal lattice. Receptors recruited in clathrin coated pits are broken down into two class groups. Class I receptors (e.g. transferrin and mannose-6-phosphate) are clustered into coated pits and internalised regardless of ligand association. Class II, in contrast demonstrate ligand-dependent clustering and internalisation, as seen with the signalling receptors such as EGFR. Upon formation of the clathrin coated lattice, GTPase dynamin directed action, releases a clathrin coated vesicle greater than 100 – 150 nm in diameter. Clathrin coated pits are small areas on the plasma membrane into which ligand-receptor complexes or dimers with ligand : receptor ratio of 2:2 are recruited. Vesicle budding at these coated regions occurs rapidly following inward invagination of the membrane. Two major structural components involved in this process are the adaptor proteins and clathrin itself, which is composed of 3 copies each of heavy and light chains forming a triskelion (Belting *et al.*, 2005). Clathrin coats the plasma membrane cytoplasm face through interactions with the adaptor proteins AP-2 complex, while the other proteins present in these pits perform a regulatory function. These endocytic vesicles meet and fuse with the endosome, responsible for sorting the receptor and ligands to their various intracellular destinations. The endosomes can be categorised into early, intermediate and late endosomes. It has been noted that an intravesicular pH drop occurs from 6 – 6.5 in early endosomes to 4.5 – 5.5 in the late endosomes and lysosomes, which relates to the ligand-receptor complex dissociation. Upon invagination of the coated pits into the coated endocytic vesicles, the clathrin and associated proteins must return to form new coated pits on the membrane (Sorkin, 1998; Grandal and Madhus, 2007).

**Clathrin Dependent Endocytosis**

**Clathrin Independent Endocytosis**

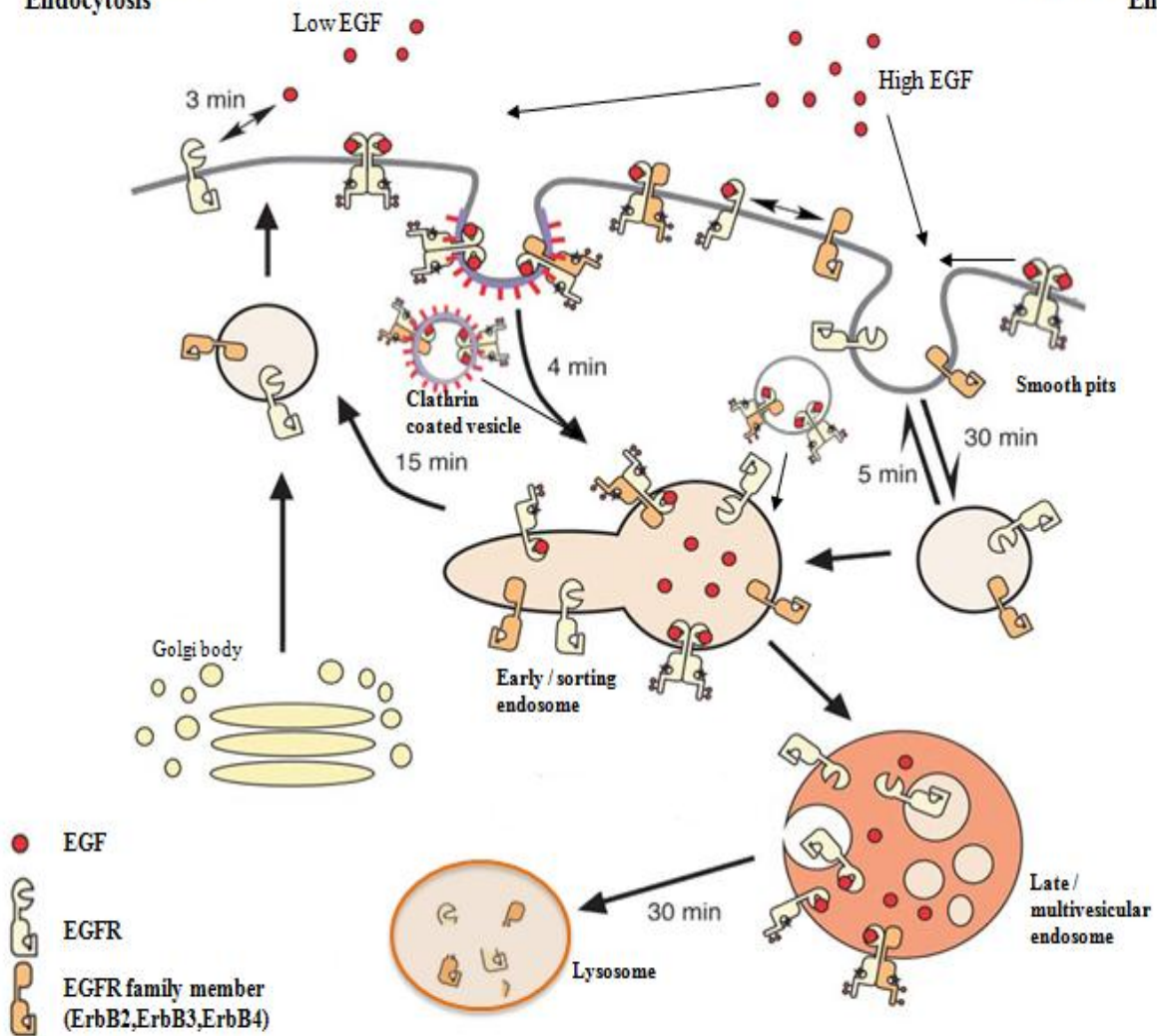


**Figure. 1.11:** Cellular entry mechanisms favoured by the EGFR family. Activated EGFR homo- and hetero-dimers are internalized through a clathrin coated pit pathway, other receptor family members are likely internalized by a smooth pit pathway (caveolin mediated endocytosis). Clathrin mediated endocytosis is the preferred mechanism of endocytosis by EGFR, particularly in the presence of physiological quantities of EGF. When inundated with higher levels of EGF, however, some overflow enters the clathrin independent mechanisms for entry. Thus easing the burden on the clathrin mediated pathway. Approximate mean times for specific processes (where available) have been included based on literature. (adapted and modified from Wiley, 2004; Abella and Park 2009; Haguld and Dikic, 2012).

In the absence of activation, cell cultures displaying amplified expression of the EGFR show a receptor turnover time of 24 hrs or more. Comparatively, those receptors showing low to moderate levels ( $\leq 200000/\text{cell}$ ) have a turnover time of 6 – 10 hrs. The constitutive recycling rate of inactive receptors has been shown to be higher than the rate of internalisation (Sorkin and Goh, 2009). During clathrin mediated endocytosis, the endosome matures from the early endosome to form multivesicular bodies (MVBs) and late endosomes. Accumulation of the EGF-EGFR complexes within the intraluminal membranes of the MVBs prevents plasma membrane recycling. Receptor recycling does not take place since EGF does not dissociate significantly from its receptor resulting in an intact complex being recycled. Two mechanistically and kinetically different pathways are involved in this recycling. One pathway is rapid and efficient at low temperature and takes place via the early endosome, while the other displays far slower kinetics and is blocked at low temperature. This second pathway is believed to involve the MVBs membranes. Fusion of these membranes with the lysosome leads to the rapid degradation of the intraluminal components. Degradation of the primary lysosomal vesicles is caused by the proteolytic enzymes present. The receptor-ligand complex is reported to retain signaling activity, even within the endosomes. These endosomes have also shown great importance not only as sorting systems, but also as contributors to signal specificity and diversification. In this dual signal role, the endosomes are able to sustain signals produced at the plasma membrane level, as well as generate original and unique signals restricted to the plasma membrane (Sorkin and Goh, 2009; Scita and Difore, 2010; Xiang and Zhang, 2013).

Activation of the EGFR kinase through ligand binding has been identified as a key factor in the recruitment of the receptor complex into the clathrin coated pits. Moreover, the c-Src tyrosine kinase activation has been implicated in the phosphorylation of the heavy chain of the clathrin triskelion and thus in the regulation of EGFR CME. Recent studies have indicated that tyrosine kinase activity may not be as essential as previously implied. Receptor dimerisation has been revealed to be necessary for kinase activation as well as internalisation. EGFR efficiently activates MAPK in HeLa and HepG2 cells, which due to overexpression of the dominant negative dynamin, is conditionally defective in this type of endocytosis (Wang, 2012). Internalisation of the EGFR is mediated by binding of the RING-finger E3 ubiquitin ligase (Cbl). This is an

important part of receptor trafficking as it promotes receptor ubiquitination enabling receptor targeting for endocytosis and endosomal sorting (Mills, 2007; Ceresa, 2011; Wang, 2012).

While the predominant nature of CME is clearly evident, there still exists the need for non-CME or clathrin-independent endocytosis. Research into the pathway of EGFR endocytosis, has shown that the concentration of the associative ligand and the extent of ubiquitylation, play a defining role in the internalisation pathway. As mentioned earlier, at physiological concentration of the ligand representing a relatively moderate or low level, clathrin-dependent endocytosis is preferred. In contrast, at higher ligand concentrations the receptors enter a clathrin-independent endocytic pathway. It has been previously proposed that this influenced choice of pathway, is actually determined by the internalisation pathways saturability and capacity. In this regard, the high concentrations of the ligand together with receptor overexpression, overwhelm the CME pathway, necessitating non-CME internalisation. Cells displaying moderate levels of endogenous EGFR have been found to be capable of coping with high levels of EGF-receptor stimulation and subsequent internalisation. Previous studies involving A-431 (epidermoid carcinoma) cells displaying extremely high levels of EGFR were reported to engage micro- and macropinocytic vesicles in addition to membrane ruffling with an absent clathrin coat. Those receptors internalised by CME have been shown not to undergo targeting for degradation, but plasma membrane recycling. This prolongs the signalling effect and receptor induced biological responses. In contrast, clathrin-independent mechanisms show preferential targeting toward degradation (Sorkin and Goh, 2008; Halgund and Dikic, 2012).

Multiple clathrin-independent mechanisms have been revealed, including caveolar-type endocytosis, clathrin-independent carriers GPI-AP enriched early endosomal compartment (CLIC-GEEC)-type endocytosis, phagocytosis, macropinocytosis, flotillin-associated endocytic structures, entosis, and dorsal ruffles (waves). Dorsal ruffle internalisation involves ruffles on the plasma membrane and has been observed in many cell lines, requiring kinase activity, dynamin, and PI3-Kinase (Sorkin and Goh, 2008). Caveolar mediated endocytosis involving cholesterol rich lipid rafts has been proposed and identified in response to high prevalence and engagement of EGF and EGFR in Hela cells. Despite higher rates of receptor internalisation, all clathrin-

independent pathways occur at far slower rates than that achieved with CME (Sorkin, 1998; Lundmark and Carlsson, 2010; Xiang and Zhang, 2013).

Within the caveolae mediated mechanism, the flask-like invaginations or caveolae on the plasma membrane consist of caveolin proteins, sphingolipids and cholesterol. Morphologically, the caveolae resemble lipid rafts. The number of EGF receptors available for binding, and not the ligand binding affinity, determines EGF binding and cholesterol loading or depletion. Caveolin, a resident protein of the lipid raft is known to induce caveolae formation at the cell surface. Two mechanisms have been proposed for the involvement of caveolae in EGFR internalisation. One proffers that the caveolae encases the EGF-EGFR complexes, allowing a single wave process of trafficking that completely depletes the cell surface of caveolae. The second revolves around a rapid turnover of the caveolae, where internalised complexes have their membrane positions replaced (LeRoy and Wrana, 2005; Roepstorff *et al.*, 2008).

## **1.6. Aims and Objectives**

This investigation aims to produce a potential vector system which will lead to improved levels of hepatotropism in gene delivery. For this purpose two major functional modifications were investigated. Firstly, to afford shielding properties, DSPE-PEG was integrated to the vector for enhanced circulation, particularly under *in vivo* conditions. The second modification was the incorporation of the EGF peptide which allows for the exploitation of the overexpressed receptors on the cellular surfaces of the studied cancer cells (HepG2). For the purpose of this study, focus was placed on two major objectives.

1. The synthesis of DSPE-PEG shielded liposomes, EGF tagged liposomes, as well as standard cationic liposomes for control purposes.
2. The analysis of these potential vector systems in the *in vitro* environment, under numerous investigative assessments to thoroughly ascertain successful vector implementation.

A detailed examination of these objectives are presented per chapter in the thesis outline below.

## 1.7. Thesis Outline

Cationic lipofection vectors, through the inclusion of targeting moieties have shown significant levels of tumour cell specificity and together with the addition of a polymer coating, provides for a sustained circulation time allowing for the expression of the transgene in the desired cell, tissue or organ. This thesis attempts to address the issue of safe and efficient delivery of genes *in vitro* using novel epidermal growth factor targeted cationic liposome systems that show promise and that may be considered for further development. Chapter one provides an up to date review on the literature surrounding gene delivery systems and the attractiveness of EGF as a targeting ligand for improved hepatotropism.

With the aim of this research in mind, a number of cationic liposome formulations were prepared, two of which are basic preparations consisting of the zwitterionic lipid DOPE in conjunction with cytofectins Chol-T and MS09 respectively. Two stealth preparations were formulated as above but with the additional inclusion of DSPE-PEG<sub>2000</sub>, affording these liposomes shielding to cytosolic proteins, and allowing improved circulation time for effective transfection. Targeted preparations were achieved through the adsorption of the EGF peptide to the preformed liposomes. Targeted preparations were assessed on the basis of the target receptor being overexpressed in tumour cell lines, such as the EGFR-positive hepatocellular carcinoma cell line HepG2. Chapter two describes the various materials and procedures utilised in the formulation of the liposomes, the physicochemical characterisation of the liposomes and their complexes with DNA, cytotoxicity studies of these gene delivery vehicles to mammalian cells [hepatocellular carcinoma HepG2 and chinese hamster ovary CHO-K1 cell lines] in culture, and the eventual cellular expression of transgenes.

The physicochemical characteristics such as structural morphology, size distribution and surface charge of these eight (targeted and untargeted) liposome formulations were determined by transmission electron microscopy using a negative staining-vitrification protocol, and nanoparticle tracking analysis (NTA). The formation and nature of the liposome-DNA complexes were established through band shift, ethidium bromide displacement and nuclease protection studies. Attachment of the EGF ligand to the liposome surface was confirmed using

an EGF-ELISA kit for protein determination, based on a set of predetermined EGF standards. The MTT growth inhibition assay was used to determine the levels of cytotoxicity, while the levels of transgene expression was measured using the luciferase reporter gene assay utilising the pCMV-*luc* plasmid DNA and GFP protein assay using the pCMV-GFP plasmid DNA. The latter was quantified after fluorescence microscopy by flow cytometric analyses. Confirmation of EGF receptor mediated endocytosis was carried out through competition transfection studies using the YI-12 synthetic peptide as the competing ligand. Results of these analyses are discussed in chapter three, showing successful formulation of liposomes, DNA condensing capability, cellular tolerance and expression.

To conclude, Chapter four provides a summarising discussion on the achievements of the formulated liposomes reported in this thesis relative to currently available literature. While the basis for these formulations stem from well established cytofectins and liposomal development, the addition of the epidermal growth factor (EGF) polypeptide as well as the method of attachment provide a novel approach to gene delivery vector production. The EGF tag present on the liposome surface enables specific targeting, which although previously explored, has been limited with regard to liver cancer therapy. Moreover, the ease of its inclusion through simple mixing, provides a fast and reliable method for the development of EGF targeted cationic liposomes. These aspects show the significance of the development of these novel liposome vector systems, herein examined.

## CHAPTER TWO

### 2. MATERIALS AND METHODS

#### 2.1. Synthesis and Formulation

##### 2.1.1. Materials

Dioleoylphosphatidylethanolamine (DOPE) was purchased from the Sigma Chemical Company, St Louis, USA. Chol-T  $3\beta$ [N-(N',N'-dimethylaminopropane)-carbamoyl] cholesterol and  $3\beta$ [N(N',N',-dimethylaminopropylsuccinamidohydrazido)-carbamoyl] cholesterol (MS09) cationic lipids were synthesized at the University of Kwazulu-Natal, Discipline of Biochemistry, Westville, South Africa. The epidermal growth factor, human (h EGF) was procured from Roche Diagnostics, Mannheim, Germany. The 2-[4-(2-hydroxyethyl)-1-piperazinyl] ethanesulphonic acid (HEPES) was purchased from Merck, Darmstadt, Germany. Plasmid DNA: pCMV-*luc* DNA was purchased from Plasmid Factory, Bielefeld, Germany. All other chemicals were of analytical grade.

##### 2.1.2. Methods

###### 2.1.2.1. Cytfectin synthesis

###### 2.1.2.1.1. Chol-T Synthesis

The Chol-T cytofectin used, was synthesized as previously described by Singh and co-workers (2001) as shown in Figure 2.1. Briefly, a solution of 3-dimethylaminopropylamine ( $\approx 3$  mmole) was introduced to a mixture of cholesteryl chloroformate ( $\approx 1$  mmole) in 1 ml dichloromethane. The reaction mixture was allowed to proceed at room temperature for an hour; thereafter a sample of the prepared mixture was retained for analysis by thin layer chromatography (TLC results not shown). The solvent of dichloromethane and excess 3-dimethylaminopropylamine, was removed through Büchi Rotavapor-R rotary evaporation. Crystallisation of the resulting residue was allowed to form overnight after being dissolved in absolute ethanol. After recrystallisation, a stream of dry nitrogen gas was used to filter the product, which was thereafter dried by rotary evaporation producing crystals of Chol-T.

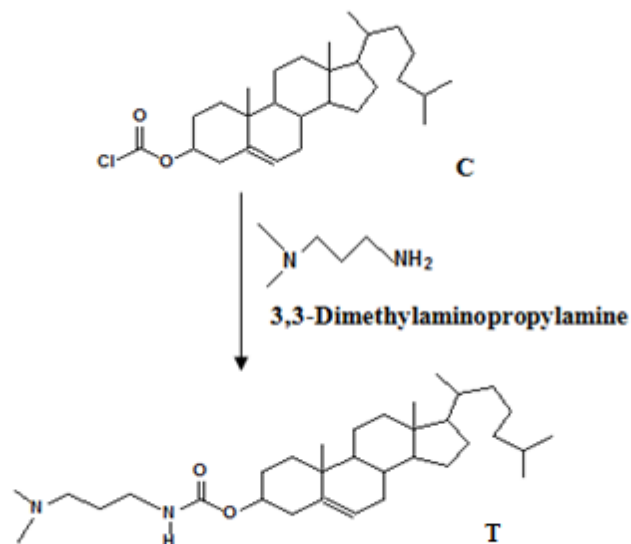


**Figure 2.1:** Reaction scheme showing the preparation of the cationic cholesterol derivative Chol-T (T) from cholesteryl chloroformate (C) and 3-dimethylaminopropylamine.

#### 2.1.2.1.2. MS09 Synthesis

MS09 was synthesized as detailed previously by Singh and Ariatti (2006), as described below (Figure 2.2). Succinic anhydride (0.5 mmole) in dimethylformamide:pyridine (5 ml) was used to treat cholesterylformylhydrazide (MSO4) (0.5 mmole). This was incubated at room temperature overnight, followed by subsequent rotary evaporation for solvent removal. Cholesterylformylhydrazide hemisuccinate (MSO8) was obtained in a crystalline state from absolute ethanol. MSO8 (0.34 mmole), dicyclohexylcarbodiimide (DCCI) and N-hydroxysuccinimide (0.68 mmole) were mixed in DMF and warmed to  $\pm 50^{\circ}\text{C}$ . Thin layer chromatography was used to monitor the progress of the reaction, using silica gel 60F<sub>254</sub> plates in 9:1 (v/v) chloroform:methanol. Dicyclohexylurea crystals were produced after overnight incubation and subsequently removed through filtration followed by filtrate evaporation under vacuum. Excess N-hydroxysuccinimide was extracted from chloroform solution using water. Thereafter the chloroform layer was evaporated, and excess DCC was removed using petroleum ether. The final MS09 product was recrystallized from ethanol.

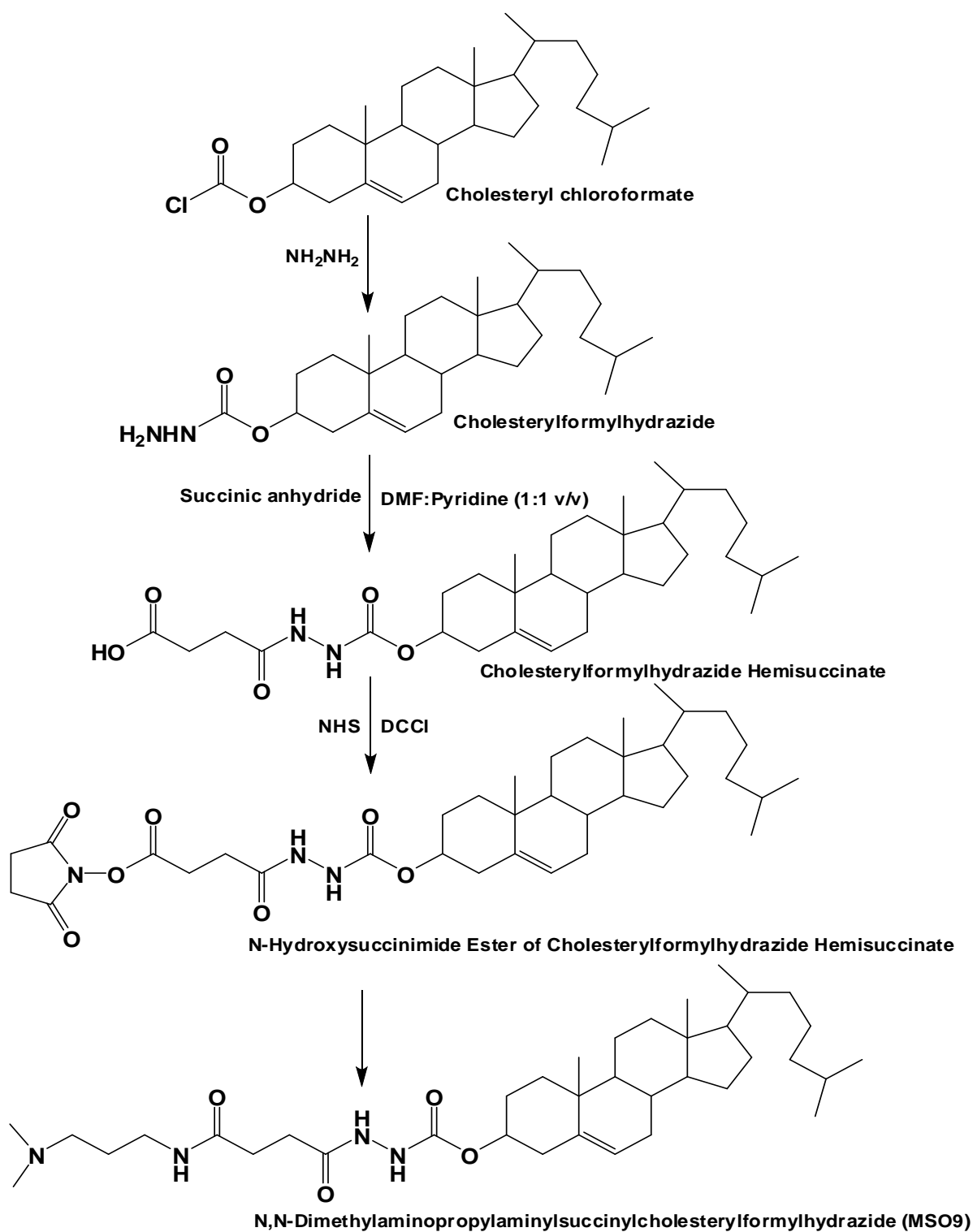


**Figure 2.2:** Reaction scheme representing the preparation of the cationic cholesterol derivative, 3 $\beta$ [N(N',N',-dimethylaminopropylsuccinamidohydrazido)-carbamoyl]cholesterol (MS09)

### 2.1.2.2. Formulation and storage of the EGF peptide

The human epidermal growth factor (hEGF) polypeptide lyophilised powder (100 µg) was resuspended in 400 µl of 18 Mohm water, creating a stock of 0.25 µg/µl. This was split into 50 µl aliquots for storage and future use, to prevent degradation from repeated freeze-thaw cycles.

### 2.1.2.3. Preparation of Liposomes

The cationic liposomes were synthesized in accordance with an adaptation of the protocol employed by the team of Gao and Huang (1991). The molar ratios and mass of the liposomal components are outlined in Table 2.1. The plain and PEG-functionalised (Figure 2.3) liposome preparations were made up to a total of 4 µmoles of lipid in chloroform (1 ml). The preparation was then subjected to rotary evaporation using a Büchi Rotavapor-R, and the lipid components were deposited as a thin film on the inside of a quick fit test tube. The samples were dried further in a Büchi TO-50 drying pistol. Thereafter the samples were rehydrated in 1 ml sterile HEPES buffered saline (20 mM HEPES; 150 mM NaCl pH 7.5). All liposomal suspensions were vortexed and left over night at 4 °C. Thereafter the suspensions were briefly sonicated (5 minutes) in a bath sonicator to produce unilamellar liposomes.

**Table 2.2:** The total lipid composition of the prepared cationic liposomes

CATIONIC LIPOSOMES	MOLAR RATIOS (µmole)			MASS (mg)		
	Cytofectin	DOPE	DSPE-PEG <sub>2000</sub>	Cytofectin	DOPE	DSPE-PEG <sub>2000</sub>
Chol-T	2	2	0	1.03	1.49	0
Chol-T/PEG	2	1.92	0.08	1.03	1.43	0.16
MS09	2	2	0	1.26	1.49	0
MS09/PEG	2	1.92	0.08	1.26	1.43	0.16

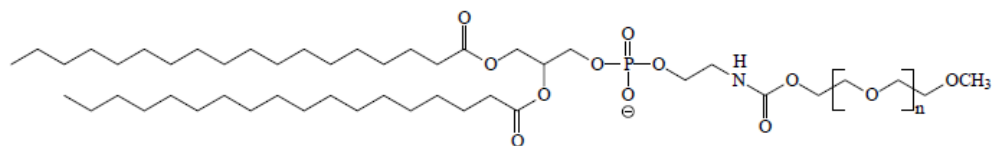


**Figure 2.3:** A representative image of the DSPE-PEG molecule employed for liposomal synthesis, where  $n = 45$  for DSPE-PEG<sub>2000</sub>.

Targeted lipoplexes were formulated adapting the method used by Buñuales and co-workers (2011). Briefly the EGF was incubated with the preformed liposomes prior to lipoplex preparation. EGF at a concentration of 1  $\mu\text{g}/\mu\text{g}$  pDNA was introduced to each of the four liposomes. This was allowed to incubate at room temperature for 15 minutes. Thereafter the liposome-EGF samples were transferred to individual Amicon Ultra-2 3K centrifugal devices (3000 nominal molecular weight limit, NMWL) and exposed to ultrafiltration, by centrifugation with a swinging bucket rotor (Eppendorf centrifuge 5810) at 3202 x g for 15 minutes to concentrate the sample and to remove any unbound or free EGF. This was immediately followed by a recovery spin (1000 x g for 2 min) to collect the liposome-EGF samples. Recovery of sample concentrates with a swinging bucket rotor was achieved at approximately 85- 98%. These liposome quantities as outlined in Table 2.1 were used to determine the optimal ratio of liposome to DNA binding, dissociation and protection (sections 2.2.2.3; 2.2.2.5 and 2.2.2.5).

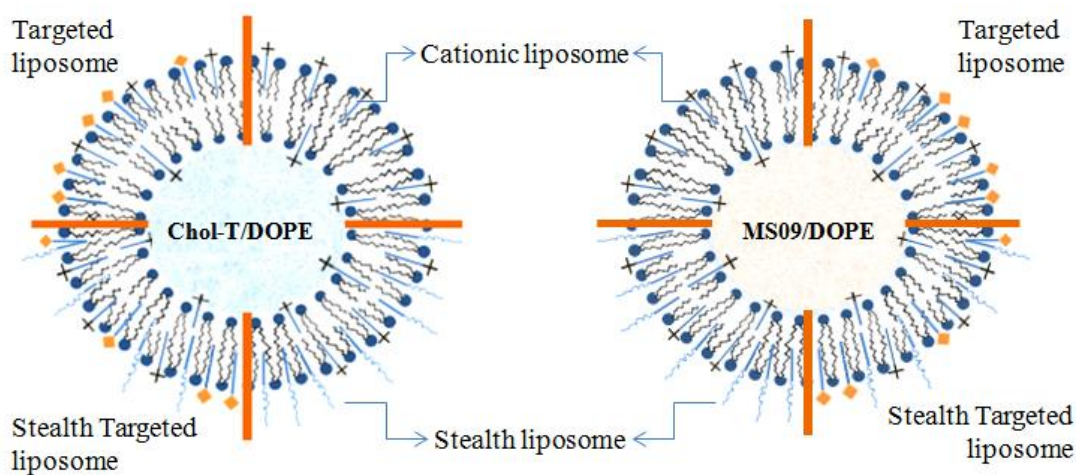


**Figure 2.4:** Illustration of the eight different liposome test preparations derived from the four originally formulated cationic liposomes, analysed for hepatotropic DNA delivery

#### 2.1.2.4. Amplification of pCMV Control Vector

The pCMV-*luc* control vector (Figure 2.5) was amplified in the non-viral gene delivery laboratory, Discipline of Biochemistry, University of KwaZulu-Natal according to a standard protocol. The DNA purity and concentration was determined spectroscopically using a Thermo Electron Corporation Biomate 3 spectrophotometer. The isolated DNA was run on a 1% agarose gel against a control DNA sample to confirm purity and identify the different forms of DNA. The NanoDrop 2000c from Thermo Scientific was used to further confirm purity and measure concentration of the amplified DNA.

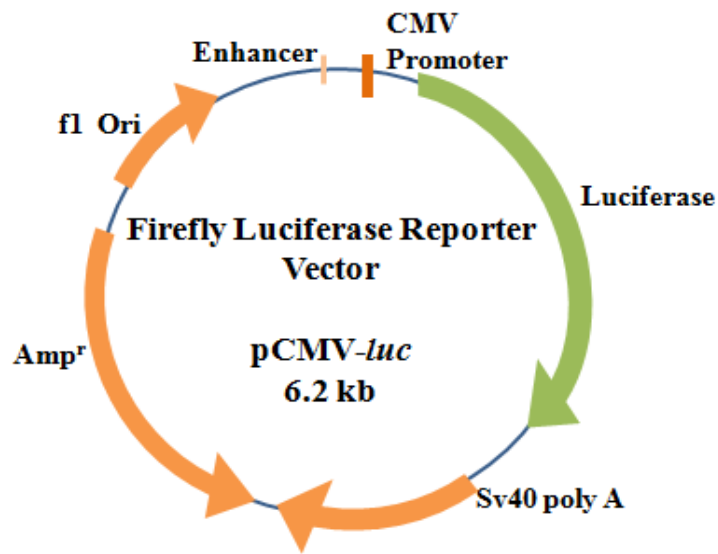


**Figure 2.5:** Map of the pCMV-*luc* vector. The vector is driven by the cytomegalovirus (CMV) promoter and consists of the cDNA of the firefly luciferase (*luc*) gene and an ampicillin resistance (Amp<sup>r</sup>) gene for selection (adapted from <http://www.plasmidfactory.com>, accessed 07/02/2014).

### 2.1.2.5. Preparation liposome-DNA complexes or lipoplexes

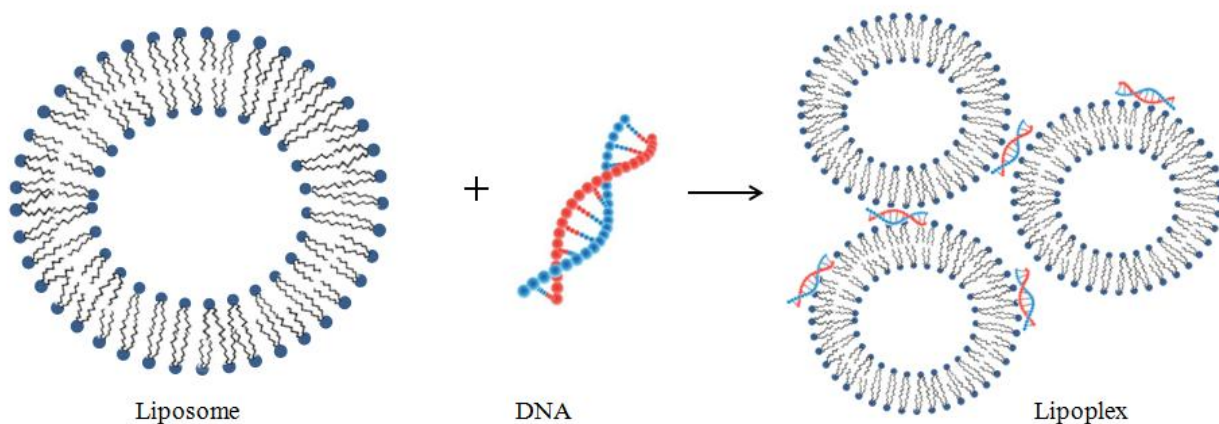


**Figure 2.6:** Lipoplex formation from the simple interaction of a liposome with DNA. Image of DNA sourced from Icke, 2010.

Varying amounts of liposome preparation were incubated with plasmid DNA of a constant concentration, resulting in the production of the lipoplex (Figure 2.6). All liposome preparations were vortexed and sonicated in a bath sonicator for 5 minutes before use. The liposome samples were incubated with pCMV-*luc* DNA for 15 – 30 minutes at room temperature to enable complex formation. For targeted formulations, liposomes were incubated with EGF as described above in section 2.1.2.3. Thereafter, 1  $\mu\text{g}$  of pCMV-*luc* DNA was added and the resulting liposome-EGF-DNA containing suspensions were vortexed and allowed to incubate at room temperature for 15 minutes, for formation of targeted lipoplexes.

## 2.2. Liposome and Liposome-DNA Characterisation

### 2.2.1. Materials

Uranyl acetate (American Chemical Society-ACS grade reagent) of molecular weight 425.15 Daltons, depleted of radioactivity was obtained from Ted Pella Inc. Ultra pure DNA grade agarose was acquired from Bio-Rad Laboratories, Richmond, USA. Ethidium bromide and 2-[4-(2-hydroxyethyl)-1-piperazinyl] ethanesulphonic acid (HEPES) was obtained from Merck, Darmstadt, Germany. Targeting ligand hEGF was purchased from Roche Diagnostics, Mannheim, Germany. Human EGF ELISA Kit (hEGF) (96 tests) for protein analysis was

obtained from Invitrogen Corporation, Camarillo, CA 93012. All other chemicals were of analytical grade.

## **2.2.2 Methods**

### **2.2.2.1 Transmission Electron Microscopy**

Cationic liposome preparations were diluted 1:5 with HBS to promote fluidity of the samples. Aliquots of 1  $\mu$ l of each diluted sample were placed on Formvar-coated copper grids with a 1  $\mu$ l aliquot of 1% (w/v) uranyl acetate negative stain. The coated grids were then allowed to stand for 3 – 5 minutes after which the excess liquid was removed with filter paper. The samples were immediately vitrified by plunging into liquid nitrogen-cooled propane gas at -183 °C, using a spring-loaded Leica CPC system (Vienna, Austria). Grids were then transferred to a GATAN cryotransfer system and viewed using a JEOL 1010 (Tokyo, Japan) transmission electron microscope (TEM) without warming above -150°C. The electron micrographs obtained from this negative staining – vitrification methodology, were digitally captured using an Olympus MegaView III camera and SIS iTEM software (Tokyo, Japan), which also facilitated measurements of liposomes on the calibrated image.

#### **2.2.2.2. Zeta sizing and Zeta potential determination**

Liposome and lipoplex preparations described below were analysed for particle size and  $\zeta$ -potential using nanoparticle tracking analysis (NTA). Initially liposomes were vortexed for 5 minutes followed by sonication for a period of 10 minutes. Plain and EGF-targeted lipoplex formulations were prepared as described in section 2.1.2.5. Thereafter, the liposome and lipoplex suspensions were diluted 1:1000 ( $v/v$ ), and vortexed for 1 minute prior to analysis. This dilution ensured sample concentrations were maintained between  $10^6$ –  $10^9$  particles/ml. All measurements were taken in HBS (diluted to 3% in 18 Mohm H<sub>2</sub>O, pH. 7.0), with a dielectric constant of 80. The NTA experiments were performed on each formulation using the NanoSight NS500 system (Malvern Instruments Ltd., Worcestershire, UK). Measurements were read at 25°C.

The NanoSight NS500 system was first configured by priming the fluidics of the operating system and ensuring that the stage zero position/thumbprint was appropriately centralized and focused prior to sample analysis. Two 90 s video images were captured with the samples undergoing Brownian motion and under electric current (24V, current maintained between 40 – 60  $\mu$ A). Four 30 s video images were captured thereafter to correct for the effects of electro osmosis, and the detection threshold set to discount any crossing over of particle tracks. The system tracks each particle and its speed through the sample, using a 405 nm laser with high sensitivity. All data are presented in chapter 3, section 3.1.3, and contain the mode and standard error across all video image data obtained for each sample. The analysis of liposomes and lipoplexes was carried out using the NanoSight nanoparticle tracking analysis software v3.0 (Malvern Instruments Ltd., Worcestershire, UK).

#### **2.2.2.3. Agarose gel retardation analysis**

A 1% agarose gel was prepared by dissolving 0.2 g of agarose in 18 ml 18 Mohm water. This was then heated to boiling until the solution was clear. Once the temperature dropped to approximately 75°C, 2 ml of 10 x electrophoresis buffer was added. This was followed by the addition of 1.5  $\mu$ l of ethidium bromide (1  $\mu$ g/ml). Once the temperature had dropped to approximately 65°C, the gel was poured into a sealed gel tray containing an 8 well comb. The gel was allowed to set for 45 -60 min. A fixed amount of pCMV-*luc* DNA (0.5  $\mu$ g) was added to increasing amounts of cationic liposome, as shown in Table 2.2. These were made up to a final volume of 10  $\mu$ l with HBS. Complexes were allowed to incubate for 30 minutes at room temperature. Thereafter 2  $\mu$ l of gel loading buffer (50% glycerol, 0.05% bromophenol blue, 0.05% xylene cyanol) was added to all samples. The samples were subjected to electrophoresis on 1% agarose gels in a Bio-Rad mini-sub electrophoresis tank containing 1 x electrophoresis buffer (36 mM Tris-HCl, 30 mM sodium phosphate, 10 mM EDTA pH 7.5), for 90 minutes at 50 volts. The gels were thereafter viewed under UV transillumination and images captured using the Vacutec Syngene G:Box gel documentation system (Syngene, Cambridge, UK).

**Table 2.2:** Liposome mass range tested for DNA binding. pCMV-*luc* DNA was used at a constant amount of 0.5  $\mu\text{g}$  in each lipoplex preparation.

<b>Lipoplex</b>	<b>Liposome test range (<math>\mu\text{g}</math>)</b>							
<b>Chol-T - DNA</b>	0	1	1.5	2	2.5	3	3.5	4
<b>MS09 – DNA</b>	0	4	4.5	5	5.5	6	6.5	7
<b>Chol-T-PEG - DNA</b>	0	2	2.5	3	3.5	4	4.5	5
<b>MS09-PEG - DNA</b>	0	3.5	4	4.5	5	5.5	6	6.5

#### **2.2.2.4. Liposomal display of hEGF protein for targeted formulations**

To confirm the presence of the EGF polypeptide on the surface of the prepared liposome formulations, an EGF ELISA kit was employed. All reagents were allowed to equilibrate to room temperature. Liposomes were prepared as described in section 2.1.2.5 in accordance with optimal levels for DNA binding as determined by agarose retardation analysis. EGF-liposomes were diluted 1:200 using the standard diluent buffer supplied with the kit. Two 8 well antibody coated strips were used on a 96 well microtitre plate. One strip was used for determination of hEGF protein standards ranging from 0 – 250 pg/well, and the second for analysis of targeted liposome formulations in duplicate (100  $\mu\text{l}$ /well). One well containing only 100  $\mu\text{l}$  of standard diluent buffer served as a chromogen blank.

Once all the samples had been added to the coated wells in the plate, they were gently mixed by tapping the side of the plate. This increases the availability of the samples to the antibody. The plate was then covered with a plate cover and allowed to incubate at room temperature for 2 hrs. Post incubation the residual fluid was removed and the wells washed four times using a working wash buffer (25x wash buffer stock diluted 1:24), to dissolve any precipitated salts. The wash buffer was left to incubate in the wells for 15 – 20 seconds between each wash. This was followed by the addition of a biotin conjugate (100  $\mu\text{l}$ ) and incubation for 1 hr at room temperature. Wells were then aspirated and washed (4x) with the working wash buffer.

Thereafter 100 µl of streptavidin – horse radish peroxidase working solution (contains 3.3 mM thymol) (viscous 100x stock in glycerol diluted 1:100 with streptavidin-HRP diluent) was introduced to all test and standard wells except the blank and incubated at room temperature for 30 min. Thereafter the solution was removed and the wells washed as previously described. The stabilised chromogen (tetramethylbenzidine – TMB) was introduced to the wells at 100 µl/well and the plate incubated at room temperature in the dark for 30 mins to allow for the development of the blue colour. At the end of this incubation 100 µl of stop solution was added to each well, and after gentle mixing a colour transition from blue to yellow was noted.

Within 2 hrs of adding the stop solution, absorbances of the samples were read at 450 nm using a Mindray MR-96A microplate reader (Vacutec, Hamburg, Germany). A standard curve was produced using the standard absorbance values obtained and the concentration of EGF on targeted liposome samples determined, indicating the presence of hEGF.

#### **2.2.2.5. Nuclease Protection Assay**

To determine the degree of protection afforded to the plasmid DNA cargo against nuclease attack, lipoplexes were prepared for analysis, as per Table 2.2. Varying amounts of cationic liposome, as determined from retardation studies, were added to a constant amount of pCMV-*luc* DNA (1 µg). This was made up to a volume of 10 µl with HBS. The samples were allowed to incubate for 30 minutes at room temperature. Foetal bovine serum (FBS) was thereafter added to the complexes to a final concentration of 10%. Two controls were employed, a negative control containing pCMV-*luc* DNA only, and a positive control consisting of pCMV-*luc* DNA and FBS. The samples were then incubated for 4 hours at 37°C. Post incubation, ethylenediaminetetraacetic acid (EDTA) was added to the samples to a final concentration of 10 mM together with sodium dodecyl sulphate (SDS) at a final concentration of 0.5% (<sup>w</sup>/<sub>v</sub>). This was followed by further incubation for 20 minutes at 55°C. Samples were subjected to electrophoresis on a 1% agarose gel (as per 3.2.2.1) for 120 minutes at 50 volts. Images were captured using the Vacutec Syngene G:Box gel documentation system as in 2.2.2.3.

**Table 2.3:** Varying liposome quantities tested for nuclease protection. DNA was constant at 1  $\mu\text{g}$  and EGF used at 1  $\mu\text{g}$  for all targeted formulations.

<b>Liposome Preparation</b>	<b>Liposome (<math>\mu\text{g}</math>)</b>		
Plain			
<b>Chol-T – DNA</b>	4	5	6
<b>MS09 – DNA</b>	11	12	13
<b>Chol-T-PEG - DNA</b>	7	8	9
<b>MS09-PEG - DNA</b>	10	11	12
Targeted			
<b>Chol-T-EGF – DNA</b>	4	5	6
<b>MS09 – EGF-DNA</b>	11	12	13
<b>Chol-T-PEG- EGF-DNA</b>	7	8	9
<b>MS09-PEG- EGF-DNA</b>	10	11	12

#### 2.2.2.6. Ethidium bromide intercalation assay

In order to ascertain the ability of the liposomes to compact DNA an ethidium displacement or ethidium bromide intercalation assay was carried out on a Glomax™ multidetection system set at an excitation wavelength of 520 nm and an emission wavelength of 600 nm. Initially 2  $\mu\text{l}$  (0.2  $\mu\text{g}$ ) of an ethidium bromide stock solution (100  $\mu\text{g}/\text{ml}$ ) was added to 100  $\mu\text{l}$  of HBS in a single well of a black 96 well culture plate. This baseline measurement was recorded as a relative fluorescence of 0%. Subsequently a representative 100% relative fluorescence was determined by introducing 4.8  $\mu\text{l}$  (1.2  $\mu\text{g}$ ) of pCMV-*luc* DNA to the mixtures. Thereafter 1  $\mu\text{l}$  (2.5  $\mu\text{g}$ ) aliquots, of liposome preparation were systematically added to the mixture until a plateau in readings was reached. In order to ensure an accurate reading the solution was mixed by vortexing the plate for 2 seconds before each reading to promote dispersion of the liposome suspension thereby allowing for complete compaction of the DNA. The results obtained were plotted relative to the 100% fluorescence value. The procedure explained was then performed for all Chol-T, MS09, Chol-T-PEG, MS09-PEG and targeted liposome varieties assayed.

### **2.2.2.7. Statistical analysis**

A comparison of the particle sizes of the different lipoplexes was analyzed using a paired student t-test and the one-way ANOVA test. *P* values of less than 0.05 were considered to be of statistical significance. All statistical analysis on particle size was carried out using the Graphpad prism 6.0 software analysis system (©2015 GraphPad Software, Incorporated) based on the mean diameter of 5 liposome particles in the TEM imaging frame. These sizes were then evaluated against each formulation prepared and examined in the same manner. Particle size based on NTA analysis (section 2.2.2.2.) was additionally assessed for significant variation between the different samples.

## **2.3. Transfection and Cytotoxicity Analyses *in vitro***

### **2.3.1. Materials**

CHO-K1 and HepG2 cells together with irradiated foetal bovine serum (FBS) were obtained from Highveld Biological (PTY) LTD., Lyndhurst, South Africa. Eagle's Minimum Essential Medium (MEM) containing Earle's salts and L-glutamine together with the trypsin-versene and penicillin/streptomycin mixtures was purchased from Lonza BioWhittaker, Walkersville, USA. Lipofectin<sup>®</sup> reagent was obtained from Invitrogen life technologies, Invitrogen Corporation, Carlsbad, CA. The pCMV-*luc* and pCMV-*GFP* vectors were purchased from the Plasmid Factory, Bielefeld, Germany. The Luciferase Assay kit was obtained from the Promega Corporation, Madison, USA. The bicinchoninic acid (BCA) assay reagents were purchased from the Sigma-Aldrich Co., St. Louis, USA. The YI-12 (C75H97N17O19) competitive peptide was synthesized by GL Biochem, Shanghai. Phosphate-buffered saline (PBS) tablets were purchased from Calbiochem, Canada. The MTT salt (3-(4,5-dimethylthiazol-2-yl)- 2,5-diphenyltetrazolium bromide) was purchased from Merck, Darmstadt, Germany. All sterile plastic ware for tissue culture were obtained from Corning Inc., Corning, NY, USA. All other reagents were of analytical grade.

## **2.3.2. Methods**

### **2.3.2.1. Cell Culture Procedure and Cell Maintenance**

Ampoules of cryopreserved HepG2 and CHO-K1 cells were removed from storage in a biofreezer (-80°C) and thawed to 37°C. Cells were sedimented by centrifugation at 1000 rpm for 5 minutes. Upon reconstitution of the pellet into fresh complete medium (EMEM + 10% foetal bovine serum +100 µg / ml penicillin, 100 µg/ ml streptomycin) under aseptic conditions, cells were maintained in a semi confluent state until the log phase of cell growth was reached.

Cells were trypsinised once they had reached confluency. For trypsinisation the spent medium was decanted and cells washed with 5 ml of phosphate buffered saline solution (PBS; 150 mM NaCl, 2.7 mM KCl, 1 mM KH<sub>2</sub>PO<sub>4</sub>, 6 mM Na<sub>2</sub>HPO<sub>4</sub>; pH 7.5), followed by the addition of 1 ml of trypsin-versene to dislodge the cells from the culture flask. The trypsinisation process was monitored under a Nikon TMS inverted light microscope (Nikon, Tokyo, Japan) until cells had rounded off. Thereafter, 2 ml of serum containing medium was introduced to the flask to halt the trypsinisation procedure. Culture flasks were then firmly tapped against the palm to completely dislodge cells. The cells were then seeded into multiwell plates for the various analyses or split in predetermined ratios into separate flasks containing 5 ml of complete medium, or alternatively cryopreserved (2.3.2.1a) for future use. Growing cells were supplemented with fresh growth medium when needed ensuring maintenance of pH and elimination of waste products.

#### **2.3.2.1.1. Cryopreservation of cells**

Following trypsinisation, cells were pelleted by centrifugation at 1000 rpm for 5 minutes. Pelleted cells were resuspended in 0.9 ml EMEM + 10% FCS and 0.1 ml of a cryoprotective medium dimethylsulphoxide (DMSO). Cells were then aliquoted into 2 ml cryovials and frozen at a rate of -1°C per minute in a Nalgene™ “Mr Frosty” Cryo 1°C freezing container containing isopropanol to a temperature of -70°C. Cells were stored temporarily in a -80°C biofreezer (Nuaire, Lasec Laboratory and Scientific Equipment), or in liquid nitrogen for long term storage.

### 2.3.2.2. Transfection Studies

#### 2.3.2.2.1. MTT growth inhibition analysis

The control cell line CHO-K1 and targeted cell line HepG2 cells were trypsinised and seeded into two 48 well plates at seeding densities of  $1.6 \times 10^4$  and  $8.16 \times 10^4$  cells/well respectively, and incubated at  $37^\circ\text{C}$  for 24 hours to allow for attachment of cells. The cells were prepared by replacing the spent medium with fresh complete growth medium (EMEM+FBS+antibiotics). All liposome solutions were briefly sonicated prior to formation of reaction complexes with the pCMV-*luc* DNA. Three concentrations correlating with the sub-optimal, optimal and supra-optimal DNA binding ratios as determined from retardation studies (Table 2.3) were used for lipoplex preparation as outlined in section 2.1.2.5. Once formed the lipoplex formulations were introduced to the cells. The assays were carried out in triplicate. Cells were incubated for 48 hours at  $37^\circ\text{C}$  in a Steri-cult  $\text{CO}_2$  incubator HEPA Class 100 (Thermo-Electron Corporation, Waltham Massachusetts, USA).

Following the incubation period, cells were assayed for growth inhibition using the MTT cell proliferation assay. For the assay, the spent medium in each well was removed and replaced with fresh medium (200  $\mu\text{l}$ ) and MTT reagent (200  $\mu\text{l}$ ; 5  $\text{mg ml}^{-1}$  in sterile PBS, pH 7.4). The plates were allowed to incubate for 4 hrs at  $37^\circ\text{C}$ . Thereafter, the medium was carefully removed and 200  $\mu\text{l}$  of DMSO added to each well to ensure cell permeation and solubilisation of formazan crystals (Figure 2.7). Absorbances were read at 540 nm using a Mindray MR-96A microplate reader (Vacutec, Hamburg, Germany). The percentage cell viability was calculated using the following formula: % cell survival =  $[A_{540 \text{ nm}} \text{ treated cells}] / [A_{540 \text{ nm}} \text{ untreated cells}] \times 100$ .

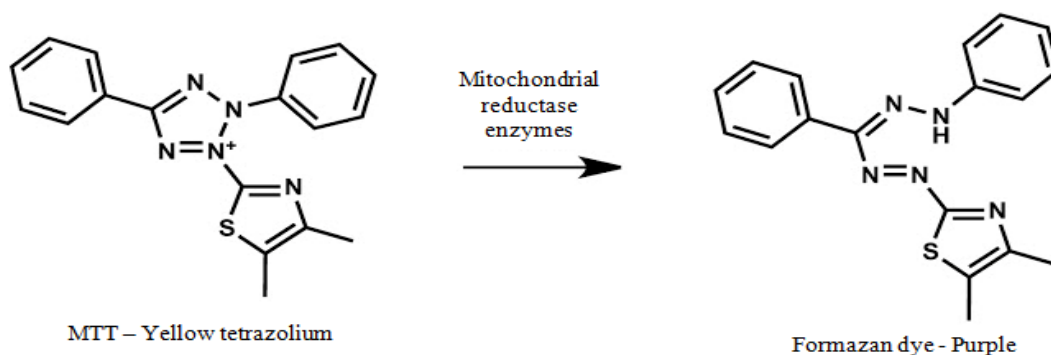


**Figure 2.7:** Reaction showing the reduction of MTT by mitochondrial succinate dehydrogenase enzymes to the MTT-formazan product (Heasley, 2012).

#### **2.3.2.2.2. Reporter gene analysis**

Both cell lines were trypsinised and seeded into two 48 well plates at seeding densities of  $2 \times 10^4$  cells/well and then incubated at 37°C for 24 hours. The cells were allowed to attach and grow to semi-confluence. The transfection complexes were prepared in triplicate as described in section 2.1.2.5 and Table 2.3. The cells were prepared by discarding the medium and replacing it with 0.5 ml fresh complete medium (EMEM + 10% foetal bovine serum + antibiotics). The transfection complexes were then added to the cells. Two controls were set up, one containing cells only and the other containing cells and naked DNA (1 µg). The cells were then incubated at 37°C for 48 hours. Following the incubation period, the cells were assayed for luciferase activity as described below (2.3.2.2.2a).

#### **2.3.2.2.2a. Luciferase Assay**

The luciferase assay was carried out using the Promega Luciferase Assay kit. The luciferase assay reagent (20 mM tricine, 1.1 mM magnesium carbonate hydroxide pentahydrate, 2.7 mM magnesium sulphate, 0.1 mM EDTA, 33.3 mM dithiothreitol, 270 µM coenzyme A, 470 µM luciferin, 530 µM ATP), was prepared by adding 10 ml of the luciferase assay buffer to one vial of lyophilised luciferase assay substrate. The cell culture lysis reagent (5x) (25 mM tris-phosphate, pH 7.8; 2 mM dithiothreitol, 2 mM 1,2-diaminocyclohexane – N, N, N'N'- tetra-acetic acid, 10% (v/v) glycerol, 1% (v/v) triton X-100), was diluted with distilled water to produce a 1x stock. Both reagents were allowed to equilibrate at room temperature.

The cells were prepared by first removing the growth medium and carefully washing twice with PBS. Approximately 80 µl of 1x cell lysis reagent was added to the wells to cover the cells and the multi-well plate was then placed on a Scientific STR 6 platform shaker for 15 minutes at 30 rev /min. Thereafter the attached cells were dislodged from the wells using a cell scraper and the resultant cell suspension was briefly centrifuged (5 seconds) in an Eppendorf microcentrifuge at 12 000 x g to pellet the debris. The cell free extracts (supernatant) were retained to be assayed for luciferase activity and protein content. For the luciferase assay 20 µl of each cell free extract was transferred to a white 96 well plate, to which 50 µl of luciferase assay reagent was

immediately introduced, thoroughly mixed and luminescence immediately read using a GloMax™ multidetection system (Promega Biosystems, Sunnyvale, USA). Protein determination was performed on the cell free extracts using the bicinchoninic acid (BCA) assay, and readings obtained using the Mindray MR-96A microplate reader preset for protein determination at 562 nm. All luminescence readings were normalized against the protein content and expressed as relative light units per milligram protein (RLU/mg protein)

#### **2.3.2.2.2b. Competitive transfection in HepG2 Cell Line**

Competitive HepG2 cellular transfection was conducted as described below, in the presence of the YI-12 synthetic peptide. Synthesis of this peptide (NMR spectra provided in Appendix 3) was based on the GE11 synthetic peptide produced by Li *et al.* (2005). The HepG2 (receptor positive) cell line was seeded at a cell density of  $2 \times 10^4$  cells per well into a 48 well cell culture plate. The plate was incubated at 37°C for 24 hours. Thereafter, the spent medium was replaced with 0.3 ml fresh complete medium (MEM+Antibiotics+10%FBS). The targeted lipoplexes were prepared and allowed to incubate at room temperature as detailed in section 2.1.2.5. During this time 25 µl (0.5 mM) of the competitive peptide YI-12 (Figure 2.8) of a 5 mM stock, was added to the cells prior to addition of the targeted lipoplexes. The peptide was allowed to incubate with the cells for 45 minutes at 37°C. Thereafter the targeted lipoplexes were introduced to compete for epidermal growth factor receptor binding. Cells were then incubated for 48 hours at 37°C. At the end of this period, the cells were assayed for luciferase reporter gene activity as outlined in section 2.3.2.2.2a.

#### **Tyr-His-Trp-Tyr-Gly-Tyr-Thr-Pro-Gln-Asn-Val-Ile**

**Figure 2.8:** Amino acid sequence of the Y-12 EGF competitor peptide

#### **2.3.2.2.2c. Lipofectin® mediated transfection**

To assay for transfection activity, cells were added to a 48 well plate at a seeding density of  $6.6 \times 10^4$  cells/well and incubated overnight. Thereafter, the growth medium was removed, cells washed with 0.25 ml PBS and replenished with fresh medium. Lipofectin®: DNA complexes

were prepared according to manufacturer's protocol in quadruplicate. Lipofectin<sup>®</sup> reagent (4, 6, 8, 10 µg), and pCMV-*luc* (1 µg) were separately diluted in 25 µl serum free EMEM. These individual solutions were allowed to stand at room temperature for 30 min. They were thereafter combined and incubated for a further 15 min at room temperature, for formation of lipoplexes. Lipoplexes were then introduced to the cells according to the given transfection protocol and cells were allowed to incubate for 48 hrs at 37°C. Thereafter luciferase activity was determined as per the luciferase assay protocol outlined in section 2.3.2.2.a.

#### 2.3.2.2.d. GFP reporter gene Analysis

Both HepG2 (receptor positive) and Cho K1 (receptor negative) cells were seeded at cell densities of  $1.2 \times 10^5$  and  $1.6 \times 10^5$  cells per well respectively, into a 12 well cell culture plate and incubated for 24 hours at 37°C. Thereafter, the spent medium was replaced with fresh complete medium. EGF-targeted and untargeted lipoplexes were prepared as described in section 2.1.2.5 with pCMV-GFP (plasmid map shown in Figure 2.9) at a DNA concentration of 0.25 µg/µl and final EGF/pDNA ratio equivalent to 1:1 (<sup>w/w</sup>). Lipoplexes were introduced to the cells and incubated at 37°C for 48 hours.

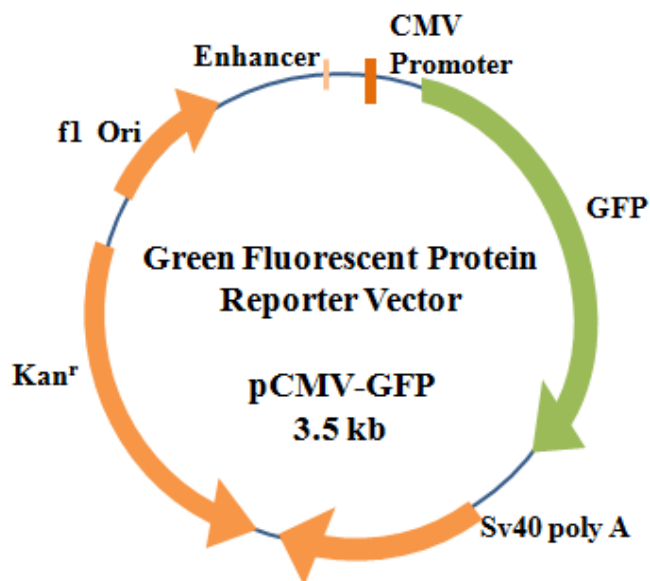


**Figure 2.9:** Map of pCMV-GFP reporter vector. The vector expresses the green fluorescent protein (GFP) reporter gene and the kanamycin resistance ( $Kan^r$ ) gene. The GFP gene is driven by the cytomegalovirus immediate-early (CMV) promoter ((adapted from pCMV-*luc* plasmid map <http://www.plasmidfactory.com>, accessed 07/02/2014).

### **a. Flow Cytometry**

GFP expression was further quantified by flow cytometry using the Accuri C6 Flow cytometer (BD Biosciences, trademark property of Becton, Dickinson, and Company; ©2013 BD). Prior to use, the flow cytometer was configured for accuracy each day through routine processing of eight peak bead samples followed by the six peak bead samples. This confirmed the run parameters were in the correct working order. For quantification of green fluorescent protein expression, the 488 nm laser was used with the cytometer filter set at 533/30 for the FL1 detector. The standard laser configuration for the BD Accuri C6 is the three Blue – one Red, within which the 533/30 filter is in the FL1, 585/40 in FL2, 670 LP in FL3, 675/25 in FL4. Once the cytometer was prepared the transfected cell populations were examined. For analysis the cells in the 12-well plate were trypsinised using 0.1 ml trypsin-versene. To this 0.2 ml of complete medium was immediately introduced and the contents of each well transferred to micro-centrifuge tubes and centrifuged at 1000 rpm for 5 minutes. Thereafter, the supernatant (cell free medium) was removed and the pelleted cells resuspended in phosphate buffered saline (PBS).

FACS analysis was carried out on all samples based on GFP expression determined via the recording of 10000 events over a 1 minute period (total of 30000 events). A back-flush was carried out between the additions of the different samples to ensure that there was no contamination across readings. In comparison to the non-expressing control, GFP expression in a population of cells was examined and relevant histograms obtained for analysis. Data analysis was performed using the FloJo analysis software from TreeStar Inc., Ashland, Oregon, USA.

#### **2.3.2.2.3. Statistical analysis**

Statistical analyses were performed using ANOVA (one-way analysis of variance), (GraphPad Prism version 6, GraphPad Software Inc., USA). The Dunnett multiple comparison and Tukey honestly significant difference (HSD) tests were used as post hoc test comparatives between groups and a preset control, and across groups, respectively. *P* values less than 0.05 were regarded as significant.

## CHAPTER THREE

### 3. RESULTS AND DISCUSSION

#### 3.1. Synthesis and Characterization of Non-Viral Liposome Systems

##### 3.1.1. Liposome and lipoplex preparation

Four cationic liposomes were successfully prepared as per Table 2.1., following the thin film rehydration method outlined in section 2.1.2.3. The four EGF targeted preparations were also successfully formulated by addition of the EGF polypeptide post synthesis, to two previously synthesized cytofectins, Chol-T (Singh *et al.*, 2001) and MS09 (Singh and Ariatti, 2006) respectively. The chemical composition and structure of the cytofectin is an important factor determining the physical and chemical properties of liposomal formulations, the level of cytotoxicity and transfection activities, and cellular interaction (Zhao *et al.*, 2011). Each cytofectin in this study was synthesized to display four components that confer charge (head group), stability (anchor), and binding potential and biodegradability (spacer and linker bond). While the Chol-T preparation displays a carbamoyl linker bond and a three carbon spacer arm, the MS09 cytofectin presents a 15Å spacer arm length (Singh and Ariatti, 2006). Both cationic lipids display the dimethylamino head group and a cholesterol ring anchor. Inclusion of such cationic lipids confer liposomes with a net positive charge that would enable nucleic acid binding, in addition to enhancing the attachment to cell surface molecules (sulphated proteoglycans and sialic acids) that exhibit a negative surface charge (MacLachlan, 2007).

The liposome preparations, separated into untargeted (plain and stealth) and targeted (plain and stealth) liposomes were formulated with each of the cytofectins at a 50% mole composition. The neutral lipid DOPE was the helper lipid used for all formulations, and is known to impact significantly on the overall functionality of the liposome. DOPE serves to improve interactions with cell membranes through its fusogenic capabilities, particularly at the endosomal level, where membrane disruption and cargo release is crucial (Litzinger and Huang, 1992; Farhood, *et al.*, 2005; MacLachlan, 2007). Moreover, liposome structure can be affected by the interaction of the cationic and neutral lipid constituents. Here interaction of the cytofectin headgroup of either Chol-T or MS09 offers a potential ion-pair formation that could have a knock on effect on the

physiochemical lipid-bilayer surface and solvent-lipid relationships (Ferrari, 2001). Mukherjee and co-workers (2005) have proposed a formulation to improve cationic lipid based cellular transfection *in vivo*, using combined equimolar quantities of the neutral lipids DOPE and cholesterol, for cases where the cationic-DOPE liposomes have shown to be ineffective in transfection in comparison to cationic-cholesterol liposomes (Zhu and Mahato, 2011).

The positive nature and fusogenic characteristics of these liposomes, makes it possible for non-specific interactions to occur. Hence, the transient shielding of the vector using the polymer polyethylene glycol (PEG) was included so as to positively impact on gene delivery (Chen, *et al.*, 2011). This protective shielding is thought to result in increased circulation times of the lipoplexes especially *in vivo*, which is advantageous for improved gene/drug delivery (Torchilin, 2005, MacLachlan, 2007, Opanasopit, *et al.*, 2011). It has been previously observed that the percentage composition of this polymer influences the interaction of the liposome with DNA. It was observed by Singh and coworkers (2011) that the use of a 5% molar composition of PEG seemed to obscure the positive charge of the liposome resulting in higher binding ratios and lower transfection. Hence, a 2% molar composition which proved favourable was employed for the stealth liposomes investigated in this study.

The EGF polypeptide was used to provide targeting potential to the liposome formulations in an effort to improve their liver cell specific transfection. While the asialoglycoprotein receptor has proved effective and popular in this regard, the rapid internalisation of the EGF-EGFR system into coated pits could prove to be an alternative for targeting liposomes to the liver (Buñuales *et al.*, 2011). The abundance of the EGF receptor on the hepatocyte cell surface further supports the inclusion of this small polypeptide as a targeting moiety.

Liposome-DNA complexes or lipoplexes have been described over the years to form in a number of ways, thereby producing numerous morphological configurations. Cationic liposomes are known to form spontaneous associations with the negative backbone of the DNA through ion-pair interactions. It has also long been accepted that cationic colloids interact at the surface with the DNA, compared to DNA binding through entrapment by negatively charged vesicles. These

liposomes show, in general, a relative retention of size and shape upon complexation, despite known condensation effects (Behr, 1986; Felgner and Ringold, 1989; Gershon *et al.*, 1993).

This packing morphology of the lipoplex affects cellular transfection efficiency. Some documented morphologies are the: ‘beads on a string’ (Felgner and Ringold, 1989), spaghetti and meatballs (Sternberg *et al.*, 1994); the phase models such as the inverted hexagonal phase ( $H_I$ ) (Klibanov *et al.*, 1990), and the multilamellar structure ( $L^C_a$ ) (Ishii *et al.*, 2001), as well as the map-pin and sliding columnar phase (O’Hern & Lubensky, 1998). Due to the dynamic and rapid binding observed between DNA and cationic liposomes, Pozarski and colleagues (2003) proposed that this complex production could be an endothermic process, driven by entropic inflation resulting from counterions being released from between the lipid bilayers and the DNA (Pozarski, and MacDonald, 2003; Ewert *et al.*, 2004). This formation produces a simultaneous collapse of the DNA structure. The condensation and compaction were examined in the present study with the results discussed in section 3.2.2.

Factors other than liposome composition also affect lipoplex formation and morphological characteristics. This includes the method of preparation e.g. the introduction of DNA to the cationic liposome seems to produce incremental increases in the size of lipoplex particles, whereas the addition of liposome to DNA, has been found to display no drastic change in lipoplex size. Other factors include ionic strength, temperature and charge ratio (N/P ratio of lipid/DNA) (Zhu and Mahato, 2011).

### **3.1.2. Transmission electron microscopy of liposome and lipoplexes**

Cryogenic transmission electron microscopy (Cryo-TEM) was used to ascertain the general morphology and average size of liposome and lipoplex formulations within a specific field of view. The system has proved an effective tool over the years, being suitable for protein solutions and liposomes, as it retains the aqueous integrity of the sample through rapid vitrification and offers high resolution (Rangelov *et al.*, 2010; Fox *et al.*, 2014). Cryo-TEM also provided a platform from which to discern the physical effects of the liposome constituents. In this regard, the Chol-T and MS09 untargeted plain liposomes appeared as distinctly spherical structures with slight invaginations along the circumference as seen in Figures 3.1.a., and 3.2.a. respectively.

This corresponds to earlier TEM studies by Singh and co-workers (2001; 2006; 2011) of plain liposome formulations. The Chol-T and MS09 liposomes were found to be between 42 – 135 nm and 104 – 250 nm in size respectively. While an apparent size differential exists between the two size ranges, particle aggregation, may contribute to some of the increased size effects observed.

**Table 3.1:** The mean diameters of the various liposome suspensions examined. The data are presented as means,  $\pm$ S.D. (n = 5).

Preparation	Liposome		Lipoplex		EGF-Lipoplex	
	Mean diameter (nm)	Standard deviation (nm)	Mean diameter (nm)	Standard deviation (nm)	Mean diameter (nm)	Standard deviation (nm)
<b>Chol-T</b>	77.81	43.92	65.72	44.35	58.10	24.09
<b>Chol-T-PEG</b>	75.80	28.74	104	21.59	99.35	63.66
<b>MS09</b>	131.96	64.79	54.71	22.18	57.83	64.79
<b>MS09-PEG</b>	92.36	52.46	59.98	19.44	104.25	46.75

The physiochemical characterization by TEM of the untargeted liposome formulations, revealed a morphological disparity between the plain and stealth functionalised liposomes (Figures 3.1. and 3.2.d) with the latter showing a more elongated structure with almost tapered ends compared to the more traditional spherical structures. Rangelov and colleagues (2010) ascribe this elliptical formation to the presentation of three dimensional objects from two dimensional images (Almgren *et al.*, 2000). Moreover, the average size diameters of the liposomes ranging between 47- 120 nm, and 65 – 200 nm show a nominal decrease in size in comparison to the plain liposomes, as can be seen in Figure 3.3. These untargeted, plain and stealth liposomes produced an overall standard deviation (n = 5) ranging from 28.74 – 64.79 nm, showing that even in this restricted viewing platform, a relatively broad size range exists within the liposome suspensions.

In terms of the lipoplex variations, it is understood, based on DNA binding interaction that the lipoplex is a condensed structure. The level of this DNA condensation and compaction is

examined later in the ethidium dye exclusion analysis (section 3.2.2). From the electron micrographs of Figures 3.1 and 3.2 the plain and stealth formulations appear to favour the formation of agglutinates, mostly produced from smaller sized particle aggregation. The Chol-T and Chol-T-PEG lipoplexes displayed a tendency to form smaller clusters with individual lipoplexes of varying size ranges. In contrast, the MS09 lipoplexes showed an irregular, almost continuous aggregation of the smaller lipoplexes, with singular unattached lipoplexes close to the larger aggregates. MS09-PEG lipoplexes showed a propensity to present as sac-like formations, housing smaller lipoplexes within. The overall lipoplex average sizes (Figure 3.3.) inclusive of aggregates were generally small, with the Chol-T-PEG and MS09-PEG lipoplexes however appearing larger, by comparison. Aggregation such as this is not an uncommon occurrence in cationic lipid–DNA interactions (Bordi *et al.*, 2004; Sennato *et al.*, 2005).

Targeted lipoplexes, that included the EGF polypeptide (1EGF : 1DNA ;  $w/w$ ), produced a drop in lipoplex size for Chol-T based targeted plain and stealth lipoplexes. The lipoplexes appear to be bound in a membranous film, within which lipoplexes of smaller sizes reside. In particular, the Chol-T-EGF lipoplexes (Figure 3.1.c), present as individual sac like structures containing numerous small lipoplexes, with the average size range observed between 25–90 nm. In comparison, MS09-EGF lipoplexes showed smaller aggregate clusters and individual lipoplexes present in close proximity to each other within the observed population, with sizes ranging between 30–188 nm. The Chol-T-PEG-EGF and MS09-PEG-EGF lipoplexes (Figure 3.1.f., and 3.2.f.) indicate a more linked lipoplex structure, while the targeted Chol-T-PEG lipoplexes appeared to be encased in a membranous network, and the MS09-PEG-EGF lipoplexes produced the more common grape-like or berry-like structure. Letrou-Bonneval and co-workers (2008) described similar grape-like morphologies for lipoplex structures in their effort to produce a multimodular non-viral gene delivery system specific for transfer to primary hepatocytes.

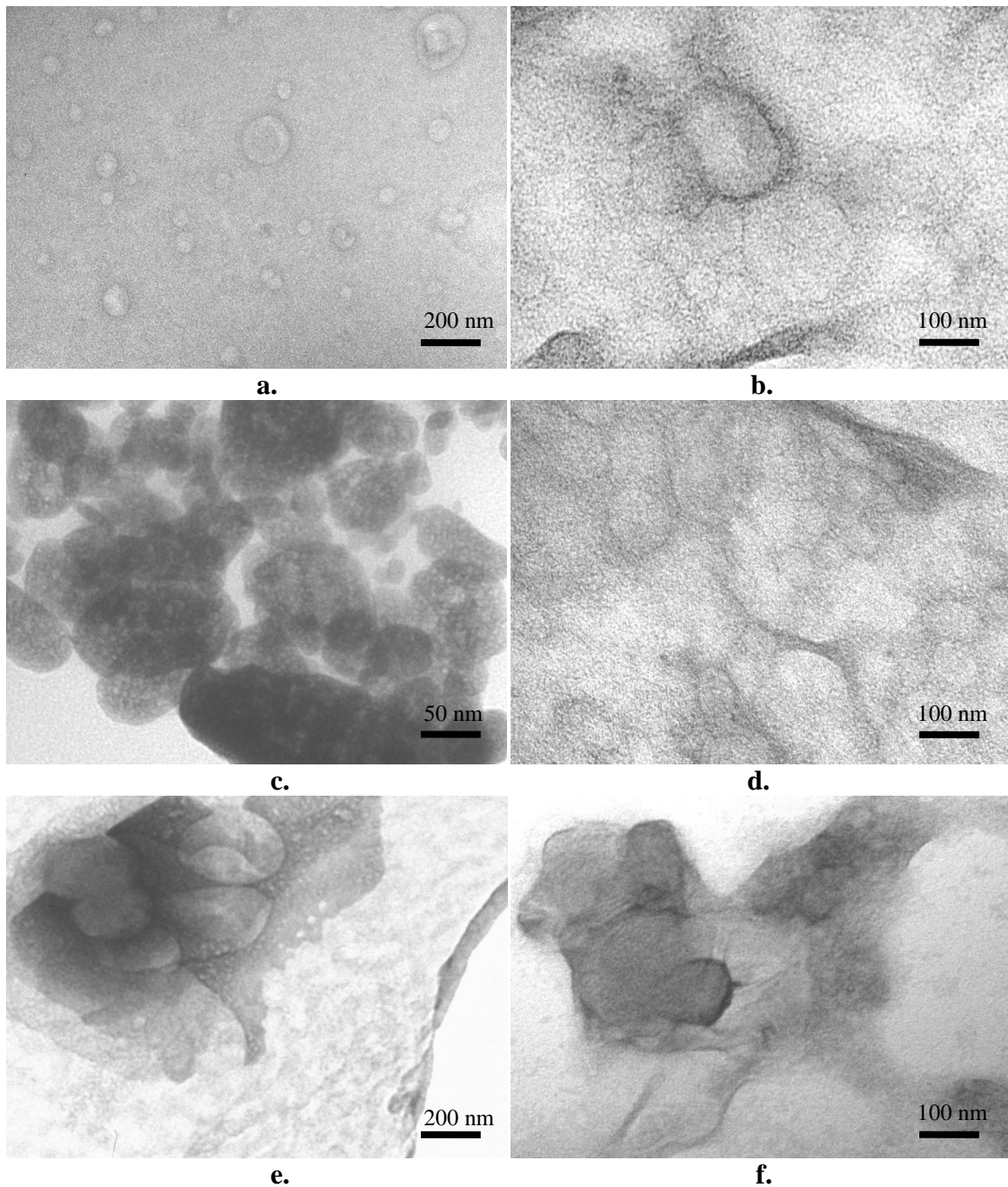


**Figure 3.1:** Transmission electron micrographs of cytofectin Chol-T based plain and stealth liposomes, Lipoplexes and EGF targeted lipoplex formulations, **a.** Chol-T, **b.** Chol-T - DNA, **c.** Chol-T-EGF - DNA, **d.** Chol-T-PEG, **e.** Chol-T-PEG - DNA, **f.** Chol-T-PEG-EGF - DNA. Lipoplexes were assembled with pCMV-*luc* DNA. Scale Bar (a, and e) = 200 nm; (b, d, and f.) = 100 nm and (c.) = 50 nm.

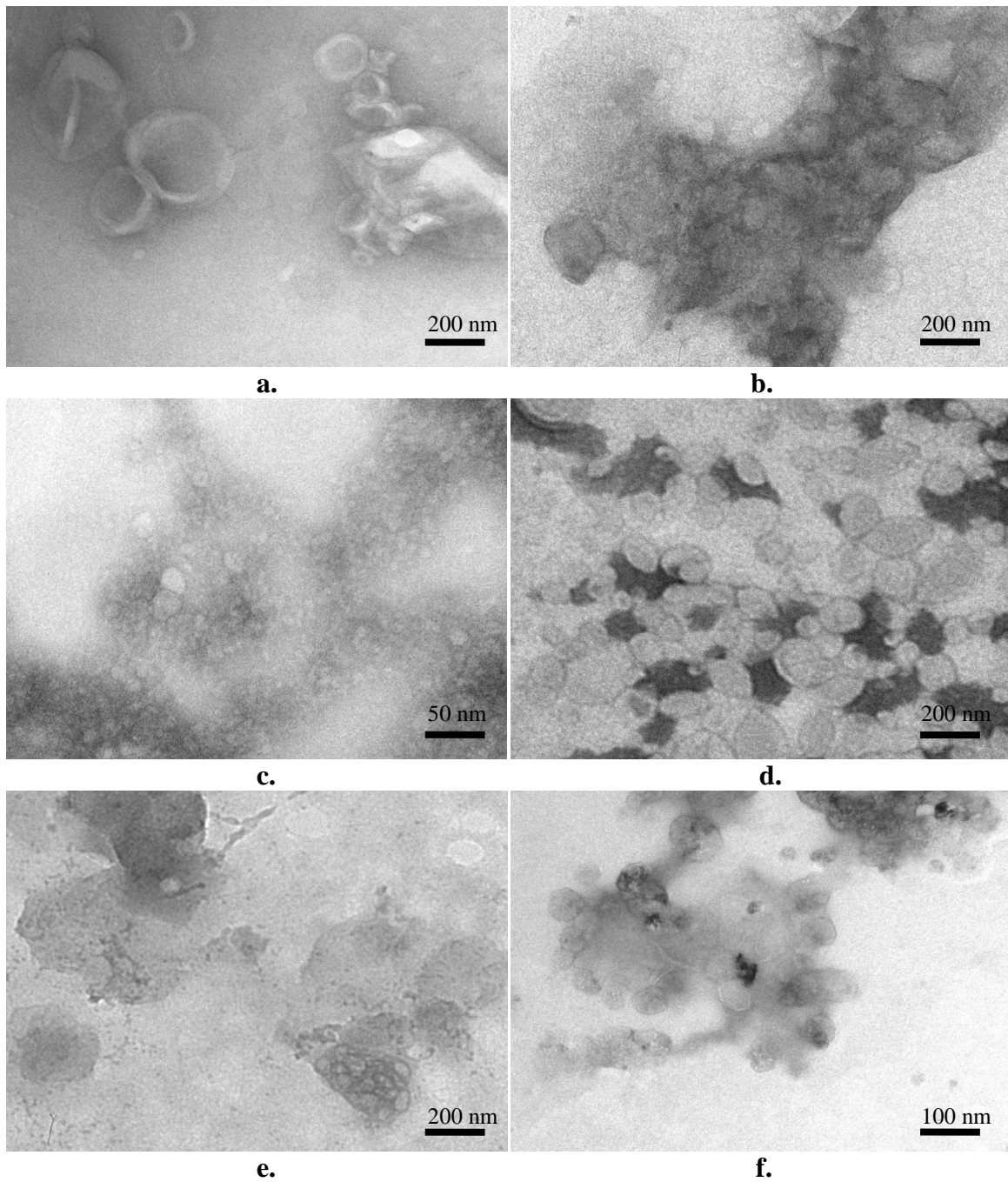


**Figure 3.2:** Transmission electron micrographs of cytofectin MS09 based plain and stealth liposomes, Lipoplexes and EGF targeted lipoplex formulations, **a.** MS09, **b.** MS09 - DNA, **c.** MS09-EGF - DNA, **d.** MS09-PEG, **e.** MS09-PEG - DNA, **f.** MS09-PEG-EGF - DNA. Lipoplexes were assembled with pCMV-*luc* DNA. Scale Bar (a, b, d, and e) = 200 nm; (f.) = 100 nm and (c.) = 50 nm.

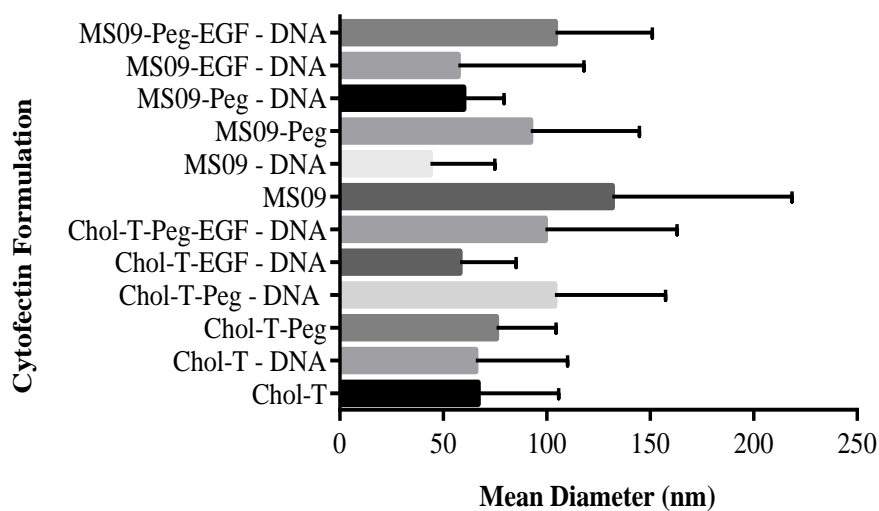


**Figure 3.3:** Bar graph depiction of average mean diameter and population size deviations as determined from Cryo-TEM micrographs  $\pm$ S.D. (n = 5).

Based on the size ranges and average size diameters provided (Table 3.1), together with the TEM micrographs, the different formulations presented as generally spherical to elliptical unilamellar structures with large size and morphology variations. This potentiates the presence of poly-dispersed sample preparations, which is supported by the large standard deviations observed for all liposome and lipoplexes preparations. However, no significant size differences were observed on comparison of each preparation.

As mentioned earlier, TEM, while useful in providing a visual understanding of liposome and lipoplex appearance and size, has drawbacks which include rapid dehydration, loss of sample, and over staining which can be accompanied by separate grid areas of under staining. These disadvantages, together with the retention of a single micrograph representation of a selected viewing area, ensured the need for complementary analysis such as nanoparticle tracking analysis (NTA).

### 3.1.3. Zeta sizing and surface potential

The *in vitro* investigation to determine cellular uptake and eventual transfection of cultured cell lines (e.g. CHO-K1 and HepG2, section 3.3) plays a vital role in the estimation of the eventual desired treatment efficiency *in vivo*. Hence, the cationic liposomes produced here were initially characterized through Cryo-TEM analysis above, in an effort to discern any physiochemical traits which could potentially affect their cellular internalization capability. These two dimensional micrographic analyses, however, cannot account for the hydrodynamic particle size, nor do they provide any evaluation of particle charge. Lipoplex size and charge are known to increase with an increase in the lipid : DNA (<sup>w/w</sup>) ratio. While the size of a liposomal carrier may not give a direct indication of transfection capability, it does influence the gene transfer to cells undergoing active endocytosis (Eastman *et al.*, 1997; Ross and Hui, 1999; Wasungu and Hoekstra, 2006; Ma *et al.*, 2007).

The need for diminutive-sized particles such as liposomes for improved rates of transfection may prove more evident *in vivo* than *in vitro* (Ma *et al.*, 2007; Pathak *et al.*, 2009). Although *in vitro* conditions attempt to mimic that of the *in vivo* environment, sedimentation factors, faster transfer, and supposedly improved cell surface contact, has often resulted in larger complexes effecting successful *in vitro* transfection. The liver fenestrae, as mentioned earlier, restrict the passage of particles into surrounding tissues. As such, the smaller complexes would be advantageous compared to the larger particles, which experience phagocytic effects and capillary entrapment. Sizes thus required for successful liver and lung gene transfer correlate to 100 – 200 nm and 40 – 80 nm respectively, in contrast to the larger 200 – 400 nm lipoplex size effective *in vitro* (Zhdanov *et al.*, 2002; Lee *et al.*, 2003; Kneuer *et al.*, 2000; Ma *et al.*, 2007; Jacobs *et al.*, 2010).

For accurate identification of liposome and lipoplex size, nanoparticle tracking analysis (NTA) was performed (section 2.2.2.2). This analysis shows superior functionality and accuracy compared to more traditional technologies, such as TEM and dynamic light scattering (DLS), as measurement is based directly on particle diffusion within the dispersion. This technique was thus applied for additional determination of zeta potential ( $\zeta$ -) within a buffered medium

(Malloy, 2011). It is important to note here, that no polydispersity index (PdI) measurement is provided from this technique. The level of particulate dispersion is rather determined through evaluation of size dimension displayed by different particle concentrations within the formulation. For the purposes of this study, particle distribution width was determined using standard deviation rather than PdI, as is required for DLS systems that are intensity weighted average (z-average) based.

A colloid system can be described as the minuscule presence of any one of the fundamental states of matter in another. Liposome systems, as with other colloid suspensions, may experience aggregate formation as a consequence of inter particle adhesion and attraction. The zeta potential is a function of the repulsive potential as considered for the DVLO theory of colloid system stability, put forward by researchers; Derjaguin, Verwey, Landau and Overbeek in the early 1940's. In this regard, the system stability is dependent on the sum of the attractive (Van de Waals) and repulsive (electric charge double-layer) forces that occur between approaching particles undergoing Brownian motion. The repulsive force provides an energy barrier to the two particles' adherence. Zeta potential has thus served as a good index for colloid particle interaction and subsequent system stability (Derjaguin and Landau, 1941; Verwey and Overbeek, 1988).

The zeta potential of a formulation has often been accepted as the measure of surface charge; however, it more accurately reflects the charge at the diffuse layer surrounding particles within a colloid dispersion. Hence, the zeta measurement provides a good estimate of colloidal stability, where particles displaying potential  $\geq \pm 30$  mV at either extreme are considered stable (Leite and Ribeiro, 2012; Honary and Zahir, 2013). With a distance of only  $\approx 0.2$  nm between the actual particle surface to the diffuse layer, the zeta potential measurement offers a realistic evaluation of particle behaviour within the suspension. At a more positive zeta potential, lipoplexes may display aggregated morphologies of the multilamellar structure ( $L^C_o$ ), while more negative values would be indicative of more loosely bound nucleic acid. In this instance, low level lipid content may result in free or exposed plasmids at the external display of the liposomes (Ma *et al.*, 2007). Furthermore, this measurement is affected by the pH, conductivity (ionic constituents) of the medium and the preparation constituent concentration. An inversely

proportional relationship exists between the zeta potential and experienced bulk pH, where a negative zeta potential is observed at high pH, while low pH produces positive potentials. Isoelectric or zero potential points exist between +/- 15 mV and represents the region of highest instability, where formulations appear flocculated / or in an aggregated state (Leite and Ribiero, 2012). Higher ionic strength of the bulk suspension affects the thickness of the double layer, by producing greater compression at the surface.

The sizes and zeta potential of the different preparations listed in Table 3.2, show general small hydrodynamic sizes and negative  $\zeta$ -potential for all cytofectin based formulations. Lipoplexes of the Chol-T and MS09 liposomes displayed size increases by a factor of  $\approx 2$  compared to their un-complexed counterparts. The Chol-T liposome displayed multiple population peaks with different size dimensions, and an overall SD =  $76.6 \pm 4.2$  nm. The concentration versus size graph of the MS09 liposome produced a major peak having a smaller population size variation and lower standard deviation. This indicates that the Chol-T formulation is more polydispersed and heterogeneous in nature than the MS09 cationic liposomes. Both lipoplex formulations can be considered polydispersed following irregular peak presentation and population size with a standard deviation of  $\approx 60$  nm. These lipoplexes displayed significant ( $P \leq 0.0001$ ) zeta potential increase toward the negative for the Chol-T and MS09 liposomes. The Chol-T lipoplex zeta shift displays a stable formulation presenting zeta measurements of only just above -30 mV.

**Table 3.2:** Sizes and Zeta potential of liposomes and lipoplexes.

Preparation	Lipid : DNA (w/w)	Liposome		Lipoplex		EGF-Lipoplex	
		<sup>a</sup> Particle size (nm) ± SE	<sup>a</sup> ζ-Potential (mV) ± SE	<sup>a</sup> Particle size (nm) ± SE	<sup>a</sup> ζ-Potential (mV) ± SE	<sup>a</sup> Particle size (nm) ± SE	<sup>a</sup> ζ-Potential (mV) ± SE
Chol-T	5	100.9 ± 3.4	-23.0 ± 0.1	181.3 ± 26.1****	-47.9 ± 0.8****	74.3 ± 1.0####	-22.3 ± 1.9####
Chol-T-PEG	8	171.6 ± 8.8	-14.3 ± 0.6	113.2 ± 10.8***	-33.7 ± 0.8****	88.0 ± 1.3****	-20.8 ± 0.9###
MS09	12	68.4 ± 1.7	-30.6 ± 0.3	132.3 ± 9.7	-41.7 ± 0.2**	79.8 ± 2.3##	-23.4 ± 1.9 <sup>b</sup> *c.####
MS09-PEG	11	125.2 ± 10.6	-18.7 ± 0.8	118.9 ± 4.4	-41.2 ± 2.7****	101.9 ± 3.6	-15.3 ± 2.2####

<sup>a</sup> Each value is representative of the mode and ±standard error (n=2) across the standard deviation. Analysis was performed over five video images per two sets of sample nanoparticle tracking. The mode presents the largest concentration of particles in each sample population displaying the indicated size. These were obtained from the concentration (particles/ml) vs. size and concentration vs. ζ-potential peaks for each liposome and lipoplex assessed for size and Zeta potential (Appendix 2).

<sup>b</sup> \**P* < 0.05, \*\*\**P* < 0.001, \*\*\*\**P* < 0.0001 vs. original liposome formulations;

<sup>c</sup> #*P* < 0.05, ####*P* < 0.001, #####*P* < 0.0001 vs. the untargeted lipoplexes.

Chol-T-PEG and MS09-PEG liposomes were found to be larger in comparison to the plain-non-stealth liposomes. This is in contrast to earlier knowledge of PEGylated liposomes and current TEM analysis (3.1 and 3.2). These liposomes upon complexation with DNA produced a decrease in particle size as determined by the largest particle concentration peak. Here again the Chol-T cytofectin based formulation showed greater variation in size within the formulation (SD = 84 ± 13.1 nm), compared to that observed for the MS09-PEG preparation. On comparison, the lipoplex variants show the MS09-PEG lipoplex to be more heterogeneous in nature, with particle concentration peaks displaying almost individual size distributions (SD = 73 ± 20.1 nm).

The zeta measurements observed, are indicative of lipoplexes with highly negative ζ-potential, allowing greater formulation stability compared to the liposomes which border on the zero-ζ-position (±15 mV). Hence, the PEG-liposomes seem to present as weak to strong aggregates at

any time, as well as displaying a propensity to continuously combine forming agglomerates. This fact could account for the larger hydrodynamic size observed for these liposomes, which is not in agreement with the stabilizing effect often seen with PEG-liposomes. As such, it can be proposed that the mushroom presence of the PEG moiety is not at a sufficient density to overcome particle – particle aggregation (Leite and Ribiero, 2012; Yin and Alivisatos, 2005; Jun *et al.*, 2006).

The addition of the EGF targeting moiety to the liposomal formulations produced a ubiquitous size decrease from that observed for the original liposome or lipoplex. The Chol-T, Chol-T-PEG and MS09-EGF targeted preparations displayed a size range of 74.3 nm – 88 nm with an average  $\zeta$ -potential of  $\approx -22$  mV. This was indicative of these formulations exhibiting moderate stability with a potential for aggregate formation, which is in accordance with Cryo-TEM micrographs (Figure 3.1, and 3.2 c. and f.) of these lipoplexes. In spite of potential aggregation, relatively small sizes were observed, which is in contrast to previous EGF-lipoplex size determinations. Furthermore, Buñuales and co-workers (2011) reported positive zeta potentials for cationic lipoplexes bearing EGF targeting at higher EGF : DNA concentrations (up to 5:1), while results reported here were on an EGF : DNA ( $^w/w$ ) of 1:1 at pH 7.0. The MS09-PEG-EGF lipoplex displayed the largest size of all targeted formulations, together with  $\zeta$ -potential which is reflective of high instability in suspension. This potential for high level aggregation as observed for Cryo-TEM studies may also affect downstream cytotoxicity. The particle concentration versus size curves for all preparations showed mostly polydispersed formulations, with the exception of the Chol-T-EGF lipoplex. The population size display of this lipoplex shows the overlay peaks lying closely within the same size range or population width, which is indicative of a more mono-dispersed suspension.

The reduced zeta potential of these EGF lipoplexes can be postulated to be due to the post-formulation introduction of the EGF moiety to the liposomes disrupting the bilayer and producing lower level stabilisation (Marqués-Gallego and de Kroon, 2014). Additionally, the incorporation of the negatively charged EGF polypeptide produced a more positive  $\zeta$ -potential probably due to the naturally acidic nature of the peptide. The reduced pH of this suspension could also result in the observed zeta shift (Benedetta *et al.*, 2002; Gratton *et al.*, 2008; Honary and Zahir, 2013).

## 3.2. Liposome – DNA Interactions

### 3.2.1. Agarose gel retardation

The agarose retardation or electrophoretic mobility shift assay was first described more than three decades ago. It is a simple and commonly used methodology for the investigation of DNA : lipid interactions. This assay allows for the determination of the ability of the positively charged liposome molecules to completely neutralize the negatively charged DNA phosphate backbone creating electroneutral complexes with restricted electrophoretic migration patterns (Huang *et al.*, 1998; Hasegawa *et al.*, 2002). The net charge presented by the lipoplex is known to affect the transfection capability of the lipoplex, since the lipoplex surface charge is a determining factor for lipoplex interaction either *in vitro* or *in vivo*. The charge ratio of the liposome : DNA complexes is a primary point of interest for determination of colloidal properties, rather than the constitution of the lipoplex (Zhu and Mahato, 2011; Segura, 2003). Positive and negative charge ratios are known to present different packaging of the nucleic acid with the lipidic component. Neutral lipoplex charge display approaching 1 has in general shown a tendency toward agglomeration (Zhdanov *et al.*, 2002). Higher charge ratios have been found effective under *in vitro* conditions, while the *in vivo* environment may necessitate the need for reduced surface charge. Increases in charge ratio are known to produce increases in zeta potential, which may be coupled with non-specific interactions within the cellular environment as well as potential cytotoxicity (Segura, 2003; Ma *et al.*, 20007; Zhu and Mahato, 2011).

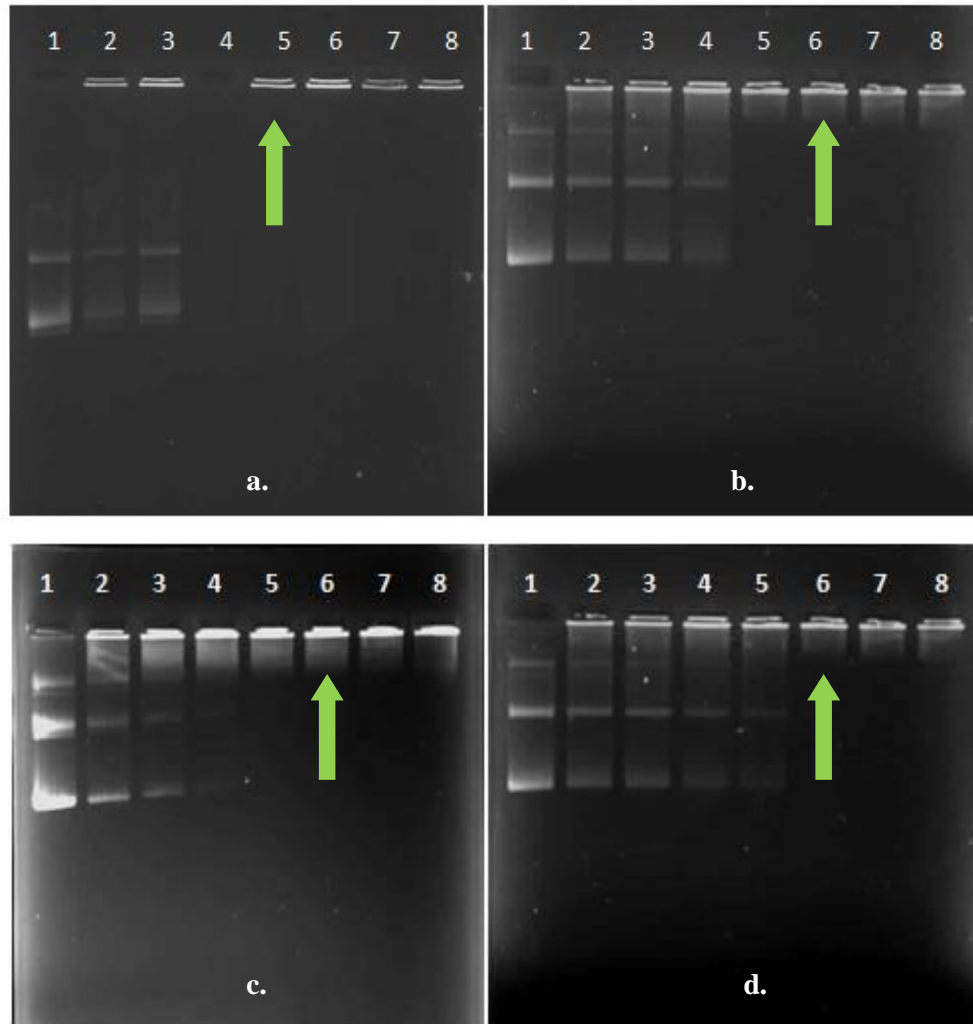


**Figure 3.4:** Agarose retardation gels showing liposome – DNA binding of the different reaction mixtures tested. Preparations made up in 20 mM HEPES, 150 mM NaCl (10  $\mu$ l, pH 7.5) consisted of varying amounts of liposome in lanes 1 – 8 (shown below), while the pCMV-*luc* DNA was maintained at a constant 0.5  $\mu$ g. a. Chol-T : DNA, (0, 1, 1.5, 2, 2.5, 3, 3.5,4  $\mu$ g), b. MS09 : DNA, (0, 4, 4.5, 5, 5.5, 6, 6.5, 7  $\mu$ g), c. Chol-T-PEG : DNA, (0, 2, 2.5, 3, 3.5, 4, 4.5, 5  $\mu$ g), d. MS09-PEG : DNA, ( 0, 3.5, 4, 4.5, 5, 5.5, 6, 6.5  $\mu$ g).

**Table 3.3:** DNA : Liposome ratios for complete and optimal binding

Liposome Preparation	Optimal Retardation conditions		
	Liposome ( $\mu\text{g}$ )	DNA: Liposome Ratio (w/w)	DNA: Liposome Charge Ratio (-ve/+ve)
Chol-T : DNA	2.5	1 : 5	1 : 1.3
MS09 : DNA	6	1 : 12	1 : 2.9
Chol-T-PEG : DNA	4	1 : 8	1 : 2
MS09-PEG : DNA	5.5	1:11	1 : 2.6

The four liposome preparations were assessed for their ability to bind to the pCMV-*luc* plasmid DNA. The DNA was kept constant (0.5  $\mu\text{g}$ ) while the liposomal formulations were varied in concentration. From the agarose gels presented in Figure 3.3, it can be seen that the different formulations were able to effectively bind the DNA at the point of electroneutrality. Chol-T (Figure 3.3a.) produced DNA binding with the lowest concentration of liposome when compared to MS09, Chol-T-PEG, and MS09-PEG. The MS09 liposomes required 6  $\mu\text{g}$  (Figure 3.3b.) to completely bind DNA. At the point of electroneutrality, the negatively charged DNA is completely bound and cannot migrate toward the anode as seen at lower liposome : DNA ratios, where the different conformations of the DNA are still visible on the agarose gel. Hence for the MS09 lipoplex, a higher positive charge (Table 3.3) was observed.

PEG functionalised Chol-T and MS09 liposomes resulted in good DNA binding, however, as with the MS09 plain liposome, each of these PEGylated liposomes were required at higher amounts in order to completely neutralize the negatively charged pCMV-*luc* DNA. Consequently, higher charge ratios were observed with binding occurring at 1:2 and 1:2.6 for Chol-T-PEG and MS09-PEG respectively. The PEG moiety was included in formulations on the basis of predicted improved liposomal stability and enhanced shelf-life, through minimisation of non-specific interactions this. However, this was not confirmed by the zeta potential observed for these liposomes, which was closely related to the region of system instability (Zhu and Mahato, 2011).

Despite all formulation calculations of charge ratio being within the net positive range,  $\zeta$ -measurements differed, exhibiting moderate to highly negative potential within the suspension. The possibility exists that some of the cytofectin positive charge may be presented within the lumen of the liposomes. However, it is important to note that this only gives an indication of the charges available based on cytofectin present, and not the overall lipoplex surface charge.

Based on the evidence produced, it can be noted that the optimal DNA binding ratio for each liposome was successfully determined. For a thorough analysis of the charge effect on the effectivity of the liposome formulation, the sub-optimal, optimal, and super-optimal ratios were evaluated in further investigations. These ratios were also employed for the preparation of EGF targeted lipoplexes, based on effective liposome–DNA binding.

### **3.2.2. Ethidium bromide intercalation**

The binding of a liposome carrier to DNA has long been understood to result in a condensed lipoplex structure. Scazello and colleagues (2005) described a ‘ring-like’ pattern as a consequence of DNA compaction by cationic liposome formulations. This condensation is believed to produce an ordered toroidal structure of DNA. Additionally, the lipid component has been found to undergo condensation and modification of its own, during the complexation process (Bloomfield, 1997; Xu *et al.*, 1999; Simberg *et al.*, 2001; Scarzello *et al.*, 2005).

This property of the lipoplex systems prepared here, was assessed by the ability of the liposome formulations to displace the intercalating ethidium bromide dye from the DNA. This assay is based on measurement of the intense fluorescence produced on DNA base pair intercalation of the ethidium dye, which gradually diminishes upon liposome inclusion. The ability to condense DNA to a particular level would impact on the point and rate of DNA release from the carrier (Xu and Szoka, 1996; Lasic *et al.*, 1997). The displacement of the ethidium bromide by introduction of the respective liposome formulations can be seen in Figure 3.5.a. and b.

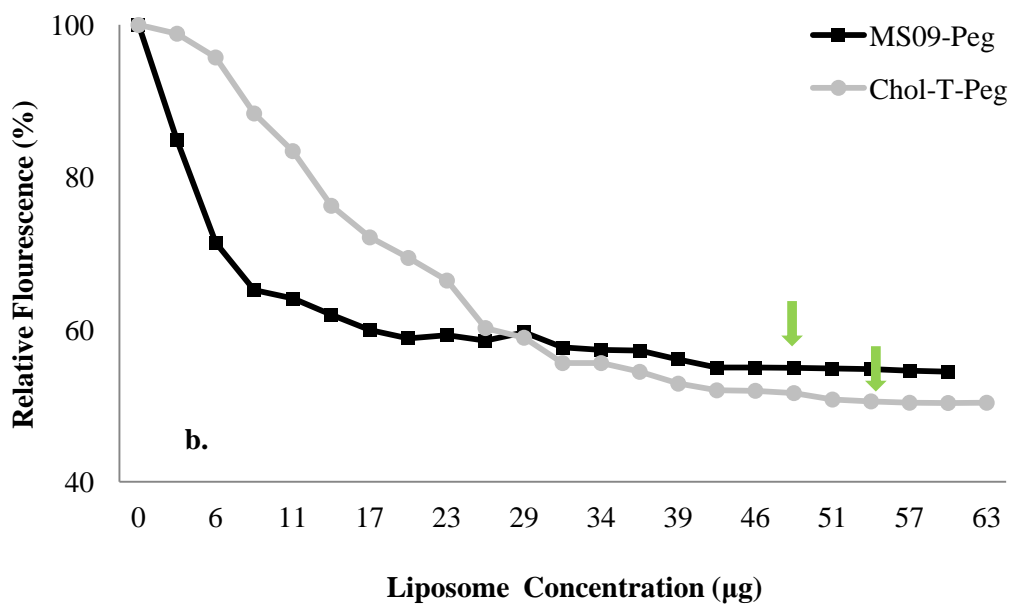
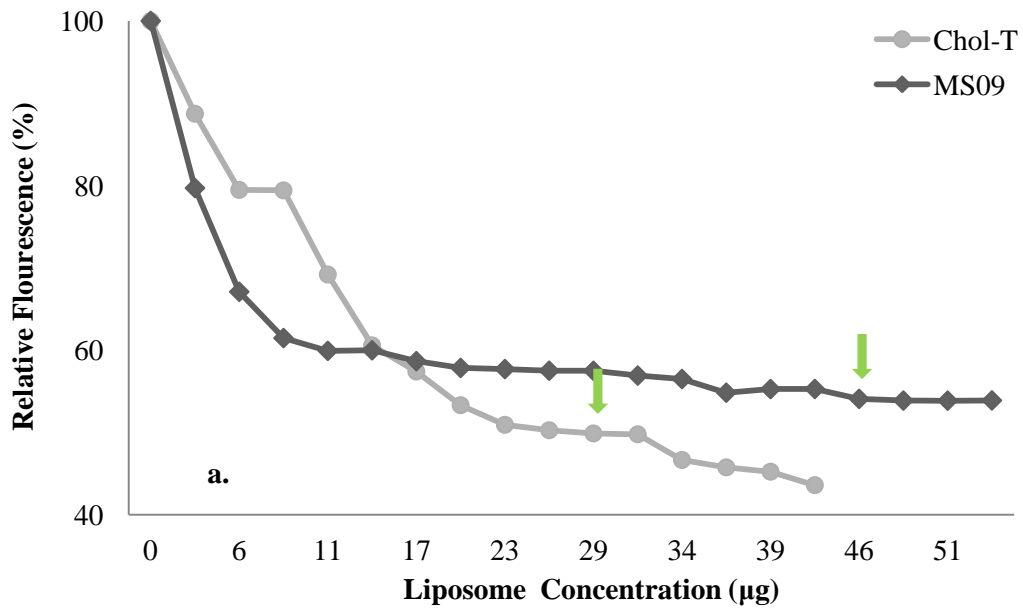


**Figure 3.5:** Ethidium bromide intercalation assay for cationic liposomes in a total of 100 µl incubation mixtures containing 1.2 µg pCMV-*luc* DNA and increasing amounts of liposome in HBS. a. Chol-T, and MS09; b. Chol-T-PEG, and MS09-PEG.

All liposome formulations were able to successfully displace the ethidium bromide dye from the DNA, producing a quenching of the fluorescence until a plateau in fluorescence readings was observed. At this point no further reduction in fluorescence will occur as the DNA is maximally compacted. Any drop in fluorescence will be due to turbidity brought about by the high concentration of the liposomal suspension. This assay is hence often considered a good corroborative assessment of the gel mobility shift analysis. With the exception of the Chol-T liposome, the Chol-T-PEG, MS09, and MS09-PEG liposomes all produced binding and condensation of the plasmid DNA at lower liposome concentrations than were obtained for agarose DNA binding determinations. These liposomes were able to produce condensation of the DNA at a DNA : lipid ( $^w/w$ ) ratio of 1: 6.98, 1: 8.5, and 1: 7.25, respectively. The Chol-T liposome in correlation with retardation analysis showed binding at 1: 5.06 ( $^w/w$ ).

An average drop in fluorescence was observed ranging from 45 – 53 % over all examined preparations. At the lower levels of fluorescent decay, the strength of condensation of the pCMV-*luc* plasmid is reduced. This may result in early release of the nucleic acid, exposure to nucleases and ultimately degradation of the DNA cargo. A steep decline in fluorescence, could suggest too compact a complex, which could prove disadvantageous for vector-DNA dissociation which is required for effective transgene transfection and expression. By and large, all preparations examined displayed good DNA condensing capability. The rate of fluorescence reduction, may also serve as a good indicator of complex stability. Hence it can be observed that the Chol-T-PEG and MS09-PEG liposomes (Figure 3.5.b) exhibit an initial rapid decrease in fluorescence, followed by gradual plateau formation. This coupled with the lower overall percentage drop in fluorescence could be postulated as being indicative of less stable liposome dispersions. This is in accordance with  $\zeta$ -potential determinations, which were above -30 mV and around the  $\pm 15$  mV range of instability and known flocculent formation. MS09 produced the most gradual decline toward electroneutral DNA complexation, corroborating higher potential stability determined by  $\zeta$ -measurements. Of all the evaluated liposomes, the Chol-T formulation was required at the lowest concentrations to produce effective DNA binding and condensation.

### 3.2.3. Liposomal display of hEGF protein for targeted formulations

In order to effectively exploit the excessive display of EGF receptors by HepG2 cells for improved hepatotropic capability, EGF, a polypeptide containing 53 amino acid residues was introduced to preformed liposomes. The amount of EGF added to the cationic liposomes was based upon the predetermined ratios obtained from agarose gel retardation studies (section 3.2.1) at optimal liposome-DNA binding.

To ascertain if the EGF-liposomes were able to successfully display the EGF targeting ligand, the human epidermal growth factor (hEGF) ELISA assay was performed as described in section 2.2.2.4. This assay served as a quantitative measure of the relative prevalence of the polypeptide on each liposome. The positive identification and quantification of other targeting ligands have been performed in a similar manner or with the use of radiolabelling, e.g. quantification of the TAT peptide was accomplished by radiolabelling the TAT peptide with indium<sup>111</sup> (111-In) (Mullen and Banaszak Holl, 2011; Portnoy *et al.*, 2011).

With numerous preparation protocols available for ligand-liposome complexes, a need for some form of covalent coupling remains, although the negative charge of the EGF molecule may inevitably undergo some form of electrostatic interaction with the cationic liposomes (Buñuales, 2011).

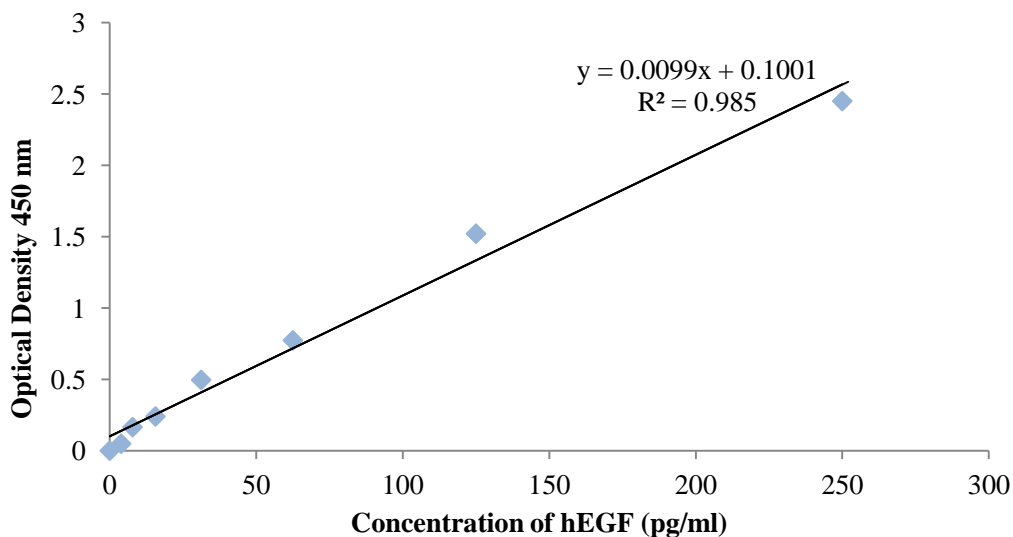


**Figure 3.6:** Standard curve of hEGF sample standards from 0 – 250 pg/ml. The linear regression equation was used to determine the concentration of the various liposome formulations.

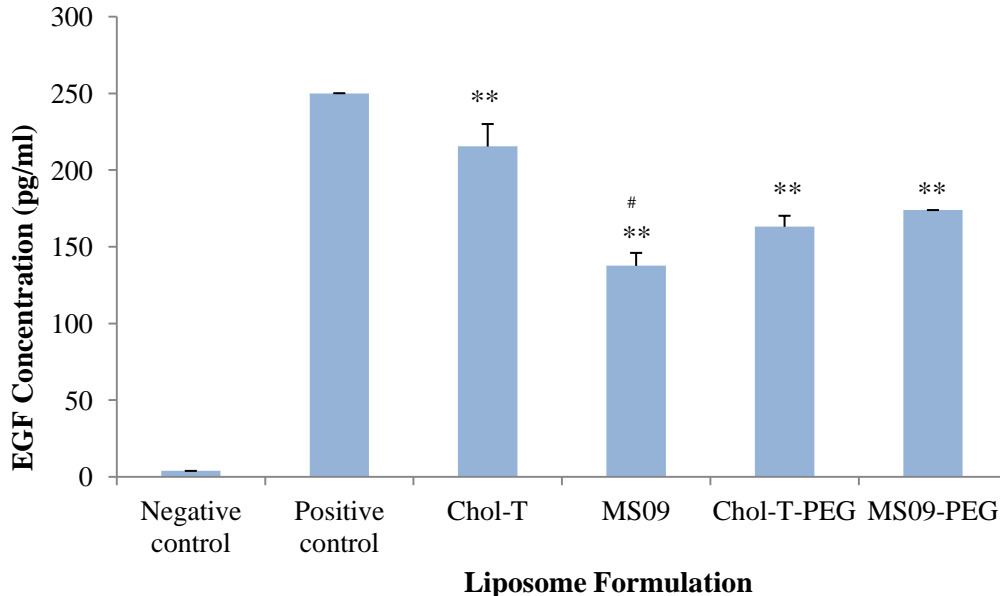


**Figure 3.7:** Concentration of EGF present in each liposome formulation as determined from the linear regression equation of Figure 3.6 above. A high positive control (250 pg/ml) was used and allowed for a clear comparative of positive EGF presence. \* $P < 0.05$ , \*\* $P < 0.01$ , vs. negative control (0.39 pg/ml); # $P < 0.05$  vs. positive control.

Two control groups were employed (positive and negative) based on the outlying EGF concentrations used to produce the EGF standard curve (Figure 3.6). These offered stable boundaries within which the presence and concentration level of EGF displayed per sample could be evaluated. All liposome formulations tested for the retention of the EGF ligand, displayed a significant (\*\* $P < 0.01$ ) concentration of EGF present. Detection of the EGF occurred following a sandwich ELISA protocol, so termed, because the hEGF antigen binds to an immobilised antibody; which is followed by the hEGF specific biotinylated monoclonal antibody which then binds to the immobilised hEGF-antibody. Finally an enzyme, streptavidin-peroxidase was introduced to produce a four member sandwich, which upon introduction of the tetramethylbenzidine chromogen substrate, produced a colour intensity allowing for the determination of the EGF concentration.

The results shown in Figure 3.7 clearly indicate the varying prevalence of EGF on each formulation. Chol-T-EGF displays approximately 215 pg/ml, the highest EGF concentration of all liposomes examined, in contrast to the MS09-EGF liposomes, which displayed the lowest

proportion of EGF (138 pg/ml). Concentrations of 163 pg/ml and 174 pg/ml for the Chol-T-PEG and MS09-PEG targeted preparations were observed. Reduced retention of the polypeptide could be attributed to steric interference from the PEG shield, as well as the longer spacer of the MS09 cytofectin component of the liposomes.

### **3.2.4. Nuclease protection Assay**

The systemic delivery of nucleic acid is limited not only by the lipoplexes physiochemical characteristics, but also to poor levels of cellular interaction, uptake and target specificity. This could be partly due to the serum nucleases present within the physiological environment that provide an additional barrier to cellular access and eventual transgene expression. Furthermore, intracellular trafficking of the complexed plasmid DNA via the endocytic pathways, can result in the DNA being completely degraded by the lysosomal enzymes. (Poutona *et al.*, 1994; Wattiaux *et al.*, 2000). This was believed to be ablated by the condensation of DNA into compact supramolecular structures capable of protecting DNA (Kisoon *et al.*, 2002). These lipoplexes, however, are still required to traverse the nuclease ridden environment, and as such, have often been limited in their transgene expression capability (Vasir and Labhasetwar, 2006; Esposito *et al.*, 2006; Obata *et al.*, 2009).

From the different DNA conformations, it has been observed that the open circular conformation, rather than either the linear or supercoiled, produces higher levels of expression. The degradation of nucleic acid in the serum, is dependent on the divalent cation activation of the DNase enzyme for DNA degradation (Hill *et al.*, 2001). Consequently metal ion chelators have been used to stop DNA degradation by this enzyme in laboratory assays. EDTA, is one such chelator, and was employed in this assay to stop the enzyme activity and to prevent any further DNA degradation. This was followed by addition of a detergent, SDS, for release of the DNA from the vector, allowing visualization of the DNA bands on the agarose gel. The lipoplexes were analysed at the sub-optimal, optimal, and super-optimal ratios as determined by the retardation studies, and the structural integrity of the DNA evaluated by agarose gel electrophoresis, as an indication of the degree of protection afforded by the liposomes. The results from the nuclease protection assay are shown in Figure 3.8.

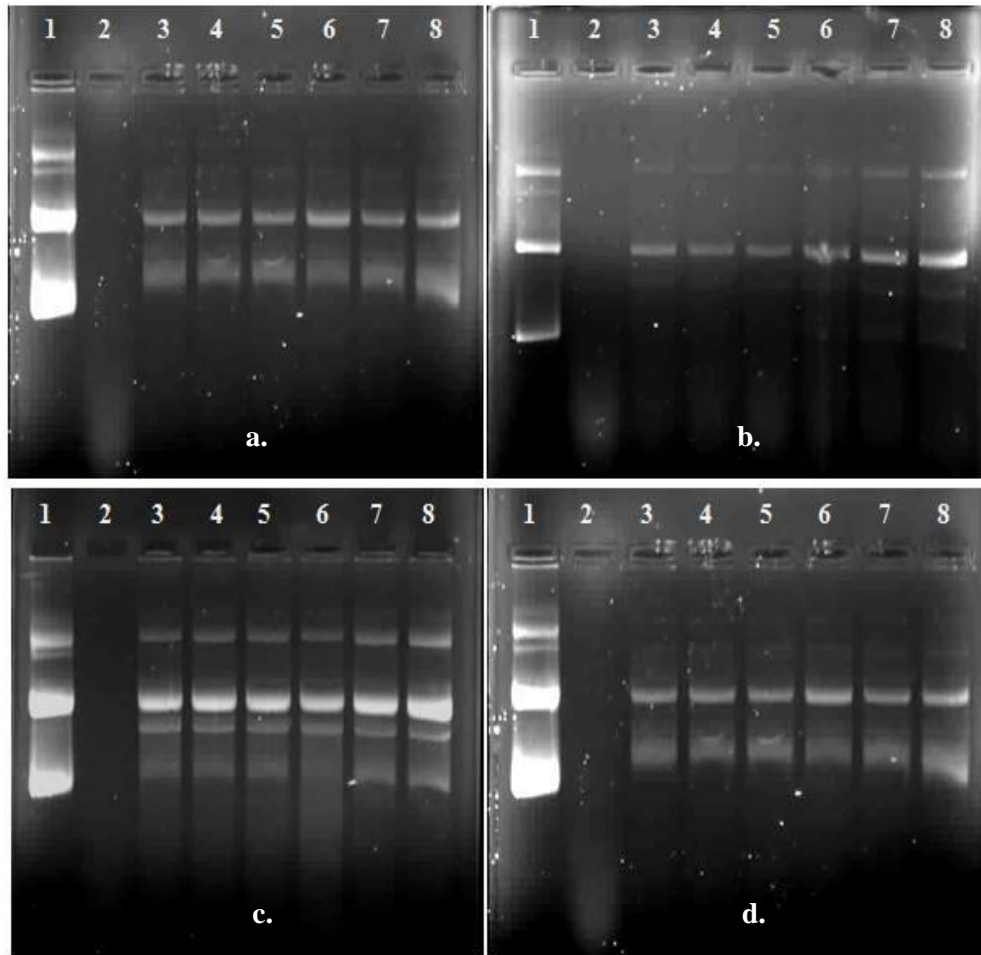


**Figure 3.8:** Serum nuclease protection assay of the DNA-cationic liposome complexes (lipoplexes) containing; a. Chol-T and MS09, b. Chol-T/EGF and MS09/EGF, c. Chol-T-PEG and MS09-PEG, and d. Chol-T-PEG/EGF and MS09-PEG/EGF, respectively. Lanes one and two were consistent over all four nuclease assessments. Lane 1: pCMV-*luc* DNA (1 µg). Lane 2: Naked pCMV-*Luc* DNA (1 µg) in the presence of 10% (v/v) serum. a. Lanes 3-5: lipoplexes with Chol-T (4, 5 and 6 µg). Lanes 6-8: lipoplexes with MS09 (11, 12 and 13µg). b. Lanes 3-5: lipoplexes with Chol-T/EGF (4, 5 and 6 µg). Lanes 6-8: lipoplexes with MS09/EGF (11, 12 and 13µg). c. Lanes 3-5: lipoplexes with Chol-T-PEG (7, 8 and 9 µg). Lanes 6-8: lipoplexes with MS09-PEG (10, 11 and 12 µg). d. Lanes 3-5: lipoplexes with Chol-T-PEG/EGF (7, 8 and 9 µg). Lanes 6-8: lipoplexes with MS09-PEG/EGF (10, 11 and 12 µg).

Having determined the binding and condensation of the untargeted liposome preparations, the next important assessment was the determination of protection afforded to the nucleic acid by the liposomes under degradative conditions. Here the untargeted (plain and stealth) liposomes were analysed in conjunction with the EGF targeted formulations, so as to ascertain the effects, if any, of the EGF polypeptide on the protection of the DNA cargo.

In each agarose gel image (Figure 3.8) a positive control of naked DNA displaying the circular, linear and supercoiled conformations was employed. A second control of naked DNA exposed to serum was used as a measure of the degradative effect of the nucleases on the plasmid DNA. Each liposome was thereafter examined against these controls to determine DNA protection within the lipoplex. As all transfection studies were carried out under the effects of serum containing medium, so as to mimic the physiological environment, the ability of the different formulations to safely transport plasmid DNA within this environment is noteworthy.

Figure 3.8.a. shows the effects of serum nucleases on the plain cationic liposomes, Chol-T and MS09. These liposomes display good DNA protection with only partial degradation or nicking of the linear and supercoiled bands observed. The nuclease digestion assessment of the EGF targeted formulations (Chol-T-EGF and MS09-EGF) is shown in Figure 3.8.b, which clearly displays a partial disintegration of the DNA to the linear conformation. The MS09-EGF liposomes appear to show improved protection of the supercoiled DNA when compared to Chol-T-EGF preparation.

Stealth formulations of Chol-T-PEG and MS09-PEG clearly indicate improved levels of DNA shielding when compared to the plain preparations. Both liposomes display only minimal nicking of the circular and partial degradation of the supercoiled conformer. Similarly the targeted formulations (Chol-T-PEG-EGF and MS09-PEG-EGF) show good protection of the plasmid DNA, although to a less extent than the non-target preparations, with loss of the linear conformation and little degradation of the supercoiled forms. The shielding properties of the PEG liposomes are evident, confirming the proposal that the PEG molecules can limit serum nuclease interaction. It has been suggested that, higher charge ratios could result in more of the DNA sites for the DNA degradation enzyme attack being blocked, allowing improved nucleic acid

protection (Narang *et al.*, 2005; Penacho *et al.*, 2008). Furthermore, the degree of protection afforded by the EGF targeted preparations could be linked to the reorganisation of the liposome bilayer resulting from post-formulation ligand attachment, and the possible rearrangement of the lipoplexes conformation with DNA. This, together with the lower charge ratio may result in some exposure of the plasmid DNA (Rao, 2010).

With the liposomes analysed exhibiting a propensity to maintain relatively good DNA integrity under standard *in vitro* conditions, these plain, stealth and targeted formulations were further assessed for their cytotoxic ability and cellular transfection potential.

### **3.3. Cell Line Maintenance and Transfection Activity**

#### **3.3.1. Cell line maintenance**

Mammalian cells in culture exhibit a rather fragile disposition, requiring gentle handling. Maintenance of the the two cell lines, CHO-K1 and HepG2 required a precise working protocol that included no vigorous action with respect to either cell line, despite firm adherence to the culture flask. Additionally the cells were at no point exposed to centrifugation above 1500 x g. Both cell lines were maintained and propagated in complete EMEM (FBS + antibiotics) for the entire duration of the study. All cell culture procedures were carried out in a class II Biohazard hood, with all cell growth and background routinely monitored using an inverted phase contrast microscope. Cell growth, as expected was associated with waste product generation and consequent pH alterations which was accomodated for by the frequent replenishment of the cells with fresh complete medium.

Both the CHO-K1and HepG2 cell lines, upon reconstitution after cryopreservation, underwent an early lag phase of approximately two weeks prior to reaching semi confluency (Figure 3.9.a. and b.). This slow initial rate of cell developement could be attributed to the prolonged period of cryopresevation, storage of cell populations already recylced to the lag phase, or previous vigorous propagation and trypsinisation. Cell numbers did improve over time, due to the production of growth factors during cellular division, and those present in the growth medium,

promoting further cell growth and development of the cell populations. Cell lines were propagated approximately 6 times prior to cryopreservation.

Both cell lines were employed to test the effectivity of the prepared targeted formulations in cell specific receptor targeting. The EGFR expressing cell line, HepG2, was selected as a positive control, and a cell model for liver targeting (Aramaki *et al.*, 2003; Buñuales *et al.*, 2011), while the CHO-K1 cell line was utilized as a receptor negative cell line, as it has been stated that they have little to no expression of the EGFR on their surface (Jo *et al.*, 2003; Slanina *et al.*, 2014).

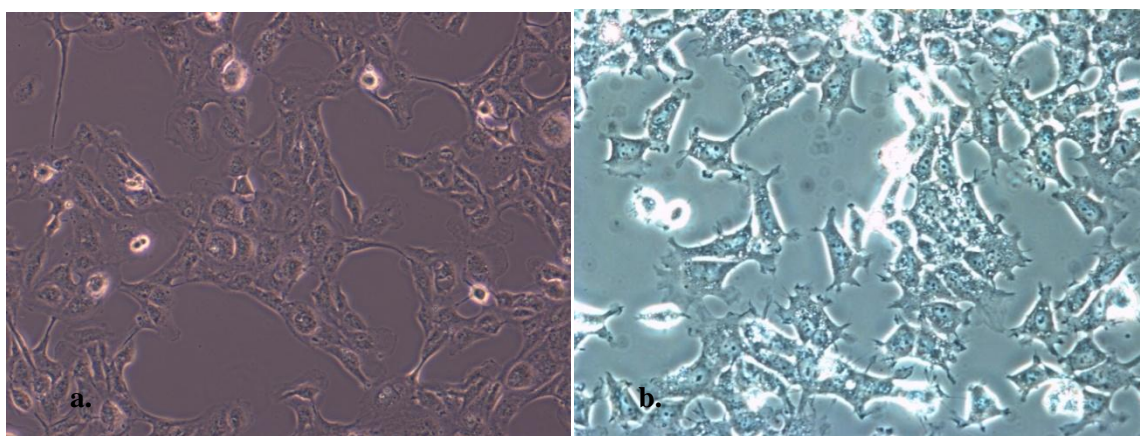


**Figure 3.9:** Semi confluent distribution of a. CHO-K1, and b. HepG2 cells, as viewed under an Olympus inverted microscope (20x)

### 3.3.2. Cytotoxicity testing

Cationic liposomes have been used to bind, protect and safely deliver the nucleic acid /drug to target cells. An often a neglected aspect of this system, is carrier-nucleic acid associated cytotoxicity. Intravenous administration of drug associated nanoparticles displaying increased target organ toxicity has been observed (Gelmon *et al.*, 1999; Gabizon, 2001). Human cell culture models, such as those employed here, were utilised in an effort to better determine the cytotoxic effect of the formulated liposomes. This *in vitro* analysis may provide an idea of the associated toxicity, prior to an animal model investigation (Wilkening *et al.*, 2003). Cationic amphiphilic constituents are known to influence the ultimate cytotoxic effect of transfection-bound lipoplexes. Thus tertiary amphiphiles are believed to be less toxic when in liposomal

formulations than their quarternary amine variants. The hydrophobic domain of the cytofectin comprising one, or more than two aliphatic chains may induce cytotoxic effects or decreased levels of cellular entry (Mahato *et al.*, 1997; Tang and Hughes, 1999; Zhi *et al.*, 2010; Zhu and Mahato, 2011).

The MTT colorimetric assay was employed for the detection of metabolic and mitochondrial activity in both the CHO-K1 and HepG2 cell lines upon treatment with different liposome formulations. The results of these cytotoxicity evaluations in both cell lines can be seen in Figures 3.10 – 3.11.

### 3.3.2.1. Cytotoxicity in the Cho K1 and HepG2 cell lines

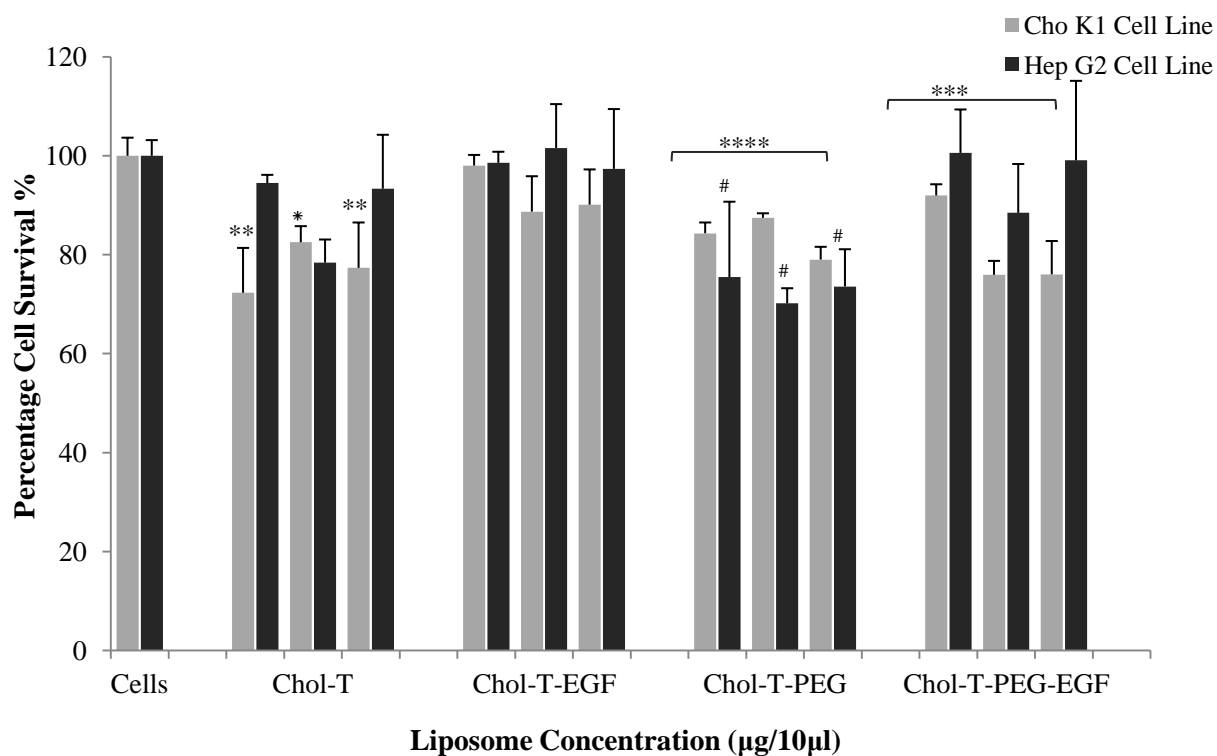


**Figure 3.10:** Growth inhibition studies of cationic liposome: pCMV-*luc* DNA complexes in CHO-K1 and HepG2 cells *in vitro*. DNA was kept constant at 1 µg while varying amounts of liposome used were; Chol-T (4, 5, and 6 µg), Chol-T/EGF (4, 5, and 6 µg), Chol-T-PEG (7, 8 and 9 µg), Chol-T-PEG/EGF (7, 8 and 9 µg). Data are presented as a percentage of the control sample (no liposomes, 0 µg) and are represented as means ±S.D. (n=3). \* $P < 0.05$ , \*\* $P < 0.01$ , \*\*\* $P < 0.001$ , \*\*\*\* $P < 0.0001$  for the CHO-K1 cell line against the untreated control, and # $P < 0.05$ , ## $P < 0.01$ , ### $P < 0.001$ , #### $P < 0.0001$  for the HepG2 cell line against the untreated control.

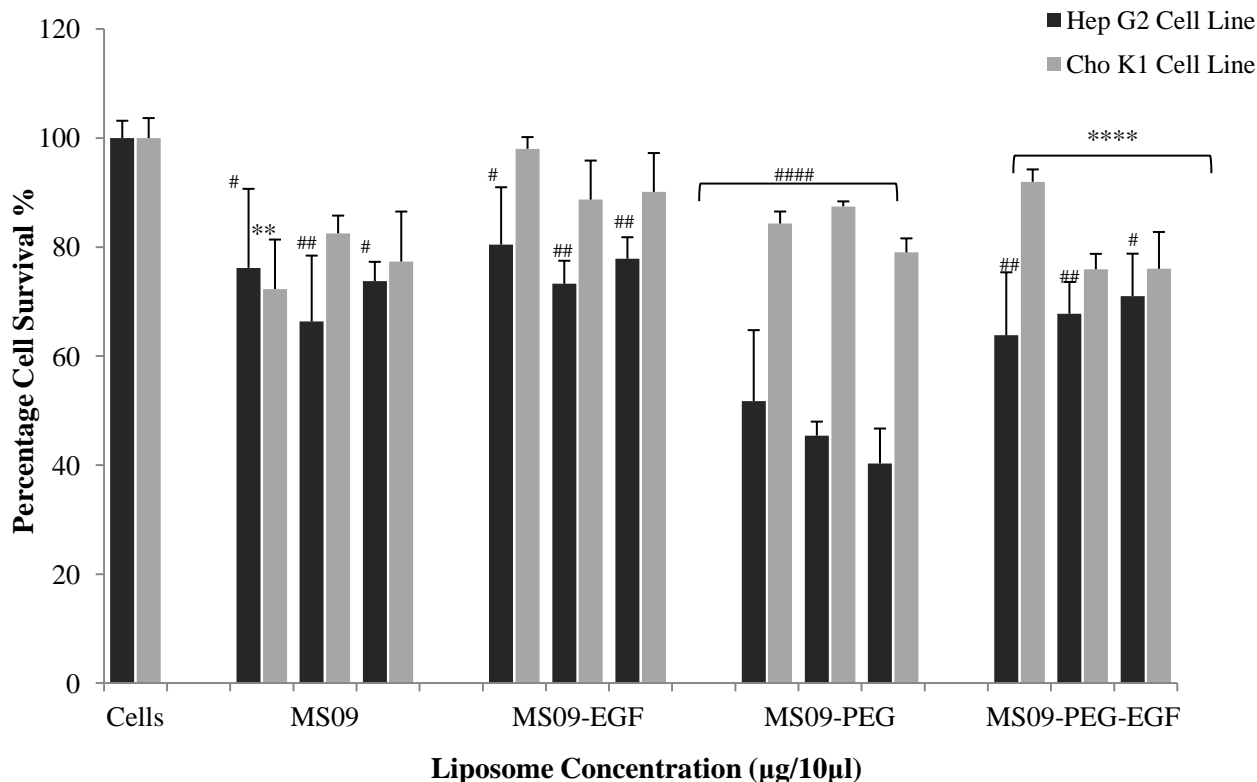


**Figure 3.11:** Growth inhibition studies of cationic liposome: pCMV-*luc* DNA complexes in CHO-K1 and HepG2 cells *in vitro*. DNA was kept constant at 1 µg while varying amounts of liposome were used; MS09 (11, 12, and 13 µg), MS09/EGF (11, 12, and 13 µg), MS09-PEG (10, 11 and 12 µg), MS09-PEG/EGF (10, 11 and 12 µg). Data are presented as a percentage of the control sample (no liposomes, 0 µg) and are represented as means ±S.D. (n=3). \* $P < 0.05$ , \*\* $P < 0.01$ , \*\*\* $P < 0.001$ , \*\*\*\* $P < 0.0001$ , for the CHO-K1 cell line against the untreated control, and # $P < 0.05$ , ## $P < 0.01$ , ### $P < 0.001$ , #### $P < 0.0001$  for the HepG2 cell line against the untreated control.

In both examined cell lines the plain cationic lipoplexes were reasonably well tolerated. The Chol-T and MS09 lipoplexes showed minimal cytotoxic effect with cell survival averaging 77% and 84% respectively in the CHO-K1 cell line. These lipoplexes were just as well tolerated within the HepG2 cell line; however, with the Chol-T liposome slightly better tolerated than the MS09 formulation. An overall mortality of just 12 – 28 % in both cell lines implies a good platform for cellular transfection. The Chol-T and MS09 lipoplexes displayed maximal cytotoxic effect at sub-optimal and optimal DNA : lipid charge ratios within the CHO-K1 cell line, and at transfection optimal ratios for HepG2 cells.

The stealth Chol-T-PEG and MS09-PEG formulations also displayed maximal cytotoxicity at optimal DNA : lipid ratios in HepG2 cells, in contrast to its cytotoxicity at the super-optimal (more positive) charge ratio within the CHO-K1 cell line. These PEGylated lipoplexes exhibited high biocompatibility with the CHO-K1 cells with average cell death of only 17% and 11% respectively. This was not the case for the HepG2 cells, where the MS09-PEG formulation portrayed the highest cell death (55%) from all the preparations and across both cell lines. Similarly, Chol-T-PEG did show a decrease in HepG2 cell biocompatibility although this was less pronounced. Hence, it can be noted that at optimal transfection ratios, the Chol-T-PEG and MS09-PEG exhibited an increase in cytotoxicity, which is in conflict with earlier reports of cell tolerance and enhanced biocompatibility (Singh *et al.*, 2011; Narainpersad *et al.*, 2012).

Incorporation of the EGF polypeptide for cellular targeting, clearly showed (Figures 3.10 – 3.11) improved levels of cell survival in the HepG2 cell line compared to the CHO-K1 cell line and to that of their non-targeted counterparts. The Chol-T-EGF and MS09-EGF lipoplexes were well tolerated on cellular internalisation, leading to 93% and 76%, and 99% and 77% cell survival in the CHO-K1 and HepG2 cell lines respectively. Furthermore, Chol-T-EGF lipoplexes showed a 10% improvement over that displayed by the plain Chol-T lipoplexes in HepG2 cells. PEGylated targeted formulations, correspondingly, showed improved cellular survival when measured against non-targeted formulations. The Chol-T-PEG-EGF lipoplexes produced 81% and 96% cell survival in the CHO-K1 and HepG2 cell lines respectively, correlating to an approximate 23% increase in cell-specific biocompatibility. The MS09-PEG-EGF lipoplexes produced an average cell survival of 62% and 67% in the CHO-K1 and HepG2 cell lines. Hence, this addition of EGF resulted in improved cell survival rates compared to the higher cytotoxicity levels observed for the untargeted MS09-PEG lipoplexes in the same cell line.

The observed increase of cellular survival noted for the targeted formulations in the HepG2 receptor positive cell line was anticipated, since EGF is a growth factor and is known to increase cell growth and survival. It has often been observed that the introduction of EGF at appropriate quantities improves cell growth by promoting propagation, and as such, has been identified for its potential in wound healing experiments (Raymond *et al.*, 2004; Buñuales *et al.*, 2011).

Of all the examined preparations, the MS09 cytofectin containing lipoplexes displayed a greater cytotoxicity compared to those containing the Chol-T cytofectin, particularly in the HepG2 cell line. Although, EGF targeting increased survival in the HepG2 cell line, the MS09-PEG and MS09-PEG-EGF lipoplexes were more cytotoxic by comparison, with maximal and significant cell death at 60% (HepG2) and 46% (CHO-K1) respectively.

Lipoplex toxicity may be influenced by the cationic amphiphile, incubation time and specific cell type, which is evident in the toxicity based results reported in this study. The zeta potential and likewise charge ratio present further influence the cytotoxicity elicited in each cell line by the different liposomes. Where higher charge ratios exist (MS09, MS09-PEG, and MS09-PEG-EGF), increased lipid content arises, resulting in lipid composition derived toxicity as well as the potential for toxic synergism between the liposomes and DNA (Dass and Choong, 2006). Formulation stability is also significant, where low stability as determined by  $\zeta$ -measurements of the MS09-PEG liposome, could indicate a potential for agglomeration, resulting in a higher cytofectin presence and which can be related to cellular shrinking or cytoplasmic vacuolisation and thus cytotoxicity (Mohr *et al.*, 2001).

### **3.3.3. Reporter gene expression**

The firefly luciferase and green fluorescent proteins are two of the most popularly employed molecular reporters and have been applied for this study. The luciferase assay system (Figure 3.12) examines transient gene expression and is substrate (luciferin) dependent. It presents a chemiluminescent assay for luciferase activity that is both sensitive and rapid (Torchilin, 2003). The assay is based on the lack of luciferase enzyme expression by mammalian cell systems, and the low levels of cellular autoluminescence. The GFP reporter derived from the *Aequorea Victoria* jelly fish, while requiring no substrate for fluorescence production, chromophore development by the posttranslational cyclisation and oxidation reaction is fairly slow (Heim and Tsien, 1996; Day *et al.*, 1998).

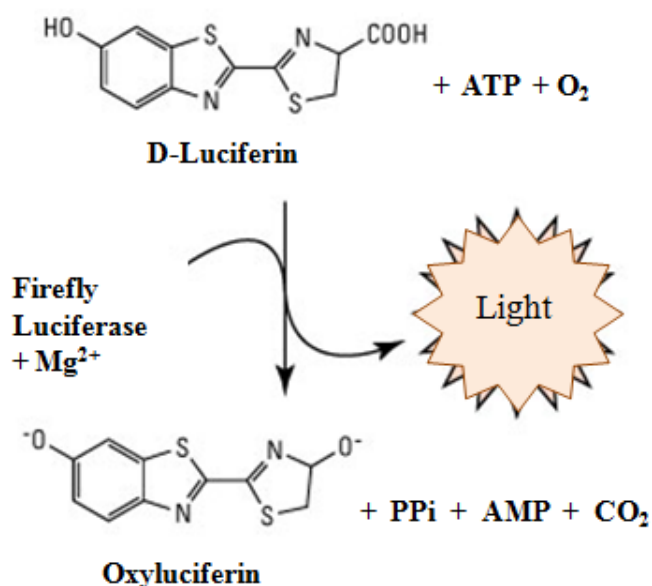


**Figure 3.12:** The firefly luciferase reaction. The intensity of light emitted is quantified by a luminometer, providing a measure of the level of gene expression (<http://www.piercenet.com>, accessed 16/03/2014)

Expression of the luciferase reporter gene (pCMV-*luc* DNA) was used to measure the efficiency of the prepared liposomal formulations as gene delivery vehicles. The primary focus of this investigation was tailored toward the effective targeting of liver hepatocytes based on the presence of EGF receptors. To completely understand the nature and effect of the targeted liposomes potential against the non-targeted plain and stealth liposomes, a series of controls were employed. Here the CHO-K1 cell transfection served as a receptor negative transfection control, thereby eliminating transfection through EGF-EGFR endocytic channelling. To further establish effective receptor targeting, HepG2 cellular transfection was carried out in the presence of excess of the synthetic peptide (YI-12) which is capable of EGF-related EGFR association. Finally the effects of a commercially successful liposome formulation Lipofectin<sup>®</sup> was examined, providing a positive control for effective transfection of the HepG2 cell line, against which the obtained transfection results could be evaluated.

The GFP reporter was thereafter employed for further estimation of the transfection capabilities of the various liposomes to the HepG2 cell line. In this regard, quantification of GFP expression within the cell line was determined using flow cytometric analysis as reported in section 3.3.3.5a.

The results of the cationic liposome mediated transfection studies in the CHO-K1 cell line can be seen in Figures 3.13 – 3.14, while transfection in the HepG2 cell line can be viewed in Figures 3.15– 3.16.

### 3.3.3.1. Luciferase reporter gene analysis in the Cho K1 cell line

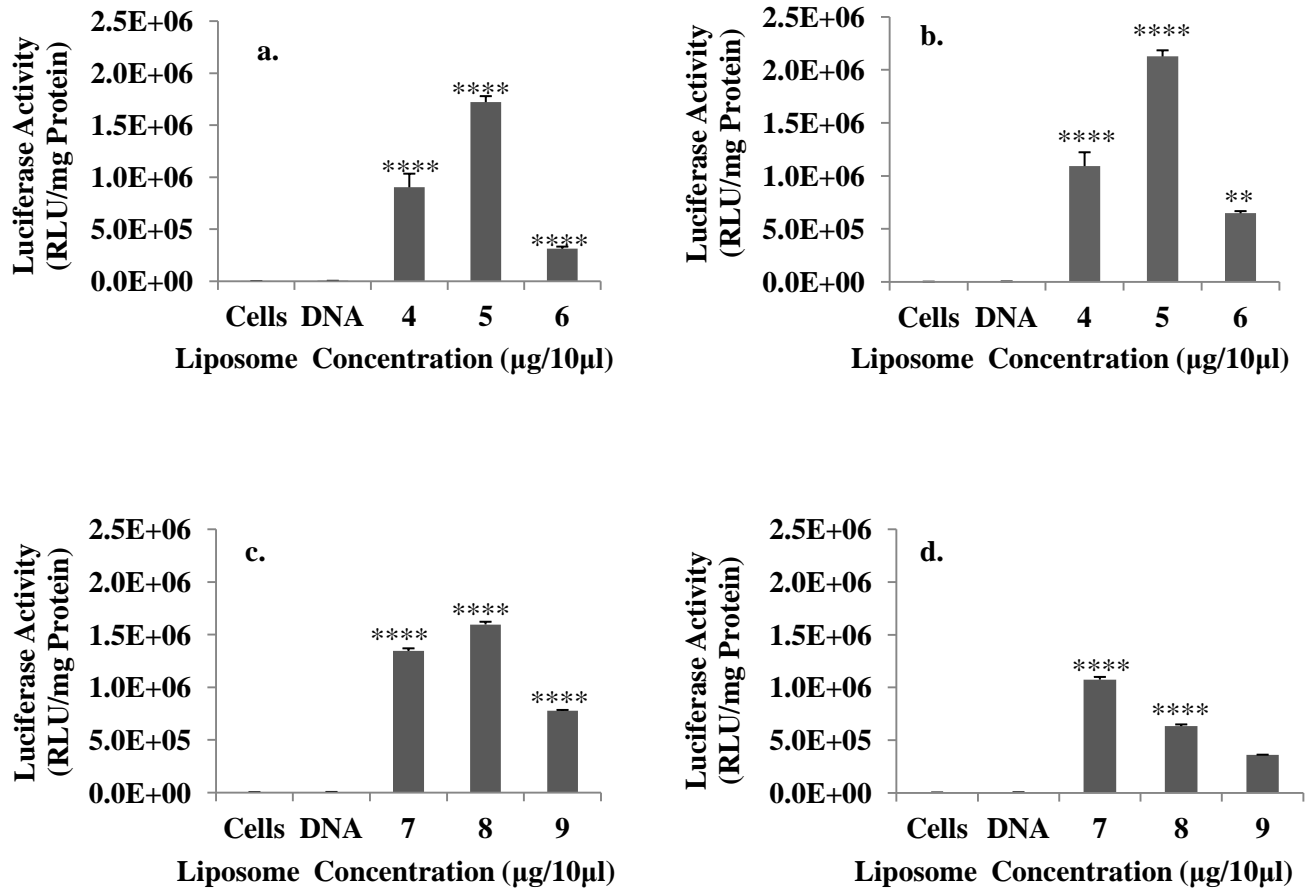


**Figure 3.13:** Transfection studies of cationic liposome: pCMV-*luc* DNA complexes in CHO-K1 cells *in vitro*. DNA was kept constant at 1 µg. Liposomes were introduced at varying amounts. **a.** Chol-T (0, 4, 5, and 6 µg), **b.** Chol-T/EGF (0, 4, 5, and 6 µg), **c.** Chol-T-PEG (0, 7, 8 and 9 µg), **d.** Chol-T-PEG/EGF (0, 7, 8 and 9 µg). Data are presented as means ±S.D. (n=3). \**P* < 0.05, \*\**P* < 0.01, \*\*\**P* < 0.001, \*\*\*\**P* < 0.0001 vs. the DNA control for the respective liposomes.

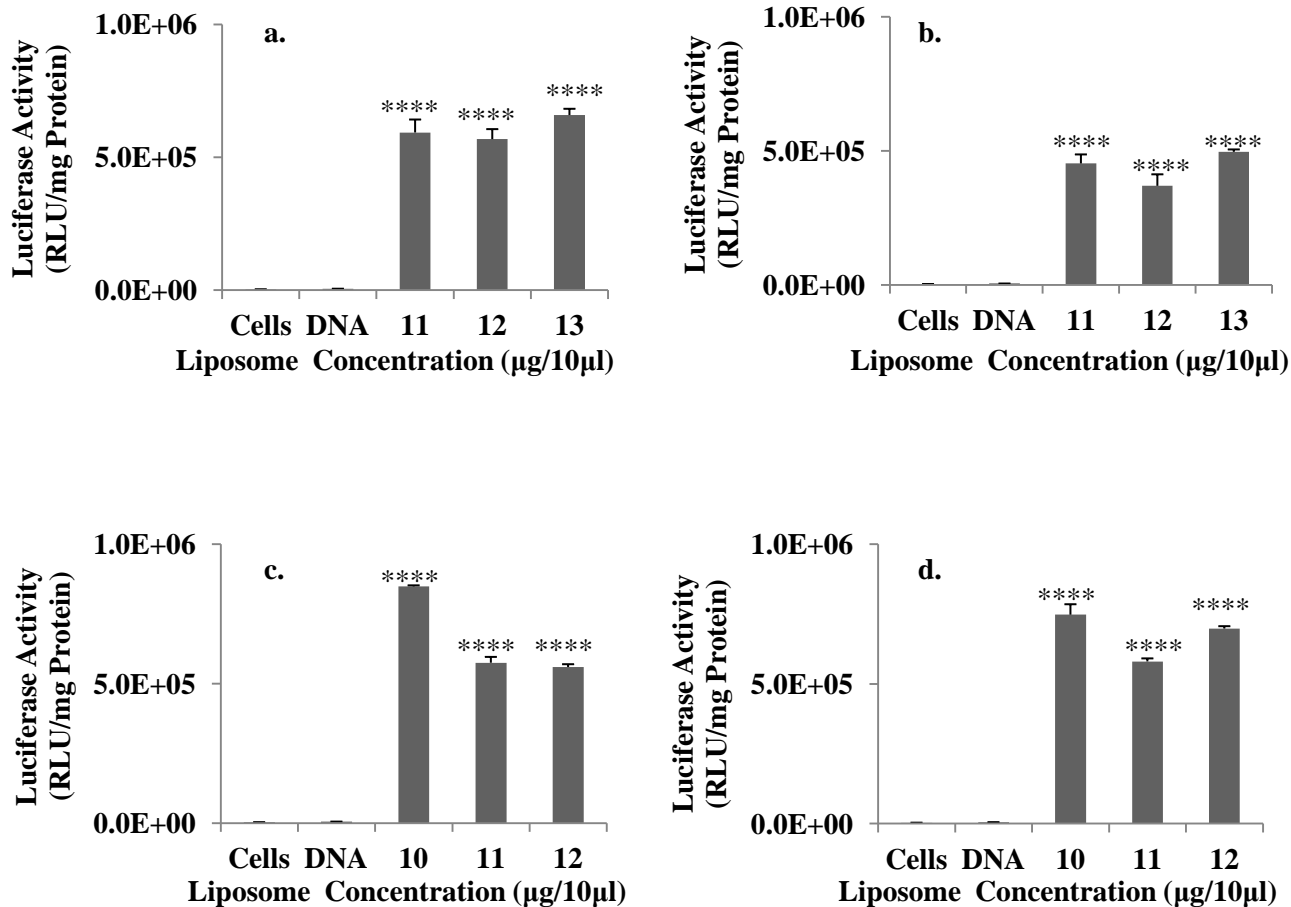


**Figure 3.14:** Transfection studies of cationic liposome: pCMV-*luc* DNA complexes in CHO-K1 cells *in vitro*. DNA was kept constant at 1 µg. Liposomes were introduced at varying amounts. **a.** MS09 (0, 11, 12, and 13 µg), **b.** MS09/EGF (0, 11, 12, and 13 µg), **c.** MS09-PEG (0, 10, 11 and 12 µg), **d.** MS09-PEG/EGF (0, 10, 11 and 12 µg/10 µl). Data are presented as means ±S.D. (n=3). \* $P < 0.05$ , \*\* $P < 0.01$ , \*\*\* $P < 0.001$ , \*\*\*\* $P < 0.0001$  vs. the DNA control for the respective liposomes.

From the graphs above, it can be noted that all liposome formulations produced good transfection of the CHO-K1 cell line with significant levels of luciferase activity in comparison to the naked DNA control. Furthermore, in spite of the smaller hydrodynamic size of the MS09 liposomes, a trait generally favourable for transfection, the Chol-T based formulations produced the greater transgene activity. The Chol-T plain formulations, however, clearly produces the highest level of luciferase gene expression across all evaluated liposomes in the CHO-K1 cell line. Since this liposome displays an overall neutral to positive DNA : lipid charge ratio with minimal effect on cell growth, the high level transfection and gene expression were expected.

The MS09 liposome similarly produced good CHO-K1 transfection, with no significant improvement in transgene expression over an increase in liposome concentration.

The effect of the PEGylated formulations, Chol-T-PEG and MS09-PEG can be considered in a comparative manner, with Chol-T-PEG producing appreciable luciferase expression at the sub- and optimal DNA : lipid ratios (1 : 7 and 1 : 8). Good cell survival rates and improved longevity together with the relatively small size as determined by Cryo-TEM and NTA suggest that this liposome preparation provides a good platform for effective transfection *in vitro*. The MS09-PEG formulation by comparison achieved good transgene expression, with a notable decline at higher liposome concentrations. Higher charge ratios may potentially result in the presentation of free liposomes in suspension and as such limit the transfer of plasmid DNA.

The targeted EGF liposomes which were well tolerated by the cell line showed good transfection capability. Chol-T-EGF produced good expression at optimal DNA binding ratios, while Chol-T-PEG-EGF produced good overall expression levels with a measurable decrease at higher lipid concentrations. The lowest level of luciferase expression was observed for the MS09-EGF liposome, which like MS09 alone, displays the highest overall DNA : lipid charge ratios, where the higher lipid content may play a role in the transfection observed. Despite poor biocompatibility in this cell line MS09-PEG-EGF, showed good cellular transfection and transgene expression at the sub- and super-optimal DNA: lipid ratios (1 : 10 and 1 : 12). A drop in transfection was noted at the optimal charge ratio, corresponding to the highest levels of cytotoxicity.

Overall, the Chol-T liposome appears to be the most favourable for gene delivery and transgene expression in the cell lines studied. The moderate levels of expression obtained for the EGF targeted liposomes despite their smaller size could be designated to their hepatotropic design and the absence of EGFR on the CHO-K1 cell surface (Jo *et al.*, 2003). The smaller size of these liposomes as well as the PEG-shielding of the stealth liposomes may prove to be more advantageous under *in vivo* conditions, which provides a more favourable environment for particles below 200 nm, showing that size and cell specificity are indeed noteworthy under early *in vitro* evaluations such as these.

### 3.3.3.2 . Luciferase reporter gene analysis in the HepG2 cell line

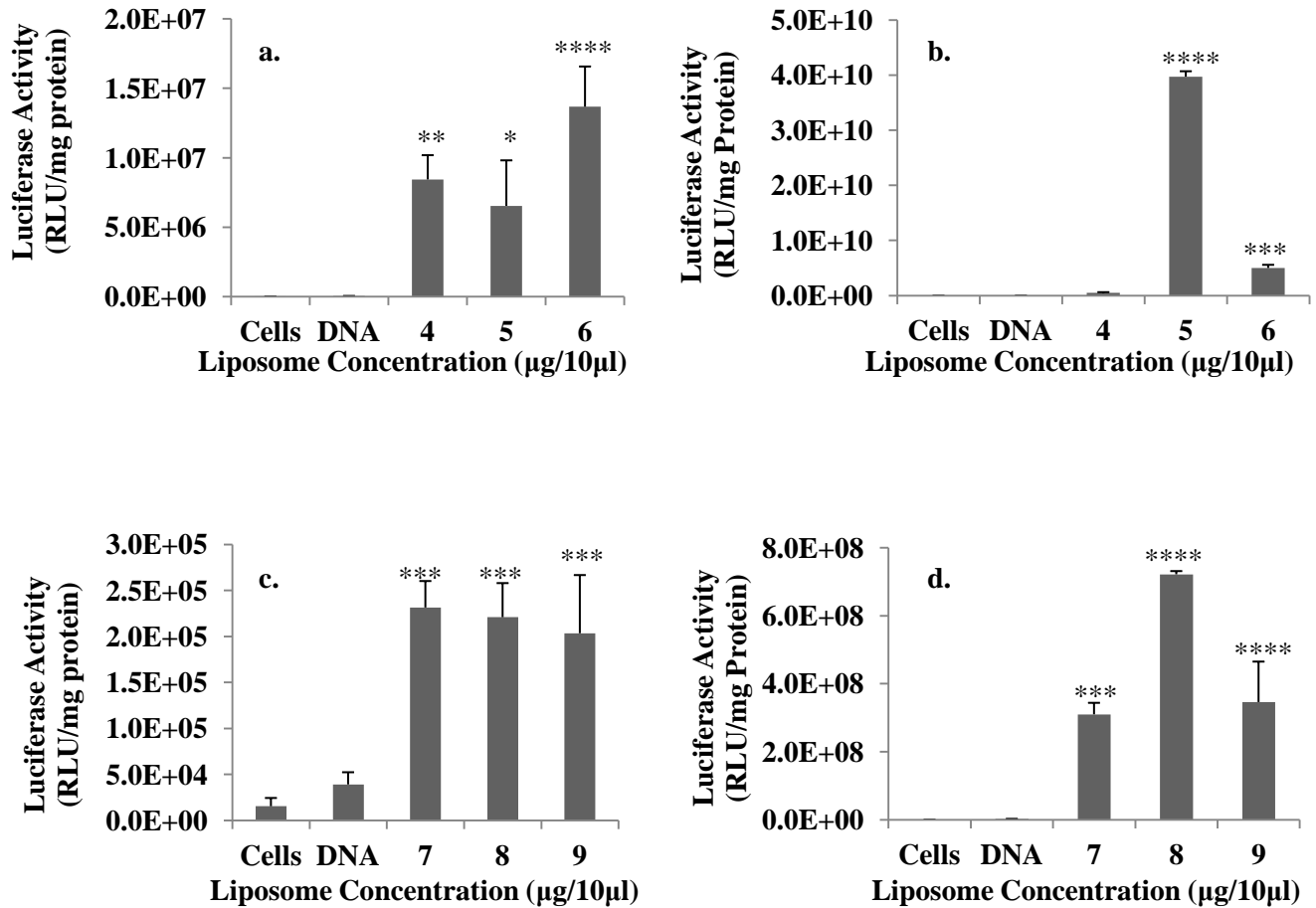


**Figure 3.15:** Transfection studies of cationic liposome: pCMV-*luc* DNA complexes in HepG2 cells *in vitro*. DNA was kept constant at 1 µg. Liposomes were introduced at varying amounts. **a.** Chol-T (0, 4, 5, and 6 µg), **b.** Chol-T/EGF (0, 4, 5, and 6 µg), **c.** Chol-T-PEG (0, 7, 8 and 9 µg), **d.** Chol-T-PEG/EGF (0, 7, 8 and 9 µg). Data are presented as means ±S.D. (n=3). \* $P < 0.05$ , \*\* $P < 0.01$ , \*\*\* $P < 0.001$ , \*\*\*\* $P < 0.0001$  vs. the DNA control for the respective liposomes.

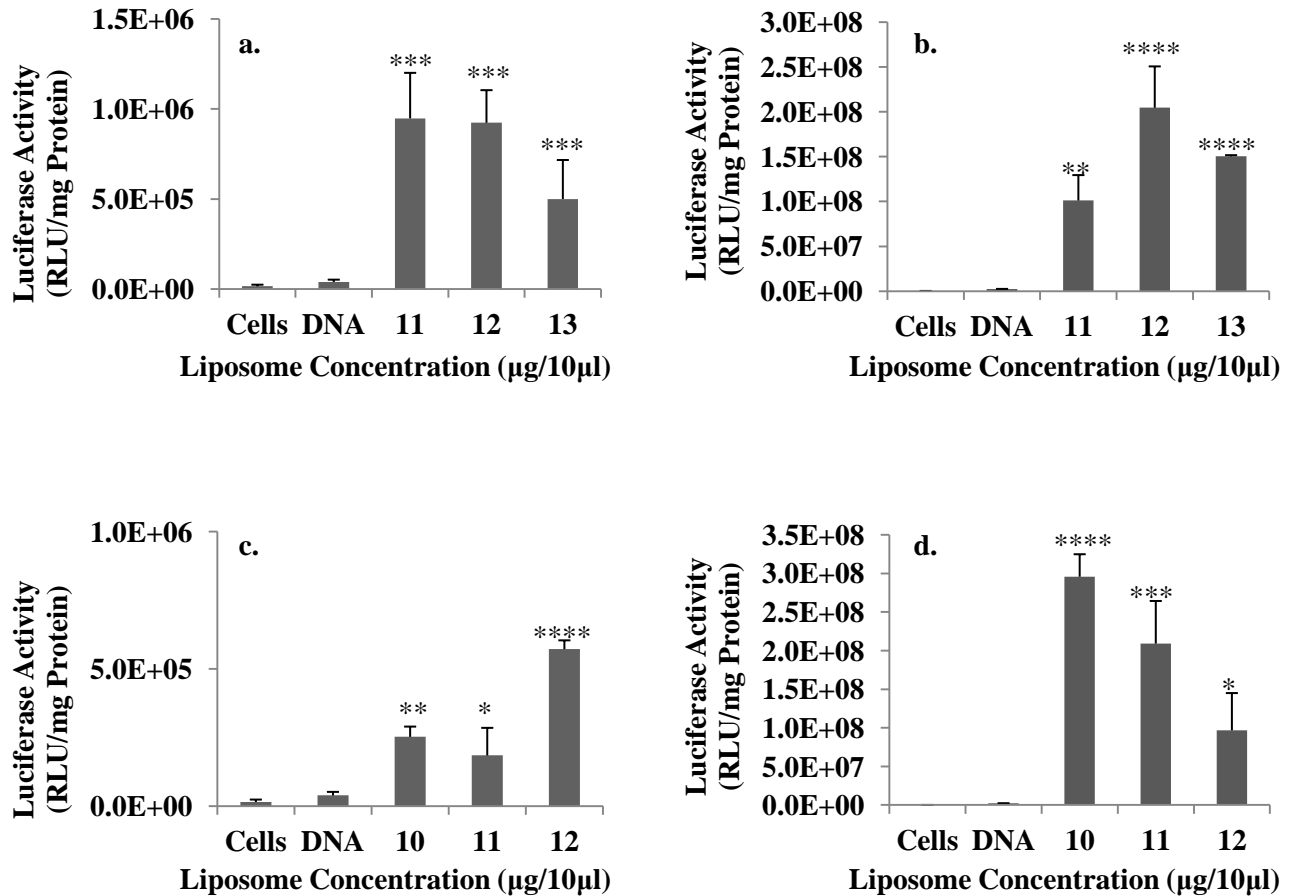


**Figure 3.16:** Transfection studies of cationic liposome: pCMV-*luc* DNA complexes in HepG2 cells *in vitro*. DNA was kept constant at 1 µg. Liposomes were introduced at varying amounts. **a.** MS09 (0, 11, 12, and 13 µg), **b.** MS09/EGF (0, 11, 12, and 13 µg), **c.** MS09-PEG (0, 10, 11 and 12 µg), **d.** MS09-PEG/EGF (0, 10, 11 and 12 µg). Data are presented as means ±S.D. (n=3). \**P* < 0.05, \*\**P* < 0.01, \*\*\**P* < 0.001, \*\*\*\**P* < 0.0001 vs. the DNA control for the respective liposomes.

Expression of the luciferase transgene in the targeted cell line (HepG2) mediated by the different liposome formulations was indicative of a successful transfection protocol. The plain Chol-T and MS09 cationic liposomes were able to yield moderate to good levels of gene expression. Chol-T was the better performer of the two, showing very good transfection at the super-optimal DNA : lipid charge ratio (1 : 1.6). Transfection activity produced by the MS09 liposome showed that an increase in lipid content at higher charge ratios resulted in lower levels of transgene expression. However, both liposomes showed improved levels of transgene expression in the HepG2 cell line compared to that observed in the CHO-K1 cell line. Chol-T was 4 fold more effective in the HepG2 cell line compared to the CHO-K1 cell line at optimal transfection ratios, which

significantly increased to almost 21 fold at the super-optimal ratio. Comparatively the MS09 liposomes produced only a 2 fold increase in transfection.

Stealth liposomes are considered useful functionalised formulations *in vivo*, capable of ensuring delivery and therefore, expression. This is thought to be attributed to the shielding of the liposomes from the external cellular forces and serum effects. While these PEGylated preparations displayed good retention of DNA integrity under the action of serum nucleases (section 3.2.4., Figure 3.8c., and d.) they, however, did show some degree of cytotoxicity in the HepG2 cell line as well as poor cellular transfection. The average gene expression produced by the Chol-T-PEG liposome showed an observable decrease in transfection at higher lipid concentrations. Notably the MS09-PEG formulation brought about the lowest overall transfection of the HepG2 cell line at the optimal DNA : lipid charge ratio, with a subtle increase in expression at the super-optimal ratio. This coincided with only a 1 fold improvement in expression when compared to that achieved in the CHO-K1 cell line.

The positive shielding effect mentioned above, indicate that the PEGylated liposomes may be more successful *in vivo*. Two presumptions exist, based on membrane interaction inhibition produced by the presence of the PEG modality. The first involves steric interference between the PEG-grafted liposome surface and the cell target (Deshpande *et al.*, 2004; Chen *et al.*, 2011). The second relates to the presentation and molecular weight of the PEG graft in relation to the lipid component. Here the presence of the PEG moiety may impede contact with the endosomal membrane by fusogenic lipids, such as DOPE. The lack of membrane destabilization at this critical point, results in DNA degradation rather than transgene expression (Song *et al.*, 2002; Remaut *et al.*, 2007). Chen and colleagues (2011) described the arrangement of the PEG graft (DSPE-PEG<sub>2000</sub>), present at low concentrations (< 4 mol %) to be in the mushroom conformation as opposed to the brush-type arrangement observed at higher concentration (> 8 mol %). At 2 mol %, as used for this investigation, it can be assumed that the PEG-lipid graft exists in the mushroom orientation on the liposome surface (Kenworthy *et al.*, 1995; Chen *et al.*, 2011).

The use of the EGF targeted liposomes was to improve the cellular transfection of the plasmid DNA via the receptor mediated endocytic pathway. All liposomes showed significant luciferase

gene expression compared to that achieved by the naked DNA (control). The Chol-T-EGF liposome produced the highest luciferase gene expression at the optimal and super-optimal charge ratios. This was followed by the Chol-T-PEG-EGF preparation, which brought about significant ( $P \leq 0.0001$ ) transfection at its optimal DNA binding ratio (1 : 8). MS09-EGF exhibited a distinct increase in transgene expression with an increase in lipid content, while the MS09-PEG-EGF liposomes displayed the opposite. In addition to showing significant ( $P \leq 0.05$ ,  $P \leq 0.0001$ ) overall transfection at observably higher magnitudes compared to that achieved by naked pCMV-*luc* DNA, these targeted formulations also produced significantly higher expression levels compared to their untargeted counterparts.

The Chol-T-EGF preparation at optimal and super-optimal ratios showed significantly ( $P \leq 0.0001$ ) improved transfection compared to all other evaluated targeted formulations. The Chol-T-PEG-EGF liposome similarly produced comparatively significant expression at its optimal charge ratio compared to MS09-EGF ( $P \leq 0.05$ ) and MS09-PEG-EGF ( $P \leq 0.01$ ). Overall, Chol-T-EGF, Chol-T-PEG-EGF, MS09-EGF and MS09-PEG-EGF at their observed effective transfection charge ratios, confirmed that transfection occurred via the EGFR mediated endocytosis pathway of the HepG2 cell line when viewed against the expression levels in the receptor negative control cell line (CHO-K1). This evaluation identified substantial averages of 140 – 23000 fold increases of cellular transfection levels per liposomal ratio over those attained in the CHO-K1 cell line. This provides clear evidence of effective targeting of the EGF receptors on the HepG2 cell surface.

While almost neutral to highly positive charge ratios were determined for all liposomes evaluated,  $\zeta$ -determinations using nanoparticle tracking analysis has shown the relative surface charge to be moderately to highly negative. Gratton and co-workers (2008) identified nanoparticle surface charge to significantly affect cellular internalization. Their work showed that a pH induced shift in zeta potential resulted in reduced percentage cell population transfection. However, it is important to consider that zeta potential is a measure of the potential difference between the layer of stationary fluid particles on the surface of the dispersed liposome and the dispersion medium. Moreover, this measurement is significantly influenced by the pH of the bulk fluid or dispersion medium. At high pH, negative zeta potential is observed, while at

more acidic pH the zeta potential reflects a positive value (Honary and Zahir, 2013). Based on this premise, the liposomes and lipoplexes presented here may not necessarily display a negative surface charge, however, at pH 7.0, under bulk buffered solution, they present a net negative zeta potential, which did not hinder the degree of transfection observed.

Early literature in this regard, has proposed that the cell surface possesses points of cationic charge interspersed with larger anionic domains, which allow clusters of small particles displaying negative zeta potential to bind (Patil *et al.*, 2007). This, however, cannot be confirmed as no recorded evidence of this kind has been observed for either investigated cell line. In spite of this, a possibility exists that the negative charge surrounding the lipoplexes in the dispersion medium, limit interactions with serum components, thus allowing improved traversal of the cytoplasm for delivery and expression of the transgene. This could be true, especially for the EGF targeted lipoplexes that require uninterrupted transport to the EGFR on the HepG2 cells for effective transfection.

### **3.3.3.3. Competition Studies in the HepG2 Cell Line**

Competitive binding studies, in general involve transfection of cells pre-exposed to an excess of the target ligand, being evaluated. This creates a blockage of the available receptor sites on the cell surface, resulting in measurable reductions in transgene expression mediated by the transfecting vector system. Therefore to adequately evaluate the receptor mediated endocytic internalisation of EGF targeted lipoplexes, the target HepG2 cells would require initial receptor quenching with excess EGF polypeptide. For the purposes of this investigation, the YI-12 peptide, mimicking the function of the GE11 peptide (Li *et al.*, 2005) which showed good EGF-comparative receptor binding was synthesized as a competitive binding functionality.

For further confirmation of positive EGFR directed transfection having taken place within the HepG2 cell line, the transfection protocol was duplicated and cellular transfection allowed to proceed in the presence of the synthesized competitor peptide (section 2.3.2.2.2b.). All targeted formulations were found to display a significant drop in transfection activity, as seen in Figure 3.17.

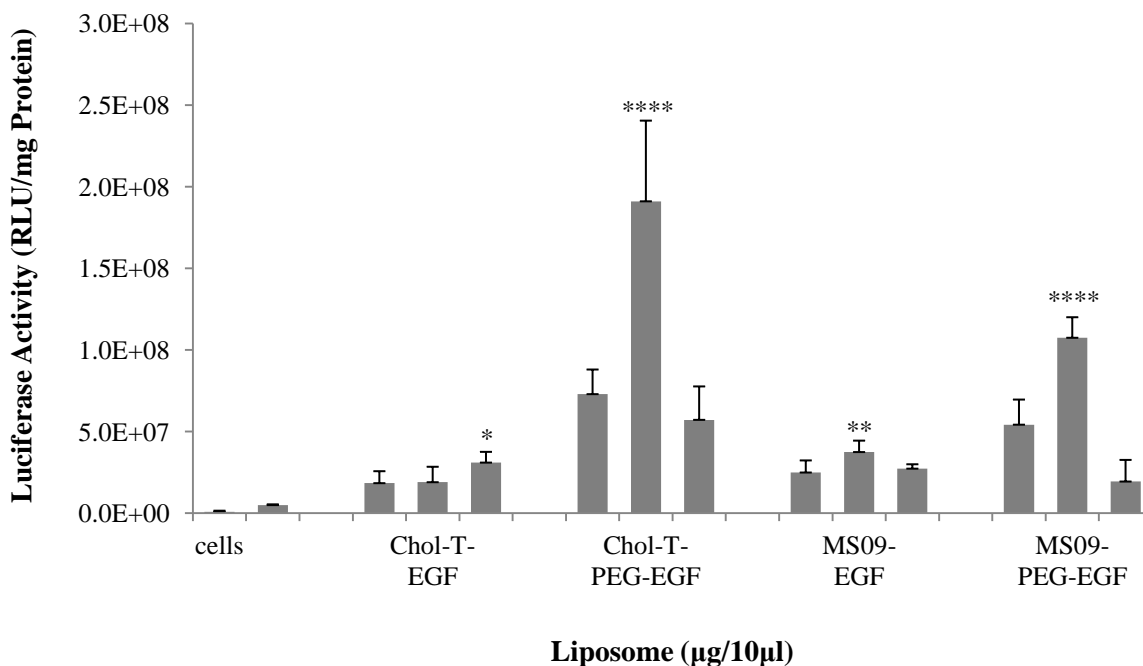


**Figure 3.17:** Transfection studies of targeted cationic liposome: pCMV-*luc* DNA complexes in HepG2 cells *in vitro* in the presence of YI-12 peptide (0.5 mM). DNA was kept constant at 1 µg. Liposomes were introduced at varying amounts. **a.** Chol-T-EGF (0, 4, 5, and 6 µg), **b.** Chol-T-PEG-EGF (0, 7, 8, and 9 µg), **c.** MS09-EGF (0, 11, 12 and 13 µg), **d.** MS09-PEG-EGF (0, 10, 11 and 12 µg). Data are presented as means ±S.D. (n=3). \* $P < 0.05$ , \*\* $P < 0.01$ , \*\*\* $P < 0.001$ , \*\*\*\* $P < 0.0001$ , for the respective liposomes vs. the DNA control.

As seen in Figure 3.17, the Chol-T-EGF and MS09-EGF liposomes produced comparatively diminished gene expression in the presence of the competitor. Under these conditions each liposome achieved highest transfection at the respective super-optimal and optimal charge ratios. In particular, the Chol-T-EGF liposome demonstrated a 30, 2000, and 160 fold decrease respectively, in observed luciferase activity, when having to compete for binding with the YI-12 peptide. Similarly the MS09-EGF liposome displayed a drop in gene expression of approximately, 4, 6, and 8 fold at the sub-, optimal and super-optimal charge ratios. The Chol-T-PEG-EGF and MS09-PEG-EGF liposomes likewise, exhibited an average decrease in transgene expression of 2 – 6 fold. While all formulations showed a marked reduction in observable gene expression, the stealth targeted formulations achieved higher level transfection than their non-PEG counterparts in the presence of the competitor. This could be attributed to the mushroom conformation of the PEG graft on the liposome surface interfering with, or limiting, the EGF presence for receptor targeting. Despite this observation, the Chol-T-PEG-EGF liposomes still

show significantly diminished luciferase gene expression compared to that observed in the absence of the YI-12 peptide (Figure 3.15).

The ability of the above liposomes to still elicit significant levels of transgene expression, despite the presence of the competing peptide can be postulated to result from the lower affinity of the synthetic peptide to bind the EGFR compared to the EGF polypeptide. Firstly YI-12, like GE11, is a 12 amino acid peptide and is therefore substantially smaller than the 53 amino acid EGF polypeptide (Li *et al.*, 2005). EGF undergoes receptor binding at the extracellular amino terminal of EGFR comprising the L1 and L2 domains, instigating receptor dimerisation (Ogiso *et al.*, 2002; Jorissen *et al.*, 2003). The smaller size of the YI-12 peptide would therefore inadequately bind the receptor at the EGF binding pocket, presumably only being able to bind one domain at any time. This inaccurate binding would not induce downstream signalling and may potentially enable the EGF targeted formulations to still affect some level of transgene expression (Li *et al.*, 2005).

Overall significant reductions of cellular transfection under the effects of this YI-12 synthetic peptide of  $\approx 2 - 2000$  fold, together with the observed comparative transfection levels in CHO-K1, provides compelling evidence that confirm EGF-receptor mediated endocytosis is the primary avenue for the cellular entry of EGF targeted cationic liposomes.

#### **3.3.3.4. Lipofectin<sup>®</sup> transfection in HepG2 cell line**

Many lipid and liposome based formulations (e.g. lipofectamine, DC-Chol, DOTAP and lipofectin<sup>®</sup>) have achieved success as effective cellular transfection agents. As such they have come to light as highly effective positive standards of transfection, against which carriers under investigation may be examined. For the currently investigated liposome formulations, the commercial lipofectin transfection reagent was utilised as a comparator for transfection of the HepG2 cell line. This commercial liposome formulation has the renowned capability to produce transfection of and transgene expression in established, primary, and even 'hard-to-transfect' cell types such as the HepG2 cells (Bennett *et al.*, 1992).

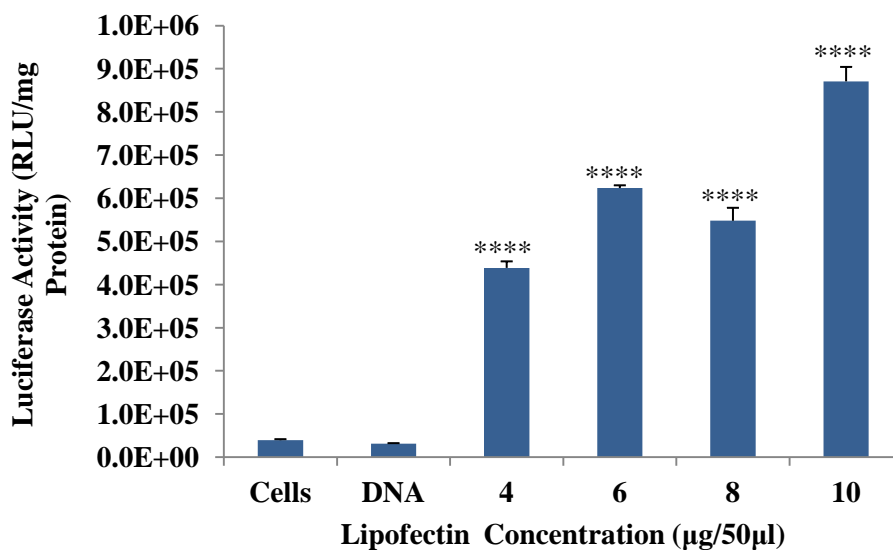


**Figure 3.18:** Transfection studies of commercial Lipofectin : pCMV-*luc* DNA complexes in HepG2 cells *in vitro*. DNA was kept constant at 1 µg. Lipofectin was introduced to DNA and HepG2 cells as per manufacturer protocol ratios of DNA : Lipofectin (<sup>w/w</sup>); 1:4, 1:6, 1:8, and 1:10. Data are presented as means ±S.D. (n=4). \**P* < 0.05, \*\**P* < 0.01, \*\*\**P* < 0.001, \*\*\*\**P* < 0.0001, for the respective liposomes *vs.* the DNA control.

Lipofectin, composed of DOTMA : DOPE (Felgner *et al.*, 1987) produced stable successful transfection of the HepG2 cells, as displayed in Figure 3.20 above. This assay was conducted in accordance with manufacturer determined guidelines, against a negative control of cells alone where no expression was expected, but background luminescence was observed. A second control of naked DNA was also included, as was the case for all the other transfection analyses.

All DNA : lipofectin ratios tested showed significant improvement in DNA based transfection of the HepG2 cell line compared to the DNA control. Good overall luciferase expression was observed, particularly at the DNA : lipofectin ratio of 1: 10 (<sup>w/w</sup>). In contrast, the plain cationic liposome formulations (Chol-T and MS09) showed comparable, if not a slightly heightened lipofection in this target cell line, as evidenced by Figures 3.15, and 3.16. Furthermore, both untargeted stealth liposomes, Chol-T-PEG and MS09-PEG demonstrated relatively low levels of transfection. All transgene expression levels were found to be below that observed for lipofectin, with the exception of the comparable MS09-PEG liposome at the super-optimal charge ratio.

All EGF targeted liposomal systems exhibited high transfection across all lipofectin ratios assessed. The production of an approximate 70000 fold disparity in transfection capability between Chol-T-EGF and lipofectin proves that this preparation can produce high levels of luciferase reporter gene transfection in the target HepG2 cell line, when compared to the commercially successful and widely used carrier lipofectin.

### **3.3.3.5. GFP reporter gene analysis by Flow cytometry in the HepG2 cell line**

While GFP is prominent as a determining tool for *in vivo* gene expression, it's *in vitro* aptitude as a quantitative reporter of gene expression has been highlighted here through the application of flow cytometry (Soboleski *et al.*, 2005). GFP unlike the luciferase reporter requires no need for additional substrate or co-factors, as it is capable of spontaneous intracellular fluorophore formation. With no breakdown of additional substrate or external activity, the fluorescence intensity observed may be entirely attributed to GFP expression. Furthermore, flow cytometric assessment of this expression provides advantageous single cell quantification (Ducrest *et al.*, 2002). Flow sorting per particle enables separation of individual particles or cells present in a heterogeneous population. An obvious advantage of this GFP reporter system is the direct visualisation of protein accumulation in live cells prior to quantification and detection of per cell GFP gene expression. GFP fluorescence detection by flow cytometry has also been regarded as ten times more sensitive than fluorescence microscopy examinations (Soboleski *et al.*, 2005).

The results of the GFP gene expression quantification by flow cytometry are shown below in Figures 3.19 – 3.21.

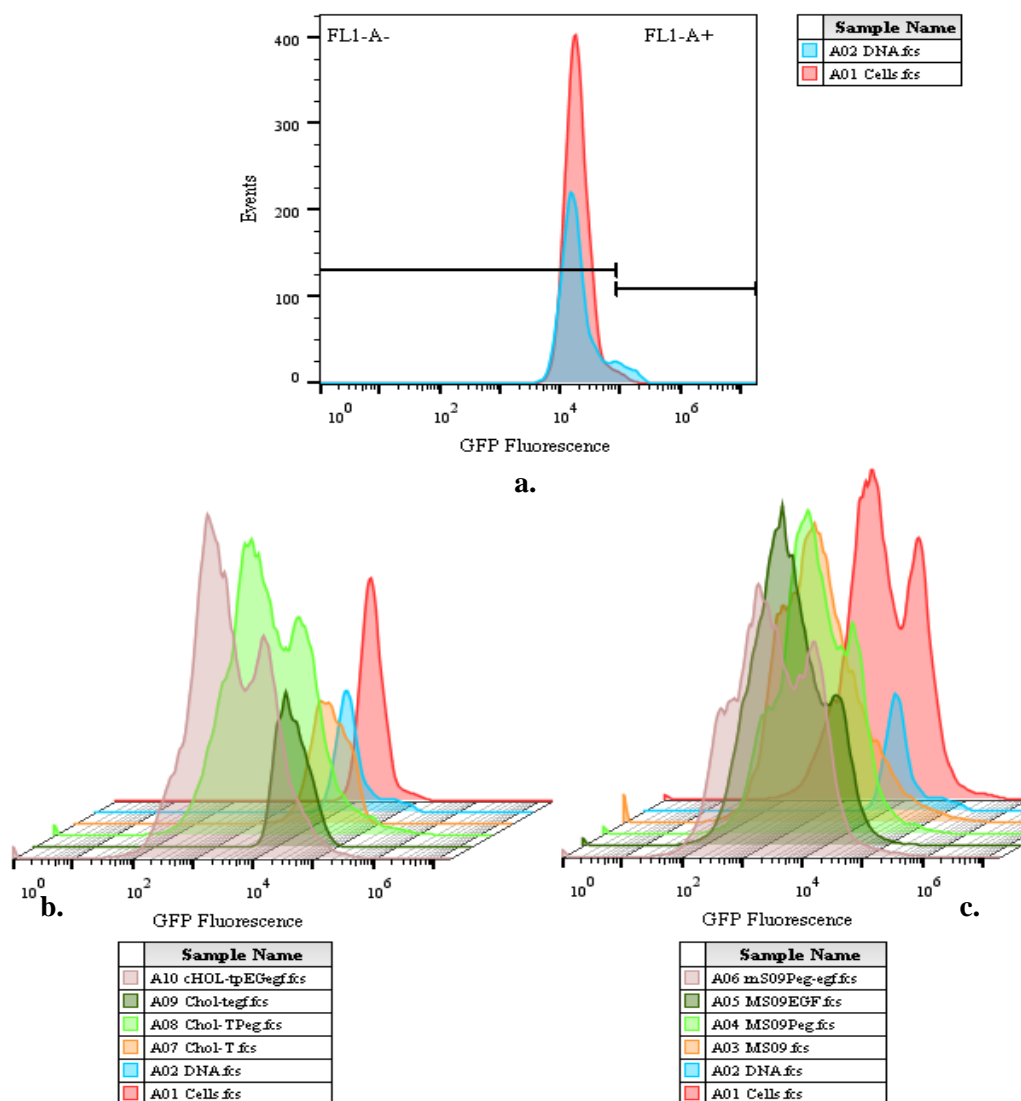
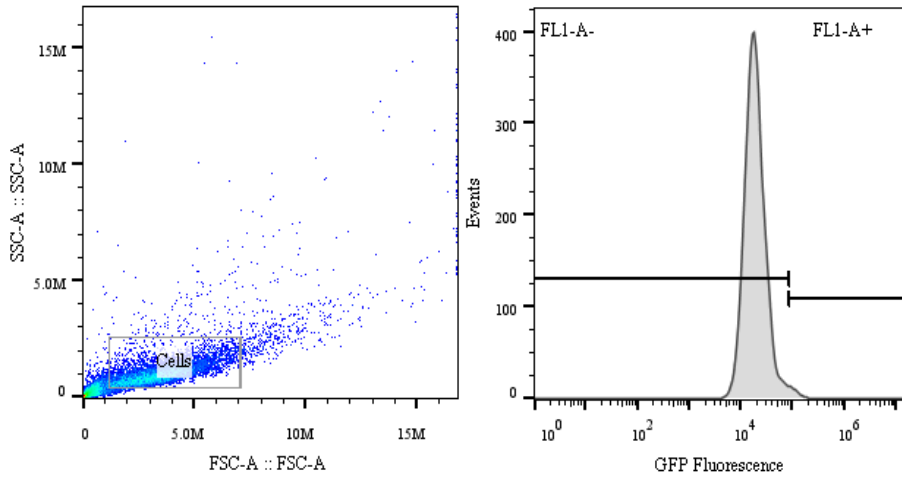
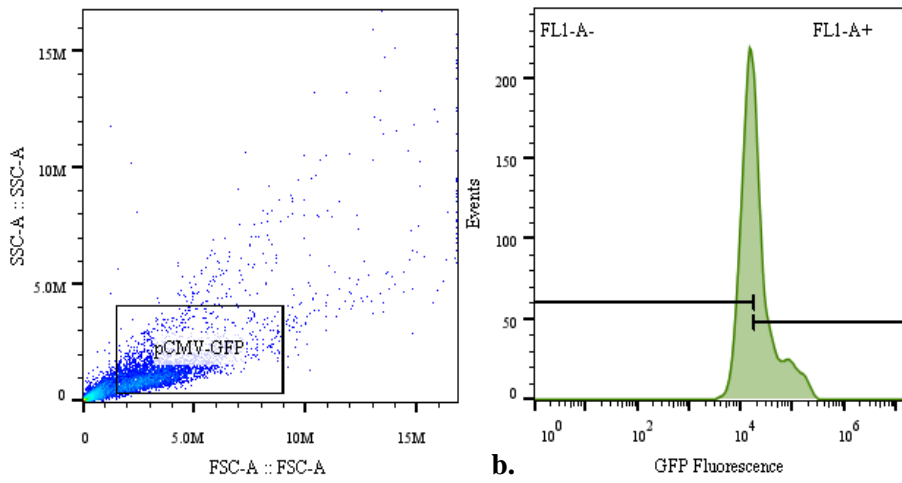


**Figure 3.19:** Staggered overlay histograms illustrating the cytometric quantisation of GFP fluorescence produced by the varying liposomes at transfection optimal ratios. Histogram a. shows an overlay of the negative control (HepG2 cells alone) with that of the positive pCMV-GFP control (naked DNA in HepG2 cells). The staggered histograms b. and c., Chol-T and MS09 cytofectin containing liposomes respectively, represent expression of GFP against the two controls. GFP expression data was plotted against the events counted for each cell population.

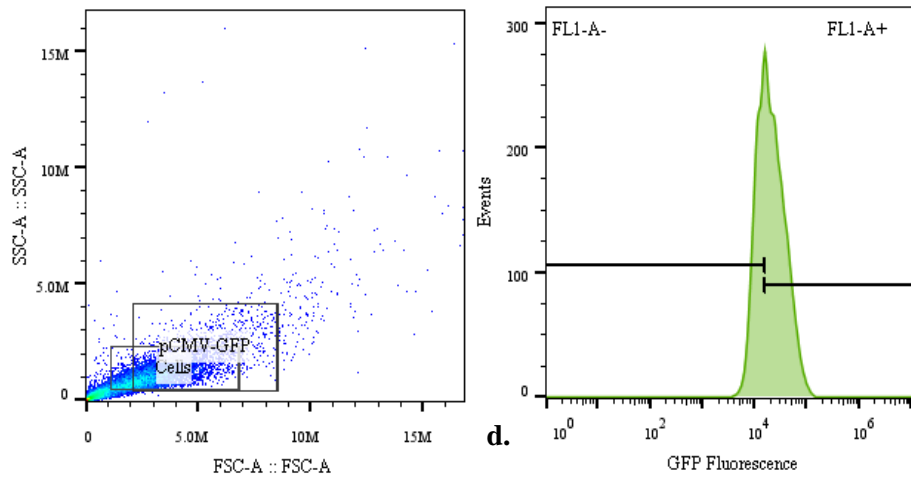
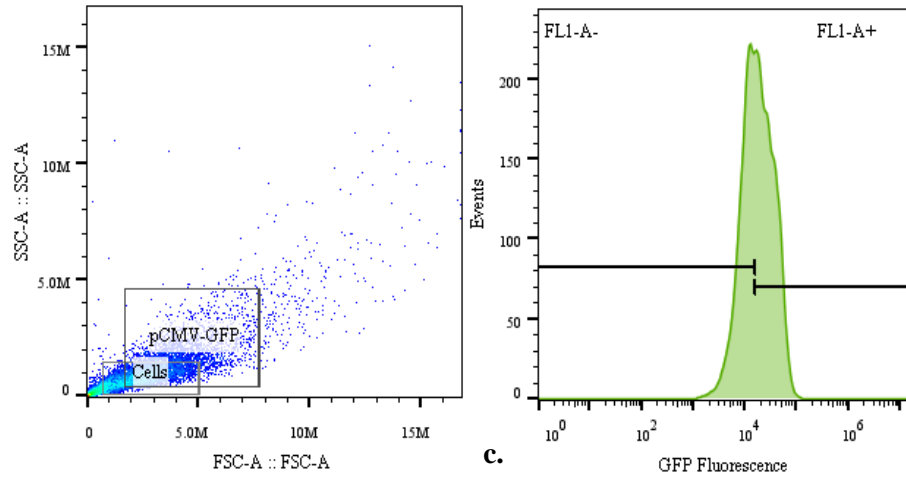


**a.**

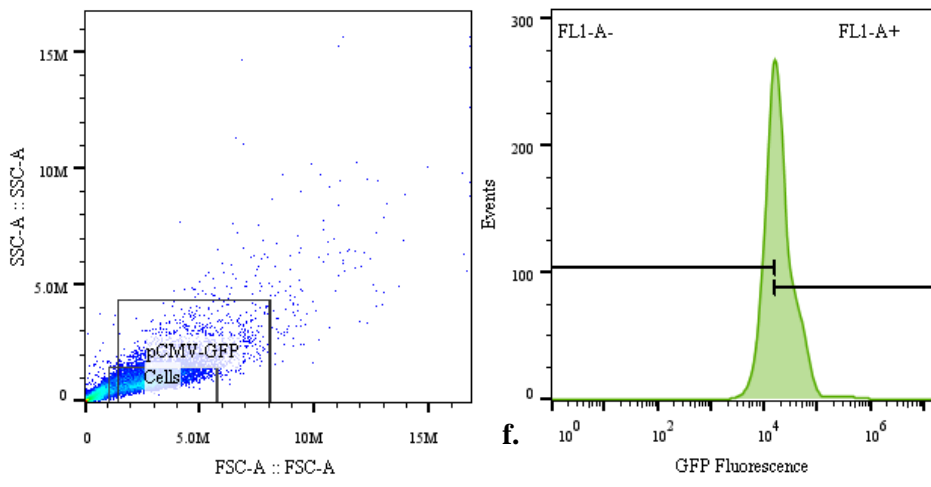
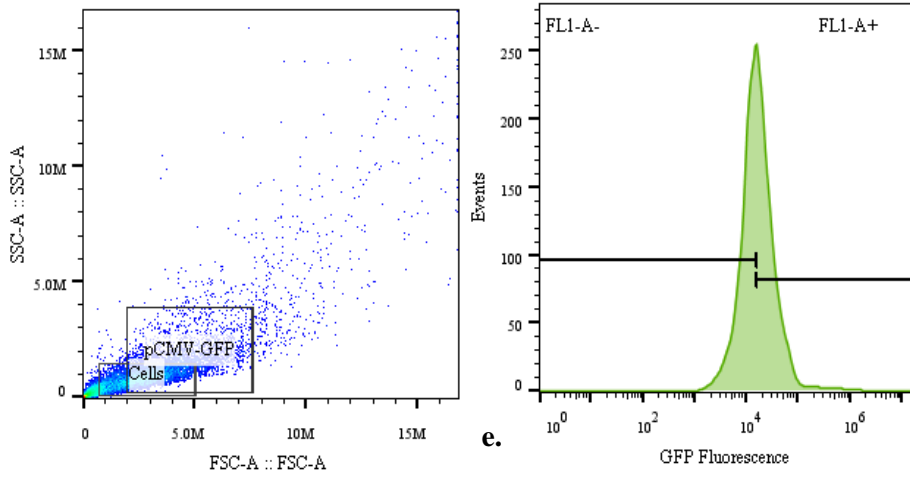


**b.**

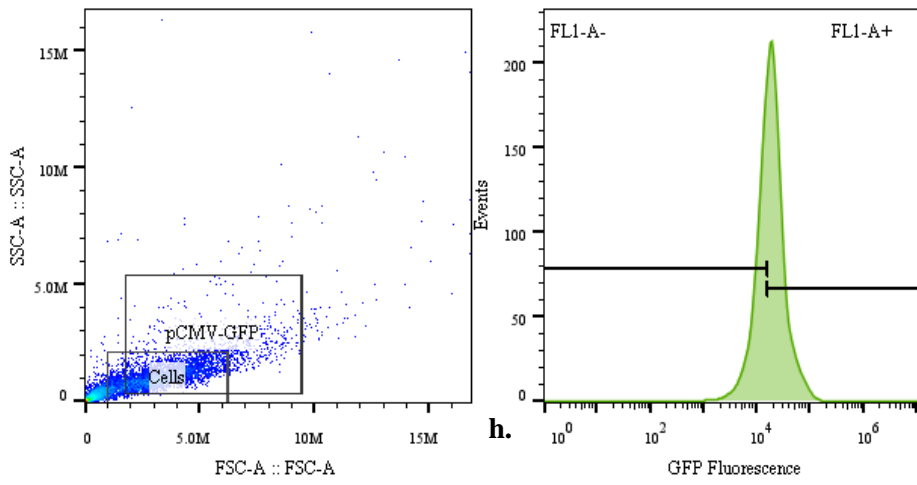
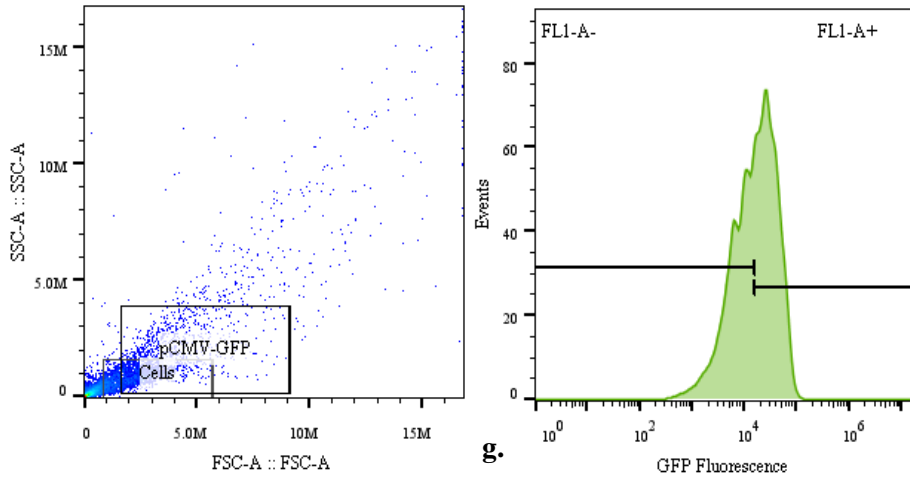
Preparation	Count	Median	CV	% GFP+
<b>a. HepG2 Cells</b>	6676	3686	47	1.41
<b>b. pCMV-GFP</b>	4129	2610	80	48.1



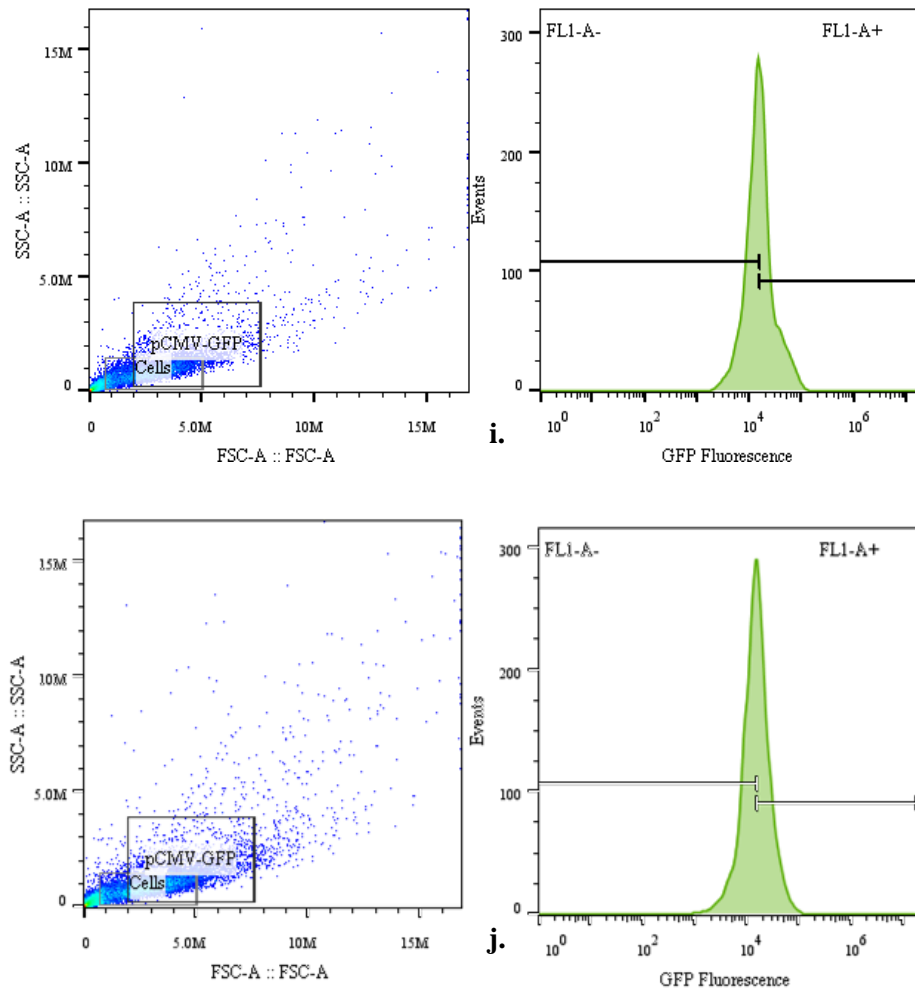
Preparation	Count	Median	CV	% GFP+
<b>c. Chol-T</b>	6464	2984	81	53.6
<b>d. Chol-T-EGF</b>	6455	2762	71.6	60.9



Preparation	Count	Median	CV	% GFP+
<b>e. Chol-T-PEG</b>	6112	3223	72	48.4
<b>f. Chol-T-PEG-EGF</b>	5389	3210	70.4	56.8



Preparation	Count	Median	CV	% GFP+
<b>g. MS09</b>	2603	1514	98	52.5
<b>h. MS09-EGF</b>	4149	2310	53	58.4



Preparation	Count	Median	CV	% GFP+
<b>i. MS09-PEG</b>	5100	2960	57	44.4
<b>j. MS09-PEG-EGF</b>	5708	2853	57.3	43.7

**Figure 3.20:** Dot plot and histogram representations of GFP fluorescent intensity produced by the different liposome formulations against a positive and negative control within the HepG2 cell line. The negative (a. HepG2 cells alone) and positive (c. pCMV- GFP) gated controls, set according to a single healthy cell population within the negative control and the population showing GFP expression in the positive control. These gates were set for all formulations examined. Remaining dot plots show a single cell population delineated by the negative and positive control gates, while the histogram overlays depict the GFP fluorescence intensity within the gated population. Liposomes c. – h., represent, c. Chol-T, d. Chol-T-EGF, e. Chol-T-PEG, f. Chol-T-PEG-EGF, g. MS09, h. MS09-EGF, i. MS09-PEG, j. MS09-PEG-EGF, respectively. All statistics presented above were produced using the FloJo analysis software Vx10.

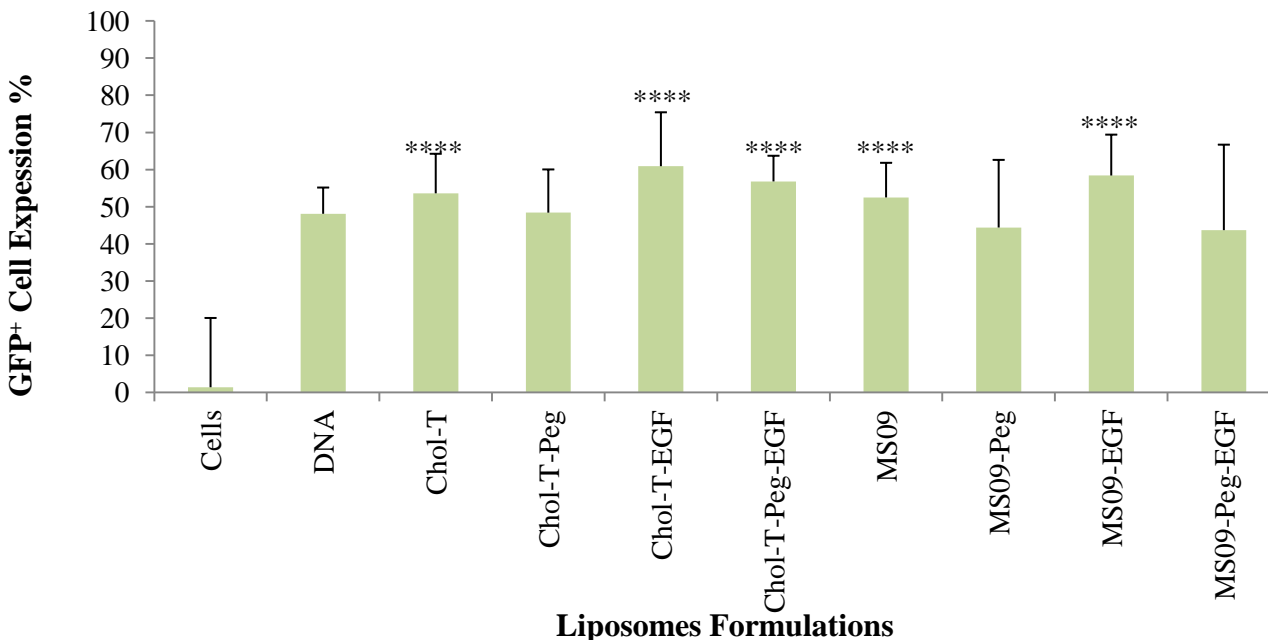


**Figure 3.21:** GFP fluorescence expressed as percentage produced per liposome as quantified by flow cytometry. The percentage GFP expression was determined from the number of GFP+ events counted within the gated cell population. SD was determined using the floJo analysis software, based on 30000 events of the HepG2 cell line ( $n = \pm 5986$  counted events).

For this analysis of GFP expression by the formulated liposomes, two controls were applied, as was performed for assessment of luminescence production by luciferase expression. Firstly, the cellular or fluorescence negative control (Figure 3.20a.) was gated such that the forward and side scatter signals were restricted to only single HepG2 viable cells, of the 30000 events counted per sample. This was applied across all GFP measurements. Moreover, the threshold between the positive GFP (pCMV-GFP) and negative fluorescent control was set so that  $> 98.6\%$  of the untransfected HepG2 cells could be considered as negative for GFP, thereby limiting background fluorescence effects. The DNA control of cells transfected with the naked plasmid was assumed positive for GFP expression, as any GFP fluorophore expression or activity would be detected per cell evaluated within the gated cell population, thus providing an expected positive result.

Following evaluation of the supplied histogram plots of the different liposome preparations, it becomes apparent that only a small population of cells were able to produce GFP fluorescent intensity at detectable levels, when compared with the 30000 overall evaluated events. Despite

this, the different liposomes examined here, were able to elicit GFP fluorescence at comparable to elevated levels against the pCMV-GFP DNA control (Figure 3.21).

The Chol-T-EGF preparation largely represented the uppermost level of detected fluorescence with approximately 60.9% of the counted cell population producing GFP expression under the direction of this liposome. This was followed by the MS09-EGF and Chol-T-PEG-EGF suspensions (Figure 3.20 h., and f.) generating an average of 58.4% and 56.8% respectively of GFP positive population expression. With the exception of MS09-PEG-EGF, a clear trend of EGF-liposome derived, superior HepG2 cell population expression was noted over that achieved by the non-targeted lipoplexes. Furthermore, with an average cell count of  $\approx 5986$  within the gated viable cell population, the MS09 and MS09-EGF treated populations showed decreased viable cell numbers. This could result from the observed cytotoxic effect of these samples compared to the Chol-T cytofectin formulations, in addition to the larger size of the plasmid being transported. Evaluation of the coefficient of variation (CV) across all liposome treatments of HepG2, highlighted the potential need for a larger data subset, or increased event count per second of up to 100 x more events (Hoy, 2006). In general the expected norm for this within the biological field should be at or around the order of 5%. Increased events evaluated would lead to decreases in the observed CV, since a wider range of GFP positive cells or events would be available for detection.

Notwithstanding this, the discernible percentage of cells expressing GFP fluorescence, shows a good correlation with lipoplex performance trends observed for the luciferase reporter gene expression. While this may be comparative, the apparent percentage of GFP expression may be elevated through the use of more GFP reporter plasmid. By comparison, even with single cell expression detection and high level mechanical sensitivity, the higher sensitivity of the luciferase reporter assay may necessitate the requirement for more GFP plasmid, which would provide a sounder signal (fluorescence) : background (auto-fluorescence). This comes from the fact that certain primary cells such as macrophages and monocytes are auto-fluorescent, despite no GFP-mammalian cell nativity (Ducrest *et al.*, 2002; Soboleski *et al.*, 2005).

A comparative representation of GFP expression capabilities of the examined lipoplexes, based on cytofectin composition can be seen in Figure 3.21. The Chol-T-EGF, Chol-T-PEG-EGF and MS09-EGF preparations produced a significant increase in the events expressing GFP fluorescence. MS09-PEG and MS09-PEG-EGF, by contrast, showed a significant reduction in the number of GFP positive events within the sample population.

## CHAPTER FOUR

### 4. CONCLUSION

Despite the vast array of gene delivery vehicles already available, novel gene therapy systems continue to be explored. The development of viral vectors remains active, while the utilisation of the many established non-viral chemical techniques for direct gene transfer into mammalian cells, have proved to be an effective base for modification or functionalisation for treatment realisation (Suda *et al.*, 2009, Guo and Huang, 2012). The effective transition of cationic liposome mediated transfection from laboratory cell culture analysis, to clinical trial application for gene therapy, and possible successful commercial marketability as transfection positive agents (Ravikant, 2014), has isolated this system as a positive basis for the current investigation.

The cellular size and steric hindrance associated with these gene delivery vectors, as well as undesired cytoplasmic interactions are barriers known to reduce efficiency of these colloidal systems for therapeutic effect. For liver directed targeting, in particular, the size of the associated fenestrae, lung entrapment and transfection, as well as possible kupffer cell rather than parenchymal uptake, makes initial cell specific vector manipulation imperative (El-Aneed, 2003; Suh *et al.*, 2007). The success of the PEG surface attachment for improved stability and *in vivo* delivery of non-viral vectors, explains its use in the liposomal system investigated here. This study was thus aimed at producing safe and efficient hepatocyte targeted cationic liposomes utilising the PEG polymer for shielding and EGF ligand for cell specific targeting in an *in vitro* system.

The novel lipoplex systems examined, contained cationic cytofectins Chol-T and MS09 that had shown efficacy in previous gene delivery experiments. Four different liposome formulations were prepared containing Chol-T and MS09 with and without DSPE-PEG<sub>2000</sub>. The EGF-polypeptide was then adsorbed onto these formulations for evaluation of the cationic liposome hepatotropism. The untargeted cationic (Chol-T and MS09) and stealth (Chol-T-PEG and MS09-PEG) liposomes and lipoplexes, as well as the targeted cationic (Chol-T-EGF and MS09-EGF) and stealth (Chol-T-PEG-EGF and MS09-PEG-EGF) lipoplexes were observed as roughly spherical in structure with varying degrees of aggregation. Cryo-TEM analysis showed that the

addition of PEG and EGF to the untargeted cationic liposomes displayed a tendency for aggregation, compared to the more homogeneous distribution of the non-functionalised liposomes. Microscopic analysis together with nanoparticle tracking analysis (NTA) identified that all formulations were nano-sized and under 200 nm. The NTA, being more sensitive and specific was able to distinguish these formulations as being generally heterogenous in size distribution, with the Chol-T-EGF preparation showing the greatest tendency toward a more monodispersed population size. Zeta determinations of these liposome and lipoplex systems indicated the relative surface charge of the formulations to be net negative in the dispersion buffer. This formulation stability in suspension was in accordance with the observed levels of aggregation, recorded by Cryo-TEM studies. All EGF targeted lipoplexes displayed an average  $\zeta$ -potential of -22 mV, indicative of colloidal propensity toward aggregate formation. This increase in the zeta potential compared to the non-target lipoplexes, is associated with a drop in pH of the lipoplex formulation due to the presence of EGF, which even on agglomerate formation, was small in size. Although, the untargeted stealth lipoplexes (Chol-T-PEG and MS09-PEG) displayed lower hydrodynamic sizes, improved stability and highly negative zeta potentials compared to the non- stealth liposomes, higher levels of aggregation were noted.

Gel retardation and ethidium bromide displacement studies revealed that these liposomes were able to effectively bind and compact plasmid DNA, with the MS09 liposome and the PEG-stabilised liposomes required at higher concentrations for formation of an electroneutral complex with DNA. The serum nuclease protection assay, revealed that the PEG-grafted liposomes offered the best nuclease protection. Overall, all liposomes showed the ability to protect and prevent complete digestion of the pCMV-*luc* DNA cargo by nucleases. The degree to which the EGF ligand was bound to each of the examined targeted formulations was confirmed through sandwich ELISA analysis. This identified the Chol-T-EGF preparation to possess the highest concentration of EGF at its surface, and as such expected to produce the highest overall transfection in the HepG2 cell line.

Cytotoxicity studies *in vitro*, showed that the EGF containing liposomes produced negligible cytotoxicity in both the CHO-K1 and HepG2 cells. Cell viability in the HepG2 cell line showed levels of cell growth that remained relatively constant with that of the untreated cell control. The

MS09-PEG lipoplex, produced a significant drop in HepG2 cell survival. While the Chol-T based (cationic, stealth, and targeted) lipoplexes produced higher luciferase gene expression compared to that observed by the MS09 preparations in both cell lines, the EGF targeted formulations proved to be far superior. The Chol-T-EGF lipoplex affected maximal luciferase gene expression in the HepG2 cell line at the optimal and super-optimal DNA binding ratios, and the Chol-T-PEG-EGF at the optimal DNA binding ratio. These targeted lipoplexes clearly displayed higher transgene expression in the target cell line (HepG2) compared to the receptor negative CHO-K1, where transfection efficiency was relative to that of the non-target preparations.

Effective EGFR targeting to the HepG2 cell line was further confirmed by competitive transfection of this cell line in the presence of excess YI-12 synthetic peptide, which significantly reduced the transfection activity due to receptor blocking by the peptide preventing the targeted lipoplex from effectively binding. The Chol-T-EGF, Chol-T-PEG-EGF, MS09-EGF, and MS09-PEG-EGF formulations displayed a, 2000, 4, 6, and 2 fold decrease in the transfection efficiency, further confirming the process of EGFR mediated endocytosis. Gene expression from the targeted transfection to the HepG2 cell line was up to 70000 fold greater than the expression seen for the commercial transfection agent, Lipofectin. Flow cytometric quantification of the GFP reporter gene expression in the HepG2 cell line for the targeted formulations did confirm their transfection efficiency and displayed a similar trend to the luciferase transgene activity. Overall moderate GFP expression was observed based on positively expressing cell populations, with the Chol-T-EGF lipoplex displaying the highest percentage (60.9%) cell population displaying positive GFP fluorescence.

The above cationic systems afford simplicity, efficiency of formulation, and the capacity for cell specific tailoring. Although the inclusion of the PEG polymer coating showed reduced transgene activity under the *in vitro* conditions, it does not directly correlate to its possible effect *in vivo*, where the longer circulation time and steric interruption would come into play. The improved efficiency of the targeted EGF cationic lipoplexes, particularly, the Chol-T-EGF and Chol-T-PEG-EGF warrants their further optimisation and investigation as hepatotropic non-viral gene delivery systems for future *in vivo* studies. Their ability to effectively achieve specific receptor

targeting drives the need for further investigation using additional preliminary examinations of GFP fluorescence and confocal imaging, ultimately leading to experiments in the *in vivo* animal model. This *in vivo* analysis affords the option of live animal imaging, as well as reporter gene expression. To begin with, the mouse model would be the first step, thereafter studies in larger animal systems would be necessary prior to reaching the clinical trial status. Several gene therapy systems have been evaluated in pre-clinical and clinical trials, with approximately 3000 patients being treated by gene therapy (Lundstrom and Boulikas, 2003). With this being the definitive goal of investigations such as these, the successful outcome of *in vivo* investigations involving the Chol-T-EGF and Chol-T-PEG-EGF lipoplexes could eventually lead to clinical trial evaluation, as an effective gene delivery system for the treatment of hepatocellular carcinoma.

## REFERENCES

- A, Wells. "EGF Receptor." *International Journal of Biochemistry and Cell Biology*, 13, no. 6 (1999): 637-43.
- Abella, J.V., and Park, M. " Breakdown of endocytosis in the oncogenic activation of receptor tyrosine kinases." *The American Journal of Physiology - Endocrinology and Metabolism*, 296, (2009): 973–984.
- Allen, T.M. "Ligand-targeted therapeutics in anticancer therapy." *Nature*, 2, (2002): 750 - 763.
- Almgren, M., Edwards, K., and Karlsson, G."Cryo transmission electron microscopy of liposomes and related structures." *Colloids and Surfaces A: Physicochemical and Engineering Aspects*, 174, (2000): 3-21.
- Amin, D. N., Hida, K., Bielenberg, D.R., and Klagsbrun, M. "Tumor Endothelial Cells Express Epidermal Growth Factor Receptor (EGFR) but not erbb3 and Are Responsive to EGF and to EGFR Kinase Inhibitors." *Cancer Research*, 66, no. 4 (2006): 2173-2180.
- Aramaki, Y., Lee, I., Arima, H., Sakamoto, T., Magami, Y., Yoshimoto, T., Moriyasu, F., Mizuguchi, J., Koyanagi, Y., Nikaido, T. And Tsuchiya, S. "Efficient Gene Transfer to Hepatoblastoma Cells through Asialoglycoprotein Receptor and Expression under the Control of the Cyclin A Promoter." *Biological and Pharmaceutical Bulletin*, 26, no. 3 (2003): 357 - 360.
- Arkipov, A., Shanemail, Y., Das, R., Endres, N.F., Eastwood, M.P., Wemmer, D.E., Kuriyan, J., and Shaw, D.E. "Architecture and Membrane Interactions of the EGF Receptor." *Cell*, 52, no. 3 (2013): 557–569.
- Arteaga, C.L."erbb-targeted therapeutic approaches in human cancer." In *The EGF Receptor Family Biologic Mechanisms and Role in Cancer*, edited by G. Carpenter, 127 - 135 . California and London: Elsevier Academic Press, (2004).
- Arteaga, C.L."erbb-targeted therapeutic approaches in human cancer." *Experimental Cell Research*, 284, (2003): 122–130.

Arteaga, C.L. "The Epidermal Growth Factor Receptor: From Mutant Oncogene in Nonhuman Cancers to Therapeutic Target in Human Neoplasia." *Journal of Clinical Oncology*, 19, no. 18 (2001): 32s - 40s.

Ashwell, G., and Harford, J. "Carbohydrate-specific Receptors of the Liver." *Annual Reviews in Biochemistry*, 51, (1982): 531–554.

Bangham, A.D., Standish, M.M., and Watkins, J.C. "Diffusion of univalent ions across the lamellae of swollen phospholipids." *Journal of Molecular Biology*, 13, (1965): 238-252.

Bangham, C. R. M., Cannon, M. J., Karzon, D. T., & Askonas, B. A. "Cytotoxic T-cell response to respiratory syncytial virus in mice." *Journal of Virology*, 56, (1985): 55-59.

Bangham, C.R.M., and Askonas, B.A. "Marine Cytotoxic T Cells Specific to Respiratory Syncytial Virus Recognize Different Antigenic Subtypes of the Virus." *Journal of General Virology*, 67, (1986): 623-629.

Barnham, K.J., Torres, A.M., Alewood, D., and Alewood, P.E. "Role of the 6-20 disulfide bridge in the structure and activity of epidermal growth factor ." *Protein Science*, (1998): 71738-1749.

Basarkar, A., and Singh, J. "Nanoparticulate systems for polynucleotide delivery." *International Journal of Nanomedicine*, 2, no. 3 (2007): 353-360.

Behr, J.P. "Gene Transfer with synthetic Cationic Amphiphiles: Prospects for Gene Therapy." *Bioconjugate Chemistry*, 5, (1994): 382 - 389.

Belting, M., Sandgren, S., and Wittrup, A. "Nuclear delivery of macromolecules: barriers and carriers." *Advanced Drug Delivery Reviews* 57, (2005): 505-527.

Benedetta, A., Benitez, S., and Komives, E.A. "Disulfide Bond Plasticity in Epidermal Growth Factor." *Proteins: Structure, Function, and Genetics*, 40, (2000): 168–174.

Bennett, C. F., Chiang, M. Y., Chan, H., Shoemaker, J.E., and Mirabelli, C.K. "Cationic lipids enhance cellular uptake and activity of phosphorothioate antisense oligonucleotides." *Molecular Pharmacology*, 41, (1992): 1023–1033.

Bhattacharai, N.R., Auwera, G.V., Rijal, S., Picado, A., Speybroeck, N., Khanal, B., Doncker, S., Das, M.L., Ostyn, B., Davies, C., Coosemans, M., Berkvens, D., Boelaert, M., and Dujardin, J.C. "Domestic animals and Epidemiology of Visceral Leishmaniasis." *Emerging Infectious Diseases*, 16, no. 2 (2010): 231-237.

Bloomfield, V. A. "Condensation of DNA by multivalent cations: Considerations on mechanism." *Biopolymers*, 31, (1991): 1471–1481.

Bordi, F., Cametti, C., Diociaiuti, M., Gaudino, D., Gili, T., and Sennato, S. "Complexation of anionic polyelectrolytes with cationic liposomes: Evidence of reentrant condensation and lipoplex formation." *Langmuir*, 20, (2004): 5214–5222.

Bunuales, M., Duzgunes, N., Zalba, S., Garrido, M.J., and Tros de Ilarduya, C. "Efficient gene delivery by EGF-lipoplexes in vitro and in vivo." *Nanomedicine*, 6, no.1 (2011): 89 - 98.

Burney, T.J., and Davies, J.C. "Gene therapy for the treatment of cystic fibrosis." *Dovepress*, 5, (2012): 29 – 23.

Candotti, F., Shaw, K.L., Muul, L., Carbonaro, D., Sokolic, R., Choi, C., Schurman, S.H., Garabedian, E., Kesserwan, C., Jagadeesh, G.J., Fu, P.Y., Gschweng, E., Cooper, A., Tisdale, J.F., Weinberg, K.I., Crooks, G.M., Kapoor, N., Shah, A., Abdel-Azim, H., Yu, X.J., Smogorzewska, M., Wayne, A.S., Rosenblatt, H.M., Davis, C.M., Hanson, C., Rishi, R.G., Wang, X., Gjertson, D., Yang, O.O., Balamurugan, A., Bauer, G., Ireland, J.A., Engel, B.C., Podsakoff, G.M., Hershfield, M.S., Blaese, R.M., Parkman, R., and Kohn, D.B. "Gene therapy for adenosine deaminase-deficient severe combined immune deficiency: clinical comparison of retroviral vectors and treatment plans." *Blood*, 120, no. 18 (2012): 3635 – 3646

Carpenter, G., and Cohen, S. "Epidermal growth factor." *Journal of Biological Chemistry*, 265, (1990): 7709-7712.

Ceresa, B.P. "Endocytic Trafficking of the Epidermal Growth Factor Receptor in Transformed Cells." In *Breast Cancer - Carcinogenesis, Cell Growth and Signalling Pathways*, edited by M. Gunduz. Intech, creative commons, (2011).

Cevher, E., Sezer, A.D., and Çağlar, E.S. "Gene Delivery Systems: Recent Progress in Viral and Non-Viral Therapy." In *Recent Advances in Novel Drug Carrier Systems*, 437-470. Intech, (2012).

Chamberlain, J.S. "Gene therapy of muscular dystrophy." *Human Molecular Genetics*, 11, no. 20 (2002): 2355 – 2362.

Chen, J-L., Wang, H., Gao, J-Q., Chen, H-L., Liang, W-Q. "Liposomes modified with polycation used for gene delivery: Preparation, characterization and transfection in vitro." *International Journal of Pharmaceutics*, 343, (2007): 255 - 261.

Chen, Y., and Li, C.H. "Novel Therapeutic Targets for hepatocellular carcinoma treatment." In *Hepatocellular Carcinoma - Basic Research*, , edited by J.W.Y Lau. Intech, (2012).

Chena, C., Wang, L., and Huang, Y. "Electrospun phase change fibers based on polyethylene glycol/cellulose acetate blends." *Applied Energy*, 88, no. 9 (2011): 3133–3139.

Cho, K., Wang, X., Chen, Z. And Shin, D.M. "Therapeutic Nanoparticles for Drug Delivery in Cancer." *Clinical Cancer Research*, 14, no.5 (2008): 1310 - 1316.

Chonn, A., and Cullis, P.R. "Recent advances in liposomal drug-delivery systems." *Current Opinion in Biotechnology*, 6, (1995): 698-708.

Chou, L.Y.T., Ming, K., and Chan, W.C.W. "Strategies for the intracellular delivery of nanoparticles." *Chemical Society Reviews, The Royal Society of Chemistry*, 40, (2011): 233–245.

Ciadiello, F. and Tortora, G. " A novel approach in the treatment of cancer: targeting the epidermal growth factor receptor." *Clinical Cancer Research*, 7, (2001): 2958–2970.

Coura, R.d.S., and Nardi, N.B. "A role for adeno-associated viral vectors in gene therapy." *Genetics and Molecular Biology*, 31, no. 1 (2008): 1-11.

Cristiano, R.J., and Roth, J.A. "Epidermal Growth Factor Mediated DNA Delivery into Lung Cancer Cells via the Epidermal Growth Factor Receptor." *Cancer Gene Therapy*, 4, no. 1 (1996): 4-10.

Cross, D., and Burmester, J.K. "Gene therapy for cancer treatment: Past, Present and Future." *Clinical Medicine and Research*, 4, no. 3 (2006): 218 – 227.

Czyzewska, J. "Human Epidermal Growth Factor Receptor Family (HER) in Gastric Cancer." In *gastric carcinoma - molecular aspects and current advances*, edited by M. Lotfy, 141 - 159 . Croatia: Intech, (2011).

Dass, C.R., and Choong, P.F.M. "Targeting of small molecule anticancer drugs to the tumour and its vasculature using cationic liposomes: lessons from gene therapy." *Cancer Cell International*, 6, no.17 (2006): 1 – 9.

Day, B.L., Thompson, P.D., Harding, A.E., and Marsden, C.D. "Influence of vision on upper limb reaching movements in patients with cerebellar ataxia." *Brain: A Journal of Neurology*, 121, (1998): 357–372.

Degennes, P.G. "Conformations of polymers attached to an interface." *Macromolecule*, 13, no. 5 (1980): 1069–1075.

Derjaguin, B.V., and Landau, L.D. "Theory of the stability of strongly charged lyophobic solutions and of the adhesion of strongly charged particles in solution of electrolytes. ." *Acta Physicochimica, U.R.S.S.*, 14, (1941): 633–652 .

Deshpande M.C., Davies M.C., Garnett M.C., Williams P.M., Armitage D., Bailey L., Vamvakaki M., Armes S.P. and Stolnik S. "The effect of poly(ethylene glycol) molecular architecture on cellular interaction and uptake of DNA complexes." *Journal of Controlled Release*, 97, (2004): 143-156.

Dollinger, M., and Rosenbaum, E. "What happens in chemotherapy." In *Everyone's Guide to Cancer Therapy: How cancer is diagnosed, treated, and managed day to day*, edited by M., Rosenbaum, E., and Cable, G. Dollinger. Kansas City: Andrews McMeel Publishing, (1997).

Ducrest, A.-L., Amacker, M., Lingner, J., and Nabholz, M. "Detection of promoter activity by flow cytometric analysis of GFP reporter expression." *Nucleic Acids Research*, 30, no. 14 (2002).

Eastman, S. J., Sigel, C., Tousignant, J., Smith, A.E., Cheng, S.H., and Scheule, R.K. "Biophysical characterization of cationic lipid:DNA complexes." *Biochimica et Biophysica Acta.*, 1325, (1997): 41–62.

Edwin, F., Singh, R., Endersby, R., Baker, S.J., and Patel, T.B. "The tumor suppressor PTEN is necessary for human Sprouty 2-mediated inhibition of cell proliferation. ." *Journal of Biological Chemistry*, 281, (2006): 4816–4822.

El-Aneed, A. "Targeted Cationic Liposomes, Technologies, and developments." *Pharmaceutical Technology*, 27, no. 12 (2003): 58 - 62.

Eming, S.A., Krieg, T. And Davidson, J.M. "Gene therapy and wound healing." *Clinics in Dermatology*, 12, (2007): 79 - 92.

Esposito, C., Generosia, J., Mossab, G., Masottic, A., and Castellan, A.C. "The analysis of serum effects on structure, size and toxicity of DDAB–DOPE and DC-Chol–DOPE lipoplexes contributes to explain their different transfection efficiency." *Colloids and Surfaces B: Biointerfaces*, 18, no. 2 (2006): 187–192.

Ewert, F., Rounsevell, M.D.A., Reginster, I., Metzger, M.J., and Leemans, R. "Future scenarios of European agricultural land use. Estimating changes in crop productivity." *Agriculture, Ecosystems and Environment*, 107, (2005): 101–116.

Fan, Y., and Wu, J. "Polylipid Nanoparticle, A Novel Lipid-Based Vector for Liver Gene Transfer." In *Gene Therapy - Tools and Potential Applications*. Intech, (2013).

Fan, Y-X., Wong, L., and Johnson, G.R. "EGFR kinase possesses a broad specificity for erbB phosphorylation sites, and ligand increases catalytic-centre activity without affecting substrate binding affinity." *Biochemical Society Journal*, 392, (2005): 417–423.

Farhood, H., Serbina, N. And Huang, L. "The role of dioleoylphosphatidylethanolamine in cationic liposome mediated gene transfer." *Biochimica et Biophysica Acta*, 1235, (1995): 289-295.

Felgner, J.H., Kumar, R., Sridhar, C.N., Wheeler, C.J., Tsai, Y.J., Border, R., Ramsey, P., Martin, M. and Felgner, P.L. "Enhanced Gene Delivery and Mechanism Studies with a Novel

Series of Cationic Lipid Formulations." *The Journal of Biological Chemistry*, 269, no. 4 (1994): 2550 - 2561 .

Felgner, P. L., and Ringold, G. M. "Cationic liposome-mediated transfection." *Nature*, 337, (1989): 387-388.

Felgner, P.L., Gadek, T.R., Holm, M., Roman, R., Chan, H.W., Wenz, M., Northrop, J.P., Ringold, G.M. and Danielsen, M. "Lipofection: A Highly Efficient, Lipid-Mediated DNA-transfection Procedure." *Proceedings of the National Academy of Sciences of the United States of America*, 84, no. 21 (1987): 7413-7417.

Ferguson, K.M. "Structure-based view of epidermal growth factor receptor regulation." *Annual Review of Biophysics*, 37, (2008): 353-73.

Ferrari, M.E., Rusalov, D., Enas, J. And Wheeler, C.J. "Trends in lipoplex physical properties dependent on cationic lipid structure, vehicle and complexation procedure do not correlate with biological activity." *Nucleic Acids Research*, 29, no.7 (2001): 1539 - 1548.

Fox, C.B., Mulligan, S.K., Sung, J., Dowling, Q.M., Fung, H.W.M., Vedvick, T.S., and Coler, R.S. "Cryogenic transmission electron microscopy of recombinant tuberculosis vaccine antigen with anionic liposomes reveals formation of flattened liposomes." *International Journal of Nanomedicine*, 9, (2014): 1367–1377.

Franklin, M.C., Carey, K.D., Vajdos, F.F., Leahy, D.J., de Vos, A.M., and Sliwkowski, M.X. "Insights into erbb signaling from the structure of the erbb2-pertuzumab complex." *Cancer Cell*, 5, (2004): 317-328.

Franzen, U., Vermehren, C., Jensen, H., and Østergaard, J. "Physicochemical characterization of a pegylated liposomal drug formulation using capillary electrophoresis." *Electrophoresis*, 32, (2011): 1-11.

Gabizon, A.A. "Stealth Liposomes and Tumor Targeting: One Step Further in the Quest for the Magic Bullet." *Clin Cancer Res February*, 7, no. 223 (2001).

Gao, X. and Huang, L. "A novel cationic liposome reagent for efficient transfection of mammalian cells." *Biochemical and Biophysical Research Communications*, 179, no. 1 (1991): 280 - 285.

Gao, X., Kim, K.S. and Liu, D. "Non-viral Gene Delivery: What We Know and What is Next." *The AAPS Journal*, 9, no. 1 (2007): 92 - 104.

Gascón, A.R., Pozo-Rodríguez, A.D., and Solinís, M.A. "Non-Viral Delivery Systems in Gene Therapy." In *Gene Therapy - Tools and Potential Applications*, edited by Francisco Martin Molina, 1 - 32 . Creative Commons, (2013).

Gelmon, K.A., Eisenhauer, E.A., Harris, A.L., Ratain, M.J., and Workman, P. "Anticancer agents targeting signalling molecules and cancer cell environment: challenges for drug development?" *Journal of National Cancer Institute*, 91, (1999): 1281-1287.

Gershon, H., Ghirlando, R., Guttman, S.B., and Minsky, A. "Mode of Formation and Structural Features of DNA-Cationic Liposome Complexes Used For Transfection." *Biochemistry*, 32, (1993): 7143 - 7151 .

Goker-Alpan, O. "Optimal therapy in Gaucher disease." *Therapeutics and Clinical Risk Management*, 6, (2010): 315 – 323.

Goodsell, D. *Epidermal growth factor*. RCSB Protein Data Bank, (2010), (accessed October 13, 2013).

Gottschalk S., Cristiano, R.J., Smith L.C. and Woo, S.L. "Folate receptor mediated DNA delivery into tumor cells: potosomal disruption results in enhanced gene expression." *Gene Therapy*, 1, no. 3 (1994): 185-91.

Grandal, M.V., and Madshus, I.H. " Epidermal growth factor receptor and cancer: control of oncogenic signalling by endocytosis." *Journal of Cell and Molecular Medicine*, 12, (2008): 1527-1534.

Guo, X., and Huang, L. "Recent Advances in Non-viral Vectors for Gene Delivery." *Accounts of Chemical Research*, American Chemical Society, 45, no. 7 (2012): 971-979.

Haglund K., and Dikic I. "The role of ubiquitylation in receptor endocytosis and endosomal sorting." *Journal of Cell Science*, 125, (2012): 265–275.

Han, S-E., Kang, H., Shim, G.Y., Suh, M.S., Kim, S.J., Kim, J-S. And Oh, Y-K. "Novel cationic cholesterol derivative-based liposomes for serum-enhanced delivery of siRNA." *International Journal of Pharmaceutics*, 353, (2008): 260 - 269 .

Harris, J.M., and Chess, R.B. "Effect of pegylation on Pharmaceuticals." *Nature Reviews, Drug Discovery*, 2, no. 3 (2003): 214 - 221.

Hasegawa, S., Hirashima, N., and Nakanishi, M. "Comparitive Study of Transfection Efficiency of Cationic Cholesterols Mediated by Liposome-Based Gene Delivery." *Bioorganic and Medicinal Chemistry Letters*, 12, (2002): 1299 - 1302 .

He, L., and Hristova K. "Consequences of replacing EGFR juxtamembrane domain with an unstructured sequence." *Scientific Reports*, 2, no. 854 (2012): 1–8.

Heasley, B.H. "Potent Antiproliferative Activity of Steroidal Natural Products is Mediated by Oxysterol-Binding Proteins." *Modern Steroid Science*. March 6, 2012.  
<http://modernsteroid.blogspot.com> (accessed October 13, 2013).

Heim, R., and Tsien, R.Y. "Engineering green fluorescent protein for improved brightness, longer wavelengths and fluorescence resonance energy transfer." *Current Biology*, 6, no. 2 (1996): 1178-1182.

Hoffman, M.S., Michael, M., Thomson, B., and Hicks, R.J. "How to treat: Neuroendocrine Tumours." *Australian Doctor*, (2011): 33–40.

Holohan, C., Schaeysbroeck, S.V., Longley, D.B., and Johnston, P.G. "Cancer drug resistance: an evolving paradigm." *Nature Reviews Cancer*, 13, (2013): 714–726.

Honary, S., and Zahir, F. "Effect of Zeta Potential on the Properties of Nano-Drug Delivery Systems - A Review (Part 1)." *Tropical Journal of Pharmaceutical Research* April 12, no. 2 (2013): 255-264.

Hoy, T. "Flow Sorting." In *Flow Cytometry : An educational guide*, edited by S. Wulff. Fort Collins, Colorado: Dako, (2006).

Huang, C-Y., Uno, T., Murphy, J.E., Lee, S., Hamer, J.D., Escobedo, J.A., Cohen, F.E., Radhakrishnan, R., Dwarki, V., and Zuckermann, R.N. "Lipitoids - novel cationic lipids for cellular delivery of plasmid DNA in vitro." *Chemistry and Biology*, 5, (1998): 345 - 354 .

Huang, J., Byong H. Kang, B.H., Pancera, M., Jeong Hyun Lee, J.H., Tommy Tong, T., Feng, Y., Imamichi, H., Georgiev, I.S., Gwo-Yu Chuang, G-W., Druz, A., Doria-Rose, N.A., Laub, L., Slieden, K., van Gils, M.J., de la Peña, A., and Derk, R. "Broad and potent HIV-1 neutralization by a human antibody that binds the gp41-gp120 interface." *Nature*, 515, (2014): 138–142.

Huang, S-L. "Liposomes in ultrasonic drug and gene delivery." *Advanced Drug Delivery Reviews*, 60, (2008): 1167 - 1176.

Icke, D. "Doing To Others ... What Was Done To Us ...?" May 7, 2010.

<http://www.davidicke.com> (accessed June 18, 2013).

Immordino, M.L., Dosio, F., and Cattell, L. "Stealth liposomes: review of the basic science, rationale, and clinical applications, existing and potential." *International Journal of Nanomedicine*, 1, no. 3 (2006): 297-315.

Ishii, M., Hirao, T., Nagashima, C., Negata, T., Sato, S., and Yao, Y. "K-Band spectroscopy of luminous young stella objects." *The Astronomical Journal*, 121, (2001): 3191-3206.

Jacobs, F., Gordts, S.C., Muthuramu, I., and De Geest, B. "The Liver as a Target Organ for Gene Therapy: State of the Art, Challenges, and Future Perspectives." *Pharmaceuticals (Basel)*, 5, no. 12 (2012): 1372–1392.

Jacobs, F., Wisse, E., and De Geest, B. "The role of liver sinusoidal cells in hepatocyte-directed gene transfer." *American Journal of Pathology*, 176, no. 1 (2010): 14-21.

Jo, M., Thomas, K.S., O'Donnell, D.M., and Gonias, S.L. "Epidermal Growth Factor Receptor-dependent and -independent Cell-signaling Pathways Originating from the Urokinase Receptor." *The Journal of Biological Chemistry*, 278, no. 3 (2003): 1642–1646.

Jokerst, J. V., Lobovkina, T., Zare, R. N., & Gambhir, S. S. "Nanoparticle pegylation for imaging and therapy." *Nanomedicine*, 6, no. 4 (2011): 715–728.

Jong, W.H.D., and Bom, P.J.A. "Drug delivery and nanoparticles: Applications and Hazards." *International Journal of Nanomedicine* 3, no. 2 (2008): 133-149.

Jorissen, R.N., Walker, F., Pouliot, N., Garrett, T.P., Ward, C.W., and Burgess, A.W. "Epidermal growth factor receptor: mechanisms of activation and signalling." *Experimental Cell Research*, 284, no. 1 (2003 ): 31-53.

Jun, I.-W., Choi, J.-S., and Cheon, J. "Shape control of semiconductor and metal oxide nanocrystals through nonhydrolytic colloidal routes." *Angewandte Chemie International Edition*, 45, (2006): 3414–3439 .

Kaasgaard, T., and Andresen, T.L. "Liposomal cancer therapy: exploiting tumor characteristics." *Expert Opinion on Drug Delivery*, 7 , no. 2 (2010): 225-243.

Kamimura, K., Abe, H., Suda, T., Aoyagi, Y., and Liu, D. "Liver-directed Gene Therapy." *Journal of Science and Medicine in Gastroenterology and Hepatology*, 1, no. 1 (2013).

Katragadda, C. S., Choudhury, P. K., and Murthy, P. N. "Nanoparticles as non-viral gene delivery vectors ." *Indian Journal of Pharmacy Education and Research*, 44 , no. 2 (2010): 109-120.

Kawakami, S., Fumoto, S., Nishikawa, M., Yamashita, F., and Hashida, M. "In Vivo Gene Delivery to the Liver Using Novel Galactosylated Cationic Liposomes." *Pharmaceutical Research*, 17, no. 3 (2000): 306–313.

Kawakami, S., Higuchi, Y. and Hashida, M. "Nonviral Approaches for Targeted Delivery of Plasmid DNA and Oligonucleotide." *Journal of Pharmaceutical Sciences*, 97, no. 2 (2008): 726 - 745.

Kawakami, S., Yamashita, F., Nishikawa, M., Takakura, Y., and Hashida, M. "Asialoglycoprotein Receptor-mediated Gene Transfer Using Novel Galactosylated Cationic Liposomes." *Biochemical and Biophysical Research Communications*, 252, no. 1 (1998): 78-83.

Kenworthy A.K., Hristova K., Needham D. and McIntosh T.J. "Range and magnitude of the steric pressure between bilayers containing phospholipids with covalently attached poly(ethylene glycol)." *Biophysical Journal*, 68, (1995): 1921-1936.

Khalil, I.A., Kogure, K., Akita, H. And Harashima, H. "Uptake Pathways and Subsequent Intracellular Trafficking in Nonviral Gene Delivery." *Pharmacological Reviews*, 58, (2006): 32 - 45 .

Kikuchi, A., Sugaya, S., Ueda, H., Tanaka, K., Aramaki, Y., Hara, T., Arima, H., Tsuchiya, S., and Fuwa, T. "Efficient Gene Transfer to EGF Receptor Overexpressing Cancer Cells by Means of EGF-labeled Cationic Liposomes." *Biochemical and Biophysical Research Communications*, 227, no. 3 (1996): 666–671.

Kisoon, N., Ariatti, M. and Moodley, T. "Novel cationic cholesterol derivative, its formulation into liposomes, and the efficient transfection of the transformed human cell lines HepG2 and Hela." *Drug Delivery*, 9, (2002): 161 – 167.

Klibanov, A.L., Maruyama, K., Torchilin, V.P., and Huang, L. "Amphipatic polyethylenglycols effectively prolong the circulation time of liposomes." *The Federation of European Biochemical Societies*, 268, (1990): 235-237.

Kneuer, C., Ehrhardt, C., Bakowsky, H., Kumar, M.N.V., Oberle, V., Lehr, C.M., Hoekstra, D., and Bakowsky, U. "The Influence of Physicochemical Parameters on the efficacy of Non-viral DNA Transfection Complexes: A Comparative Study." *Journal of Nanoscience and Nanotechnology*, 6, no. 9-10 (2006): 2776-2782.

Koynova, R., and Tenchov, B. "Cationic Lipids: Molecular Structure/Transfection Activity Relationships and Interactions with Biomembranes." *Topics in Current Chemistry*, 296, (2010): 51-93.

Ladislau, T., Madeira, K.P., Daltoé, R.D., Guimarães, I.S., Teixeira, S.F., Lyra-Júnior, P.C.M., Valadão, I.C., Rangel, L.B.A., and Herlinger, A.L. "Target Cancer Therapy." In *Cancer Treatment - Conventional and Innovative Approaches*, 38 - 62. Intech, Creative Commons, (2013).

Lasic, D.D., Strey, H., Stuart, M.C.A., Podgornik, R., and Frederik, P.M. "The Structure of DNA- Liposome Complexes." *The Journal of The American Chemical Society*, 119, (1997): 832 - 833.

Le Roy, C., and Wran, J.L. "Clathrin- and non-clathrin-mediated endocytic regulation of cell signalling." *Nature Reviews Molecular Cell Biology*, 6, (2005): 112-126.

Leahy, D.J. "The Ins and Outs of EGFR Asymmetry." *Cell*, 142, no. 4 (2010): 513–515.

Lechardeur, D., Sohn, K.J., Haardt, M., Joshi, P.B., Monck, M., Graham, R.W., Beatty, B., Squire, J., O'Brodovich, H., and Lukacs, G.L. "Metabolic instability of plasmid DNA in the cytosol: a potential barrier to gene transfer." *Gene therapy*, 5, no. 4 (1999): 482-497.

Lee, H., Kim, T.H. and Park, T.G. "A receptor-mediated gene delivery system using streptavidin and biotin-derivatized, pegylated epidermal growth factor ." *Journal of Controlled Release*, 83, no. 1 (2002): 109-119 .

Lee, R.J. "Liposomal delivery as a mechanism to enhance synergism between anticancer drugs." *Molecular Cancer Therapy*, 5, no. 7 (2006): 1639 - 1640.

Leite, E.R., and Ribeiro, C. "Basic Principles: Thermodynamics and Colloidal Chemistry." In *Crystallization and Growth of Colloidal Nanocrystals*, edited by E.R., and Ribeiro, C. Leite. Springerbriefs in Materials, (2012).

Letrou-Bonneval, E., Chèvre, R., Lambert, O., Costet, P., André, C., Tellier, C. And Pitard, B. "Galactosylated multimodular lipoplexes for specific gene transfer into primary hepatocytes." *The Journal of Gene Medicine*, 10, (2008): 1198 – 1209.

Li, S. And Huang, L. "Nonviral gene therapy: promises and challenges." *Gene Therapy*, 7, (2000): 31 - 34 .

Li, Z., Zhao, R., Wu, X., Sun, Y., Yao, M., Li, J., Xu, Y., and Gu, J. "Identification and characterization of a novel peptide ligand of epidermal growth factor receptor for targeted delivery of therapeutics." *Journal of the Federation of American Societies for Experimental Biology*, 19, (2005): 1978–1985 .

Liang, W., and Lam, J.K.W. "Endosomal Escape Pathways for Non-Viral Nucleic Acid Delivery Systems." In *Molecular Regulation of Endocytosis*, edited by B. Ceresa. (2012).

Lim, H.Y. "Cancer Gene Therapy: A Novel Strategy for Cancer Treatment." *Ajou Medical Journal*, 4, no. 1 (1999): 1 - 8 .

Litzinger, D.C., and Huang, L. "Phosphatidylethanolamine liposomes: Drug Delivery, Gene transfer and immunodiagnostic applications." *Biochimica et Biophysica Acta*, 1113, (1992): 201-227.

Lundmark, R., and Carlsson, S.R. "Driving membrane curvature in clathrin-dependent and clathrin-independent endocytosis." *Seminars in Cell and Developmental Biology*, 4, (2010): 363-370.

Lundstrom, K., and Boulikas, T. "Viral and Non-Viral Vectors in Gene Therapy: technology Development and Clinical Trials." *Technology in Cancer Research and Treatment*, 2, no. 5 (2003): 471 – 485.

Luo, D. And Saltzman, W.M. "Synthetic DNA delivery systems." *Nature Biotechnology*, 18, (2000): 33 - 37 .

Ma, B., Zhang, S., Jiang, H., Zhao, B. And Lv, H. "Lipoplex morphologies and their influence on transfection efficiency in gene delivery." *Journal of Controlled Release*, 123, (2007): 184 - 194 .

Maclachlan, I. "Liposomal Formulations for Nucleic Acid Delivery." In *Antisense drug technologies, Second edition*, 237-269. Taylor & Francis Group, LLC, (2007).

Mahato, R.I., Takemura, S., Akamatsu, K., Nishikawa, M., Takakura, Y., and Hashida, M. "Physicochemical and disposition characteristics of antisense oligonucleotides complexed with glycosylated poly(L-Lysine)." *Biochemical Pharmacology*, 53, (1997): 887-895.

Mäkelä, A. *Towards Therapeutic Gene Delivery to Human Cancer Cells*. Jyväskylä : Jyväskylä Studies In Biological and Environmental Science, (2008).

Malloy, A. "Count, size and visualise nanoparticles." *Materials Today*, 14, no. 4 (2011): 170-173.

Mamot, C., and Rochlitz, C. "Targeting the epidermal growth factor receptor (EGFR) – a new therapeutic option in oncology?" *Swiss Medical Weekly*, 136, (2006): 4–12.

Mamot, C., Drummond, D.C., Greiser, U., Hong, K., Kirpotin, D.B., Marks, J.D., and Park, J.W. "Epidermal Growth Factor Receptor (EGFR)-targeted Immunoliposomes Mediate Specific and Efficient Drug Delivery to EGFR- and egfrviii-overexpressing Tumor Cells." *Cancer Research*, 63, (2003): 3154–3161.

Marqués-Gallego, P., and de Kroon, A.I.P.M. "Ligation Strategies for Targeting Liposomal Nanocarriers." *Biomedical Research International*, (2014): 1-12.

Mccrudden, C.M., and mccarthy, H.O. "Cancer Gene Therapy – Key Biological Concepts in the Design of Multifunctional Non-Viral Delivery Systems." In *Gene Therapy - Tools and Potential Applications*, edited by F.M. Molina, 213 - 247. Creative Commons, (2013).

McMenamin, M.M., and Wood, M.J.A. "Progress and Prospects: Immunobiology of gene therapy for neurodegenerative disease: Prospects and Risks." *Gene Therapy*, 17, (2010): 448 – 458.

Medina-Kauwe, L.K., Maguire, M., Kasahara, N., and Kedes, L. "Nonviral Gene Delivery to Human Breast Cancer Cells by Targeted Ad5 Penton Proteins." *Gene Therapy*, 8, no. 23 (2001): 1753–1761.

Mendelsohn, J. "Targeting the epidermal growth factor receptor for cancer therapy." *The Journal of Clinical Oncology*, 20, no. 18 (2002): 1 - 13.

Mercer, J., and Helenius, A. "Virus entry by macropinocytosis." *Nature Cell Biology*, 11, (2009): 510-520.

Milla, P., Dosio, D., and Cattel, L. "Pegylation of Proteins and Liposomes: a Powerful and Flexible Strategy to Improve the Drug Delivery." *Current Drug Metabolism*, 13, (2012): 105-119.

Mohr, L., Yoon, S-K., Eastman, S.J., Chu, Q., Scheule, R.K., Scaglioni, P.P., Geissler, M., Heintges, T., Blum, H.E., and Wands, J.R. "Cationic Liposome-Mediated Gene Delivery to the liver and to Hepatocellular carcinomas in mice." *Human Gene Therapy*, 12, (2001): 799 - 809.

Morille, M., Passirani, C., Vonarbourg, A., Clavreul, A., and Benoit, J-P. "Progress in developing cationic vectors for non-viral systemic gene therapy against cancer." *Biomaterials*, 29, (2008): 3477 - 3496.

Mountain, A. "Gene therapy: the first decade." *Trends in Biotechnology*, 18, 2000: 119 - 128.

Mukherjee, K., Sen, J., and Chaudhuri, A. "Common co-lipids, in synergy, impart high gene transfer properties to transfection-incompetent cationic lipids." The Federation of European Biochemical Societies, *FEBS Letters* 579, no. 5 (2005): 1291-300.

Mullen, D.G., and Banaszak Holl, M.M. "Heterogeneous ligand-nanoparticle distributions: a major obstacle to scientific understanding and commercial translation." *Accounts of Chemical Research*, 44, no. 11 (2011): 1135–1145.

Muraoka-Cook, R.S., Sandahl, M., Husted, C., Hunter, D., Miraglia, L., Feng, S.-M., Elenius, K., and Earp III, H.S. "The Intracellular Domain of erbb4 Induces Differentiation of Mammary Epithelial Cells." *Molecular Biology of the Cell*, 17, (2006): 4118–4129.

Narainpersad, N., Singh, M. and Ariatti, M. "Novel neoglycolipid: formulation into pegylated cationic liposomes and targeting of DNA lipoplexes to the hepatocyte-derived cell line HepG2." *Nucleosides, Nucleotides and Nucleic Acids*, 31, no. 3 (2012): 206 – 223.

Narang, A.S., Thoma, L., Miller, D.D., and Mahato, R.I. "Cationic Lipids with Increased DNA Binding Affinity for Nonviral Gene Transfer in Dividing and Nondividing Cells." *Bioconjugate Chemistry*, no. 16 (2005): 156-168.

Nathanson, D.A., Gini, B., Mottahedeh, J., Visnyei, K., Koga, T., Gomez, G., Eskin, A., Hwang, K., Wang, J., Masui, K., Paucar, A., Yang, H., Ohashi, M., Zhu, S., Wykosky, J., and Reed, R. "Targeted Therapy Resistance Mediated by Dynamic Regulation of Extrachromosomal Mutant EGFR DNA." *Science*, 343, no. 6166 (2014): 72-76.

Nguyen, T.H., and Ferry, N. "Liver gene therapy: advances and hurdles." *Gene Therapy*, 11, (2004): S76–S84.

Niidome, T., and Huang, L. "genetherapy Progress and Prospects: Nonviral vectors." *Gene Therapy*, 9, (2002): 1647 - 1652.

Nishikawa, M., and Huang, L. "Non-viral Vectors in the New Millenium: Delivery Barriers in Gene Transfer." *Human Gene Therapy*, 12, (2001): 861 - 870.

O'Hern, C.S., and Lubensky, T.C. "Sliding Columnar Phase of DNA-Lipid Complexes." *Physical Review Letters*, (1998): 4345-4348.

Obata, Y., Saito, S., Takeda, N., and Takeoka, S. "Plasmid DNA-encapsulating liposomes: Effect of a spacer between the cationic head group and hydrophobic moieties of the lipids on gene expression efficiency." *Biochemica et Biophysica Acta*, 1778, (2009): 1148 - 1158 .

Ogiso, H., Ishitani, R., Nureki, O., Fukai, S., Yamanaka, M., Kim, J.H., Saito, K., Sakamoto, A., Inoue, M., Shirouzu, M., and Yokoyama, S. "Crystal structure of the complex of human epidermal growth factor and receptor extracellular domains." *Cell*, 110, no. 6 (2002): 775-787.

Ogris, M., and Wagner, E. "Targeting tumors with non-viral gene delivery systems." *Therapeutic Focus : Reviews* 7, (2002): 479-485.

Olayioye MA, Neve RM, Lane HA and Hynes NE. "The erbb signaling network: receptor heterodimerization in development and cancer." *The European Molecular Biology Organisation, EMBO Journal*, 19, (2000): 3159-3167.

Opanasopit, P., Tragulpakseerojn, J., Apirakaramwong, A., Ngawhirunpat, T., Rojanarata, T., and Ruktanonchai, U. "The development of poly-L-arginine-coated liposomes for gene delivery." *International Journal of Nanomedicine*, 6, (2011): 2245–2252.

P., Torchilin V. *Liposomes: a practical approach*. 2nd. New York: Oxford University Press, (2003).

Parker, A.L., Newman, C., Briggs, S., Seymour, L., and Sheridan, P.J. "Nonviral gene delivery: techniques and implications for modern medicine." *Expert Reviews in Molecular Medicine*, 5, no. 3 (2003).

Pathak, A., Patnaik, S. and Gupta, K.C. "Recent trends in non-viral vector-mediated gene delivery ." *Biotechnology Journal*, 11, no. 4 (2009): 1559 – 1572.

Patil, S., Zhang, L., Martenyi, F., Lowe, S.L., Jackson, K.A., Andreev, B.V., Avedisova, A.S., Bardenstein, L.M., Gurovich, I.Y., Morozova, M.A., Mosolov, S.N., Neznano, N.G., Reznik, A.M, Smulevich, A.B., Tochilov, V.A., Johnson, B.G., Monn, J.A., and Schoepp, D. D. "Activation of mglu2/3 receptors as a new approach to treat schizophrenia: a randomized Phase 2 clinical trial." *Nature Medicine*, 13, (2007): 1102 - 1107.

Penacho, N., Filipe, A., Simões, S., and de Lima, M.C.P. "Transferrin-Associated Lipoplexes as Gene Delivery Systems: Relevance of Mode of Preparation and Biophysical Properties." *Journal of Membrane Biology*, 221, (2008): 141–152.

Perry, J.L., Reuter, K.G., Kai, M.P., Herlihy, K.P., Jones, S.W., Luft, J. C., Napier, M., Bear, J.E., and Desimone, J.M. "Pegylated PRINT Nanoparticles: The Impact of PEG Density on Protein Binding, Macrophage Association, Biodistribution, and Pharmacokinetics. ." *Nano letters*, 12, no. 10 (2012): 5304-5310.

Pines, G., Köstler, K.J., and Yarden, Y. "Oncogenic mutant forms of EGFR: lessons in signal transduction and targets for cancer therapy." *Federation of European Biochemical Societies Letters*, 584, no. 12 (2010): 2699–2706.

Plasmid Factory. 2014. [Http://www.plasmidfactory.com](http://www.plasmidfactory.com) (accessed February 7, 2014).

Podesta, J.E., and Kostarelos, K. "Engineering Cationic Liposome:siRNA Complexes for In Vitro and In Vivo Delivery." In *Methods in Enzymology*, Vol. 464, edited by N. Düzgüneş, 343-354. Burlington: Academic Press, (2009).

Portnoy, E., Lecht, S., Lazarovici, P., Danino, P., and Magdassi, S. "Cetuximab-labeled liposomes containing near-infrared probe for in vivo imaging." *Nanomedicine: Nanotechnology, Biology, and Medicine*, 7, no.4 (2011): 480–488.

Poutona, C.W., and Seymour, L.W. "Key issues in Non-viral gene delivery." *Advanced Drug Delivery*, (2001): 187-213.

Pozharski, E., and Macdonald, R.C. "Thermodynamics of Cationic Lipid - DNA Complex Formation as Studied by Isothermal Titration Calorimetry." *The Biophysical Journal*, 83, no. 1 (2002): 556 - 565.

Rahman, M., Laurent, S., Tawil, N., Yahia, L., and Mahmoudi, M. "Nanoparticle and Protein Corona." In *Protein-Nanoparticle Interactions: The Bio-Nano Interface*, no. 84 (2013).

Ramaa, C.S., Tilekar, K.N., and Patil, V.M. "Liver cancer: Different approaches of targeting." *International Journal of pharmtech Research*, 2, no. 1 (2010): 834 - 842.

Rangelov, S., Momekova, D., and Almgren, M. "Structural characterization of lipid-based colloidal dispersions using cryogenic transmission electron microscopy." *Microscopy: Science, Technology, Applications and Education*, (2010): 1724-1734.

Ranson, M. "Epidermal growth factor receptor tyrosine kinase inhibitors." *British Journal of Cancer*, 90, (2004): 2250 – 2255.

Rao, N.M. "Cationic lipid-mediated nucleic acid delivery: beyond being cationic." *Chemistry and Physics of Lipids*, 163, (2010): 245 - 252.

Ravikant, G. "Lipoplexes: A non-viral delivery vehicle." *World Journal of Pharmacy and Pharmaceutical sciences*, 3, no. 8 (2014): 1577-1599.

Raymond, E., Alexandre, J., Faivre, S., Vera, K., Materman, E., Boni, J., Leister, C., Korth-Bradley, J., Hanauske, A., and Armand, J-P. "Safety and Pharmacokinetics of Escalated Doses of Weekly Intravenous Infusion of CCI-779, a Novel mtor Inhibitor, in Patients With Cancer." *American Society of Clinical Oncology*, 22, no. 12 (2004): 2336-2347.

Reddi, H.V. "Mutations in the EGFR Pathway Clinical Utility and Testing Strategies." *Clinical Laboratory News*, (2013): 1 - 6.

Remaut, K., Lucas, B., Braeckmans, K., Demeester, J. and De Smedt, S.D. "Pegylation of liposomes favours the endosomal degradation of the delivered phosphodiester oligonucleotides." *Journal of Controlled Release*, 117, (2007): 256 – 266.

Riese II, D.J., PhD. "Ligand-based receptor tyrosine kinase partial agonists: New paradigm for cancer drug discovery?" *Expert Opinion in Drug Discovery*, 6, no. 2 (2011): 185–193.

Robbins, P.D., Evans, C.H., and Chernajovsky, Y. "Gene therapy for arthritis." *Gene Therapy*, 10, (2003): 902 – 911.

Roepstorff, K., Grøvdal, L., Grandal, M., Lerdrup, M., and van Deurs, B. "Endocytosis downregulation of erbb receptors: mechanisms and relevance in cancer." *Histochemical Cell Biology*, 129, (2008): 563-78.

Ross, P.C., and Hui, S.W. "Lipoplex size is a major determinant of in vitro lipofection efficiency." *Gene Therapy*, 6, no. 4 (1999): 651–659.

Roth, J.A., and Cristiano, R.J. "Gene Therapy for Cancer: What Have We Done and Where Are We Going?" *Journal of the National Cancer Institute*, 89, no. 1 (1997).

Rozema, D.B. United States Patent US 2008/0200661 A1. (2008).

Salazar, G., and González, A. "Novel mechanism for regulation of epidermal growth factor receptor endocytosis revealed by protein kinase A inhibition." *Molecular Biology of the Cell*, 13, (2002): 1677–1693.

Savage, C.R., Jr., Inagami, T., and Cohen, S. "The Primary Structure of Epidermal Growth Factor." *Journal of Biological Chemistry*, 247, (1972): 7612-7621.

Scarzello, M., Vladimir Chupin, V., Anno Wagenaar, A., Stuart, M.C.A., Engberts, J.B.F.N., and Hulst, R. "Polymorphism of Pyridinium Amphiphiles for Gene Delivery: Influence of Ionic Strength, Helper Lipid Content, and Plasmid DNA Complexation." *The Biophysical Journal*, 88, no. 3 (2005): 2104–2113.

Scita, G., and Di Fiore, P.P. "Review Article The endocytic matrix." *Nature*, 463, (2010): 464-473.

Segatto, O., Anastasi, S., and Alemà, S. "Regulation of epidermal growth factor receptor signalling by inducible feedback inhibitors." *Journal of Cell Science*, 124, no. 1 (2011): 1785-1793.

Segura, T. "Formulations and Delivery Limitations of Nucleic-Acid-Based Therapies." In *Handbook of Pharmaceutical Biotechnology*, edited by S.C. Gad, 1013-1060. Wiley-Interscience, A John Wiley & Sons, Inc., Publication, (2003).

Sengupta, U., Ukil, S., Dimitrova, N., and Agrawal, S. "Expression-Based Network Biology Identifies Alteration in Key Regulatory Pathways of Type 2 Diabetes and Associated Risk/Complications. ." *plos ONE*, 4, no. 12 (2009): e8100, 1–17.

Sennato, S., Bordi, F., Cametti, C., Diociaiuti, M., and Malaspina, M. " Charge patch attraction and reentrant condensation in DNA/liposome complexes." *Biochimica et Biophysica Acta*, 11, (2005).

Shigematsu, H., Takahashi, T., Nomura, M., Majmudar, K., Suzuki, M., Lee, H., Wistuba, I.I., Fong, K.M., Toyooka, S., Shimizu, N., Fujisawa, T., Minna, J.D., and Gazdar, A.F. "Somatic mutations of the HER2 kinase domain in lung adenocarcinomas." *Cancer Research*, 65, no. 5 (2005): 1642-1646.

Sigot, V., Arndt-Jovin, D.J. and Jovin, T.M. "Targeted Cellular Delivery of Quantum Dots Loaded on and in Biotinylated Liposomes." *Bioconjugate Chemistry*, 21, no. 8 (2010): 1465–1472.

Simberg, D. Danino, D., Talmon, Y., Minsky, A., Ferrari, ME., Wheeler, C.J., and Barenholz, Y. "Phase behavior, DNA ordering, and size instability of cationic lipoplexes. Relevance to optimal transfection activity." *Journal of Biological Chemistry*, 276, (2001): 47453–47459.

Singh, M., Borain, J., Noor-Mahomed, N., and Ariatti, M. "The effect of pegylation on the transfection activity of two homologous cationic cholesteryl cytofectins. ." *African Journal of Biotechnology*, 10, no. 8 (2011): 1400-1407.

Singh, M., Hawtrey, A., and Ariatti, M. "Lipoplexes with biotinylated transferrin accessories : Novel, targeted, serum-tolerant gene carriers." *International Journal of Pharmaceutics*, 321, (2006): 124-137.

Singh, M., Kisoan, N. and Ariatti, M. "Receptor-mediated gene delivery to HepG2 cells by ternary assemblies containing cationic liposomes and cationized asialoorosomucoid." *Drug Delivery*, 8, no. 1 (2001): 29-34.

Skinner, M.W. "Gene Therapy for Hemophilia: Addressing the Coming Challenges of Affordability and Accessibility." *Molecular Therapy*, 21, no. 1 (2013): 1 – 2.

Slanina, H., Mündlein, S., Hebling, S., and Schubert-Unkmeir, A. "Role of Epidermal Growth Factor Receptor Signaling in the Interaction of *Neisseria meningitidis* with Endothelial Cells." *Infection and Immunity*, 82, no. 3 (2014): 1243–1255.

Soboleski, M.R., Oaks, J., and Halford, W.P. "Green fluorescent protein is a quantitative reporter of gene expression in individual eukaryotic cells." *The Journal of the Federation of American societies for experimental biology, FASEB*, (2005).

Song, L.Y., Ahkong, Q.F., Rong, Q., Wang, Z., Ansell, S., Hope, M.J. and Mui, B. "Characterisation of the inhibitory effect of PEG-lipid conjugates on the intracellular delivery of plasmid and antisense DNA mediated by cationic lipid liposomes." *Biochimica et Biophysica Acta*, 1588, (2002): 1 – 13.

Song, S., Liu, D., Peng, J., Deng, H., Guo, Y., Xu, L.X., Miller, A.D., and Xu, Y. "Novel peptide ligand directs liposomes toward EGF-R high-expressing cancer cells in vitro and in vivo." *The Journal of the Federation of American societies for experimental biology, FASEB Journal*, 23, (2009).

Sorkin A., and Goh L. K. " Endocytosis and intracellular trafficking of erbbs." *Experimental Cell Research*, 315, (2008): 3093–3106.

Sorkin, A. "Endocytosis and intracellular sorting of receptor tyrosine kinases" *Frontiers Biosciences*, 3, (1998): d729-d738.

Sorkin, A., and Goh, L.K. "Endocytosis and intracellular trafficking of erbbs." *Experimental cellular research*, 315, no. 4 (2009 ): 683-696.

Sternberg, B., Sorgi, F.L., and Huang. L. "New structures in complex formation between DNA and cationic liposomes visualized by freeze-fracture electron microscopy." *The Federation of European Biochemical Societies FEBS Letters*, 356, (1994): 361–366.

Strayer, D.S. "Current Status of gene therapy strategies to treat HIV/AIDS." *Molecular Therapy*, 11, (2005): 823 – 842.

Suda, T., Kamimura, K., Kubota, T., Tamura, Y., Igarashi, M., Kawai, H., Aoyagi, Y. and Liu, D. "Progress toward liver based gene therapy." *Hepatology Research*, 39, (2009): 325 - 340.

Suh, J., Choy, K.-L., Lai, S. K., Suk, J. S., Tang, B. C., Prabhu, S., and Hanes, J. "Pegylation of nanoparticles improves their cytoplasmic transport." *International Journal of Nanomedicine*, 2, no. 1 (2007): 735–741.

T, Yang. "Pegylation – Successful Approach for Therapeutic Protein Conjugation." *Modern Chemical applications*, 1, (2013).

Tang, C., Russell, P.J., Martiniello-Wilks, R., Rasko, J.E.J., and Khatria, A. "Concise review: Nanoparticles and cellular carriers-allies in cancer imaging and cellular gene therapy?" *Stem Cells*, 28, no. 9 (2010): 1686–1702.

Tang, F. and Hughes, J.A. "Synthesis of a single-tailed cationic lipid and investigation of its transfection." *Journal of Controlled Release*, 62, (1999): 345 - 358 .

Tang, X., Shigematsu, H., Bekele, B.N., Roth, J.A., Minna, J.D., Hong, W.K., Gazdar, A.F., and Wistuba, I.I. "EGFR tyrosine kinase domain mutations are detected in histologically normal respiratory epithelium in lung cancer patients." *Cancer Research*, 65, no. 1 (2005): 7568-72.

The International Agency for Research on Cancer. *Global battle against cancer won't be won with treatment alone. Effective prevention measures urgently needed to prevent cancer crisis.* Lyon/London: World Health Organisation, (3 February 2014).

Theresa M. Allen, T.M., and Cullis, P.R. "Liposomal drug delivery systems: From concept to clinical applications." *Advanced Drug Delivery Reviews*, 65, (2013): 36-48.

Thermo Fisher Scientific Incorporated. "Pierce Protein Biology Products." *Thermo Scientific*. <http://www.piercenet.com> (accessed March 16, 2014).

Thomas J. Lynch, M.D., Daphne W. Bell, Ph.D., Raffaella Sordella, Ph.D., Sarada Gurubhagavatula, M.D., Ross A. Okimoto, B.S., Brian W. Brannigan, B.A., Patricia L. Harris, M.S., Sara M. Haserlat, B.A., Jeffrey G. Supko, Ph.D., Frank G., and Haluska, M.D. "Activating Mutations in the Epidermal Growth Factor Receptor Underlying Responsiveness of Non–Small-Cell Lung Cancer to Gefitinib." *New England Journal of Medicine*, 350, (2004): 2129-2139.

Torchilin, V.P. "Recent advances with liposomes as pharmaceutical carriers." *Nature Reviews, Drug Discovery*, 4, (2005): 145-160.

Torchilin, V.P., Rammohan, R., Weissig, V., and Levchenko, T.S. "TAT peptide on the surface of liposomes affords their efficient intracellular delivery even at low temperature in the presence of metabolic inhibitors." *Proceedings of the National Academy of Sciences*, 98, no. 15 (2001): 8786–8791.

Van Craeyveld, E., Jacobs, F., Gordts, S.C., and De Geest, B. "Gene therapy for familial hypercholesterolemia." *Current Pharmaceutical design*. 17, no. 24 (2011): 2575 – 2591.

Vasir, J. K., and Labhasetwar, V. "Quantification of the Force of Nanoparticle-Cell Membrane Interactions and Its Influence on Intracellular Trafficking of Nanoparticles. ." *Biomaterials*, 29, no. 31 (2008): 4244–4252.

Verwey, E.J.W., and Overbeek, J.T.G. "Theory of Stability of Lyophobic Colloids." 92, *Elsevier*. Amsterdam, (1948).

Wagner, E., Cotten, M., Foisner, R. and Birnstiel, M.L. "Transferrin-polycation-DNA complexes: the effect of polycations on the structure of the complex and DNA delivery to cells." *Proceedings of the National Academy of Sciences*, 88, no. 10 (1991) : 4255-4259.

Wang, L., Chiang, H-C., Wua, W., Lianga, B., Xief, Z., Yaod, X., Maf, W., Duf, S., and Zhonga, Y. "Epidermal growth factor receptor is a preferred target for treating Amyloid- $\beta$ -induced memory loss." *Proceedings of the National Academy of Sciences of the United States of America*, 109, no. 41 (2012): 16743–16748.

Wang, X., Yang, L., Chen, Z. and Shin, D.M. "Application of Nanotechnology in Cancer Therapy and Imaging." *A Cancer Journal for Clinicians*, 58, (2008): 97 - 110.

Ward, C.W., and Garrett, T.P. "The relationship between the L1 and L2 domains of the insulin and epidermal growth factor receptors and the leucine-rich repeat modules." *Biomedical Central Bioinformatics*, 2, no. 4 (2001).

Ward, C.W., Hoyne, P.A., and Flegg, R.H. "Insulin and epidermal growth factor receptors contain the cysteine repeat motif found in the tumour necrosis factor receptor." *Proteins*, 22, (1995): 141- 153.

Ward, C.W., Menting, J.G., and Lawrence, M.C. "The insulin receptor changes conformation in unforeseen ways on ligand binding: sharpening the picture of insulin receptor activation." *Bioessays*, 35, (2013): 945-954.

Wasungu, L. And Hoekstra, D. "Cationic lipids, lipoplexes and intracellular delivery of genes." *Journal of Controlled Release*, 116, (2006): 255 - 264 .

Wattiaux, R., Laurent, N., Wattiaux-De Coninck, S. and Jadot, M. "Endosomes, lysosomes: their implication in gene transfer." *Advanced Drug Delivery Reviews*, 41, (2000): 201 - 208 .

Wiley, H.S. "Trafficking of the erbb receptors and its influence on signaling." In *The EGF Receptor Family Biologic Mechanisms and Role in Cancer*, edited by G. Carpenter. Elsevier Academic Press, (2004).

Wilkening, S., Stahl, F. and Bader, A. "Comparison of Primary Human Hepatocytes and Hepatoma Cell Line HepG2 With Regard To Their Biotransformation Properties." *Drug Metabolism and Disposition*, 31, (2003):1035 - 1042 .

Wolfram, J.A., and Donahue, J.K. "Gene therapy to treat cardiovascular disease." *Journal of the American Heart Association*, 2, (2013): 1 – 11.

Wu, G.Y. and Wu, C.H. "Receptor-mediated gene delivery and expression in vivo." *Journal of Biological Chemistry*, 263, (1988): 14621-14624.

Wu, J., Liu, P., Zhu, J., Maddukuri, S. and Zern, M.A. "Increased Liver Uptake of Liposomes and Improved Targeting Efficacy by Labeling With Asialofetuin in Rodents." *Hepatology*, 27, no. 3 (1998): 772-778.

Xiang, S., and Zhang, X. "Cellular Uptake Mechanism of Non-Viral Gene Delivery and Means for Improving Transfection Efficiency." In *Gene Therapy - Tools and Potential Applications*, 72-90. Intech, Creative Commons, (2013).

- Xu, Y., and Szoka, F.C.Jr. "Mechanisms of DNA Release from cationic Liposome/DNA complexes Used in Cell Transfection." *Biochemistry*, 35, (1996): 5616 - 5623.
- Xu, Y., Hui, S-K., Frederik, P. and Szoka, F.C.Jr. "Physicochemical Characterization and Purification of Cationic Lipoplexes." *Biophysical Journal*, 77, (1999): 341 - 353.
- Yang, X.D., Jia, X.C., Corvalan, J.R., Wang, P., and Davis, C.G. "Development of ABX-EGF, a fully human anti-EGF receptor monoclonal antibody, for cancer therapy." *Critical Reviews in Oncology and Hematology*, 38, no. 1 (2001 ): 17-23.
- Yanigahara, K., Cheng, H. and Cheng, P.W. "Effects of epidermal growth factor, transferrin, and insulin on lipofection efficiency in human lung carcinoma cells." *Cancer Gene Therapy*, 7, (2000): 59 - 65.
- Yarden, Y. "The EGFR family and its ligands in human cancer. Signalling mechanisms and therapeutic opportunities." *European Journal of Cancer*, 37, no. 4 (2001): S3-S8.
- Yin, Y., and Alivisatos, A.P. "Colloidal nanocrystal synthesis and the organic-inorganic interface." *Nature*, 437, (2005): 664–670.
- Yuan Zhang, Y., Satterlee, A., and Huang, L. "In Vivo Gene Delivery by Nonviral Vectors: Overcoming Hurdles?" *Molecular Therapy*, 20, no. 7 (2012): 1298-1304.
- Zeineldin, R., Muller, C.Y., Stack, M.S. and Hudson, L.G. "Targeting the EGF Receptor for Ovarian Cancer Therapy." *Journal of Oncology*, (2010): 1 - 11.
- Zhao, P., Yang, X., Qi, S., Liu, H., Jiang, H., Hoppmann, S., Cao, Q., Chua, M-Z., So, S.K., and Cheng, Z. "Molecular Imaging of Hepatocellular Carcinoma Xenografts with Epidermal Growth Factor Receptor Targeted Affibody Probes." *Biomedical Research International*, (2013): 1-11.
- Zhao, Y., Zhi, D., and Zhang, S. "Cationic Liposomes in Different Structural Levels for Gene Delivery." In *Non-Viral Gene Therapy*, edited by X. Yuan. Intech, (2011).
- Zhdanov, R.I., Podobed, O.V. and Vlassov, V.V. "Cationic lipid-DNA complexes - lipoplexes - for gene transfer and therapy." *Bioelectrochemistry*, 58, (2002): 53 - 64.

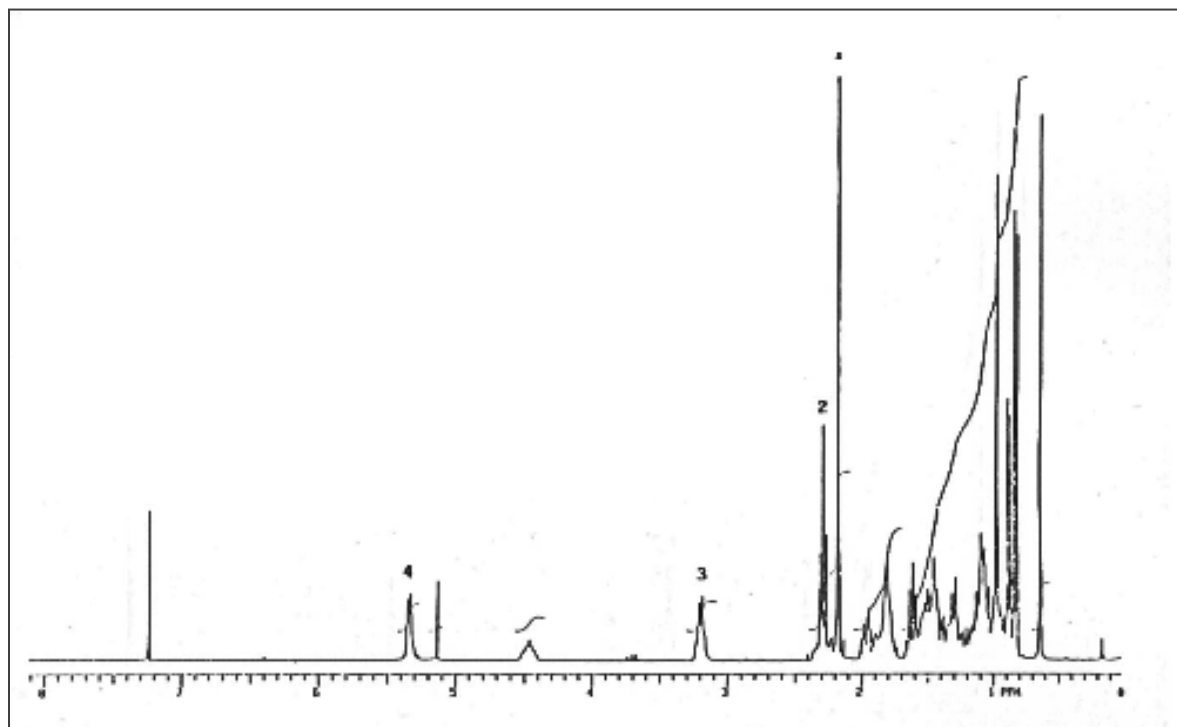
Zhenzhen, Hu., Du, J., Yang, L., Zhu, Y., Yang, Y., Zeng, D., Someya, A., Lu, L., and Gu, X. "GEP100/Arf6 Is Required for Epidermal Growth Factor-Induced ERK/Rac1 Signaling and Cell Migration in Human Hepatoma HepG2 Cells." *plos ONE*, 7, no. 6 (2012): e38777, 1–10.

Zhu, L., and Mahato, R.I. "Lipid and polymeric carrier-mediated nucleic acid delivery." *Expert Opinion in Drug Delivery*, 7, no. 10 (2010): 1209–1226.

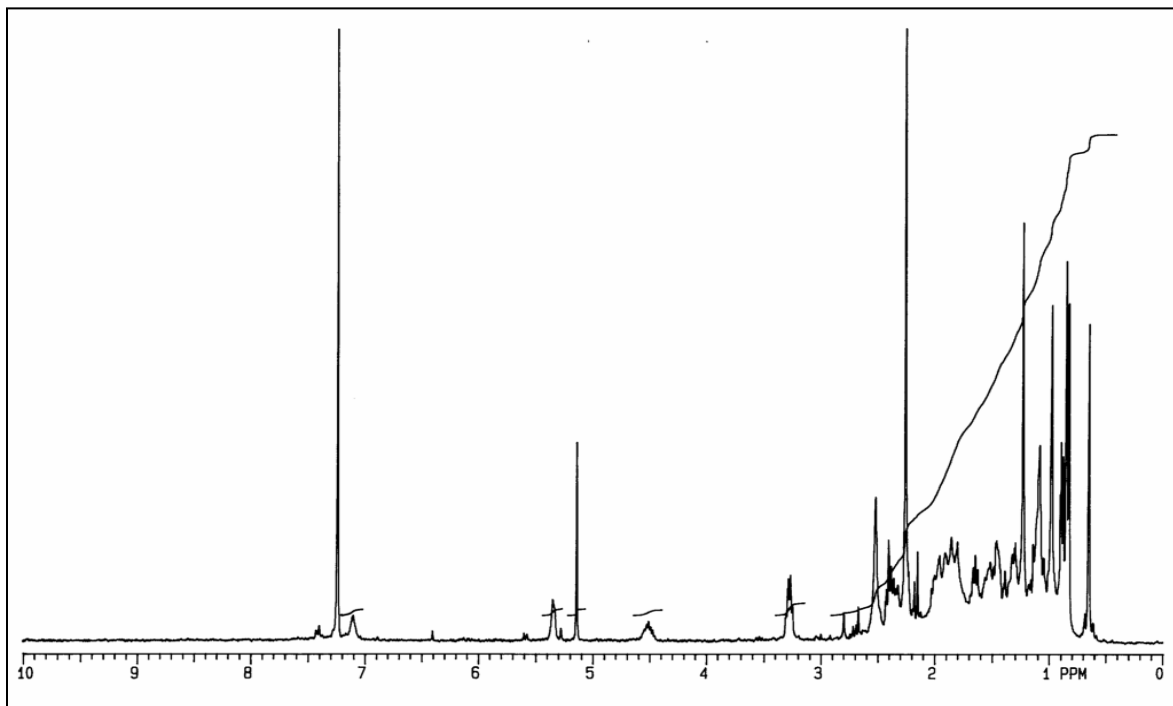
## APPENDIX 1

### NMR spectra for cationic liposome cytofectins:

#### 1. Chol-T (3 $\beta$ [N-(N',N'-dimethylaminopropane)-carbamoyl] cholesterol)



2. **MS09** (3 $\beta$ [N(N',N',-dimethylaminopropylsuccinamidohydrazido)-carbamoyl]cholesterol)



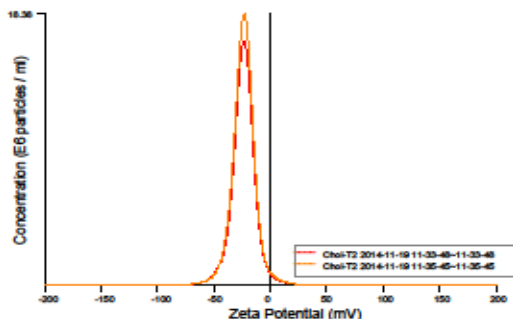
## APPENDIX 2

Nanoparticle tracking analysis for cytofectin formulations as performed with NanoSight NS500

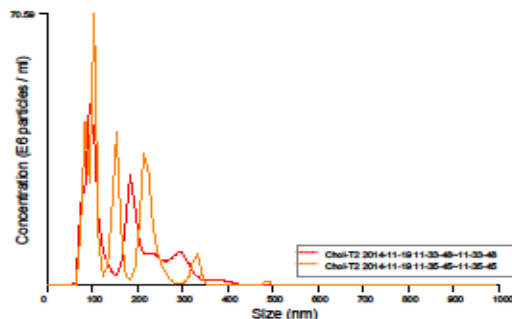
### 1.Chol-T

## NANOSIGHT

Chol-T2 2014-11-19 11-32-08



Zeta Potential / Concentration graph for Experiment:  
Chol-T2 2014-11-19 11-32-08



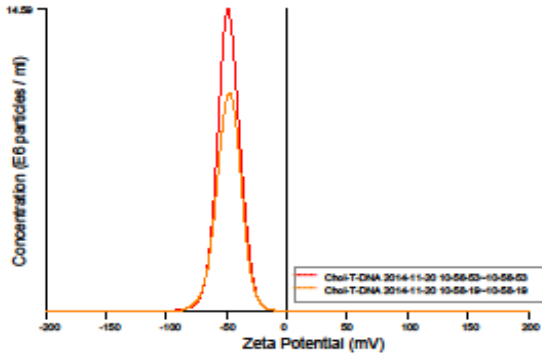
Size / Concentration graph for Experiment:  
Chol-T2 2014-11-19 11-32-08

Included Files	Results
Chol-T2 2014-11-19 11-33-48 Chol-T2 2014-11-19 11-35-45	Stats: Mean +/- Standard Error Mean: 161.3 +/- 3.9 nm Mode: 100.9 +/- 3.4 nm SD: 76.6 +/- 4.2 nm D10: 75.7 +/- 0.3 nm D50: 149.5 +/- 8.5 nm D90: 258.4 +/- 24.7 nm Concentration: 3.75e+008 +/- 1.96e+007 particles/ml 19.1 +/- 1.0 particles/frame 20.6 +/- 0.8 centres/frame
<b>Details</b>	<b>Zeta Settings and Results</b>
NTA Version: NTA 3.0 0069 Script Used: SOP Zeta Measurement 11-32-08AM 19Nov2014.txt Time Captured: 11:32:08 19/11/2014 Operator: Alisha Pre-treatment: Sample Name: Chol-T2 Diluent: 3% HBS Remarks:	Parabola fit complete Adjusted r-square: 1.00  Applied Voltage: 24.0 V Dielectric Constant: 80.00 AverageCurrent: 48.97 - 49.89 µA  Stats: Mean +/- Standard Error Mean: -24.0 +/- 0.0 mV Mode: -23.0 +/- 0.1 mV SD: 11.1 +/- 0.0 mV D10: -36.9 +/- 0.0 mV D50: -24.3 +/- 0.0 mV D90: -12.5 +/- 0.0 mV
<b>Capture Settings</b>	
Camera Type: SCMOS Camera Level: 10 Slider Shutter: 600 Slider Gain: 250 FPS: 25.0 Number of Frames: 2248 Temperature: 25.0 °C Viscosity: (Water) 0.889 - 0.889 cP Dilution factor: Dilution not recorded	
<b>Analysis Settings</b>	
Detect Threshold: 7 Blur Size: Auto Max Jump Distance: Auto: 13.0 - 13.3 pix	

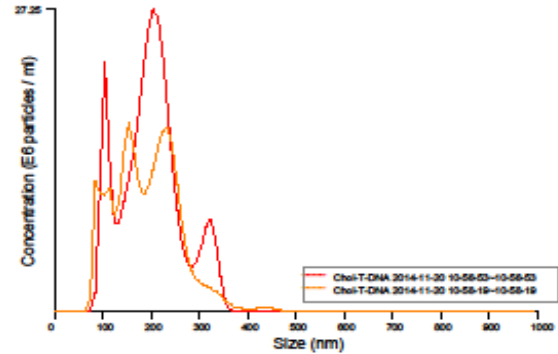
2. Chol-T-DNA (lipoplex)

# NANOSIGHT

Chol-T-DNA 2014-11-20 10-55-28



Zeta Potential / Concentration graph for Experiment:  
Chol-T-DNA 2014-11-20 10-55-28



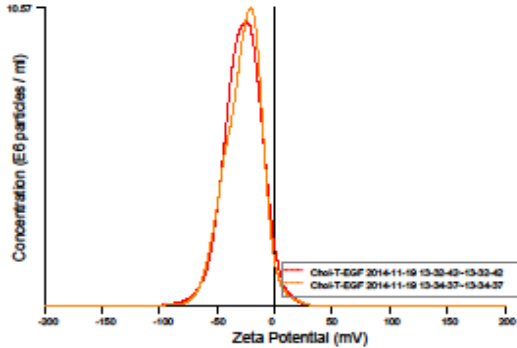
Size / Concentration graph for Experiment:  
Chol-T-DNA 2014-11-20 10-55-28

<p><b>Included Files</b></p> <p>Chol-T-DNA 2014-11-20 10-56-53 Chol-T-DNA 2014-11-20 10-58-19</p> <p><b>Details</b></p> <p>NTA Version: NTA 3.0 0069 Script Used: SOP Zeta Measurement 10-55-28AM 20Nov2014.txt</p> <p>Time Captured: 10:55:28 20/11/2014 Operator: Alisha Pre-treatment: Sample Name: Chol-T-DNA Diluent: 3% HBS Remarks:</p> <p><b>Capture Settings</b></p> <p>Camera Type: SCMOS Camera Level: 13 Slider Shutter: 800 Slider Gain: 350 FPS: 25.0 Number of Frames: 1498 Temperature: 25.0 - 25.0 °C Viscosity: (Water) 0.888 - 0.889 cP Dilution factor: Dilution not recorded</p> <p><b>Analysis Settings</b></p> <p>Detect Threshold: 3 Blur Size: Auto Max Jump Distance: Auto: 11.3 - 11.8 px</p>	<p><b>Results</b></p> <p>Stats: Mean +/- Standard Error</p> <p>Mean: 191.2 +/- 4.2 nm Mode: 181.3 +/- 26.1 nm SD: 65.6 +/- 2.4 nm D10: 95.9 +/- 3.2 nm D50: 185.5 +/- 5.1 nm D90: 274.5 +/- 13.2 nm Concentration: 3.01e+008 +/- 3.55e+007 particles/ml 15.3 +/- 1.8 particles/frame 20.4 +/- 0.3 centres/frame</p> <p><b>Zeta Settings and Results</b></p> <p>Parabola fit complete Adjusted r-square: 1.00</p> <p>Applied Voltage: 24.0 V Dielectric Constant: 80.00 AverageCurrent: 49.85 - 50.25 µA</p> <p>Stats: Mean +/- Standard Error</p> <p>Mean: -48.5 +/- 0.0 mV Mode: -47.9 +/- 0.8 mV SD: 10.8 +/- 0.4 mV D10: -61.8 +/- 0.6 mV D50: -48.9 +/- 0.1 mV D90: -36.2 +/- 0.2 mV</p>
--	--

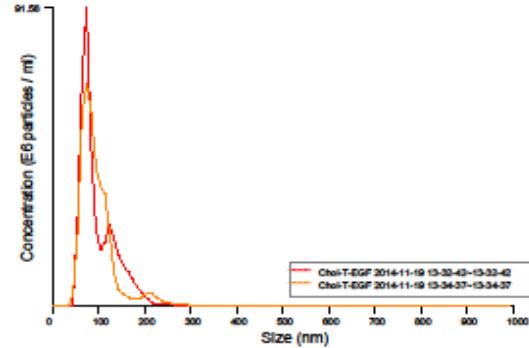
### 3. Chol-T-EGF-DNA (lipoplex)

# NANOSIGHT

Chol-T-EGF 2014-11-19 13-31-23



Zeta Potential / Concentration graph for Experiment:  
Chol-T-EGF 2014-11-19 13-31-23



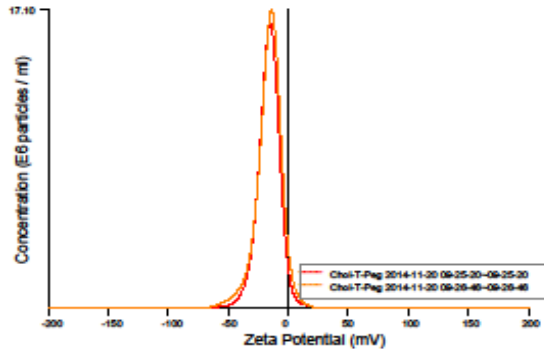
Size / Concentration graph for Experiment:  
Chol-T-EGF 2014-11-19 13-31-23

Included Files	Results
Chol-T-EGF 2014-11-19 13-32-42 Chol-T-EGF 2014-11-19 13-34-37	Stats: Mean +/- Standard Error
	Mean: 94.6 +/- 0.9 nm
	Mode: 74.3 +/- 1.0 nm
	SD: 42.9 +/- 2.1 nm
	D10: 52.4 +/- 0.3 nm
	D50: 75.8 +/- 2.2 nm
	D90: 138.7 +/- 9.7 nm
	Concentration: 4.05e+008 +/- 7.58e+006 particles/ml
	20.6 +/- 0.4 particles/frame
	21.2 +/- 0.4 centres/frame
<b>Details</b>	<b>Zeta Settings and Results</b>
NTA Version: NTA 3.0 0069	Parabola fit complete
Script Used: SOP Zeta Measurement 01-31-23PM	Adjusted r-square: 1.00
19Nov2014.txt	
Time Captured: 13:31:23 19/11/2014	Applied Voltage: 24.0 V
Operator: Alisha	Dielectric Constant: 80.00
Pre-treatment:	Average Current: 72.11 - 72.62 µA
Sample Name:	
Diluent: 3% HBS	Stats: Mean +/- Standard Error
Remarks:	Mean: -27.6 +/- 0.1 mV
	Mode: -22.3 +/- 1.9 mV
	SD: 17.0 +/- 0.1 mV
	D10: -49.3 +/- 0.5 mV
	D50: -27.1 +/- 0.6 mV
	D90: -8.4 +/- 0.7 mV
<b>Capture Settings</b>	
Camera Type: sCMOS	
Camera Level: 12	
Slider Shutter: 600	
Slider Gain: 350	
FPS: 25.0	
Number of Frames: 2248	
Temperature: 25.0 °C	
Viscosity: (Water) 0.9 cP	
Dilution factor: Dilution not recorded	
<b>Analysis Settings</b>	
Detect Threshold: 3	
Blur Size: Auto	
Max Jump Distance: Auto: 16.1 - 16.7 px	

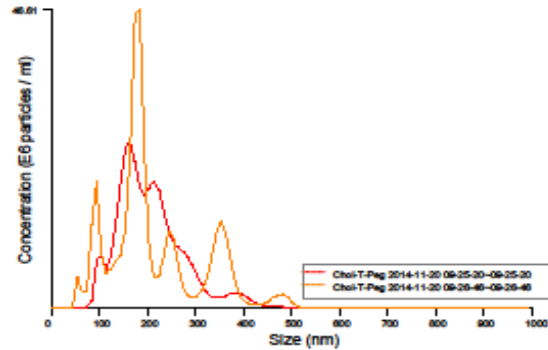
#### 4. Chol-T-PEG

# NANOSIGHT

Chol-T-Peg 2014-11-20 09-23-55



Zeta Potential / Concentration graph for Experiment:  
Chol-T-Peg 2014-11-20 09-23-55



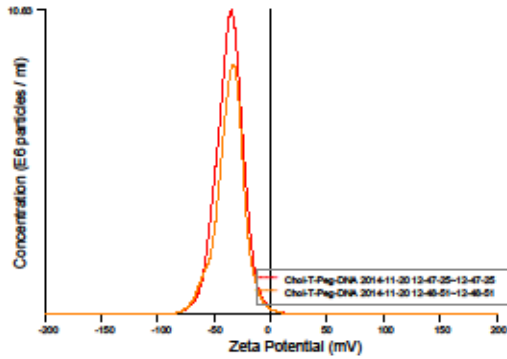
Size / Concentration graph for Experiment:  
Chol-T-Peg 2014-11-20 09-23-55

Included Files	Results
Chol-T-Peg 2014-11-20 09-25-20 Chol-T-Peg 2014-11-20 09-26-46	Stats: Mean +/- Standard Error Mean: 206.8 +/- 3.7 nm Mode: 171.6 +/- 8.8 nm SD: 84.0 +/- 13.1 nm D10: 104.6 +/- 17.3 nm D50: 181.2 +/- 5.2 nm D90: 319.9 +/- 31.2 nm Concentration: 3.58e+008 +/- 2.14e+007 particles/ml 18.2 +/- 1.1 particles/frame 28.6 +/- 4.9 centres/frame
<b>Details</b>	<b>Zeta Settings and Results</b>
NTA Version: NTA 3.0 0069 Script Used: SOP Zeta Measurement 09-23-55AM 20Nov2014.txt Time Captured: 09:23:55 20/11/2014 Operator: Alisha Pre-treatment: Sample Name: Chol-T-Peg Diluent: 3% HBS Remarks:	Parabola fit complete Adjusted r-square: 1.00  Applied Voltage: 24.0 V Dielectric Constant: 80.00 AverageCurrent: 55.36 - 55.84 $\mu$ A
<b>Capture Settings</b>	Stats: Mean +/- Standard Error Mean: -16.5 +/- 0.0 mV Mode: -14.3 +/- 0.6 mV SD: 11.1 +/- 1.0 mV D10: -29.5 +/- 0.9 mV D50: -16.2 +/- 0.4 mV D90: -5.3 +/- 0.7 mV
Camera Type: SCMOS Camera Level: 10 Slider Shutter: 600 Slider Gain: 250 FPS: 25.0 Number of Frames: 1498 Temperature: 25.0 $^{\circ}$ C Viscosity: (Water) 0.9 cP Dilution factor: Dilution not recorded	
<b>Analysis Settings</b>	
Detect Threshold: 5 Blur Size: Auto Max Jump Distance: Auto: 11.6 - 12.6 pix	

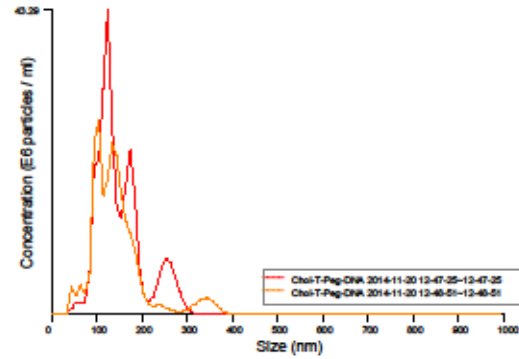
5. Chol-T-PEG-DNA (lipoplex)

# NANOSIGHT

Chol-T-Peg-DNA 2014-11-20 12-46-04



Zeta Potential / Concentration graph for Experiment:  
Chol-T-Peg-DNA 2014-11-20 12-46-04



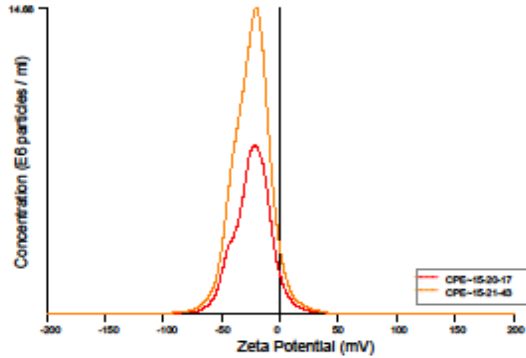
Size / Concentration graph for Experiment:  
Chol-T-Peg-DNA 2014-11-20 12-46-04

Included Files	Results
Chol-T-Peg-DNA 2014-11-20 12-47-25	Stats: Mean +/- Standard Error
Chol-T-Peg-DNA 2014-11-20 12-48-51	Mean: 144.0 +/- 3.5 nm
	Mode: 113.2 +/- 10.8 nm
	SD: 57.6 +/- 5.1 nm
	D10: 85.0 +/- 3.3 nm
	D50: 125.6 +/- 1.1 nm
	D90: 214.7 +/- 20.9 nm
	Concentration: 2.68e+008 +/- 3.01e+007 particles/ml
	13.6 +/- 1.5 particles/frame
	14.7 +/- 1.3 centres/frame
<b>Details</b>	<b>Zeta Settings and Results</b>
NTA Version: NTA 3.0 0069	Parabola fit complete
Script Used: SOP Zeta Measurement 12-46-04PM	Adjusted r-square: 0.99
20Nov2014.txt	
Time Captured: 12:46:04 20/11/2014	Applied Voltage: 24.0 V
Operator: Alisha	Dielectric Constant: 80.00
Pre-treatment:	AverageCurrent: 57.43 - 57.86 µA
Sample Name:	
Diluent: 3% HBS	Stats: Mean +/- Standard Error
Remarks:	Mean: -36.3 +/- 0.1 mV
	Mode: -33.7 +/- 0.8 mV
	SD: 13.0 +/- 0.2 mV
	D10: -53.3 +/- 0.5 mV
	D50: -36.2 +/- 0.4 mV
	D90: -21.8 +/- 0.1 mV
<b>Capture Settings</b>	
Camera Type: SCMOS	
Camera Level: 14	
Slider Shutter: 1000	
Slider Gain: 400	
FPS: 25.0	
Number of Frames: 1498	
Temperature: 25.0 - 25.0 °C	
Viscosity: (Water) 0.9 cP	
Dilution factor: Dilution not recorded	
<b>Analysis Settings</b>	
Detect Threshold: 4	
Blur Size: Auto	
Max Jump Distance: Auto: 17.6 - 19.5 pix	

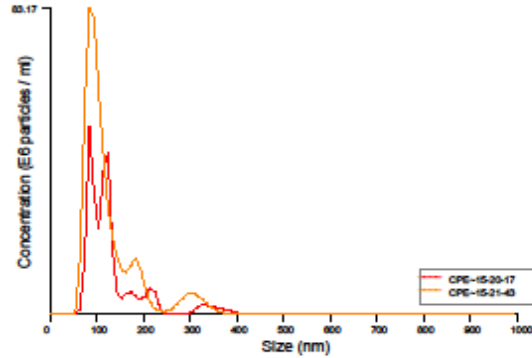
## 6. Chol-T-PEG-EGF-DNA (lipoplex)

# NANOSIGHT

CPE 2014-11-19 15-18-15



Zeta Potential / Concentration graph for Experiment:  
CPE 2014-11-19 15-18-15



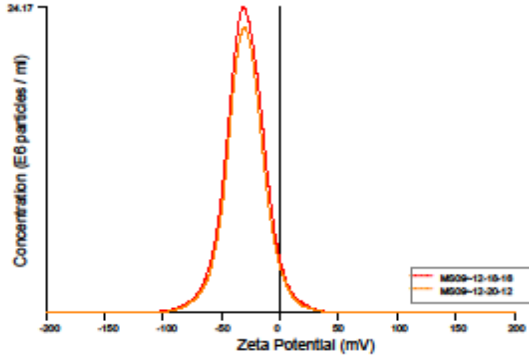
Size / Concentration graph for Experiment:  
CPE 2014-11-19 15-18-15

Included Files	Results
CPE 2014-11-19 15-20-17	Stats: Mean +/- Standard Error
CPE 2014-11-19 15-21-43	Mean: 125.5 +/- 3.6 nm
	Mode: 88.0 +/- 1.3 nm
	SD: 64.4 +/- 1.6 nm
	D10: 69.4 +/- 3.1 nm
	D50: 100.0 +/- 5.9 nm
	D90: 198.9 +/- 7.7 nm
	Concentration: 4.11e+008 +/- 1.16e+008 particles/ml
	20.8 +/- 5.9 particles/frame
	26.4 +/- 3.0 centres/frame
<b>Details</b>	<b>Zeta Settings and Results</b>
NTA Version: NTA 3.0 0069	Parabola fit complete
Script Used: SOP Zeta Measurement 03-18-15PM	Adjusted r-square: 0.96
19Nov2014.txt	
Time Captured: 15:18:15 19/11/2014	Applied Voltage: 20.0 V
Operator: Alisha	Dielectric Constant: 80.00
Pre-treatment:	AverageCurrent: 79.28 - 81.74 $\mu$ A
Sample Name: Chol-T-Peg-EGF	Stats: Mean +/- Standard Error
Diluent: 3% HBS	Mean: -24.2 +/- 0.2 mV
Remarks:	Mode: -20.8 +/- 0.9 mV
	SD: 17.0 +/- 0.1 mV
	D10: -45.6 +/- 0.3 mV
	D50: -23.9 +/- 0.3 mV
	D90: -5.5 +/- 0.3 mV
<b>Capture Settings</b>	
Camera Type: SCMOS	
Camera Level: 13	
Slider Shutter: 800	
Slider Gain: 350	
FPS: 25.0	
Number of Frames: 1498	
Temperature: 25.0 $^{\circ}$ C	
Viscosity: (Water) 0.9 cP	
Dilution factor: Dilution not recorded	
<b>Analysis Settings</b>	
Detect Threshold: 3	
Blur Size: Auto	
Max Jump Distance: Auto: 13.1 - 13.8 pix	

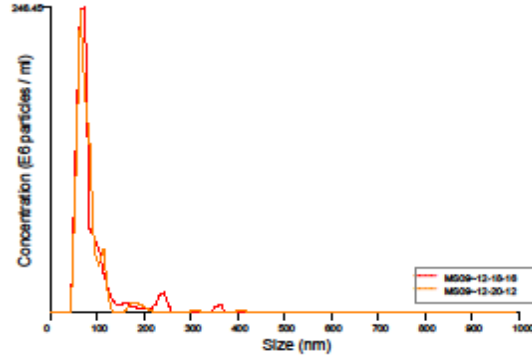
7. MS09

# NANOSIGHT

MS09 2014-11-19 12-16-58



Zeta Potential / Concentration graph for Experiment: MS09 2014-11-19 12-16-58



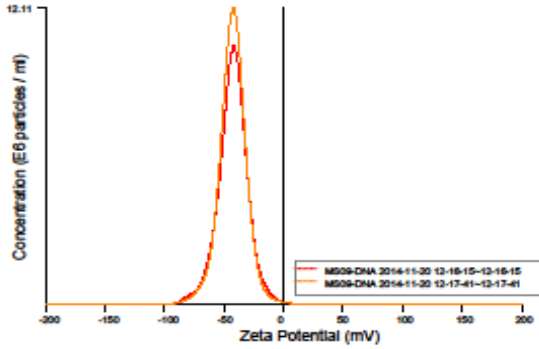
Size / Concentration graph for Experiment: MS09 2014-11-19 12-16-58

<p><b>Included Files</b></p> <p>MS09 2014-11-19 12-18-16 MS09 2014-11-19 12-20-12</p> <p><b>Details</b></p> <p>NTA Version: NTA 3.0 0069 Script Used: SOP Zeta Measurement 12-16-58PM 19Nov2014.txt</p> <p>Time Captured: 12:16:58 19/11/2014 Operator: Alisha Pre-treatment: Sample Name: MS09 Diluent: 3% HBS Remarks:</p> <p><b>Capture Settings</b></p> <p>Camera Type: SCMOS Camera Level: 13 Slider Shutter: 800 Slider Gain: 350 FPS: 25.0 Number of Frames: 2248 Temperature: 25.0 - 25.0 °C Viscosity: (Water) 0.9 cP Dilution factor: Dilution not recorded</p> <p><b>Analysis Settings</b></p> <p>Detect Threshold: 8 Blur Size: Auto Max Jump Distance: Auto: 17.1 - 17.5 pix</p>	<p><b>Results</b></p> <p>Stats: Mean +/- Standard Error</p> <p>Mean: 83.5 +/- 3.5 nm Mode: 68.4 +/- 1.7 nm SD: 48.0 +/- 5.2 nm D10: 47.9 +/- 0.3 nm D50: 64.5 +/- 0.1 nm D90: 117.9 +/- 13.7 nm Concentration: 9.09e+008 +/- 4.86e+007 particles/ml 46.1 +/- 2.5 particles/frame 49.6 +/- 2.5 centres/frame</p> <p><b>Zeta Settings and Results</b></p> <p>Parabola fit complete Adjusted r-square: 0.96</p> <p>Applied Voltage: 24.0 V Dielectric Constant: 80.00 AverageCurrent: 49.94 - 50.52 µA</p> <p>Stats: Mean +/- Standard Error</p> <p>Mean: -30.0 +/- 0.0 mV Mode: -30.6 +/- 0.3 mV SD: 18.2 +/- 0.3 mV D10: -51.6 +/- 0.3 mV D50: -30.6 +/- 0.0 mV D90: -9.0 +/- 0.3 mV</p>
---	---

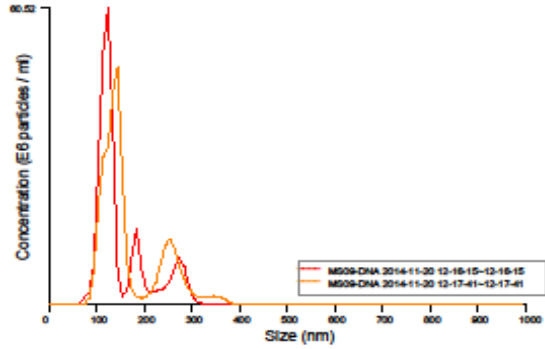
## 8. MS09-DNA (lipoplex)

# NANOSIGHT

MS09-DNA 2014-11-20 12-14-05



Zeta Potential / Concentration graph for Experiment:  
MS09-DNA 2014-11-20 12-14-05



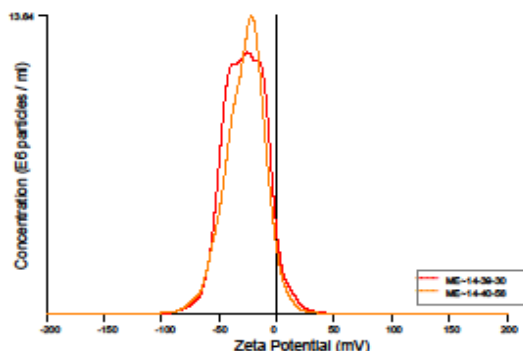
Size / Concentration graph for Experiment:  
MS09-DNA 2014-11-20 12-14-05

Included Files	Results
MS09-DNA 2014-11-20 12-16-15 MS09-DNA 2014-11-20 12-17-41	Stats: Mean +/- Standard Error
	Mean: 156.7 +/- 8.4 nm
	Mode: 132.3 +/- 9.7 nm
	SD: 61.2 +/- 3.8 nm
	D10: 98.1 +/- 2.5 nm
	D50: 126.1 +/- 8.0 nm
	D90: 256.4 +/- 2.9 nm
	Concentration: 2.98e+008 +/- 1.06e+007 particles/ml
	15.1 +/- 0.5 particles/frame
	16.7 +/- 0.4 centres/frame
	<b>Zeta Settings and Results</b>
	Parabola fit complete
	Adjusted r-square: 1.00
	Applied Voltage: 24.0 V
	Dielectric Constant: 80.00
	AverageCurrent: 57.37 - 58.00 $\mu$ A
	Stats: Mean +/- Standard Error
	Mean: -42.9 +/- 0.1 mV
	Mode: -41.7 +/- 0.2 mV
	SD: 12.8 +/- 0.4 mV
	D10: -58.5 +/- 0.8 mV
	D50: -43.1 +/- 0.1 mV
	D90: -28.7 +/- 0.7 mV
<b>Details</b>	
NTA Version: NTA 3.0 0069	
Script Used: SOP Zeta Measurement 12-14-05PM 20Nov2014.txt	
Time Captured: 12:14:05 20/11/2014	
Operator: Alisha	
Pre-treatment:	
Sample Name: MS09-DNA	
Diluent: 3% HBS	
Remarks:	
<b>Capture Settings</b>	
Camera Type: SCMOS	
Camera Level: 13	
Slider Shutter: 800	
Slider Gain: 350	
FPS: 25.0	
Number of Frames: 1498	
Temperature: 25.0 $^{\circ}$ C	
Viscosity: (Water) 0.9 cP	
Dilution factor: Dilution not recorded	
<b>Analysis Settings</b>	
Detect Threshold: 3	
Blur Size: Auto	
Max Jump Distance: Auto: 12.0 - 13.3 pix	

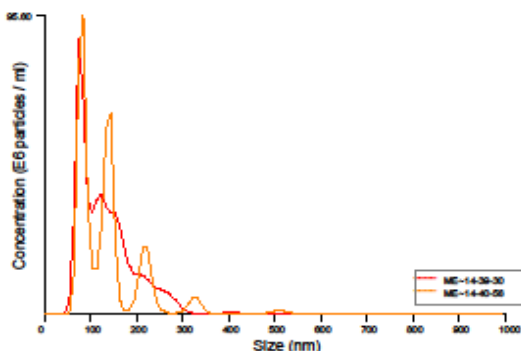
## 9. MS09 – EGF-DNA (lipoplex)

# NANOSIGHT

ME 2014-11-19 14-38-14



Zeta Potential / Concentration graph for Experiment:  
ME 2014-11-19 14-38-14



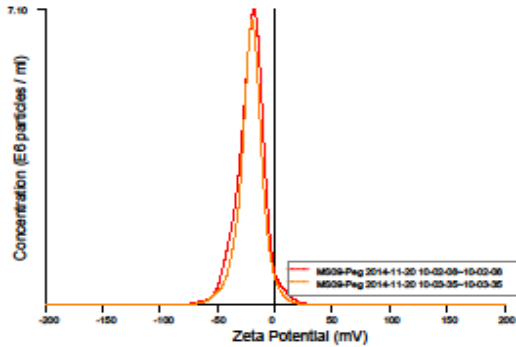
Size / Concentration graph for Experiment:  
ME 2014-11-19 14-38-14

Included Files		Results	
ME 2014-11-19 14-39-30 ME 2014-11-19 14-40-56		Stats: Mean +/- Standard Error	
<b>Details</b>		Mean:	131.8 +/- 1.0 nm
NTA Version:	NTA 3.0 0069	Mode:	79.8 +/- 2.3 nm
Script Used:	SOP Zeta Measurement 02-38-14PM 19Nov2014.txt	SD:	70.1 +/- 4.1 nm
Time Captured:	14:38:14 19/11/2014	D10:	64.0 +/- 1.1 nm
Operator:	Alisha	D50:	113.5 +/- 2.2 nm
Pre-treatment:		D90:	216.1 +/- 0.1 nm
Sample Name:	MS09-EGF	Concentration:	5.76e+008 +/- 3.44e+007 particles/ml
Diluent:	3% HBS		29.3 +/- 1.7 particles/frame
Remarks:			30.8 +/- 1.9 centres/frame
<b>Capture Settings</b>		<b>Zeta Settings and Results</b>	
Camera Type:	SCMOS	Parabola fit complete	
Camera Level:	12	Adjusted r-square:	0.99
Slider Shutter:	600	Applied Voltage:	20.0 V
Slider Gain:	350	Dielectric Constant:	80.00
FPS:	25.0	Average Current:	73.77 - 75.12 $\mu$ A
Number of Frames:	1498	Stats: Mean +/- Standard Error	
Temperature:	25.0 - 25.0 $^{\circ}$ C	Mean:	-27.5 +/- 0.1 mV
Viscosity:	(Water) 0.9 cP	Mode:	-23.4 +/- 1.9 mV
Dilution factor:	Dilution not recorded	SD:	18.4 +/- 0.4 mV
<b>Analysis Settings</b>		D10:	-50.9 +/- 0.2 mV
Detect Threshold:	4	D50:	-27.3 +/- 0.6 mV
Blur Size:	Auto	D90:	-6.3 +/- 0.8 mV
Max Jump Distance:	Auto: 13.9 - 14.7 pix		

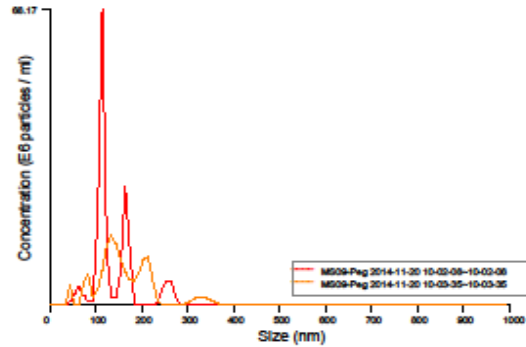
## 10. MS09-PEG

# NANOSIGHT

MS09-Peg 2014-11-20 10-00-43



Zeta Potential / Concentration graph for Experiment:  
MS09-Peg 2014-11-20 10-00-43



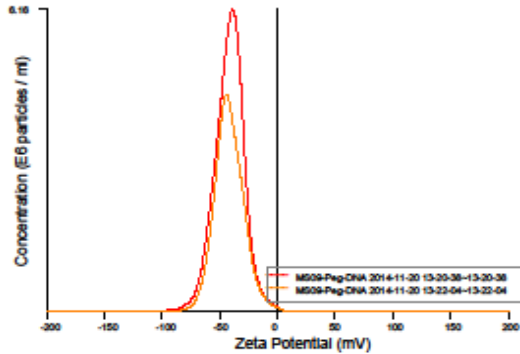
Size / Concentration graph for Experiment:  
MS09-Peg 2014-11-20 10-00-43

Included Files	Results
MS09-Peg 2014-11-20 10-02-08	Stats: Mean +/- Standard Error
MS09-Peg 2014-11-20 10-03-35	Mean: 146.2 +/- 12.1 nm
	Mode: 125.2 +/- 10.6 nm
	SD: 55.5 +/- 7.6 nm
	D10: 85.1 +/- 7.8 nm
	D50: 124.8 +/- 16.2 nm
	D90: 191.8 +/- 22.2 nm
	Concentration: 1.66e+008 +/- 1.56e+007 particles/ml
	8.4 +/- 0.8 particles/frame
	12.0 +/- 2.2 centres/frame
<b>Details</b>	<b>Zeta Settings and Results</b>
NTA Version: NTA 3.0 0069	Parabola fit complete
Script Used: SOP Zeta Measurement 10-00-43AM	Adjusted r-square: 0.99
20Nov2014.txt	
Time Captured: 10:00:43 20/11/2014	Applied Voltage: 24.0 V
Operator: Alisha	Dielectric Constant: 80.00
Pre-treatment:	AverageCurrent: 50.90 - 50.94 $\mu$ A
Sample Name: MS09-Peg	
Diluent: 3% HBS	Stats: Mean +/- Standard Error
Remarks:	Mean: -21.0 +/- 0.0 mV
	Mode: -18.7 +/- 0.8 mV
	SD: 12.4 +/- 0.6 mV
	D10: -36.6 +/- 1.2 mV
	D50: -20.9 +/- 0.1 mV
	D90: -8.1 +/- 0.5 mV
<b>Capture Settings</b>	
Camera Type: SCMOS	
Camera Level: 14	
Slider Shutter: 1000	
Slider Gain: 400	
FPS: 25.0	
Number of Frames: 1498	
Temperature: 25.0 - 25.0 $^{\circ}$ C	
Viscosity: (Water) 0.9 cP	
Dilution factor: Dilution not recorded	
<b>Analysis Settings</b>	
Detect Threshold: 9	
Blur Size: Auto	
Max Jump Distance: Auto: 14.0 - 19.2 pix	

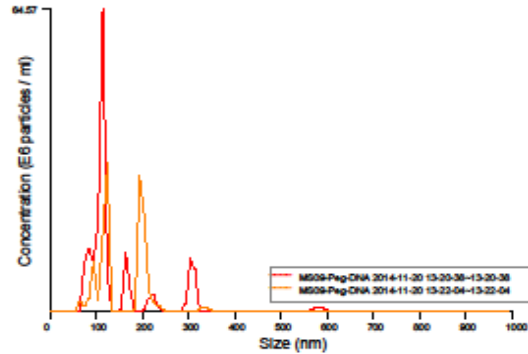
## 11. MS09-PEG-DNA (lipoplex)

# NANOSIGHT

## MS09-Peg-DNA 2014-11-20 13-19-18



Zeta Potential / Concentration graph for Experiment:  
MS09-Peg-DNA 2014-11-20 13-19-18



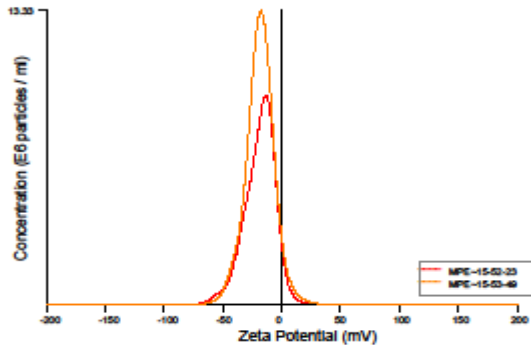
FTLA Size / Concentration graph for Experiment:  
MS09-Peg-DNA 2014-11-20 13-19-18

Included Files	Results
MS09-Peg-DNA 2014-11-20 13-20-38 MS09-Peg-DNA 2014-11-20 13-22-04	Stats: Mean +/- Standard Error Mean: 150.2 +/- 2.6 nm Mode: 118.9 +/- 4.4 nm SD: 73.0 +/- 20.1 nm D10: 80.7 +/- 5.3 nm D50: 112.3 +/- 6.8 nm D90: 247.4 +/- 48.2 nm Concentration: 1.55e+008 +/- 2.47e+007 particles/ml 7.8 +/- 1.3 particles/frame 11.7 +/- 1.1 centres/frame
<b>Details</b> NTA Version: NTA 3.0 D069 Script Used: SOP Zeta Measurement 01-19-18PM 20Nov2014.bt Time Captured: 13:19:18 20/11/2014 Operator: Alisha Pre-treatment: Sample Name: MS09-Peg-DNA Diluent: 3% HBS Remarks:	<b>Zeta Settings and Results</b> Parabola fit complete Adjusted r-square: 1.00 Applied Voltage: 24.0 V Dielectric Constant: 80.00 AverageCurrent: 52.55 - 53.02 µA Stats: Mean +/- Standard Error Mean: -42.0 +/- 0.1 mV Mode: -41.2 +/- 2.7 mV SD: 13.3 +/- 0.0 mV D10: -58.5 +/- 0.5 mV D50: -42.4 +/- 0.7 mV D90: -26.6 +/- 0.5 mV
<b>Capture Settings</b> Camera Type: SCMOS Camera Level: 14 Slider Shutter: 1000 Slider Gain: 400 FPS: 25.0 Number of Frames: 1498 Temperature: 25.0 - 25.0 °C Viscosity: (Water) 0.9 cP Dilution factor: Dilution not recorded	
<b>Analysis Settings</b> Detect Threshold: 4 Blur Size: Auto Max Jump Distance: Auto: 14.0 - 14.6 pix	

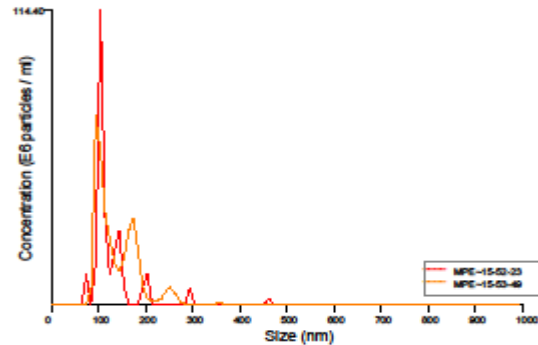
## 12. MS09-PEG-EGF-DNA (lipoplex)

# NANOSIGHT

MPE 2014-11-19 15-51-07



Zeta Potential / Concentration graph for Experiment:  
MPE 2014-11-19 15-51-07



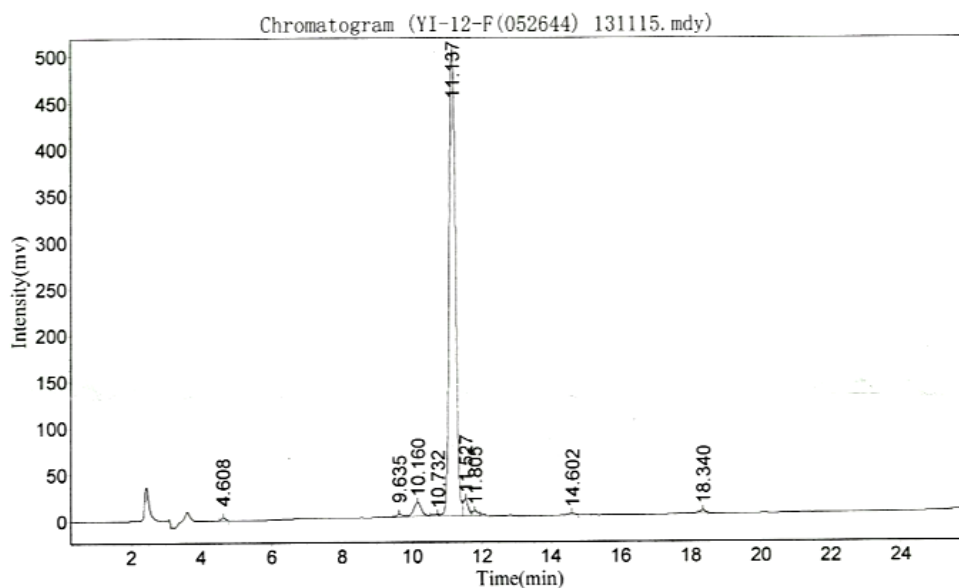
Size / Concentration graph for Experiment:  
MPE 2014-11-19 15-51-07

Included Files	Results
MPE 2014-11-19 15-52-23 MPE 2014-11-19 15-53-49	Stats: Mean +/- Standard Error
<b>Details</b>	Mean: 130.0 +/- 4.2 nm
NTA Version: NTA 3.0 0069	Mode: 101.9 +/- 3.6 nm
Script Used: SOP Zeta Measurement 03-51-07PM	SD: 52.4 +/- 5.8 nm
19Nov2014.txt	D10: 86.7 +/- 2.6 nm
Time Captured: 15:51:07 19/11/2014	D50: 106.5 +/- 6.9 nm
Operator: Alisha	D90: 182.5 +/- 2.9 nm
Pre-treatment:	Concentration: 3.24e+008 +/- 4.55e+007 particles/ml
Sample Name: MS09-Peg-EGF	16.4 +/- 2.3 particles/frame
Diluent: 3% HBS	17.6 +/- 2.7 centres/frame
Remarks:	<b>Zeta Settings and Results</b>
<b>Capture Settings</b>	Parabola fit complete
Camera Type: SCMOS	Adjusted r-square: 1.00
Camera Level: 11	Applied Voltage: 20.0 V
Slider Shutter: 600	Dielectric Constant: 80.00
Slider Gain: 300	AverageCurrent: 70.65 - 71.92 µA
FPS: 25.0	Stats: Mean +/- Standard Error
Number of Frames: 1498	Mean: -18.8 +/- 0.1 mV
Temperature: 25.0 - 25.0 °C	Mode: -15.3 +/- 2.2 mV
Viscosity: (Water) 0.9 cP	SD: 13.8 +/- 0.4 mV
Dilution factor: Dilution not recorded	D10: -36.2 +/- 1.1 mV
<b>Analysis Settings</b>	D50: -18.3 +/- 0.6 mV
Detect Threshold: 4	D90: -4.1 +/- 0.1 mV
Blur Size: Auto	
Max Jump Distance: Auto: 14.4 - 15.4 px	

## APPENDIX 3

### YI-12 Peptide for Competitive Trasfection

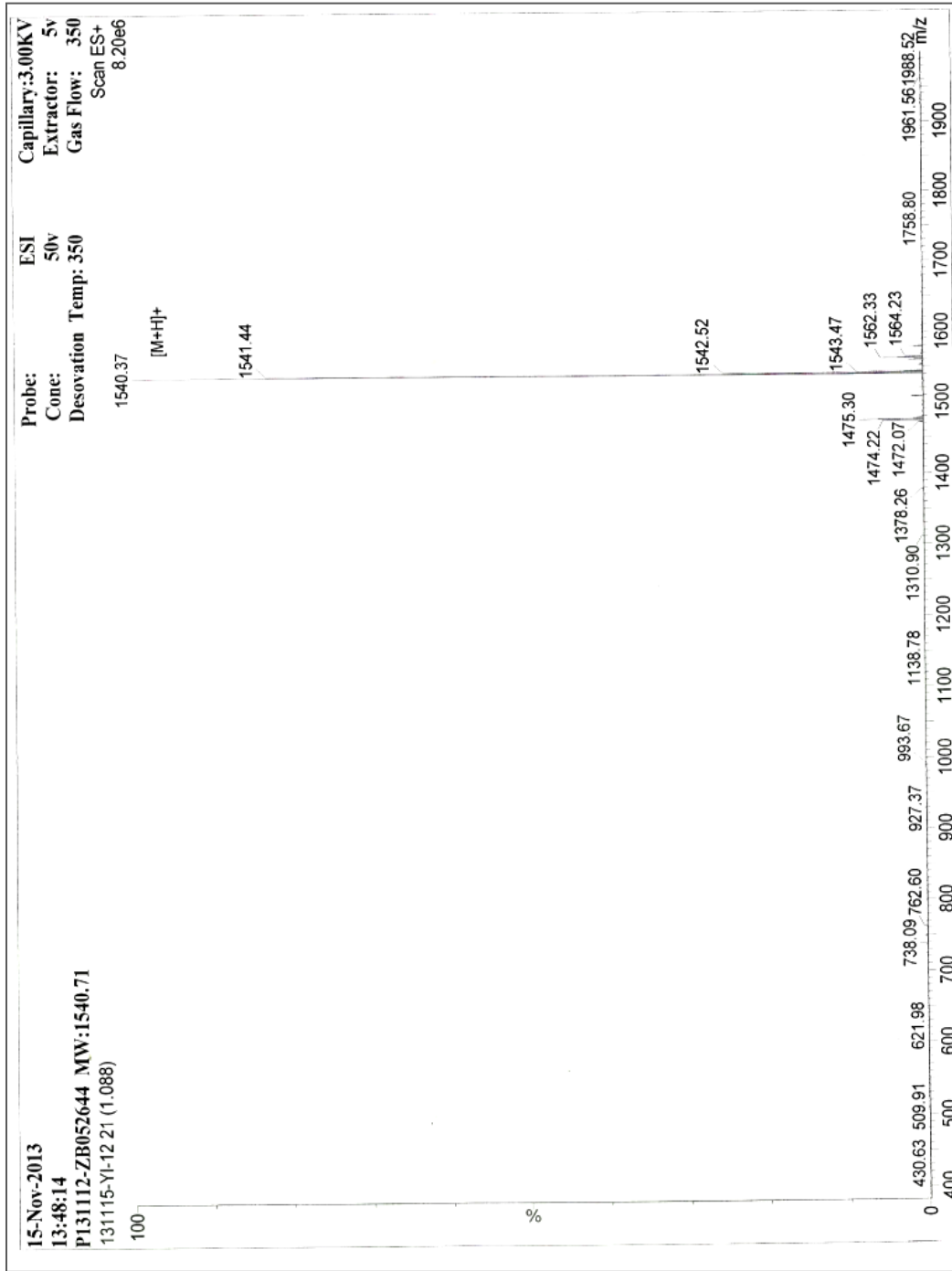
Sample Description:  
 Structure : YI-12  
 Number : 010250011  
 Lot No : P131112-ZB052644  
 Column : 4.6×250mm, Venusil MP C18-5  
 Solvent A : 0.1% trifluoroacetic in 100% acetonitrile  
 Solvent B : 0.1% trifluoroacetic in 100% water  
 Gradient :  
                   A                  B  
 0.01min      15%          85%  
 25min         40%          60%  
 25.1min     100%          0%  
 30min                  STOP  
 Flow rate : 1.0 mL/min  
 Wavelength : 220nm  
 Volumn : 5ul



#### Results

Peak No.	Peak ID	Ret Time	Height	Area	Conc.
1		4.608	3556.214	28139.049	0.4050
2		9.635	2688.268	32532.701	0.4682
3		10.160	14422.818	216378.172	3.1139
4		10.732	1169.351	11587.113	0.1668
5		11.137	501686.469	6339807.000	91.2377
6		11.527	18493.123	196333.391	2.8255
7		11.805	5783.708	61039.484	0.8784
8		11.805	2401.073	19732.484	0.2840
9		14.602	1498.995	16564.543	0.2384
10		18.340	3298.724	26558.945	0.3822
<b>Total</b>			554998.744	6948672.883	100.0000

# YI-12 Peptide Chromatogram



## APPENDIX 4

### Conference Proceedings: Published Abstract

#### POSTER PRESENTATIONS

A65

experiments, two balloon catheters were introduced simultaneously through jugular and femoral veins and were placed in cava vein close to liver entry restricting the perfusion area, the whole liver was targeted; portal outflow was blocked by intrahepatically placing another balloon catheter in main portal branch. Then, pTC7101 plasmid bearing the hAAT gene in 200 ml saline solution (20 µg/ml) was retrovenously injected (20 ml/s). The gene transfer efficiency and protein expression of both models were compared.

**Results:** The results showed: (i) the highest gene delivery (10–100 hAAT DNA copies/diploid genome) occurred with free outflow; (ii) outflow blockade mediated a slightly higher rate of transcription (~10 vs ~1 hAAT RNA copies/cell) despite a lower plasmid amount; (iii) conjugating these results, the intrinsic efficacy of outflow blocking model resulted higher ( $10^2$ – $10^3$  vs 1–10 RNA/DNA copy per cell); (iv) outflow blockade model achieved efficient protein expression (~ $10^8$  copies/cell).

**Conclusion:** Data suggest that retrovenous catheter mediated liver gene transfer is an efficient model of hepatic gene transfer with potential clinical applications and the portal outflow blocking could improve the gene expression. Partially supported by AP-151-11 and SAF2011-27002.

#### P018

##### Epidermal growth factor targeted novel cationic lipoplexes enhance transgene expression in HepG2 cell line *In vitro*

A Sewbalas<sup>1</sup>, M. Ariatti<sup>1</sup>, M. Singh<sup>1</sup>

<sup>1</sup>Non-Viral Gene Delivery Laboratory, Discipline of Biochemistry, School of Life Sciences, College of Agriculture, Engineering, and Science, University of KwaZulu-Natal, Durban, South Africa

For augmented efficiency, cationic liposomes can be modified as cell-specific gene therapy systems. Of the different ligands used for modification and exploitation of receptor mediated endocytosis, the epidermal growth factor (EGF) was chosen for this investigation. The aim of this study was to evaluate the hepatotropism of targeted liposomes for enhanced transgene expression in the HepG2 (Human hepatocellular carcinoma) cell line, known to over-express EGF.

Four liposomes, two consisting of cytofectins 3β[N-(N',N'-dimethylaminopropyl)-carbonyl] (Chol-T) and N,N-dimethylaminopropylamidolsuccinyl-cholesterylformylhydrazide (MS09) and two displaying additional distearoylphosphatidylethanolamine-polyethylene glycol 2000 (DSPE-PEG 2000), were formulated with the neutral lipid DOPE through thin film re-hydration. Preformed cationic liposomes were conjugated to the (EGF) polypeptide through a simple adsorption method prior to characterization and cell culture studies. All liposome formulations were investigated for their ability to bind, condense and protect plasmid DNA (pCMV-Luc), using the agarose gel retardation, ethidium bromide dye displacement and nuclease protection assays. All liposomes and lipoplexes were subjected to electron microscopy and zeta-sizing to determine lamellarity and size distribution. *In vitro* cytotoxicity was determined using the MITT assay, and gene expression using the luciferase reporter gene assay and fluorescence microscopy in the HepG2 cell line.

Overall targeted liposomes showed good binding and protection of plasmid DNA. These novel lipoplex systems were able to successfully transfect the HepG2 cell line with minimal cytotoxicity and greater transgene expression than the receptor negative control cell line. Initial results show that with further optimization clinically viable gene or drug delivery vehicles can be formulated.

#### P019

##### Viral vs. non-viral gene therapy to improve tendon healing: Electrotransfer leads to rapid gene expression compared to AAV-based delivery.

S Hasslund<sup>1</sup>, H Gissel<sup>1</sup>, CC Danielsen<sup>1</sup>, M Koefoed<sup>1</sup>, TG Jensen<sup>1</sup>, L Aagaard<sup>1</sup>

<sup>1</sup>Aarhus University, Denmark

Injury and repair of the flexor tendons of the human hand are often complicated by fibrotic adhesions limiting the hand function. In order to restore the tendon gliding function new treatment options are needed. Gene therapy using AAV has shown ability to improve tendon healing in model systems. In this study we sought to develop a non-viral method, in order to avoid potential inflammatory response induced by the viral vector. Indeed, inflammation is one of the factors thought to increase adhesion formation. We used electrotransfer of plasmid DNA to muscle as delivery strategy.

Using an established murine model of flexor tendon injury and healing, we transected and repaired the flexor digitorum longus tendon in the mouse foot. Following surgery we injected 10 µl of either pDNA (15 µg) or rAAV ( $2 \times 10^9$  particles) encoding a firefly luciferase reporter gene into an adjacent muscle (flexor digitorum brevis). Luciferase activity were recorded by live bioimaging at 2, 4, 8, 12, 24 hours post treatment and followed for up to 28 days. We detected luciferase activity as early as two hours after gene delivery by electrotransfer. In contrast the onset of gene expression in the viral vector treated group did not exceed our detection limit until day 3.

Electrotransfer and the rapid onset of gene expression opens new possibilities for flexor tendon gene therapy. Currently we are investigating a number of possible anti-adhesive genes of their potential to improve the tendon healing and gliding function in our murine model.

#### P020

##### Muscle-targeted incretin gene therapy for type 2 diabetes

G Patterson<sup>1</sup>, A Mahmoud<sup>1</sup>, M White<sup>1</sup>, H Marshall<sup>1</sup>, S Luli<sup>1</sup>, C Huggins<sup>1</sup>, L Todd<sup>1</sup>, E Cook<sup>1</sup>, S Niessen<sup>2</sup>, J Shaw<sup>1</sup>

<sup>1</sup>Diabetes Research Group, Newcastle University, Institute of Cellular Medicine, Newcastle upon Tyne, UK

Type 2 diabetes affects 350 million people world wide. Current treatments are somewhat effective but usually do not halt disease progression relying heavily on patient adherence. Our objective was to evaluate plasmid-mediated GLP1 gene therapy in normal and diabetic mice. Constitutively active pVR1012-GLP1; pVR1012-Ex4 (long-acting GLP1 homologue), and pVR1012-eGFP plasmids were injected into both anterior tibialis and gastrocnemius muscles in CD1 or db/db mice, with adjuvant hyaluronidase pre-treatment and electroporation. Sustained eGFP reporter gene expression was confirmed by IVIS spectrum imaging throughout study duration (CD1: Day 8–30 (n=5); db/db Day 3–41 (n=6)). Circulating Exendin-4 levels following pVR1012-Ex4 injection in normal mice (n=5) peaked at Day 15 (7095 ± 9405 pmol/l) and were maintained throughout study duration (Day 30: 1250 ± 634 pmol/l) with comparable end-point levels in db/db mice (n=6) (pre-plasmid: 95.5 ± 22.3 pmol/l; Day 14: 234 ± 35 pmol/l; Day 42: 1684 ± 1310 pmol/l). Circulating GLP1 levels in db/db mice following pVR1012-GLP1 injection were low (Day 42: 3.9 ± 3.0 pmol/l (n=6)). Glucose tolerance in db/db mice improved in the group receiving pVR1012-Ex4 (IPGTT AUC: Day 42 5022 pmol.min vs Day 0 3536 pmol.min